THE FUNCTION OF *Streptococcus mutans* YIDC1 AND YIDC2, AND THEIR ROLES IN MEMBRANE BIOGENESIS

By

SARA MARIE RASER PALMER

A DISSERTATION PRESENTED TO THE GRADUATE SCHOOL
OF THE UNIVERSITY OF FLORIDA IN PARTIAL FULFILLMENT
OF THE REQUIREMENTS FOR THE DEGREE OF
DOCTOR OF PHILOSOPHY

UNIVERSITY OF FLORIDA

2011

To everyone who believed in me and helped along the way, this would not have been possible without you

ACKNOWLEDGMENTS

First I would like to thank my high school biology teacher, Mr. Fern “Bud” Ellis. He was the first person to recognize my potential as a scientist and without his careful mentoring and passion for teaching I would not have pursued a career in science, but would probably be a struggling artist instead. My Aunt and Uncle Carolynn and Terry Palmer, who took me in and gave me a chance to make something of my life, have my sincerest appreciation. They taught me the importance of education and helped me to realize my potential as a person. I would also like to thank my Aunt Anne Palmer, who was there when I needed her at a time when I didn’t know who to ask for help. I am grateful to Dr. Linda Mansfield, who was my mentor for undergraduate research. Her lab was the first of many labs I hope to work in during my career as a scientist. She gave me a chance to see what science is all about and without her letter of recommendation graduate school would not have been possible.

I want to acknowledge Dr. Jeannine Brady, my dissertation mentor. Jeannine has been an incredibly supportive “Boss” over the last five years. She has shown compassion, understanding, and an amazing ability to handle all that life throws at you. Jeannine has been an excellent role-model and has an incredible scientific mind. I am grateful that I chose her as my mentor for so many reasons, but mostly because she challenged me to think for myself and allowed me the freedom to persue my interests. I appreciate all the opportunities she has imparted on me through the year, and I will miss working with her. I was also fortunate to know Dr. Arnold Bleiweis. He was a tremendous person and scientist and I feel much honored to have known him and benefited from his vast knowledge and understanding of *Streptococcus mutans.* I am particularly grateful of the time he took to proof-read my pre-doctoral fellowship

application as well as for all the papers he printed with me in mind. I would like to thank Paula Crowley, for all the advice and knowledge she has imparted over the past five years. I particularly want to thank her for help with proof-reading my pre-doctoral fellowship application as well as all the constructive criticism she has given me in the past. I am also indebted to Dr. Lin Zeng for his advice and help with cloning in *Streptococcus mutans*, which was integral to the completion of this project.

Last but not least, I want to acknowledge my committee members. Thank you for attending my committee meetings and providing lively discussions about my project, for asking tough questions and motivating me to be a better scientist. Thank you for taking the time to read this document and for all your criticisms, which have made it better. You have been a great committee and I strive to make you proud. In particular, I want to thank Dr. Brian Cain for the use of the equipment in his lab as well as his advice on the ATP hydrolysis assays. He has always been extremely supportive of his students and a great mentor. I am also appreciative for the letter of support he wrote on my behalf for my pre-doctoral fellowship. I owe many thanks to Dr. Ken Cline for his letter of support and for help with the Blue-Native PAGE experiments. I'm grateful to Dr. Robert Burne, for all his advice with my cloning projects and taking the time to meet to discuss my project on several occasions. I thank Dr. Paul Gulig for his insistence on excellence and dedication as a teacher in microbial genetics as well as always attending the immunology and microbiology journal clubs. His insight and contributions to these discussions have been invaluable to my education and development as a scientist.

TABLE OF CONTENTS

page

LIST OF TABLES

LIST OF FIGURES

LIST OF ABBREVIATIONS

2D-BN/SDS PAGE	2nd dimensional Blue-Native/Sodium dodecyl sulfate PAGE
AA	Amino acids
ACMA	9-amino-6-chloro-2-methoxyacridine
ACN	Acetonitrile
ATR	Acid tolerance response
BCA	Bicinchoninic acid
BHI	Brain heart infusion
BN-PAGE	Blue-Native polyacrylamide gel electrophoresis
BSA	Bovine serum albumin
CAT	Chloramphenicol acetyltransferase
DCCD	N, N'-dicyclohexylcarbodiimide
DDM	Dodecylmaltoside
DTT	Dithiothreitol
EDTA	Ethylenediaminetetraacetic acid
ELISA	Enzyme-linked immunosorbent assay
GAPDH	Glyceraldehyde-3-phosphate dehydrogenase
GTF	Glucosyltransferases
HK	Histidine kinase
HPLC	High-performance liquid chromatography
IAA	Iodoactamide
IPTG	Isopropyl β-D-1-thiogalactopyranoside
kDa	Kilodaltons
LB	Luria-Bertani
LC-MS/MS	Liquid chromatography-MS/MS

LHCP	Light harvesting chlorophyll binding protein
MS	Mass spectometry
MALDI-TOF-MS	Matrix-assisted laser desorption/ionization-time of flight -mass spectrometry
MSM	Multiple sugar metabolism
NICE	Nisin inducible controlled expression
NT	Nucleotide
OD	Optical density
O/N	Overnight
PAGE	Polyacrylamide gel electrophoresis
PBS	Phosphate buffered saline
PCR	Polymerase chain reaction
PEP-PTS	Phosphoenolpyruvate- phosphotransferase system
PFL	Pyruvate formate lyase
PK	Proteinase K
PMF	Proton motive force
Qrt-PCR	Quantitative real-time PCR
RBS	Ribosome binding site
RNAi	Ribonucleic Acid Interference
RR	Response regulator
scRNA	Small cytoplasmic RNA
SGP	*Streptococcus* GTP-binding protein
SOE PCR	Splice overlap extension polymerase chain reaction
SRP	Signal recognition particle
TCA	Trichloroacetic acid
TDM	Tereckyj Defined Media

THYE	Todd-Hewitt Yeast Extract
TIM	Translocon of inner membrane
TMD	Transmembrane domain
TOM	Translocon of outer membrane
WCL	Whole cell lysate

Abstract of Dissertation Presented to the Graduate School
of the University of Florida in Partial Fulfillment of the
Requirements for the Degree of Doctor of Philosophy

THE FUNCTION OF *Streptococcus mutans* YIDC1 AND YIDC2, AND THEIR ROLES IN MEMBRANE BIOGENESIS

By

Sara Marie Raser Palmer

May 2011

Chair: L. Jeannine Brady
Major: Medical Sciences, Immunology and Microbiology

Streptococcus mutans is a major causative agent of dental caries. It has two paralogs of the YidC/Oxa1/Alb3 family of membrane protein insertases/chaperones. Like disruption of the signal recognition particle (SRP) co-translational pathway, elimination of *yidC2* causes loss of genetic competence, stress sensitivity (acid, osmotic and oxidative), and impaired biofilm formation. It has been postulated that acid sensitivity in these mutants is due to defects in assembly of the F_1F_o ATPase, which pumps protons out of the cell during acidic growth conditions. Elimination of *yidC1* is less severe, with no observable effect on growth or stress sensitivity.

YidC2 has a longer, more positively-charged C-terminal tail than YidC1 and can complement an Oxa1 mutant in yeast. Oxa1 function depends on its C-terminal tail. Chimeric proteins were constructed to evaluate, the roles of the C-termini in stress tolerance of YidC1 and YidC2. Placing the YidC2 tail on YidC1 restored acid and osmotic stress tolerance to a *yidC2* mutant. In contrast, placing the C-terminal tail of YidC1 on to YidC2 resulted in a dominant negative effect, with decreased growth yield and sensitivity to stress, indicating the C-terminal domains play an important role in stress tolerance.

Studies revealed both YidC1 and YidC2 can function in *E. coli* to assemble an active F_1F_o ATPase in a YidC-depletion strain. In *S. mutans*, deletion of either *yidC1*or *yidC2* results in decreased membrane-associated ATPase activity, indicating that the pronounced acid sensitive phenotype of the delta *yidC2* mutant stems from further mechanisms in addition to impaired proton extrusion.

Blue-Native PAGE, which separates native membrane protein complexes, combined with LC-MS/MS revealed differences in location of glycolytic enzymes, citrate metabolic enzymes, transporters, and ribosomal proteins associated with the membrane fractions of wildtype and the *yidC* mutants. Therefore, YidC1 and YidC2 appear to contribute to assembly of membrane-associated complexes involved with glycolysis and to ribosome tethering for co-translational translocation, likely explaining the dispensability of the SRP pathway in *S. mutans*.

Collectively, these results provide evidence that the difference in stress sensitivity between the Δ*yidC1* and Δ*yidC2* mutants stems from functional differences in their C-termini.

CHAPTER 1
LITERATURE REVIEW

Streptococcus mutans and Dental Caries

Streptococcus mutans is a member of the viridans group of streptococci, which was originally characterized by partial hemolysis of red-blood cells through the production of hydrogen peroxide, giving blood agar surrounding colonies a green appearance (alpha-hemolysis). Streptococci are catalase negative, gram-positive cocci that form chains. Current classification of the viridans group relies on three tests to differentiate them from other streptococci. They are leucine aminopeptide positive, pyrrolidonylarylamidase negative and do not grow in broth with 6.5% NaCl. The viridians group is further sub-divided into the mutans, salivarius, anginosus, sanguinus and mitis groups, sometimes inaccurately referred to as the oral streptococci as they are found in other locations besides the oral cavity [reviewed in (1-2)]. *S. mutans*, a member of the mutans group, is not capable of hydrolyzing arginine, but produces acetoin, hydrolyzes esculin and can metabolize both mannitol and sorbitol. The species *S. mutans* is further divided into four serotypes; *c*, *e*, *f* and *k*, based on cell wall rhamnose-glucose polysaccharides. Most (70-80%) *S. mutans* strains isolated from the oral cavity are serotype *c*, while ~20% are type *e* and less than 5% are serotype *f* or *k.* Serotype *k* was only recently recognized, when it was isolated from blood of Japanese patients with bacteremia (3).

S. mutans is the bacterium most often associated with human dental caries (4-5). However, it has also been isolated from patients with infective endocarditis and atherosclerosis, and a serotype *f* strain has been shown to invade human coronary artery endothelial cells (6), indicating that certain serotypes of *S. mutans* may contribute

to cardiovascular disease. In an Immunology Nature review by Taubman et al., 2006, titled “The scientific and public-health imperative for a vaccine against dental caries”, the authors report that The World Oral Health Report of 2003 stated that 60-90% of school children and adults have experienced dental caries, declaring this infectious disease is a major health problem in industrialized countries (5). In the United States dental caries is the number one childhood disease, and is most prevalent in minority populations affecting ~20 million children from low-income families. In 2004 there was an estimated $75 billion spent on oral health care alone, accounting for ~5% of total healthcare costs in United States. As the consumption of refined sugars increases in developing countries, so does the incidence of dental caries and other diseases associated with poor oral health.

S. mutans possesses numerous virulence factors, both secreted and membrane associated that contribute to its disease causing properties and to its ability to contend with the harsh environment of the oral cavity, reviewed in (7). *S. mutans* forms biofilms and is able to attach to the tooth surface through sucrose-dependent and sucrose-independent mechanisms, both of which require the secretion of several proteins (4). The sucrose-dependent mechanisms involve the production of glucans (8), which allow for stable adherence to the tooth surface, while sucrose-independent adhesion involves the protein P1 (Antigen I/II, PAc) that binds to salivary agglutinin (gp340) on the pellicle of the tooth (9). *S. mutans* secretes three glucosyltransferase (GTF) proteins capable of synthesizing extracelluar glucan polymers. These polymers can be water-soluble with α-1,6 linkages of glucose synthesized by GtfD, or water-insoluble with branched α-1,3 linkages of glucose synthesized by GtfB and GtfC (8). The water insoluble glucan

polymers are known as mutans and are responsible for the formation of dental plaque (8). *S. mutans* also secretes four glucan binding proteins, GbpA, GbpB, GbpC, and GbpD, which are important for biofilm formation (8). Within the biofilm, *S. mutans* is able to transport and metabolize an enormous variety of carbohydrates, conferring much versatility and a competitive advantage over the other species of bacteria (10). It is through fermentation of carbohydrates resulting in production of organic acids that causes the erosion of tooth enamel, which is soluble between pH 5.4 to 4.4 (11). *S. mutans* is able to continue glycolysis at a pH of 4.4, which is beyond the pH of 4.8 where growth stops (12-13), further lowering the pH in plaque, inevitably dissolving the enamel, and inhibiting less acid tolerant species of bacteria. *S. mutans* is not only acidogenic; it is aciduric (acid tolerant) and is able to induce an acid tolerance response (ATR) after exposure to sublethal pH conditions. The ATR results in differential gene expression, up-regulation of stress proteins, increased H+-ATPase activity, and diversion of glycolytic metabolites to less acidic end products, ultimately allowing increased survival at what would normally be a lethal pH of 3.0 (14-16). While the glycolytic enzymes of *S. mutans* are slightly more acid resistant than other oral bacteria, it is the cytoplasmic membrane that plays the largest role in acid tolerance (13). In fact, the composition of lipids in the membrane is regulated in response to acid pH. In a study by Fozo et al. 2004, it was found that a *fabM* mutant, which is inhibited in its ability to produce unsaturated fatty acids, had a decreased ability to contend with low pH, decreased glycolytic capability, and distorted glucose PTS activity (17). This same group found that the lipid composition of the wild-type membrane rapidly changed from

short chain saturated membrane fatty acids at pH 7.0 to long-chained, monounsaturated fatty acids at pH 5.5 (18).

Despite the importance of the membrane to *S. mutans'* virulence, in comparison to *E. coli,* very little is known about the processes involved in its biogenesis or the secretion of proteins through it. The major aim of this study was to investigate the roles of two membrane associated chaperone-insertases, YidC1 and YidC2, in *S. mutans* membrane biogenesis.

Acid Tolerance

F_1F_o ATP synthase. *S. mutans* is a facultative anaerobe and does not contain a cytochrome oxidase system. Therefore, ATP production is facilitated primarily through substrate level phosphorylation during glycolysis and fermentation producing organic acids (lactate, acetate and formate), which separate into protons and their anionic forms effectively lowering the pH of the cell. The membranes of streptococci are permeable to protons, which can flow back into the cytoplasm and lower the internal pH, reviewed by Quivey et al., 2001 (19). The membrane potential or proton motive force (PMF) is maintained by pumping protons from the cytoplasm to outside the cell by the F_1F_o H^+ ATPase at the expense of ATP, as well as through the transport of metabolic end products coupled to proton extrusion (20). The F_1F_o ATPase is composed of two domains. The soluble F1 portion, found in the cytoplasm is made up of $\alpha_3\beta_3\gamma\delta\varepsilon$, which forms the catalytic domain responsible for the ATPase activity. The F_o integral membrane portion is composed of ab_2c_{10}, which forms the proton translocating channel (21). Together these subunits form a functional enzyme, which in *E. coli* utilizes the electrochemical gradient of the membrane to synthesize ATP. In *S. mutans* and other

facultative anaerobes the main function of this multi-subunit enzyme is to extrude protons through the hydrolysis of ATP. However, work by Sheng and Marquis et al. 2006, showed that the F-ATPase is also capable of brief synthase activity when starved cells are exposed to pH 3.0. This was theorized to provide ATP for concurrent proton extrusion (22). The F_1F_o ATPase is an important factor in the acid tolerance of *S. mutans*, with a pH optimum of 6.0, but nearly 75% maximal functional activity at pH 5.0 (23-24). Its expression is upregulated in response to low pH, thereby increasing this organisms' capacity to tolerate acid end products created through metabolism (12, 25). Work by Magalhaes, et al. 2005, characterized a P-type H^+ ATPase, which the authors propose to function in conjunction with the F_1F_o ATPase to extrude protons aiding in acid tolerance (26). In support of this hypothesis, a recent microarray study found the gene *pacL* encoding a cation transporting P-type ATPase, was upregulated fourfold during acid adaptation in *S. mutans* (27). The same study demonstrated upregulation of the F-ATPase operon by about threefold. The role of this P-type ATPase in acid tolerance needs further exploration.

Assembly of the F_1F_o ATPase has been investigated in *E. coli*. These studies have revealed that insertion of the F_o membrane components of F_1F_o ATP synthase requires several pathways. Insertion of subunit "b", which contains one transmembrane domain with its N-terminus located within the membrane, requires the signal recognition particle (SRP) pathway, the SecYEG translocon and the aid of YidC for insertion (28). Similarly, subunit "a", which contains five transmembrane segments, also requires the SRP, SecYEG translocon and YidC for insertion (28-29). In contrast to the "a" and "b" subunits, subunit "c" , which contains two transmembrane domains with its N and C

termini located in the periplasm, is inserted solely by the YidC only pathway in *E. coli* (30). In *S. mutans*, it is unknown which proteins mediate the insertion of the F_1F_o ATPase, however previous research from the Brady group showed a decrease in membrane associated ATPase activity in mutants of the SRP pathway, and the Δ*yidC2* mutant (31). This will be discussed in more detail below.

Carbohydrate utilization and diversion of glycolytic metabolites. *S. mutans*, and other lactic acid bacteria in the oral cavity, have many methods for dealing with the constantly changing nutrient availability found in the oral biofilm. For example, *S. mutans* has two different mechanisms for transporting carbohydrates, including ABC transporters and phosphoenolpyruvate- phosphotransferase systems (PEP-PTS). There are four possible ABC transporters involved with sugar transport, including the MSM (multiple-sugar metabolism) transporter, which transports sugars at the expense of ATP (32). Some ABC transporters consist of two membrane permeases, two membrane associated ATPases, and a solute binding protein located on the outside of the membrane. The other way carbohydrates are transported is through sugar specific phosphoenolpyruvate-sugar- phosphotransferase systems (PEP-PTS), where sugars are transported and phosphorylated by the sugar specific EII permease. *S. mutans* is predicted to have 14 PTS systems, five of which are constitutively expressed and capable of transporting glucose, fructose, maltose and sucrose at all times (32). There are also additional genes for PTS systems for transport of lactose, fructose, mannose, cellobiose, trehalose, β-glucosides, mannitol, sorbitol, ribulose and sorbose/mannose. Each PTS system is composed of two components, the EI component, which is common to all PTS systems, and the sugar specific EII component, generally composed

of domains A, B, and C (33). Domains EIIA and B are phosphorylated and in turn transfer the phosphate to the incoming sugar, which is transported by the membrane integral EIIC domain (33). The phosphocarrier protein HPr and enzyme EI facilitate the transfer of the phosphate from phosphoenolpyruvate (PEP) to the EIIAB components of the PTS systems. HPr has two phosphorylation sites, at His-15 and Ser-46 (34). Enzyme EI is responsible for phosphorylation of HPr-His-P, while HPr kinase/phosphatase is responsible for phosphorylation/dephosphorylation of HPr at Ser-46. HPr-Ser-P is a major component of carbon catabolite repression (CCR) in *S. mutans* and through the regulation of HPr kinase/phosphatase activity, allows for use of preferred carbohydrates over less desired ones, thus maximizing the energy production within the cell. Mechanisms by which *S. mutans* regulates CCR are not completely understood and probably have unique components that vary depending on the genes or pathways being regulated (35). However, the ability of *S. mutans* to perform this regulation over carbohydrate utilization is likely critical to its virulence, just as efficient energy production is important for proton extrusion. Furthermore, there is a clear association of membrane biogenesis in the process of sugar transport.

Once a sugar is transported into the cell and phosphorylated, it enters the glycolytic pathway and through substrate level phosphorylation, it is metabolized ultimately producing ATP and pyruvate. Pyruvate metabolism is a key branch point in the cell (36). Pyruvate can be used in fermentation reactions, where it is converted to lactate by lactate dehydrogenase (producing NAD+ from NADH), which restores the redox balance of the cell. Alternatively it goes the way of pyruvate formate lyase (PFL), which results in formate, ethanol, and acetate, producing an additional ATP through the

production of formate. The redox balance is also preserved in this set of reactions by bifunctional acetaldehyde Co-A/alcohol dehydrogenase, which oxidizes two NADH to two NAD+ for every pyruvate processed. When sugar concentrations are high, pyruvate is directed to the lactate branch through activation of lactate dehydrogenase by fructose-1, 6- bisphosphate. This acts as a “lactate gate”, preventing the buildup of toxic intermediates while maintaining the redox balance of the cell (20). The PFL branch is only active during anaerobic conditions as PFL is deactivated by oxygen. An alternative branch, which is implicated in acid tolerance, is oxidation of pyruvate by pyruvate dehydrogenase forming acetyl-CoA and CO_2 (36). Acetyl-CoA can be further processed by bifunctional acetaldehyde Co-A/alcohol dehydrogenase resulting in ethanol, or by acetate kinase producing acetate (36-37). Formate, with a pKa of 3.77, is the most acidic end product of *S. mutans* fermentation, compared to lactate (pKa of 3.86) and acetate (pKa of 4.76). By regulating the enzymes involved in fermentation, *S. mutans* can control acid production. In a two dimensional proteomics study by Len, et al. 2004, comparing *S. mutans* grown in continuous culture at pH 5.0 compared to pH 7.0, changes were limited to three key biochemical pathways involved with acid adaptation; glycolysis, acid production, and branched chain amino acid synthesis (14). These authors concluded that *S. mutans* diverts glycolysis toward less acidic end products such as lactate and ethanol, and diverts pyruvate to branch chained amino acid synthesis. Branch chained amino acid biosynthesis combats low pH by consuming the reducing equivalents pyruvate, 2-oxobutanoate, and NADPH, in effect preventing them from being used in pathways that produce acid. Additionally the production of

branch chained amino acids results in NH_3, which reacts with H+ to form NH_4^+, effectively increasing the internal pH of the cell (14-15).

Two-component systems and acid tolerance. Unlike *Escherichia coli* and *Bacillus subtilis*, which contain a large number of alternative sigma factors that regulate gene expression in response to stress, *S. mutans* only contains two, σ^{70} and σ^{x} (7). Consequently, two-component signal transduction systems (TCS or TCSTS) are very important for sensing environmental signals and enacting stress tolerance in *S. mutans*. All bacteria encode genes for two-component systems, reviewed in (38). In general, they contain a membrane bound sensor histidine kinase (HK) that senses a signal resulting in auto-phosphorylation followed by transfer of the phosphate to a soluble cytoplasmic response regulator (RR). This changs the conformation of the RR, which then positively or negatively regulates transcription of a target gene (38). The *S. mutans* genome is predicted to encode as many as fourteen TCSs depending on the strain, that affect expression of virulence factors, biofilm formation, competence development, stress tolerance and bacteriocin production (7, 39). A whole genome transcriptional analysis of *S. mutans* in response to acid adaptation identified a number of TCSs as being upregulated in response to pH 5.5 conditions. These included CiaHR, LevSR, LiaSR, ScnKR, Hk1037/Rr1038, and ComDE (27). Another study showed that VicK of the VicR/K TCS, is also involved in acid tolerance in *S. mutans* (40). Many of these TCSs overlap in stress response pathways, and it is believed there is cross-talk between the different TCSs (41-42). A recent study by Banu et. al. 2010, showed *pknB* and *pppL*, which encode a serine/threonine kinase and phosphatase respectively, are capable of affecting pathways regulated by the VicRK and ComDE TCSs (43). The

LiaSR is a TCS involved with adaptation to cell envelop stress, with an intramembrane-sensing histidine kinase that responds to cell wall envelope damage rather than a stress signal (44). A study by Senadheera et al. 2009, found that SMU.1727 (*yidC2*), has a CesR/LiaR binding motif upstream of its promoter and is induced under conditions of envelope stress, brought on by the lipid II cycle inhibitor bacitracin (45). Other lipid II cycle inhibitors, such as vancomycin and nisin, also induce the LiaSR TCS, activating genes involved in cell wall peptidoglycan synthesis and membrane protein biosynthesis. Using qrt-PCR a number of other proteins involved with membrane biogenesis were also identified as targets including; *ftsY*, *ropA* (trigger factor), *ftsH* and *degP* (*htrA*). Also, a hypothetical membrane protein (SMU.753) containing a PspC (phage shock protein C) domain, was up-regulated tenfold during envelop stress conditions.

Secretion and Membrane Protein Biogenesis

Escherichia coli. The bacterial general secretion pathway and membrane protein insertion has been most extensively studied in *E. coli*. Development of techniques to purify membrane proteins involved in secretion and their reconstitution into *in vitro* systems of proteoliposomes, have allowed researchers to reconstruct and evaluate minimum requirements for translocation of model substrates. Also, development of conditional expression systems of essential components has allowed researchers to evaluate roles of individual components in the secretion process *in vivo*. Through this work a model of protein secretion has been developed for *E. coli,* and recently reviewed in (46-48). Targeting begins at the ribosome for proteins destined for secretion or membrane insertion. Secreted proteins contain an amino-terminal signal sequence composed of a positively charged amino (-N) domain, a hydrophobic (-H) domain and polar carboxy-terminal (-C) domain, which is recognized by trigger factor, a chaperone

with peptidyl-prolyl *cis-trans* isomerase activity (49). Both trigger factor and the signal recognition particle (SRP) bind to ribosomal protein L23 and compete for binding to signal sequences of nascent polypeptide chains as they exit the ribosome (50). Membrane proteins contain an N-terminal signal anchor sequence that is highly hydrophobic and is preferentially bound by the SRP and targeted for co-translational translocation. Alternatively, proteins recognized by trigger factor are bound by the SecB chaperone and targeted post-translationally to the SecA molecular motor ATPase protein, which is associated with the SecYEG translocon and facilitates the translocation of secretory proteins through the membrane. As the pre-protein is secreted the signal sequence is cleaved by signal peptidase, resulting in a mature protein. In *E. coli*, the essential, universally-conserved SRP pathway is composed of Ffh, 4.5S scRNA (114 nt) and the FtsY receptor. The eukaryotic SRP pathway, which targets proteins to the Sec61αβγ complex in the endoplasmic reticulum, is more complicated with additional proteins associated with the particle. However, it does have SRP54 (Ffh homolog), a 7S RNA and a receptor composed of α/β-SR, of which the α-SR subunit is homologous to FtsY (46). Ffh and the scRNA (small cytoplasmic RNA) form a complex, which recognizes hydrophobic signal sequences of nascent polypeptide chains as they exit the ribosome and targets the ribosome-nascent chain (RNC) to the membrane receptor FtsY. Both Ffh and FtsY are GTPases, and upon binding to one another undergo a conformational change, resulting in binding subsequent hydrolysis of GTP. This allows the SRP particle to transfer the RNC to the SecYEG translocon pore, where the membrane protein is inserted co-translationally. SecY and SecE are essential in *E. coli* and are homologous to the eukaryotic Sec61α and γ proteins. SecYEG associates with

a number of accessory proteins including SecDF(YajC) and YidC. SecDF(YajC) are believed to aid in protein translocation and may regulate the cycling of SecA during translocation (51). SecA is required for insertion of membrane proteins with large hydrophilic segments. Mutants in SecD and F exhibit a cold sensitive phenotype, and deletions of SecDF results in extremely slow growth with defects in protein secretion (52-53). The YidC protein functions in both Sec-dependent and Sec-independent pathways and will be discussed in greater detail below.

Gram-positive bacteria. *B. subtilis* has been used as the model organism for secretion studies in gram-positive bacteria; however most studies have focused on secretion, with little work done on membrane biogenesis. Similar to *E. coli*, *B. subtilis* has homologs for SecYEG, SecA and SecDF(YajC), as well as the SRP pathway. However, there is no SecB homolog, and SecDF is one protein (54) instead of two separate ones as in gram-negative species. In *B. subtilis*, SecDF mutants exhibit a cold sensitive phenotype and a diminished capacity to secrete proteins in high volume (55). SecDF is absent from the Streptococci, but is found in Staphylococci, while YajC seems to be universally conserved in gram-positive bacteria. The SecE protein of *B. subtilis* and other gram-positive bacteria are smaller than the *E. coli* SecE and contain only one TMD where the *E. coli* SecE has three TMDs. However, only the C-terminal TMD and cytoplasmic domain are essential for SecE function in *E. coli* (56). This region is conserved in the SecE proteins from gram-positive bacteria (46). SecG is non-essential in *B. subtilis*, but deletion results in secretion defects and cold sensitivity. Another difference from *E. coli* is that the SRP of *B. subtilis* contains an additional protein, HBsu, with non-specific DNA binding activity. The *B. subtilis* scRNA is 270 nucleotides with an

Alu domain that is also found in scRNA's of *Clostridium perfringens*, and *Listeria monocytogenium* (55, 57), but not *S. mutans* (31). The SRP pathway is essential for growth in *B. subtilis*, and depletion of Ffh results in an altered cell morphology and a defect in protein secretion (58). The contribution of the SRP to protein secretion in *E. coli* is less apparent. When hybrid SecYEG translocons from *E. coli* and *B. subtilis* were evaluated for translocation in an *E. coli* background, SecA from *B. subtilis* bound with low affinity to SecYEG compared to SecA from *E. coli*, regardless of the source of SecYEG (59). Additionally this study found that while hybrid translocons were stable, they were inefficient at protein translocation.

A surprising finding in *S. mutans* was that the SRP pathway is dispensable for viability (60-61). Mutants in Ffh, scRNA or FtsY are, however, impaired in environmental stress tolerance (31). The SRP pathway is also dispensable in *S. pyogenes* where it is required for virulence (62). The ability of streptococci to survive without an SRP pathway is likely related to the presence of two yidC homologs, one with a longer positively-charged C-terminal tail, which will be discussed below.

A number of gram-positive species have accessory Sec proteins dedicated to secretion of a subset of proteins often involved with virulence (63). In some species of Streptococcus (*S. gordonii*, *S. pneumoniae*, *S. parasanguinis)*, Staphylococcus (*S. aureus*, *S. hemolyticus*, *S. epidemidis*), and Bacillus (*B. cereus*, *B. anthracis*, *B. thuringiensis*) the accessory Sec system includes accessory SecA2 and SecY2 proteins, which function separately from the canonical SecA and SecY proteins of the general secretion pathway. The accessory Sec locus of *S. gordonii* is located downstream of its substrate GspB, a large serine-rich cell surface glycoprotein that

binds platelets (64). Located in the same locus are several other genes required for GspB's secretion and function. These include two proteins with homology to SecE and SecG, and proteins needed for the glycosylation of GspB, which is required for its function (65). There is a similar gene organization in the accessory Sec locus in *S. parasanguinis*, with surface protein Fap1, followed by the accessory SecA2/Y2 genes and genes required for glycosylation of Fap1 (66). This is also true for *S. aureus*, *S. epidermidis*, *S. agalactiae* and *S. pneumoniae*, of which all encode serine-rich repeat (Srr) proteins involved with adhesion (66). A number of other gram-positive species, Mycobacterium, Listeria, and Corynebacterium, encode only a SecA2 gene, and there is no conservation in the gene locus of these species (63).

Another interesting finding in the Streptococci was the discovery by the Caparon group of the Exportal in *S. pyogenes*, a micro-domain containing SecA and dedicated to secretion (67-68). A similar micro-domain was identified in *S. mutans*, with SecA and Sortase A found to co-localize at a distinct site in the membrane (69). However, another group using a similar technique, found SecA to be distributed throughout the cell in *S. pyogenes* (70). An Exportal has not been identified in Bacillus, where the Sec translocon is found in several locations in a spiral arrangement along the cell (71).

It is clear there are differences in protein secretion pathways and membrane biogenesis among bacterial species. Gram-negative bacteria contain two cell membranes, with a periplasmic compartment in between, while gram-positive bacteria contain one membrane, but have a thick peptidoglycan cell wall. Much work remains to be done in gram-positive bacteria with regard to protein secretion mechanisms, including the Streptococci. It is possible there are as yet unidentified accessory proteins

or pathways involved in protein secretion and membrane biogenesis in this important genus of bacteria.

Stress Response and Membrane Biogenesis in *S. mutans*

Co-translational signal recognition particle pathway. Previously it was believed the SRP pathway was essential for viability in all cells, including bacteria (58, 72). However, a search for genes involved in acid tolerance in *S. mutans* using transposon mutagenesis yielded a mutant with a disruption of *ffh* (60). It was later demonstrated that an acid-adapted isogenic mutant of *ffh* had decreased membrane-associated ATPase activity, while the ATPase activity of permeabilized whole cells was unaffected when compared to the wild type, suggesting a defect in the assembly at the membrane in these mutants (73-74). Later it was confirmed that elimination of the entire SRP pathway of *S. mutans* is not lethal, but results in an inability to tolerate environmental stresses (acid, osmotic and oxidative), decreased biofilm formation, and loss of natural competence (31, 75). To investigate the involvement of the SRP pathway in acid tolerance, 2D-gel electrophoresis of membrane proteins was performed using cells of SRP mutants grown at pH 7.0 or pH 5.0 and compared to the wild-type cells grown under the same conditions. Results showed an increase in the molecular chaperones DnaK, GroES and the ClpP protease, as well as a decrease in a number of metabolic enzymes. The β-subunit of the F_1F_o ATPase was also decreased in the Ffh membrane preparations. Transcriptome analysis was also performed comparing the Ffh mutant and wildtype under non-stress conditions. Results were consistent with a global stress response, showing an increase in molecular chaperones and proteases, most likely caused by defects in membrane protein biogenesis (75). There was also an increase in genes involved with detoxification, including a number of oxidoreductases.

Consistent with the decrease in competence and aberrant biofilm formation seen in the *ffh* mutant, there were a number of genes downregulated in the competence pathway (75-76).

Since the SRP co-translational pathway is essential in other bacteria, there must be another mechanism for co-translational translocation in *S. mutans*. In mitochondria co-translational translocation is mediated by Oxa1, which is able to bind mitochondrial ribosomes by way of its positively charged C-terminal tail. Analysis of the *S. mutans* genome revealed there are two homologs of the YidC/Oxa1/Alb3 family, YidC1 and YidC2. Elimination of *yidC2* results in a stress-sensitive phenotype similar to the SRP pathway mutants, with growth impairment under acid, osmotic and oxidative stress conditions, decreased membrane associated ATPase activity, decreased genetic competence, and impaired biofilm formation (31). Disruption of *yidC1* has a much less severe effect, with no obvious growth defects or stress sensitivity. The *yidC1* mutant does however, display aberrant biofilm formation. Attempts to isolate double mutants in the SRP pathway and YidC2 have not been possible. Nor is it possible to eliminate both YidC1 and YidC2 simultaneously, suggesting functional redundancies in the SRP and YidC2 pathways, as well as between YidC1 and YidC2 in *S. mutans*.

YidC/Oxa1Alb3 Family of Proteins

The Oxa1/YidC/Alb3 family of proteins is universally conserved in all three domains of life (77). Oxa1 of the inner mitochondrial membrane, YidC in the bacterial cytoplasmic membrane, and Alb3 in the thylakoid membrane of chloroplasts, all possess conserved functions in insertion of respiratory chain complexes, such as the cytochrome oxidase systems, F_1F_o ATP synthases, and light-harvesting chlorophyll binding proteins in plants (78-80). There are common structural features among this

family of proteins, with the highest sequence conservation in the 5 C-terminal transmembrane domains (81). Experiments have shown cross-species complementation is possible among family members, indicating vestigial functions still remain.

Oxa1 of mitochondria. The mitochondrial YidC homolog, Oxa1, is located in the inner mitochondrial membrane and is the founding member of the Oxa1/YidC/Alb3 family of proteins. Oxa1 was discovered in a yeast mutant that lacked critical components of the cytochrome c oxidase complex and was respiration deficient, hence the name Oxa for oxidase assembly (82). Because of its highly basic C-terminal tail, which has been shown to interact with mitochondrial ribosomes, Oxa1 is capable of co-translational insertion of mitochondrial-encoded proteins. There are no SRP or SecYEG homologs in the mitochondrial inner membrane. Instead these functions are filled by Oxa1, which is also capable of post-translational insertion of nuclear-encoded proteins that are first imported into the matrix through the TOM (translocon of outer membrane) and TIM (translocon of inner membrane) complexes located in the outer and inner membranes of the mitochondria (83-85). Oxa1 is involved with the insertion of subunit 9 (homologus to subunit "c" *of E. coli*) of the F_1F_o-ATPase, CoxII of the cytochrome oxidase complex, and Oxa1 itself in *Saccharomyces cerevisiae* (84). *S. cerevisiae* contains another Oxa homolog, Cox18/Oxa2, which is also involved with cytochrome oxidase assembly (86). It is now apparent, through the work of Funes et al. (87), that Cox18/Oxa2 makes up a second branch of the Oxa1/YidC/Alb3 family, specifically involved with the biogenesis of the cytochrome *c* oxidase complex, whereas Oxa1 probably functions in a more general way for insertion of inner membrane proteins (87-

88). Oxa1 and Oxa2/Cox18 are universally conserved in mitochondria of plants, fungi, and animals and have been shown to function to varying extents in heterologous species (87-88).

YidC of *E. coli*. The YidC protein was discovered in *E. coli* when proteins that were previously thought to insert spontaneously were impaired in insertion in a y*idC* depletion strain (89). YidC from *E. coli* contains six transmembrane segments (TMs) and a large periplasmic loop between TM1 and TM2. This topology is common among YidC proteins of gram-negative bacteria. While the five C-terminal transmembrane domains are highly conserved, the periplasmic loop is variable in both length and sequence (90). The first transmembrane domain of YidC serves as an un-cleaved signal anchor and is not vital for function (91). Nor is the periplasmic loop, which even with a deletion from amino-acid 25-323, does not affect YidC function (91). Purified YidC has been shown to form both monomers and dimers (92). Furthermore, YidC has both sec-dependent and sec-independent functions. Consistent with this finding, YidC is expressed in excess of the SecYE translocon, with 2,700 copies per cell compared to 100-200, respectively (93). It has been shown that insertion of YidC itself requires the SRP, SecA and SecYEG-YidC pathways (93).

YidC is essential in *E. coli*, and the generation of a *yidC* depletion strain, JS7131 where expression of YidC was placed under the control of the AraBAD promoter, has made many functional studies of YidC possible (89). A number of YidC substrates have been identified, leading to a better understanding of YidC function. CyoA of the cytochrome *bo3*, requires both SecYEG and YidC for proper insertion (94), while subunit “c” of the F_1F_o ATPase, M13 and pf3 phage coat proteins are substrates of the

YidC only pathway (95-96). MscL, the mechanosensitive channel of large conductance, was shown to require both the SRP and YidC for proper membrane insertion, but did not need SecYEG, suggesting the SRP may target proteins to YidC for insertion (97-98). There is also evidence for YidC as a chaperone involved in the assembly of polytopic membrane proteins, such as MalF (99), LacY (100) and MltA (101). Based on these experiments it is postulated that YidC is involved with release of transmembrane domains from the translocon and possibly in the assembly of multimeric protein complexes.

Alb3 of chloroplasts. In chloroplasts of *Arabidopsis thaliana*, Alb3 is essential for viability (102). It is involved with the biogenesis and insertion of the LHCP (light harvesting chlorophyll binding proteins) complex and was first discovered in chloroplasts with an albino phenotype (102-103). Work by Gerdes et al. (104), showed the existence of a second YidC/Oxa1/Alb3 homolog in *Arabidopsis thaliana* termed Alb4 located in the thylakoid membrane (104). However, since only Alb3 is essential, the two homologs must have somewhat different functions. There are also two homologs in the unicellular algae *Chlamydomonas reinhardtii*, termed Alb3.1 and Alb3.2, with Alb3.2 being essential for viability (105). Mutations in Alb3.1 indicate that it functions in the insertion of LHC proteins, where reduction of Alb3.2 through RNAi indicate it's involved more specifically with photosystems I (PS1) and II (PSII) assembly, with little effect on LHC proteins. The thylakoid membrane is different from the mitochondrial inner membrane where Oxa1 and Oxa2 are located. The thylakoid membrane of chloroplast contain homologs of SecA, SecY and SecE, as well as an SRP pathway, reviewed in (106). Additionally, thylakoids possess a Tat pathway for transport of a subset of

proteins including folded proteins that is homologous to the bacterial Tat system (107). In chloroplasts, the cpSRP is involved in both a co-translational pathway that targets proteins to the cpSecYE complex (108), and a post-translational pathway that targets to the Alb3 translocase. The cpSRP is composed of the conserved cpSRP54 (Ffh homolog) and cpFtsY receptor. It differs from other SRP pathways in that it does not contain an RNA component, and has an additional unique protein component, cpSRP43 that is necessary for post-translational targeting of cpSRP substrates to Alb3. Recent work has shown that the C-terminal tail of Alb3 is involved with targeting of the cpSRP to the thylokoid membrane and cpFtsY, through an interaction with cpSRP43 (109-110). Alb4 also has a long C-terminal tail with similarities to that Alb3, but does not interact with cpSRP43, and instead is proposed to react with SecYE or with ribosomes (110). There is also evidence that Alb3 forms stable complexes with the cpSecYE complex (111). The Alb4 protein was shown to be involved in assembly of CF_1- CF_o ATPase, by stabilizing the interaction between the CF_1 to the CF_0 (112). Alb3 was not involved in this process.

YidC1 and YidC2 in gram-positive bacteria. While gram-negative bacteria have only one YidC, many gram-positive bacteria contain two genes encoding proteins of the Oxa1/YidC/Alb3 family (77). However, not all gram-positive bacteria encode two homologs. For example, *Staphylococcus aureus* encodes only one YidC, while the other Bacillales encode two. In general, gram-positive species in the order of Lactobacillales have two YidC homologs and one is usually shorter than the other by roughly 35 amino acids (81). Such is the case for *S. mutans*, with YidC1 containing 271 amino acids and YidC2 containing 310, with the main difference being in the length of

the C-terminal tails. Many gram-positive homologs are predicted to be lipoproteins that are processed by signal peptidase II (113). Based on a common location within the genome, it appears that *yidC1* is more closely related to *spoIIIj* from *B. subtilis* and *yidC* from *E. coli*, which are all located downstream from *rpnA*, the gene encoding ribonuclease P. In gram-positive species this locus also contains an RNA binding protein of the Jag family located downstream from the *yidC1* gene. This gene arrangement is conserved among the Streptococci and *B. subtillis.* In *S. mutans*, *yidC1* appears to be located in an operon with Ribonuclease P and the Jag RNA binding protein, while the *E. coli yidC* in not in an operon (80). The location of the YidC2 homologs is conserved in the Streptococci, with the gene for acyl phosphatase (*acp*) upstream from *yidC2*. However this arrangement in not observed for *yqjG*, the second YidC homolog of *B. subtilis.* When comparing the conserved five C-terminal transmembrane domains of the YidC/Oxa1Alb3 family using PSI-BLAST there is roughly 20 to 30% sequence identity and approximately 40 to 50% similarity between the homologs. There is a higher level of homology between closely related species. For example the sequence similarity between the *S. mutans* YidC proteins and those from *S. pyogenes*, is 64% identity and 79% similarity between YidC1 and Spy1 (275 a.a.), and 58% identity and 75% similarity between YidC2 and Spy2 (307 a.a.). When comparing the sequence of *S. mutans* YidC1 to that of YidC2, there is only 30% identity and 50% similarity between them suggesting an early gene duplication event and evolution of two separate proteins.

There is relatively little in the literature about the YidC proteins from gram-positive species compared to *E. coli* YidC. Most of the studies so far have involved the *B.*

subtilis homologs, SpoIIIj and YqjG, and the two paralogs from *S. mutans*, YidC1 and YidC2.

B. subtilis. SpoIIIJ and YqjG do not display the same differential in length between them as seen for streptococcal homologs, SpoIIIJ contains 261 amino acids and YqjG, 275 amino acids (81). SpoIIIJ was first identified as a protein essential for spore formation, while YqjG is not required for this process (114). Elimination of one or the other has very little affect on normal vegetative growth but at least one of these two proteins must be present for *B. subtilis* to grow, suggesting that overlap sustainably in function (114-115). It was also shown that SpoIIIJ and YqjG function in post-translocational folding of secreted proteins (115), which is a somewhat novel function, since in *E. coli* elimination of *yidC* has only a minor affect on secreted proteins (89). Recent work by Saller et al., 2009, found that YqjG and SpoIIIj are involved in membrane biogenesis. When over-expressed in *B. subtilis* or in *E. coli*, both co-puried with the entire F_1F_o ATPase (116). This study also showed that either SpoIIIJ or YqjG could functionally complement a *yidC* depletion strain in *E. coli*. Another study by Saller et al. 2011, showed that YqjG is involved in genetic competence development in *B. subtilis*, and through a conditional expression system showed that when *spolllj* is depleted in a Δ*yqjG* strain, the LiaSR envelope stress response is induced (117). YqjG is only expressed when SpoIIIJ is absent (118), and work by Chiba et al. 2009, showed the presence of a cis-acting ribosome-nascent chain sensor, MifM/YqzJ located directly upstream from YqjG/YidC2, that allows transcription of YqjG in the absence of SpoIIIJ (119). This regulation is similar to the SecM system that is activated in response to a secretion defect, resulting in increased SecA levels (120).

***S. mutans* YidC1 and YidC2**. Most of the available information regarding YidC1 and YidC2 has come from research from the Brady Lab and those of our collaborators. As mentioned above, elimination of *yidC2* results in a similar stress-sensitive phenotype as the SRP mutants, with an inability to grow when confronted with acid, salt or oxidative stress (31). The *yidC2* mutant also displays a pronounced lack of genetic competence, and a defect in biofilm formation (31). A C-terminal deletion mutant of YidC2 displays an intermediate stress-sensitive phenotype with a minor decrease in growth rate during non-stress conditions and a more pronounced affect under acid- and salt-stress conditions. Elimination of *yidC1* has almost no influence on growth, stress tolerance or genetic competence, but does affect biofilm formation under conditions of acid stress (unpublished data). Additionally, elimination of *yidC1* or *yidC2* affects surface adhesin P1, but in different ways (unpublished data, J. Brady and P. Crowley). In the *yidC2* mutant, the maturation of P1 is affected, as evidenced by reduced immunoreactivity of certain, but not all, monoclonal antibodies that recognize epitopes important for the function of P1 (121). This conclusion was supported by the fact that cells from the *yidC2* mutant exhibit substantially less binding to salivary agglutinin, as measured by whole cell BIAcore surface plasmon resonance assay (122). Disruption of *yidC1* resulted in increased immunoreactivity by all monoclonal antibodies and polyclonal antiserum against P1, and increased binding of whole cells to salivary agglutinin. This suggests either there is more P1 on the surface of the *yidC1* mutant, or less of other proteins resulting in increased exposure of P1 to the antibodies. Cross-species complementation studies between *S. mutans* and *Saccharomyces cerevisiae* revealed that YidC2 could mediate co-translational translocation in an Oxa1 mutant

(123). This ability was dependent on the presence of YidC2 protein's C-terminal tail. The ability of YidC1 to substitute for Oxa1 could not be assessed since it was not properly inserted into the mitochondrial membrane. Additionally, it was shown that like Oxa1, full-length YidC2 interacts with yeast ribosomes. When the reverse experiment was done, both yeast homologs Oxa1 and Cox18 were able to restore growth to a *S. mutans ΔyidC2* mutant under stress conditions, with Oxa1 showing better growth restoration than Cox18. Additionally, Oxa1, but not Cox18, fully restored membrane associated ATPase activity and partially restored genetic competence to a *ΔyidC2* mutant. This is consistent with the fact that *S. mutans* ATPase activity is similarly diminished in the *yidC2* C-terminal deletion mutant as it is in the complete *yidC2* mutant strain, indicating that the C-terminal tail is important for ATPase assembly. The C-terminal tail of Cox18/Oxa2 is shorter than that of Oxa1, and was not able to function in either of these capacities. On the other hand, genetic competence is severely affected by a complete deletion of *yidC2* and only partially by elimination of the YidC2 C-terminal tail. Therefore, there are functions of YidC2 that do and do not rely on the C-terminal tail, thus explaining the partial complementation of genetic competence by Oxa1.

Recent work by Suntharalingam et al. 2009, found that the promoter region of *S. mutans yidC2* contains a consensus binding site for LiaR, of the LiaSR two-component system involved with sensing envelop stress signals (45). They showed using qRT-PCR that *yidC2* expression is up-regulated threefold by LiaSR during the envelope stress response (induced by exposure to bacitracin). This may be homologous to the phage shock response in *E. coli* that is turned on during YidC depletion (124). Recent

findings by Saller et al. 2011 (117) discussed above, found induction of the LiaSR system in *B. subtillis* upon depletion of both SpoIIIJ and YqjG (117).

YidC1 and YidC2 from *S. mutans* are predicted to be lipoproteins processed by SPaseII, based on the presence of a consensus sequence in their signal peptides. Within the lipoprotein processing signal of the *yidC1* gene from *Enterococcus faecalis*, is a pheromone peptide involved in induction of conjugative transfer of a pheromone inducible plasmid pCF10, which encodes antibiotic resistance genes (125). This sequence is not present in the signal sequence of either *yidC1* or *yidC2* from *S. mutans*.

Summary and Specific Aims

Streptococcus mutans is an important pathogen affecting 90% of the world population. Dental cavities are so ubiquitous affecting nearly everyone at some point in their life, that many don't realize it is a preventable infectious disease. In areas of low socioeconomic status, many people cannot afford to see a dentist, and in extreme cases this disease can progress to a point where all teeth are lost or can result in systemic infections (5). Billions of dollars are spent each year in the United States alone on the treatment of tooth decay, largely the result of the acidogenic and aciduric properties of *S. mutans*. In this study, two *S. mutans* membrane proteins, YidC1 and YidC2, of the universally conserved YidC/Oxa1/Alb3 family of chaperone-insertases, were investigated. The information gained from this research could potentially be applied to other Streptococci, leading to a greater understanding of the mechanisms of pathogenesis that involve integral membrane and secreted proteins. This could ultimately result in more successful treatments and potentially prevention of this medically important genus.

Specific Aim 1: Develop Tools to Examine Compensatory or Redundant Functions in Membrane Biogenesis of *S. mutans.*

S. mutans appears to have overlapping functions between the SRP co-translational translocation pathway and YidC2. It is not yet understood why there are two YidC homologs in gram-positive bacteria. This aim strives to demonstrate that the two YidC proteins have separate distinct functions. For this purpose a conditional expression system was developed, whereby y*idC2* was placed under the control of an inducible promoter and the *yidC1* gene was eliminated. Also two chimeric proteins were made to investigate functional differences in the C-terminal domains of YidC1 and YidC2, and their respective roles in stress tolerance. Also a number of synthetic peptides were designed and used to produce antisera against YidC1, YidC2 and SecY.

Specific Aim 2: Evaluation of YidC1 and YidC2's Involvement in the Assembly of the F_1F_o ATP Synthase.

Acid tolerance has been largely attributed to the activity of the proton translocating F_1F_o ATPase in *S. mutans*. Previous work in the Brady lab found that *ffh* and *yidC2* mutants are sensitive to acid, oxidative and osmotic environmental stress (31). Also, it was found that these mutants had decreased membrane associated ATPase activity, although the *yidC1* mutant did not. Studies presented here will show that both *yidC1* and *yidC2* can function to insert the F_1F_o ATPase in *E. coli* and that deletion of *yidC1* in *S. mutans* can also result in decreased membrane associated ATPase activity. This suggests that the acid sensitive phenotype of the *ffh* and *yidC2* mutants is not entirely due to decreased F_1F_o ATPase activity.

Specific Aim 3: Determine Differences in Membrane Protein Complexes between Wildtype and Δ*yidC1* and Δ*yidC2* Mutants using Blue Native Polyacrylamide Gel Electrophoresis.

Membrane proteins play a critical role in stress tolerance and environmental adaptation in *S. mutans*. This organism can survive a wide range of environmental conditions, and challenges in part by employing TCS transduction systems that result in differential gene expression, changes in cell wall biogenesis, and metabolic pathways. Clearly, many of these processes take place at the membrane. This specific aim will address the difference in membrane protein complex composition between wildtype and *yidC* mutants of *S. mutans* using Blue-Native polyacrylamide gel electrophoresis. This method allows the separation of membrane protein complexes under non-denaturing conditions, so that differences between wildtype and mutant membranes can be analyzed by LC-MS/MS (liquid chromatography-mass spectrometry/mass spectrometry).. This technique was also combined with 2-dimensional SDS-PAGE and Western blot to locate protein complexes containing YidC1, YidC2 and SecY, whose associations within the translocation machinery are poorly understood in *S. mutans*.

CHAPTER 2
DEVELOP TOOLS TO EXAMINE COMPENSATORY OR REDUNDANT FUNCTIONS IN MEMBRANE BIOGENESIS OF *Streptococcus mutans*

Rationale for Study

A major difference between YidC1 and YidC2 is the length of their C-terminal tails. YidC2 has a longer more positively charged tail than YidC1 (Figure 2-1). To evaluate the functions of these tails chimeric proteins were constructed between YidC1 and YidC2 whereby the C-terminal domains were swapped (Figure 2-2). These proteins were then evaluated for their ability to restore acid and osmotic stress tolerance to a *yidC2* mutant by growth curve analysis in broth. The chimeric proteins were also evaluated for the ability to grow under acid-stress conditions on solid media.

The extensive understanding of gene regulation in *E. coli* has made many conditional expression systems possible and has enabled studies of many essential proteins. The available systems include inducible promoters (*tetA*, *trp* and T7) that allow over-expression of proteins, facilitating their purification. Other systems provide for tight regulation (araBAD promoter), enabling essential proteins to be depleted slowly, so that their effects can be studied [reviewed in (126)]. The arabinose inducible/glucose repressible promoter araBAD, was used in *E. coli* to conditionally express *yidC* in strain JS7131 (89), *secE* in strain CM124 (results in decreased levels of SecY) (127), *ffh* in strain WAM121 (128), and *ftsY* in strain FJP10 (129). In studies in *B. subtilis* the P*spac* promoter(130), a hybrid between a *Bacillus* phage promoter SP0-1 and the *lac* promoter of *E. coli* (regulated by IPTG via LacI), as well as the *xylA* promoter (inducible by xylose via XylR), have been successfully used to conditionally express proteins (117). Attempts to use these promoters in streptococci for controlled expression have failed because they were either poorly inducible or very leaky (131).

Use of the NICE (nisin inducible controlled expression) system in *Lactococcus latis* has been promising. This system uses plasmid based *nisRK* that encode a TCS system, which induces expression from the P*nisA* promoter in the presence of nisin (132). This system was shown to work in several Streptococcal species (*S. pyogenes*, *S. agalactiae*, and *S. pneumoniae*) but showed some leaky expression in *S. agalactiae* and *S. pneumoniae* with very little induction in the presence of nisin. On the other hand the system worked very well in *S. pyogenes*, with very little background expression and 59-fold induction in the presence of nisin (131). One of the drawbacks to this system is that it uses a plasmid to express the necessary control elements, which are not native to streptococci. Also the leaky expression in some of the streptococci indicates that tight regulation may not be possible in *S. mutans*. It is for this reason a conditional expression system that includes endogenous promoters expressed from the chromosome is needed. The cellobiose operon of *S. mutans*, characterized by Dr. Lin Zeng from the Burne group at the University of Florida, is tightly regulated through carbon catabolite repression (CCR) (133). There are two promoters in this operon, *PcelA* and *PcelB.* These were used to create promoter fusions to *yidC2* in *S. mutans*. The *yidC2* promoter fusions were integrated into the *gtfA* locus of the *S. mutans* strain NG8 chromosome and evaluated for their ability to control expression of *yidC2*. In addition *yidC1* was eliminated by allelic exchange mutagenesis using a spectinomycin marker, to generate a strain that under controlled conditions produces little YidC2 and no YidC. This *yidC* depletion strain was evaluated for differences in protein expression profiles using cell fractionation and one dimensional gradient SDS-PAGE.

Materials and Methods

Synthetic Peptide Antiserum

Synthetic peptides corresponding to C-terminal sequences of YidC1 (LEDEARE-LEAKKRRAKKKAHKKRK) and YidC2 (NPPKPFKSNARKDITPQANNDKKLITS) were designed based on membrane topology predictions using TMPred (Figures 2-3 and 2-4). These peptides were synthesized and sent to Proteintech Group, Inc (Chicago, Illinois) for immunization of two rabbits each. The resulting antisera were affinity purified (see Affinity Purification Protocol below).

In *S. mutans* SecY is predicted to be a 47,688 Da protein with 10 transmembrane domains (TMPred topology prediction program). To make antibodies against SecY, four synthetic peptides were designed that corresponded to the extracellular loop between TMD 1-2 (PGINAKSLEQLSKLPFLNML), the cytoplasmic loops between TMD 6-7 (QAEYKIPIQYKLAOGAPTN) and TMD 8-9 (VNPEKTAENLQKNASYIPSV), and to the C-terminal tail (GMKQLEQYLLKKKYVGFMNV). Peptides were designed based on topology predictions combined with sequence alignments between *S. mutans* SecY and SecY from *Methanococcus jannaschii*, for which the structure has been solved (134). All four peptides were combined and used to immunize two rabbits (Proteintech Group, Inc.). The resulting antisera were poorly reactive with too much non-specific background reactivity to be useful. Therefore the anti-peptide antibodies were affinity purified from antisera (see Affinity Purification Protocol below) before use in future experiments.

Antiserum against a synthetic peptide corresponding to a non C-terminal portion of YidC2 was also made. Two synthetic peptides were designed, one corresponding to the cytoplasmic loop between TMD 2 and 3 (SEKMAYLKPVEDPIQERMKN) and one to

an extracellular loop between TMD 3 and 4 (ALYISTRYTRYTKGIASILGI) (see Figure 2-4 for peptide locations). Each peptide was used to immunize a different rabbit. In the interest of time, affinity purification was completed by Proteintech Group, Inc. for a fraction of the resulting antisera and sent with the final bleeds. Only one of the antibody preparations, made against the cytoplasmic loop between TMD 2 and 3 (α-YidC2 TM 2/3), was reactive with YidC2, and therefore was the one used in future experiments.

Affinity purification. The procedure used to affinity purify antibodies used in this study was adapted from two protocols, one provided by Proteintech Group, and the other from GE Healthcare, the manufacturer of CNBr-activated Sepharose 4B beads (Instructions: 71-7686-00 AD). To make the affinity matrix, 5 mg of total peptide was dissolved in 5 ml Coupling Buffer (100 mM $NaHCO_3$, 500 mM NaCl, pH 8.0-8.3). Next 500 mg of CNBr-activated Sepharose 4B (Pharmacia) was hydrated in ice cold 1 mM HCl (pH 3.0) solution on ice for 10 minutes. The beads were then placed on a porcelain funnel with a vacuum and washed with 250 ml of iced cold 1 mM HCl (pH 3.0) solution. The Sepharose beads were not allowed to dry out during this wash step. Next the beads were combined with peptides dissolved in Coupling Buffer and incubated overnight at 4ºC with end-over- end rotation to allow for conjugation. Peptide coupled Sepharose beads were then washed with at least five gel volumes of Coupling Buffer, to remove unbound peptides. Remaining active groups were blocked by placing the beads in Blocking Buffer (100 mM Tris-HCl [pH 8.0]) for 2 hours at room temperature. After the peptide coupled Sepharose beads were blocked, they were washed with three cycles of alternating pH solutions (five gel volumes per wash). Each cycle consisted of one wash with 100 mM acetic acid/sodium acetate, pH 4.0, 500 mM NaCl, followed by a

wash with 100 mM Tris-HCl (pH 8.0), 500 mM NaCl. The peptide coupled Sepharose beads were then combined with 10 ml of antisera, and incubated for 4 hours at room temperature or overnight at 4ºC with end-over-end rotation. After antibodies were bound, the Sepharose beads were transferred to a 5 ml plastic column and the flowthrough was saved for subsequent ELISA testing. The beads were washed three times with five gel volumes of PBS (phosphate buffered saline), and the OD_{280} was monitored to determine when washes were sufficent. The antibodies were eluted with ice cold HCl (pH 2.5) solution. Fractions of 900 µl were collected into 1.5 ml Eppendorf tubes containing 100 µl 1 M Tris-HCl (pH8.0) to neutralize the antibody solutions immediately upon elution. Sodium azide (0.02%) was added to prevent microbial contamination. Each fraction was then analyzed by ELISA (enzyme-linked immunosorbent assay). ELISA plate wells were coated overnight at 4ºC with peptides from affinity purification at a concentration of 100 ng/well dissolved in carbonate-bicarbonate coating buffer (pH 9.6). ELISA plates were then blocked with 200 µl of PBS containing 0.3% Tween-20 (PBS-Tw) at 4ºC until used for ELISA. To determine the titer of purified antibodies each fraction was serially diluted by twofold starting at 1:500 to 1:32,000 in PBS-Tw. Pre-immune and post- immunization (final bleed) sera and the flowthrough from the affinity purification were included on each plate as controls. Whole cell lysates of *S. mutans* were then analyzed by Western blot using a dilution based on ELISA results of each fraction to determine the quality of the antibody and the success of the affinity purification.

The SecY antibody resulted in a mono-specific reagent that recognized primarily a ~37 kDa band by SDS-PAGE/Western blot. A ~75 kDa band, which could be a SecY

dimer, was occasionally detected, as well as a~20 kDa smear, which has been reported by others to be breakdown products of SecY.

The YidC1 and YidC2 C-terminal peptide antisera were also affinity purified using the synthetic peptides provided by Proteintech coupled to CNBr-activated sepharose. Once affinity purified, the YidC1 antibody preparation recognized a single ~24 kDa band by Western blot. The YidC2 antibody preparation recognized two bands after the first passage over the column, a ~28 kDa band (desired band), and a ~20 kDa band, which was also recognized by the pre-immune sera. The 20 kDa band was only present in the first 12 column fractions and was not present in the flowthrough, which still contained a considerable amount of antibody that recognized YidC2. Therefore, the flowthrough fraction was re-applied to the column, yielding a mono-specific reagent that recognized a ~28 kDa band by Western blot. The 20 resulting fractions were pooled and concentrated approximately sevenfold using Centiprep-10 columns.

Creation of Strains SP13, SP14 and SP17: C-Terminal Domain Swaps of YidC1 and YidC2.

Splice overlap extension (135) was used to create a chimeric protein comprised of YidC1 (amino acids 1-229) and the C-terminal tail of YidC2 (amino acids 247 to 310). Primers SP21F, with an *Xba*I site, and SP22RSOE (containing a 9 nucleotide overhang), were used to PCR amplify DNA encoding (-) 131 to (+) 687 *of yidC1* (including the ribosome binding site) from *S. mutans* strain UA159 genomic DNA. This PCR product was then gel purified and referred to as fragment AB. DNA encoding the C-terminal 63 amino acids of YidC2 was amplified by PCR from UA159 genomic DNA using primers SP22FSOE-YidC1 (with a 9-nt overhang corresponding to splice site with *yidC1*) and SP21R (with a *Bsr*GI site) resulting in a fragment of *yidC2* containing

nucleotides (nt) 741 to 1,009, including 76-nt after the stop codon of the YidC2 open reading frame. This fragment was also gel purified and referred to as fragment CD. Fragments AB and CD were combined through PCR overlap extension (135), using primers SP21F and SP21R. The product was initially cloned into pCR2.1®, and then excised by enzyme digestion using *Xba*I and *BsrG*I. This fragment was then cloned into integration vector pBGE that had been digested with *Xba*1 and *Bsr*G1. This vector was designed for chromosomal integration into the *gtfA* locus such that constructs are be expressed from the *gtfA* promoter and selected with an erythromycin marker (133), facilitating the cloning of genes that may be lethal to *E. coli*. Plasmid pBGE-*yidC1C2*-Erm was used to transform AH378 (NG8 *ΔyidC2*::Kan^R) to generate strain SP13.

A chimeric protein encompassing amino acids 1-247 of YidC2 and the C-terminal amino acids 227-271 of YidC1 was constructed using splice overlap extension as described above for YidC1C2. The *yidC2* gene fragment was amplified by PCR from UA159 genomic DNA using forward primer SP27F2, and reverse primer SP27RSOE (with a nucleotide overhang corresponding to *yidC1* fragment), amplifying nucleotides (-) 43 to (+) 741 of the *yidC2* gene. This was gel purified and referred to as fragment AB. The *yidC1* C-terminal fragment was generated by PCR from UA159 genomic DNA using forward primer SP28FSOE, and reverse primer SP28R (with a *Bsr*GI site) amplifying nucleotides (+) 685 to (+) 875 (this is 59 nucleotides downstream from the stop codon of *yidC1*). This PCR product was gel purified and referred to as CD. Fragments AB and CD were then used in a splice overlap extension PCR reaction using primers SP27F2 and SP28R. This PCR product was cloned into pCR2.1® and further processed as with YidC1C2 above, except that instead of an *Xba*I site in primer SP27F2

(a mistake was made during design), the *Xba*I site in pCR2.1 was used. The resultant strain was named SP14 (Δ*yidC2*::Kan^R, gtfA::*yidC2-C1*-Erm^R). Table 2-1 shows strain designations, and Table 2-2 lists primer sequences.

Strain SP17, with *yidC2* under the control of the *gtfA* promoter, was generated as the relevant positive control for experiments with SP13 and SP14. It was constructed in the same manner as SP13 and SP14 using primers SP27F2 and SP21R to PCR amplify *yidC2* from UA159 chromosomal DNA.

The *yidC2* mutant strain that was used to create SP13, SP14, and SP17 was made from the *S. mutans* strain NG8. Locations of chimeric and control genes were verified by PCR using the forward primer SP37F, which binds in the promoter of *gtfA* and reverse primer AH31R for strains SP13 and SP17 or SP21R for strain SP14. Genes were also PCR amplified from chromosomal DNA and correct construction was confirmed by DNA sequencing.

Conditional Expression of *yidC2*

In order to conditionally express *yidC2*, promoter fusions were created between the promoters of the *celA* and *celB* genes and *yidC2*. See Figure 2-5 for a schematic diagram of the construction. The region corresponding to the *celA* promoter (P*celA*, -1 to -345 nt from *celA* start), including the ribosome binding site (RBS), was amplified by PCR from *S. mutans* strain UA159 genomic DNA using forward primer SP12F with an engineered *Sma*I site and reverse primer SP12R with an *Nde*I site, which contains an ATG codon to facilitate promoter fusions (see Table 2-2 for primer sequences). The *celB* promoter (P*celB*) was amplified by PCR (-1 to -263-nt from *celB* start) using primers SP13F and SP13R with the same rationale as for the *celA* promoter. These primers were selected based on personal communication with Dr. Lin Zeng from the

Burne Lab at the University of Florida, who has experience with promoter fusions of P*celA* and P*celB* (133). The *yidC2* gene was amplified by PCR from UA159 genomic DNA using forward primer SP14F (with an engineered *Nde*I site), and reverse primer SP05R (with an engineered *Sma*1 site). Each PCR product was cloned into pCR2.1® (Invitrogen), and the resulting plasmids were restricted at a unique *Bam*HI site in pCR2.1® and the *Nde*I site (engineered into the primers) to determine orientation. The P*celA* and P*celB* clones containing ~45-bp fragments were selected for large scale plasmid preps and restriction digestion. The 45-bp fragment was removed by gel purification and the larger fragment (~5.0-Kb) was reserved for a downstream reaction. pCR2.1® clones containing *yidC2*, were selected that demonstrated a ~1.0 Kb fragment after *Bam*HI and *Nde*I digestion. This 1.0 Kb fragment was gel purified and ligated to the 5.0-Kb fragments containing either P*celA* or P*celB* from above, to create the promoter fusions P*celA*-*yidC2* and P*celB*-*yidC2*. The constructs were confirmed by DNA sequencing and then excised using the *Sma*I sites engineered into primers, gel purified and cloned into *Sma*1 digested pBGK2 (same as pBGK in (136) but with the Ap^R marker removed by the Burne lab). This is an integration vector containing a Kanamycin resistance marker and is designed for chromosomal integration into the *gtfA* locus of *S. mutans*. This resulted in plasmids pSP10 (P*celA*-*yidC2*) and pSP11 (P*celB*-*yidC2*). These plasmids were then used to transform the previously engineered *ΔyidC2* mutant strain AH398 (31), resulting in an integration of the P*celA*- and P*celB*- *yidC2* promoter fusions into the chromosome at the *gtfA* locus. Transformants were selected on THYE agar plates containing kanamycin (500 µg/ml). The resulting strains were named SP10 (P*celB*-*yidC2*) and SP11 (P*celA*-*yidC2).* The locations of the promoter

gene fusions in the chromosome were confirmed by PCR using either forward primer SP16F (binds within P*celA*) or SP17F (binds within P*celB*) and reverse primer SP16R (binds after the stop codon of *yidC2*). Primers that were the reverse complements of SP16F and SP17F were designed (SP16F RC and SP17F RC) and used in PCR reactions with SP18R, which binds after the stop codon of *gtfA*, to confirm that the promoter gene fusions were inserted in the opposite orientation as the *gtfA* gene. SP10 and SP11 were then used as the background strains to eliminate the endogenous copy of *yidC1.* SP20 and SP21 were created by natural transformation of SP10 and SP11 respectively with pCR2.1 Δ*yidC1*::SpecR (see below) and selected on THYE agar plates containing 1000 µg/ml spectinomycin.

Deletion Construction of Δ*yidC1* using a Spectinomycin Marker.

The *yidC1* gene was eliminated by allelic replacement using a spectinomycin marker. To make the deletion construct, splice overlap extension (SOE) (135) was used to combine the upstream and downstream fragments of *yidC1* with an intervening spectinomycin gene. The upstream fragment was designed not to interfere with the upstream gene *rnpA*, which overlaps into the open reading frame of *yidC1*. The spectinomycin marker was amplified by PCR from pDL278 (137) with primers SP25FSOE and SP25RSOE (see Table 2-2 for primer sequences) resulting in an 855-nt product. The upstream region of *yidC1* corresponding to -291 to +21 was amplified from UA159 genomic DNA using primers SP29F and SP24RSOE resulting in a 345-nt fragment with a 3' overhang, which binds to the 5' end of the spectinomycin fragment. A PCR reaction was performed with primers SP29F and SP25RSOE with the upstream *yidC1* and spectinomycin fragments as the template, through splice overlap extension (SOE). The downstream fragment of *yidC1* was amplified using primers SP26FSOE

and AH25R with the forward primer binding 817-nt from the translational start site and directly after the stop codon of *yidC1*. The reverse primer bound 932-nt downstream from the forward primer. This fragment was then combined with the previous SOE reaction using primers SP29F and AH25R to generate a 2,087-nt product, which was subsequently cloned into pCR2.1® (Invitrogen) to generate plasmid pCR2.1Δ*yidC*::SpecR. Before transformation into *S. mutans*, this plasmid was cut with *Hind*III resulting in a linear piece of DNA. The *yidC1* gene was replaced with the spectinomycin resistance gene, through double-crossover recombination.

Growth Curves

Cultures of *S. mutans* strains SP22, SP17, AH378, AH374, SP13, SP14, AH412, and SP16 were inoculated from glycerol stocks into 10 ml THYE and grown overnight at 37ºC (Table 2-1 for strain designations). Overnight cultures were diluted 1:20 into fresh THYE, pH 7.0, broth without antibiotics and grown to an OD_{600} of 0.4. A 100-well Bioscreen C plate (Labsystems, Helsinki, Finland) was filled with 180 µl of pre-warmed media (THYE pH 7.0, THYE pH 5.0 or THYE pH 7.0 with 3% NaCl). Wells were inoculated in triplicate with 20 µl of culture, and covered with sterile mineral oil, and placed in the Bioscreen C machine set to record optical density 600 nm every 15 minutes, with shaking for 10 seconds before each reading, for 16 hours. Doubling time (Td) was calculated by measuring the slope of the logarithmic growth phase using the formula Td = [(t2-t1)ln(2)]/[ln (OD2)-ln (OD1)] (31). Statistical analysis was performed using One-way ANOVA with Bonferroni's Multiple Comparison Post Test, using the GrapPad Prism 4 program.

Whole Cell Lysates

Whole cell lysates were prepared from 10 ml cultures grown in THYE (Todd Hewett 3% Yeast Extract). Cells were pelleted at 3,210 x g for 10 minutes and washed once in 25 mM Tris-HCl, pH 7.5, and then re-suspended in 500 µl of the same buffer. Each cell suspension was then combined with 0.5 grams glass beads (0.1 mm BioSpec Products, Inc.) and shaken for 1 minute for two cycles in a mini bead beater (Biospec Products) and iced for 1 minute between cycles. Glass beads were allowed to settle for several minutes before the supernatant was transferred to a new tube. For SDS-PAGE, 50 µl of each whole cell lysate was combined with 50 µl 2X SDS sample buffer, boiled for 5 minutes and centrifuged at 13,000 rpm for 3 minutes in a Beckman tabletop microcentrifuge. Then 15 µl was loaded on a 10% SDS-polyacrylamide gel for Western blot analysis (described under Western blot protocol below).

Cell Fractions and Gradient SDS-PAGE

Cells were harvested by centrifugation at 3,210 x g for 10 minutes in a tabletop Beckman centrifuge from a 20 ml mid log (OD_{600} 0.5) culture grown in TDM (Terleckj defined media)(138) containing 0.5% cellobiose or glucose. Proteins present in sterile-filtered culture supernatant (0.22 µm syringe filter) were precipitated by combining 500 µl of filtered supernatant with 500 µl 20% trichloroacetic acid (TCA) and incubation on ice for 20 minutes. Precipitated proteins were pelleted in a tabletop microcentrifuge at 4ºC at 13,000 rpm for 10 minutes. The pellets were washed twice with 300 µl acetone and allowed to air dry in a 55ºC oven for 10 minutes. The dried pellets were re-suspended in 100 µl 1 x SDS sample buffer. For other cellular fractions, cell pellets were harvested and washed once in 10 ml Buffer A (10 mM Tris-HCl [pH 6.8], 10 mM

Mg acetate, in 25% sucrose or raffinose) and then frozen at -20ºC until further processing could be done. For the cell wall fraction, each frozen cell pellet was thawed and re-suspended in 5 ml Buffer A with 10 µg/ml lysozyme (50 ul of 10 mg/ml lysozyme) and 100 U/ml of mutanolysin (50 µl of 10,000 U/Ml). Cells were incubated at 37^0C for 45 minutes to 1.5 hours to protoplast the cells (protoplast formation was monitored by Gram staining). Protoplasts were pelleted by centrifugation at 3,210 x g for 10 minutes. Supernatants from the cell wall digestion were filter with a 0.22 µm syringe filter and TCA precipitated (500 µl with 500 µl 20% TCA, as described for culture supernatants). Protoplasts were washed twice with 5 ml Buffer A and re-suspended in 1 ml Osmotic Lysis Buffer (50 mM Tris [pH7.5] containing 10 mM $MgSO_4$, 0.8M NaCl), transferred to a 5 ml polycarbonate tube, and 40 ul of EDTA free protease inhibitor cocktail (Complete - Roche Tablet 25 x stock solution), 10 µg/ml of DNase (10 µl of DNase1 mg/ml) and RNase (10µl of 1 mg/ml stock) were added. Protoplasts were lysed with two 10 second cycles on setting 10 of a Fisher Scientific Sonic Dismembrator 100 (cells were cooled on ice between cycles). The lysates were transferred to a 1.5 ml Eppendorf tube and unlysed protoplasts and cell debris were removed by centrifugation in a tabletop microcentrifuge at top speed (13,000 rpm) for 10 minutes. The supernatants were transferred to a 1.5 ml Beckman ultracentrifuge tube and centrifuged at 100,000 X g (45K rpm) in SW50.1 rotor for 20 minutes at 4^0C. The supernatants, which represented the cytoplasmic fractions, were TCA precipitated as described for culture supernatants and re-suspend in 200 µl 1X NativePAGE Sample Buffer (50 mM Bis-Tris [pH 7.2], 50 mM NaCl, 10% glycerol, 0.001% Ponceau S). The membrane pellets were re-suspended in 100 µl of ice cold NativePAGE sample buffer using a Teflon homogenizer

and a rounded Pasteur pipette to dislodge the sticky pellets. For SDS-PAGE, each fraction was combined with 2 X SDS sample buffer, and boiled for 5 minutes followed by centrifugation at 13,000 rpm for 3 minutes to remove insoluble material. Next 15 µl of each fraction was loaded on a BioRad Criterion 4-15% gradient SDS-PAGE gel and electrophoresed for approximately 1 hour 25 minutes at 200 volts in a BioRad Criterion Cell connected to a BioRad PowerPac Basic Power Supply.

Western Blotting

After proteins were separated by SDS-PAGE, they were transferred to an Immobilon® PDVF membrane (membrane was hydrated in 100% methanol according to the manufacturer's directions) in a Hoefer Mighty Small TE 22 Mini Transfer Tank for 1 hour at 100 volts in Transblot Buffer (25 mM Tris, 192 mM Glycine, 20% Methanol). After transfer, membranes were blocked for 1 hour at room temperature or overnight at 4°C in PBS, 0.3% Tween, 5% milk. Membranes were then reacted with primary antibody for 1 hour at room temperature. Affinity purified YidC1 C-terminal, YidC2 C-terminal and YidC2 non-C-terminal antibodies were used at 1:4000, 1:8000 and 1:6000 dilutions respectively. Affinity purified SecY peptide antiserum was used at a dilution of 1:1000. Peroxidase conjugated goat affinity purified anti-rabbit IgG (Cappel MP Biomedicals, Solon Ohio) was used as the secondary antibody, which was reacted for 1 hour at room temperature at a 1:1000 dilution. Western blots were developed using the Amersham ECL kit from GE Healthcare.

Results and Discussion

YidC2's C-Terminal Tail Contributes to Stress Tolerance in *S. mutans*

A number of *S. mutans* strains were constructed in order to evaluate the function of *yidC1* and *yidC2*. Whole cells lysates of each strain were evaluated by Western blot

to confirm proper expression of YidC1 or YidC2 (Fig. 2-6). The protein stain confirmed that similar levels of total protein were loaded for each strain. As can be seen from the Western blot reacted with α-YidC1 antiserum, all strains recognized a ~24 kDa band except for those strains in which *yidC1* had been replaced with an antibiotic marker, Δ*yidC1*::Erm, SP15 (Δ*yidC1::Spec*), and SP16 (*yidC2ΔC::Erm*, *ΔyidC1::Spec*). Also strain SP14, containing the chimeric protein YidC2C1, resulted in two bands of reactivity, one at the expected ~24 kDa corresponding to wild-type YidC1 and one slightly larger band at ~25 kDa corresponding to the chimeric YidC2C1 protein. The Western blot reacted with the α-YidC2 C-terminal antibody showed the expected reactivity, with all strains containing the YidC2 C-terminal tail reacting with a band of the correct size. Wild-type full-length YidC2 migrates as a ~28 kDa band, and was observed for NG8, Δ*yidC1*, SP15, and SP17 (Table 2-1 for strain designations). Strain SP13, containing the chimeric YidC1C2 protein, demonstrated a slightly smaller band of ~27 kDa. Reactivity with α-YidC2 TM 2/3, a YidC2 peptide antibody that recognizes a non C-terminal epitope, showed reactivity with all strains as would be expected, recognizing a ~28 kDa band in NG8, *ΔyidC1*, SP15, and SP17. Strains *yidC2ΔC* (AH412) and SP16 (*yidC2ΔC, ΔyidC1*) did not react with the α-YidC2 C-terminal antibody, but demonstrated a ~22 kDa band reactive with the non C-terminal α-YidC2 antibody.

Once proper YidC expression was confirmed, these strains were evaluated for their ability to tolerate acid- and osmotic-stress, by growth in THYE pH 5.0, and THYE 3% NaCl, compared to growth under non-stress conditions in THYE pH 7.0. Mean doubling times are shown in Table 2-3. Results indicate that in strain SP13 (Δ*yidC2*,

gtfA::*yidC1C2*) chimeric YidC2C1 was able to significantly restore acid tolerance to the Δ*yidC2* strain as well as complete unaltered YidC2 (SP17, Δ*yidC2*, gtfA::*yidC2*), while salt tolerance was restored to some extent it was not to a significant level. In contrast, the growth defect of strain SP14 (*ΔyidC2*, *gtfA*::*yidC2C1*) was significantly worse than that observed upon complete deletion of *yidC2* (strain AH378) under non-stress conditions. This indicates that replacing the C-terminal tail of YidC2 with that of YidC1 destroys its ability to function normally, perhaps by affecting necessary protein-protein interactions. The functional relevance of the YidC2 C-terminus is further supported by the fact that placing it onto YidC1 confers on YidC1 the ability to restore acid-tolerance to the *yidC2* mutant. Of note, SP17 did not grow like the wildtype strain under stress conditions when YidC2 was expressed from the *gtfA* promoter. This suggests that the *yidC*2 promoter probably also contributes to stress tolerance, perhaps by allowing for increased expression of *yidC2* under certain conditions, as was demonstrated in studies of the LiaSR TCS (45). The *yidC2* C-terminal deletion strain, AH412, showed similar acid and salt sensitivity as strain AH378 with a complete deletion of *yidC2*. However AH378 grew more slowly than the AH412 under non-stress conditions. This suggests that the YidC2 protein's C-terminal tail has a function that confers stress tolerance, and that in the absence of stress, additional non C-terminal functions of YidC2 contribute to normal growth. Deletion of *yidC1* in the AH412 background (strain SP16) further exacerbated the growth defects of the YidC2 C-terminal deletion. This suggests that in the absence of the C-terminal tail of YidC2, YidC1 can play a compensatory role in acid and salt tolerance. Perhaps the overall amount of YidC proteins is important. Attempts to delete *yidC1* from strains SP13 and SP14 were unsuccessful. This was somewhat

surprising in the case of SP13, in which YidC1C2 was able restore stress tolerance to the *yidC2* mutant strain. Perhaps, the level of expression was an issue and use of the *yidC2* promoter to express YidC1C2 would have resulted in full complementation. Alternatively, YidC1 and YidC2 may cooperate in a balanced manner that cannot be replicated by YidC1C2 in the absence of endogenous YidC1 and YidC2.

In addition to growth in broth, strains expressing chimeric YidC1C2 (SP13) and YidC2C1 (SP14) were evaluated for their ability to restore growth of the *yidC2* mutant on pH 5.0 THYE agar plates (Figure 2-7). For comparison, strains SP22 (NG8, *gtfA::Erm*), SP17 (Δ*yidC2, gtfA::yidC2*), and AH412 (*yidC2*ΔC) were included. Strain SP22, which *yidC2* is expressed from the endogenous promoter, showed the best growth. When the *yidC2* mutant was complemented with *yidC2* in the *gtfA* locus and expressed from the *gtfA* promoter (SP17), growth was restored, but not to wildtype levels. Deletion of the C-terminal tail of YidC2 (with the deletion in the chromosomal *yidC2* gene) had an intermediate phenotype on agar. In contrast, growth in broth culture of this strain was similar to that of the full *yidC2* mutant. This suggests that the C-terminal tail of YidC2 is less necessary for acid tolerance when the bacteria are grown on solid media, perhaps due to differences in oxygen tension. When YidC1C2 was expressed in the Δ*yidC2* background (SP13), it was able to restore growth of the *yidC2* mutant as well as wild-type *yidC2* (SP17). However, when the C-terminal tail of YidC1 was placed onto YidC2 (SP14), no complementation of growth of the *yidC2* mutant was observed.

Conditional Expression of *yidC2*

In order to better understand the functions of redundant pathways for protein secretion and membrane biogenesis in *S. mutans,* a conditional expression system was needed, to allow potentially lethal combinations of deletions to be made. A conditional expression system was developed for *yidC2* using the promoters from the cellobiose operon, *PcelA* and *PcelB.* It was shown by Zeng et. al., 2009 using promoter fusions of *PcelA* and *PcelB* with the CAT reporter gene (chloramphenicol acetyltransferase) followed by CAT assays after growth in different sugars, that expression from these promoters is controlled by carbon catabolite repression (CCR) in *S. mutans* strain UA159, with almost no expression in the presence of the repressing sugars glucose, fructose and mannose (133). In the current study, the constructs made were in the *S. mutans* NG8 background. While similar to UA159, there are some differences in CCR between the stains (personal communication, L. Zeng and R. A. Burne). Strains SP10 and SP11 were created first, with the *yidC2* gene fused to *PcelB* or *PcelA* respectively, and then placed into the *gtfA* locus of the *ΔyidC2* mutant (AH398) chromosome (Table 2-1). The *yidC1* gene was then replaced with a spectinomycin marker in SP10 and SP11, to create SP20 and SP21 respectively. To determine which carbon source has the most repressing effect on *yidC2* expression when under the control of *PcelA* (SP11/SP21) or *PcelB* (SP10/SP20), different growth conditions were tested followed by Western blot with α-YidC2 C-terminal and α-YidC1 C-terminal antibodies. The Western blot results of SP10 and SP20 grown in TDM with 0.5% cellobiose (inducing conditions) compared to growth in TDM 0.5% glucose (not shown), 0.5% fructose, 0.5% mannose, and THYE are shown in Figure 2-8. Overnight growth in TDM 0.5% mannose had the

most repressing effect on *yidC2* expression, while growth in TDM 0.5% fructose had only a minor repressing effect. Shown in Figure 2-9 are the Western blot results for strains SP11 and SP21 grown under the same conditions mentioned above. Somewhat surprisingly, *PcelA* expression of *yidC2* in the absence of *yidC1* (SP21) was not repressed by overnight growth in mannose to the same extent as *PcelB*-controlled expression of *yidC2* (SP20). However, when endogenous *yidC1* was present in strain SP11, expression of *yidC2* under the control of *PcelA* was more repressible (Figure 2-9, last two lanes). This was also true for SP20 and SP10. SP10 demonstrated repression of *yidC2* in the presence of glucose. In contrast, no repression of *yidC2* by glucose was observed for strain SP20 (not shown), and repression by mannose occurred only after overnight growth. The promoter fusions made in these studies were in an NG8 background. In contrast to what Zeng found in UA159, expression from the *celA* promoter in the NG8 background was very leaky in glucose, fructose and mannose, while expression from the *celB* promoter was more tightly regulated, but only in TDM 0.5% mannose (See Western blots in Figures 2-8 and 2-9).

Various cell fractions were prepared from strains NG8, Δ*yidC1*, Δ*yidC2*, and SP10 and compared to strain SP20, in which *yidC2* expression is limited in a *yidC1* negative background. Figure 2-10 shows the Western blot analysis of the membrane fractions prepared from cells grown in TDM 0.5% mannose or 0.5% cellobiose reacted with α-YidC2 C-terminal, α-YidC2 TM 2/3, and α-YidC1 C-terminal antibodies. Membranes from cells grown in TDM 0.5% mannose, where *yidC2* expression is low (SP20), and TDM 0.5% cellobiose, where *yidC2* expression is high are shown for SP10 and SP20 at different time points. Repression of *yidC2* was observed in SP10 (in which *yidC1* is

present) sooner and to a greater extent than in SP20, in which *yidC1* is absent and *yidC2* expression is regulated by CCR through the *PcelB* promoter. The Western blots also confirmed that the amount of YidC2 was negligible in SP20 when cells were grown in TDM 0.5% mannose for 7 hours. Cell wall, membrane and cytoplasmic fractions were analyzed by one dimensional gradient SDS-PAGE followed by silver stain. The protein profiles of cell wall fractions from the respective strains grown to late log phase in TDM 0.5% mannose are shown in Figure 2-11. For strains SP10 and SP20 cells were grown in TDM 0.5% mannose for 5 hours or 7 hours respectively. The protein profiles of cytoplasmic and membrane fractions from the various strains grown in TDM 0.5% mannose, or 0.5% cellobiose where indicated, are shown in Figures 2-12 and 2-13. Only minor differences, as reflected by 1D-SDS-PAGE analysis, were observed in the cell wall, cytoplasmic or membrane fractions, between the wildtype strain and the *yidC1* or *yidC2* mutants, or between the single mutants and SP20, in which YidC2 is depleted in a *yidC1* mutant background. Since YidC proteins may be involved in assembly of multimeric protein complexes, these strains were assessed further using the Blue Native PAGE technique described in Chapter 4. In a recent proteomics study of YidC depletion in *E. coli* under aerobic compared to anaerobic conditions by Price (139), the effects were less pronounced under anaerobic growth conditions. Since *S. mutans* is a facultative anaerobe, effects of YidC depletion in this bacterium could be influenced by oxygen as well, and more readily observed at the functional level of individual enzymes.

The complete mechanisms of CCR are not known is *S. mutans*, however it is clear from work by the Burne Lab at the University of Florida that it is different from CCR in *E.*

coli, and involves EIIAB^{Man}, a membrane-associated protein of the mannose/glucose PTS system (140). Mutation of EIIAB^{Man} results in loss of CCR, increased cellobiose PTS activity, decreased fructose PTS activity, decreased biofilm formation, and loss of genetic competence (141). The *S. mutans yidC2* mutant has a pronounced growth defect, with decreased growth rate and cell yield in defined media containing a number of different sugars (this effect is less pronounced when cells are grown in complex media THYE), decreased biofilm formation, and a loss of genetic competence. It would be interesting in future studies to evaluate the effects of *yidC1* or *yidC2* on CCR, which likely involves a number of membrane components. This could be tested by deletion of *yidC1* or *yidC2* from strains with CAT fusions to *PcelA* or *PcelB*, and assay of CAT activity after growth in different repressing sugars.

Use of the P*celB* or P*celA* promoters is a promising tool for conditional expression of essential genes in *S. mutans*. These could be optimized further though additional mutation for better control over gene expression in pathways that influence CCR, or by using different combinations of repressing sugars, or adjusting the concentrations of repressing sugars. It remains to be seen if YidC1 or YidC2 are involved in CCR. The results of these studies suggest this might be the case. Therefore *PcelA* and *PcelB* may be more effective at enabling conditional expression of genes that do not contribute to CCR. It is also possible that the effects of carbon source seen in SP10 and SP20 are related to a stress response that occurs in *S. mutans* and that affects CCR when essential genes are eliminated. In that case, use of CCR controlled promoters for conditional expression of essential genes may be more complicated and difficult to

achieve. Additionally, it is possible the discrepancies seen with repressing sugars are related to differences in CCR between UA159 and NG8.

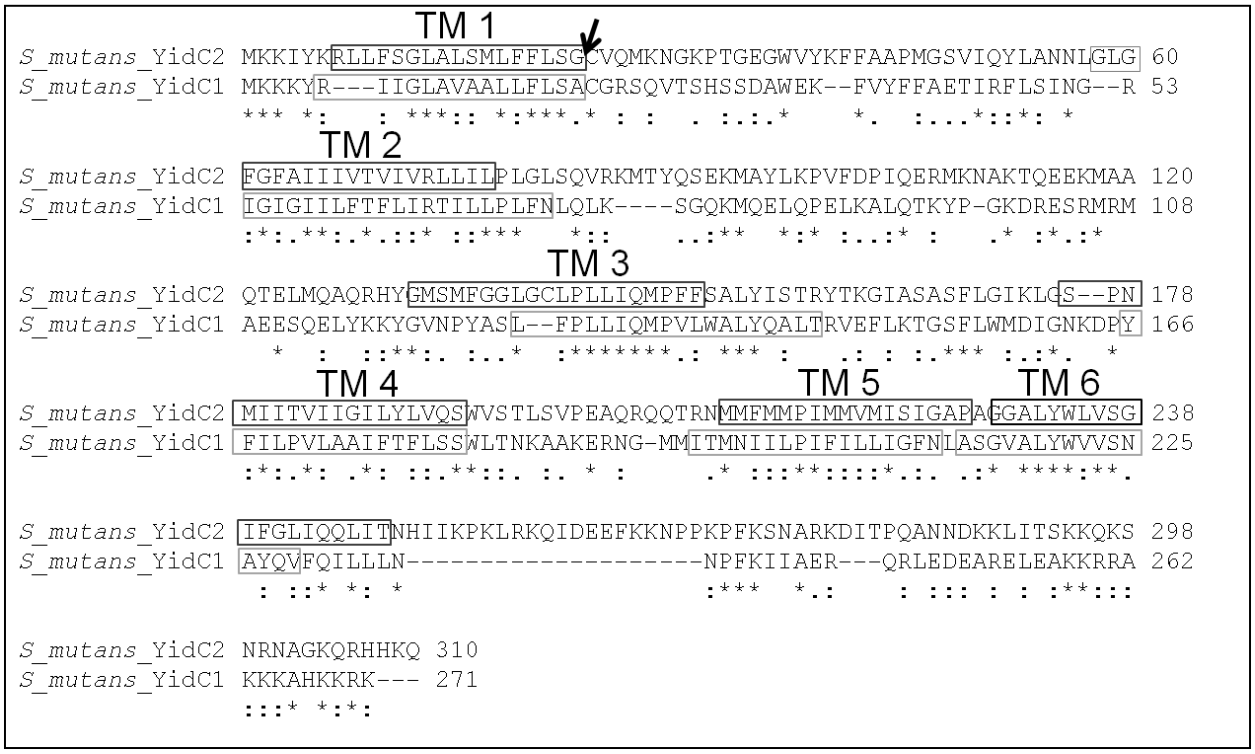

Figure 2-1. Clustal W sequence alignment of *S. mutans* YidC1 and YidC2. Sequences predicted to be transmembrane (TM) domains by TMPred are boxed and labeled 1-6. YidC1 and YidC2 are predicted to be lipoproteins that are processed by SPaseII at amino acid 23 in YidC2 and amino acid 20 in YidC1 (indicated by an arrow). N-terminal sequencing showed that YidC1 and YidC2 are further processed resulting in 218 a.a. and 253 a.a. proteins respectively (142). There is approximately 30% identity and 75% similarity between YidC1 and YidC2. Differences are seen between the C-terminal tails, with YidC2 containing a longer more basic tail (+17) than YidC1 (+10).

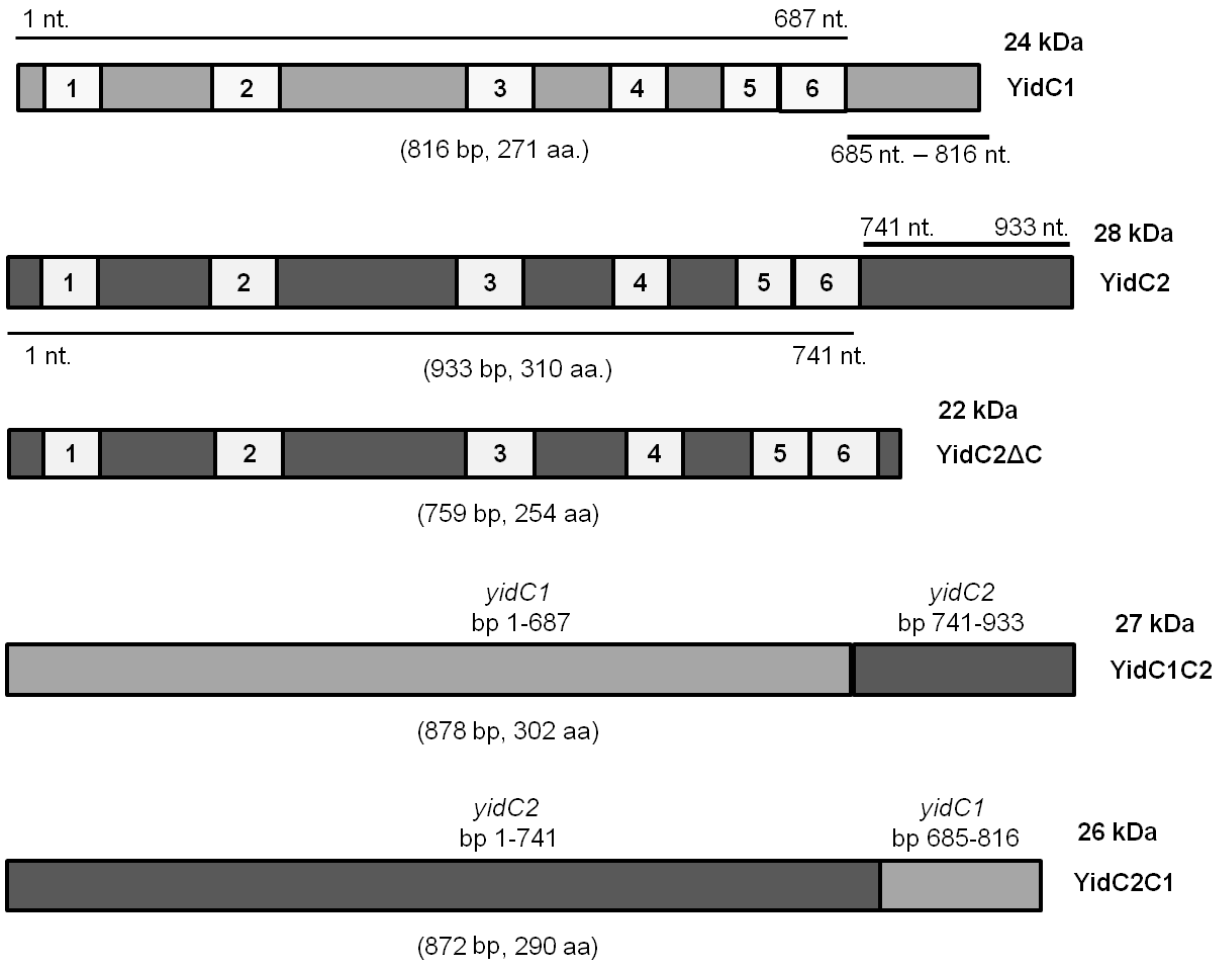

Figure 2-2. Schematic representations of *yidC1*, *yidC2*, and *yidC2*ΔC, and construction of chimeric proteins are shown. YidC1C2 was produced by strain SP13 and YidC2C1 was produced by strain SP14. Transmembrane domains are indicated in white. Predicted sizes in kilodaltons of mature proteins are indicated with the corresponding nucleotide sequences and numbers of amino acids, listed below each construct in parentheses.

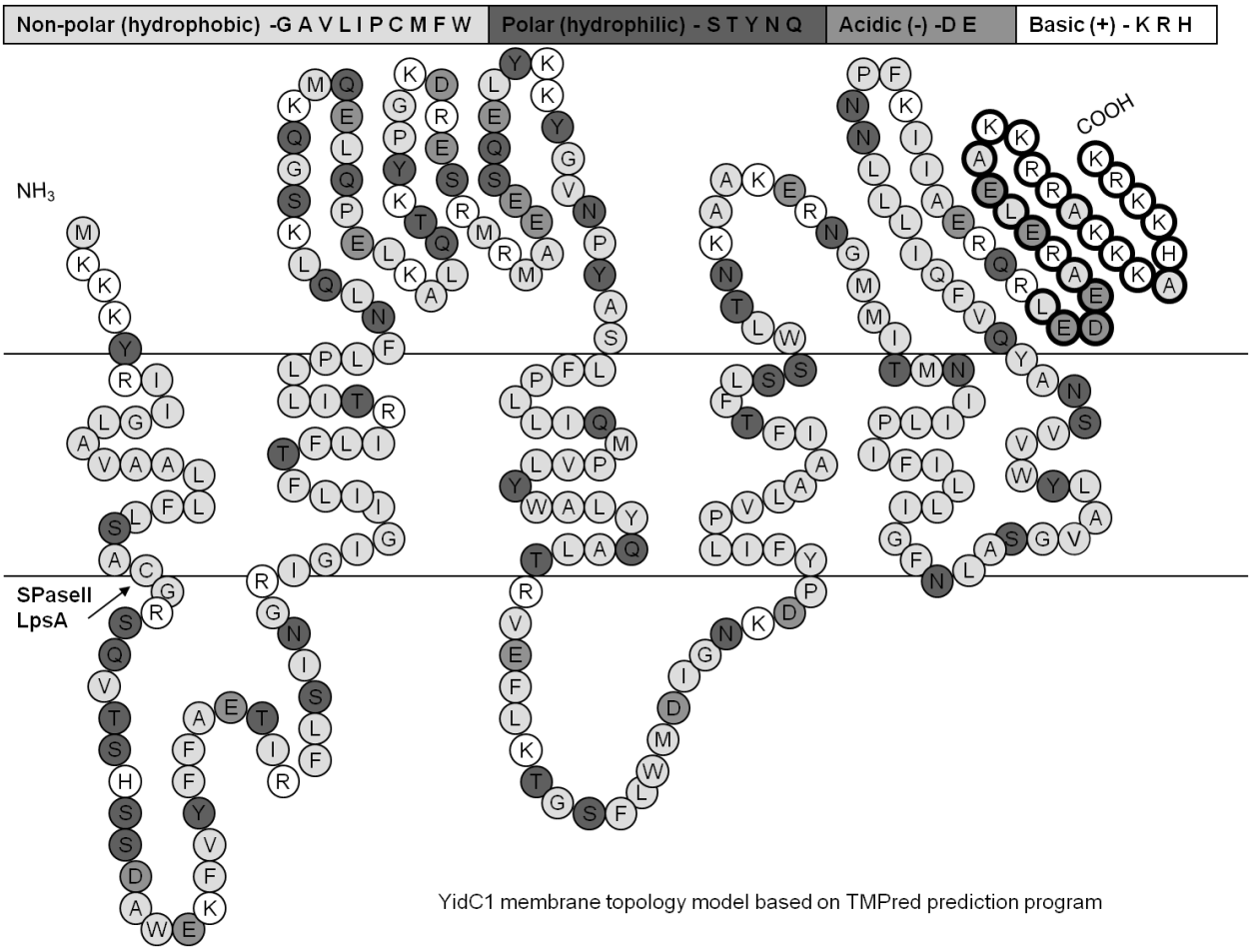

Figure 2-3. Membrane topology model of YidC1 with location of C-terminal peptide used to make C-terminal antiserum. Transmembrane domains are modeled based on the TMPred prediction program. A synthetic peptide corresponding to the amino acids located in bold circles was used to produce rabbit C-terminal peptide antiserum against YidC1. Amino acids are color coded in grey-scale based on chemical properties as indicated by the key at the top of the figure. Predicted SPaseII cleavage site is indicated by an arrow.

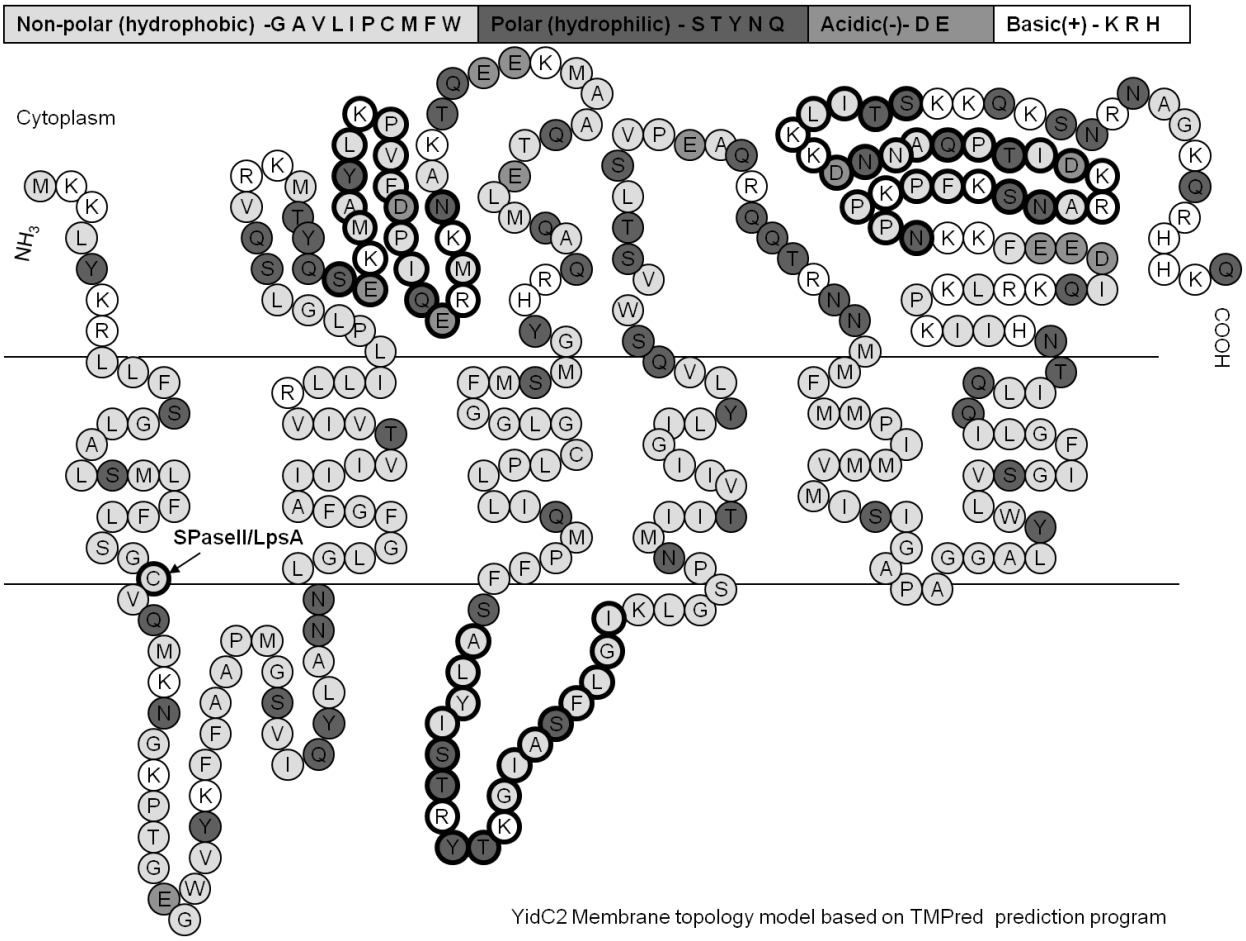

Figure 2-4. Membrane topology model and location of peptides used to make antisera against YidC2. The TMpred prediction program was used to predict the location of transmembrane domains. The predicted SPaseII cleavage site is indicated by an arrow. Residues in bold circles correspond to peptides used to immunize rabbits to produce peptide antibodies. Of the two non-C-terminal peptides, only the one corresponding to cytoplasmic loop between TM 2 and 3 (α-YidC2 TM 2/3) was used in later experiments. The antibody that was produced using the extracellular peptide between TM domains 3 and 4 had only weak reactivity against the *S. mutans* YidC2 protein. The YidC2 C-terminal peptide used to produce C-terminal antiserum is also indicated by bold circles. Amino acids are color coded in grey scale based on chemical properties. See key at top of figure for code.

Table 2-1. Bacterial strains and plasmids used in this study

Strain Name	Relevant Characteristic(s)	Source
Streptococcus mutans		
NG8	Wild-type	Brady lab
AH398	NG8 Δ*yidC2*::*erm*	(31)
AH378	NG8 Δ*yidC2*::*kan*	A. Hasona
AH374	NG8 Δ*yidC1*::*erm*	(31)
AH412	NG8 *yidC2*ΔC$^{255\text{-}310}$::*erm*	(123)
SP01	AH398/pDL289 (Kan^{R}):*yidC2*$^{1\text{-}50}$- *E. coli yidC*$^{59\text{-}548}$	(142)
SP10	AH398 *gtfA*::P$_{celB}$-*yid*C2-*kan*	This study
SP11	AH398::*gtfA::*P$_{celA}$-*yid*C2-*kan*	This study
SP12	NG8 *gtfA*::P$_{gtfA}$::*yid*C1$^{1\text{-}249}$-*yid*C2$^{246\text{-}310}$*::*Erm	This study
SP13	AH378 *gtfA*:P$_{gtfA}$::*yid*C1$^{1\text{-}249}$-*yid*C2$^{246\text{-}310}$*::*Erm	This study
SP14	AH378 *gtfA*:P$_{gtfA}$::*yid*C2$^{1\text{-}247}$-*yid*C1$^{228\text{-}271}$*::*Erm	This study
SP15	NG8 Δ*yidC1*::*spc*	This study
SP16	AH412 Δ*yidC1*::*spc*	This study
SP17	AH378 *gtfA*::P$_{gtfA}$-*yidC2*::*erm*	This study
SP20	SP10 Δ*yidC1*::*spc*	This study
SP21	SP11 Δ*yidC1*::*spc*	This study
SP22	NG8 *gtfA*::*erm*	This study
SP23	SP13 Δ*yidC1*::*spc**	This study
SP24	SP14 Δ*yidC1*::*spc**	This study
SP25	SP01 Δ*yidC1*::*spc**	This study
Plasmids		
pDL289	*E. coli- Streptococcus* shuttle vector; Kan^{r}	(143)
pDL278	*E. coli-Streptococcus* shuttle vector, Spc^{r} (*aad9*)	(137)
pBGK2	*Streptococcus* integration vector *gtf*A locus (same as pBGK, *amp*^{R} was deleted)	(136)
pBGE	*Streptococcus* integration vector *gtfA* locus, genes are expressed from the *gtfA* promoter in the chromosome	(133)
pSP10	pBGK2 with P*celA-yidC2* cloned into *Sma*1 site	This study
pSP11	pBGK2 with P*celB-yidC2* cloned into *Sma*1 site	This study
pCR2.1	T/A cloning vector, *LacZα* multiple cloning site, Amp^{r}, Kan^{r}	Invitrogen
pCR2.1-ΔyidC1SpecR	pCR2.1 with Δ*yidC1::spc* for allelic replacement of *yidC1*	This study

Antibiotics are abbreviated as; erythromycin - Erm, kanamycin- Kan, ampicillin- Amp, spectinomycin- Spc. *Attempts to delete *yidC1* in this background failed or mutants were barely viable. In the case for SP25, mutants took 4 days to grow.

Table 2-2. Oligonucleotides used in this study

Oligonucleotide primers	Sequence 5'-3' a
SP12F	GTCATAGTCAATCCCGGGTTATTTTGATAAAT
SP12R	TTAGACATATGTCTACCTCCTTTTTCTTA
SP13F	CTTCAAATGCCCGGGACATTTAAGATTAAT
SP13R	GTTTTGCCATATGATTCTAATCTCCTTT
SP14F	CAAAGGAAGATTCATATGAAAAAAATTTA
SP05R	GATTAGGTCCCGGGGTTGATAACAGCTT
SP16F	GATGCCAATTCTAGCTTTTATA
SP17F	CAGCAAATGATAAGTCAAAAATA
SP16F RC	TATAAAAGCTAGAATTGGCATC
SP17F RC	TATTTTTGACTTATCATTTGCTG
SP18R	TTAGTTCAACCATAGTCTCTC
SP21F	CCTTATTTAGGCACTCTAGATTTT
SP21R	GCTTCCGTTTGTACATGAGACGAT
SP22FSOE YidC1	TATCAGGTCACAAACCATATCATTAAACCAAAA
SP22RSOE YidC2	ATGGTTTGTGACCTGATAAGCATTTGAGAC
SP27F2*	ACGAGATCTCAGTAAAATAGATAGGTATTATTAA
SP27F2-2	ACGATCTAGACAGTAAAATAGATAGGTATTATTAA
SP27RSOE	CTGGAAGACGATCAATTGTTGGATGAGACCAAA
SP28FSOE	CAATTGATCGTCTTCCAGATTCTGTTGTTAAATAA
SP28R	CGCTGTACACTTTCAATAGCTTCTTCAAC AGTTTT
SP29F	CTGAAGGACGAAGTGTTGCCAAT
SP24RSOE	CATAGTTGTAAGTGCTGCAACAGCTAATCCAAT
SP25FSOE	GCAGCACTTACAACTATGGATATAAAATAGGTA
SP25RSOE	TTGTTCTCCGTTTCCACCATTTTTTCAATTTTT
SP26FSOE	GGTGGAAACGGAGAACAAATCATGGTATTATT
AH25R	CTTTCAACTCCTTCAATGCCAGTAAT
AH31R	AGCTTATTGC-TTATGGTGACGC
SP36F	CGCCAGCCGCAATAAGAACGATT
SP37F	GTGGCTGTTATTTTTAGGTTGAA

[a] Underlined sequences correspond to engineered restriction enzyme sites (6 nucleotides) or overhangs for splice overlap extension (9 nucleotides). *Primer SP27F2 was intended to contain an *Xba*I site, SP27F2-2 was designed to replace SP27F2 and contained an *Xba*I site.

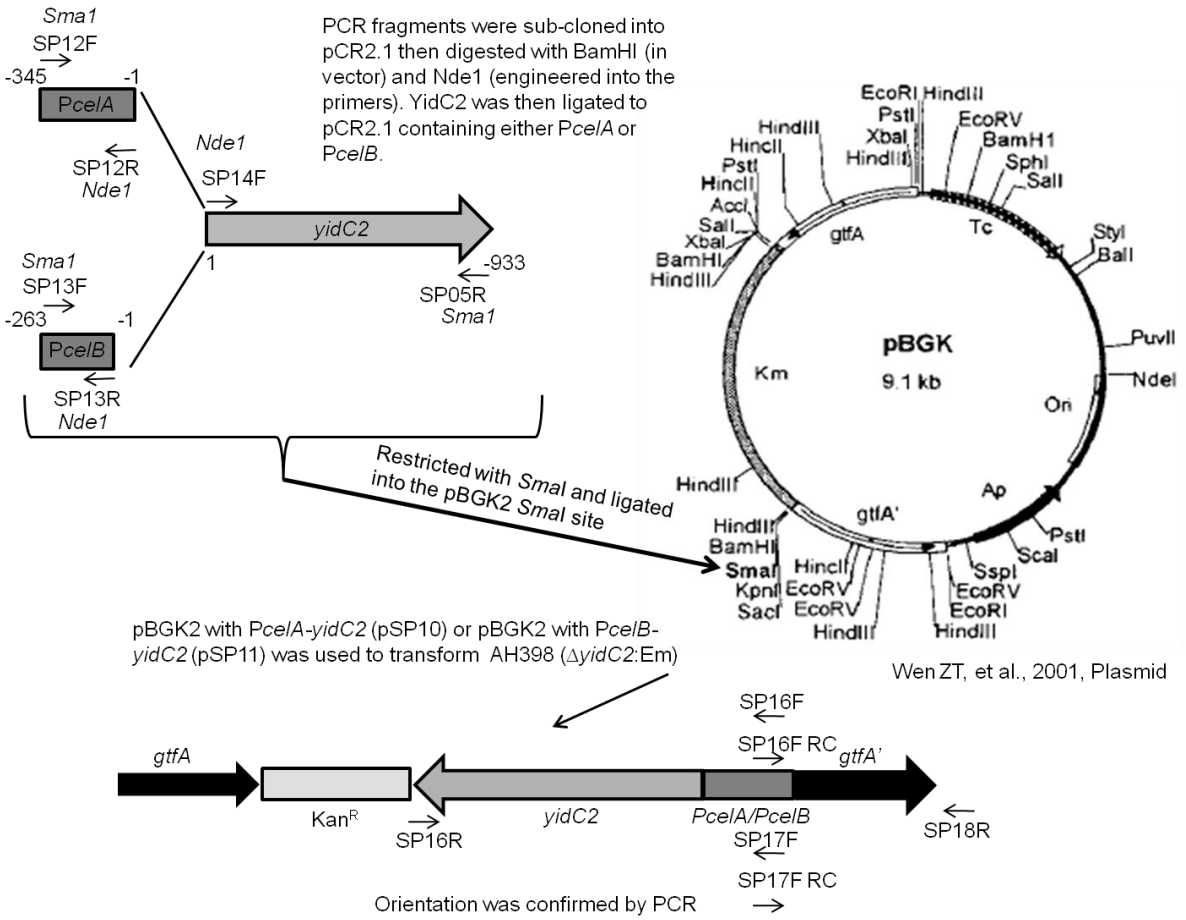

Figure 2-5. Schematic diagram of the construction of promoter fusions of P*celA* and P*celB* with *yidC2* (see text in Materials and Methods for exact protocol). Plasmid pBGK (136) is shown, however the plasmid that was used (pBGK2) had the Ap marker removed for use in streptococci. This plasmid is an integration vector, which places the cloned gene into the *gtfA* locus in the *S. mutans* chromosome through double crossover recombination. The promoter fusions were cloned in the opposite orientation as the *gtfA* gene so there would be no read-through from upstream promoters. The orientation was confirmed by PCR using primers SP16F RC (P*celA*) or SP17F RC (P*celB*) and SP18R, which binds after the stop codon of *gtfA*.

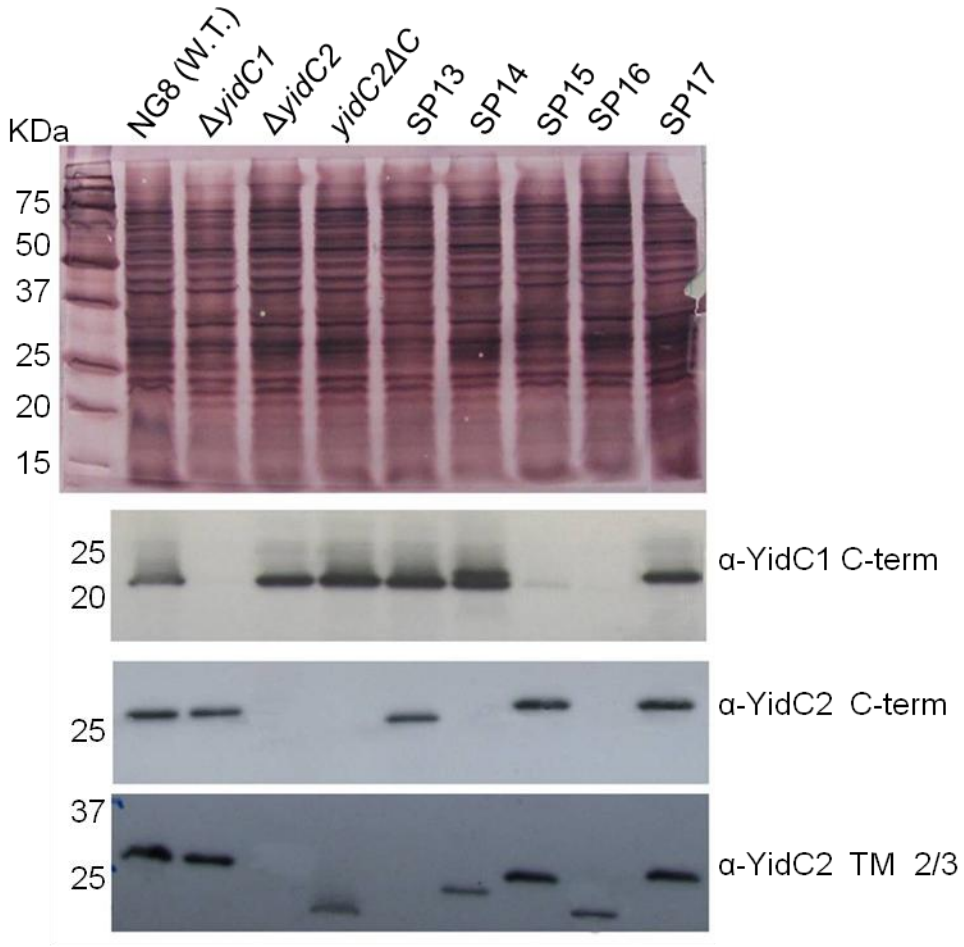

Figure 2-6. Western blot of whole cell lysates of indicated strains reacted with antibodies against YidC1 and YidC2. Top panel shows an Aurodye^{TM} protein stain, used as a loading control. Bottom panels show Western blot results with antisera of the indicated specificity. Strain genotypes are as follows: SP13 - Δ*yidC2 gtfA::yidC1C2*, SP14 - Δ*yidC2 gtfA::yidC2C1*, SP15 - Δ*yidC1*::Spc^{R}, SP16-*yidC2*ΔC, Δ*yidC1*, SP17- Δ*yidC2 gtfA::yidC2.* See Table 2-1 for detailed information.

Table 2-3. Mean doubling times (mins.)[a] of *S. mutans yidC* mutants and complemented strains under non, acid and osmotic stress conditions.

Strain	Genotype	THYE pH 7.0	THYE pH 5.0	THYE 3% NaCl
SP22	NG8 *gtfA::erm*	73±4.7	167±6.6 †	240±17.6
SP17	Δ*yidC2 gtfA::yidC2*	77±1.5 †	285±4.2 * ††	334±27.5
AH378	NG8 *ΔyidC2*::*kan*	114±1.7 *	346±19.4 *	401±24.0 *
AH374	NG8 Δ*yidC1::erm*	77±11.9 †	186±5.6 †	266±27.8 ††
SP13	AH378 *gtfA::yidC1C2*	80±1.5 †	282±19.0 * †††	346±2.7 ***
SP14	AH378 *gtfA::yidC2C1*	171±5.3 * †	390±41.7*	NG
AH412	NG8 *yidC2ΔC::erm*	83±10.0 †	367±0.0*	399±40.0
SP16	AH412 Δ*yidC1::spc*	143±3.2 * †	431±17.8* † €	NG

[a] Doubling times were calculated based on growth curves completed in triplicate in a Bioscreen C 100 well micro-titer plate and OD600 monitored in a Bioscreen C machine. NG indicates no growth. Statistical differences by One-way ANOVA are indicated compared to; SP22 * = P< 0.001, *= P< 0.01, *** = P < 0.05; AH378 †= P<0.001, ††= P< 0.01, †††=P < 0.05; AH412 € =P < 0.05.

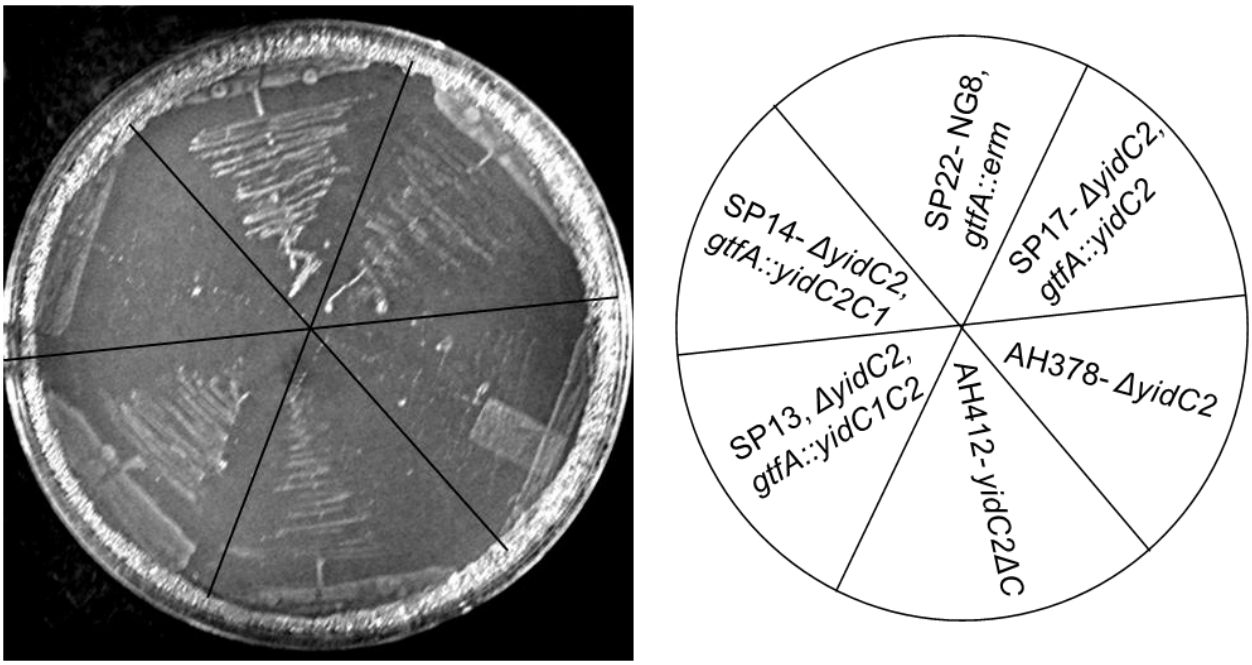

Figure 2-7. Growth on THYE pH 5.0 plates of wild type, Δ*yidC2*, *yidC2*Δ*C S. mutans* and complemented mutant strains. Panel on left shows growth after 48 hour incubation at 37ºC in a 5% CO_2.incubator. Panel on right provides a key for location of strains.

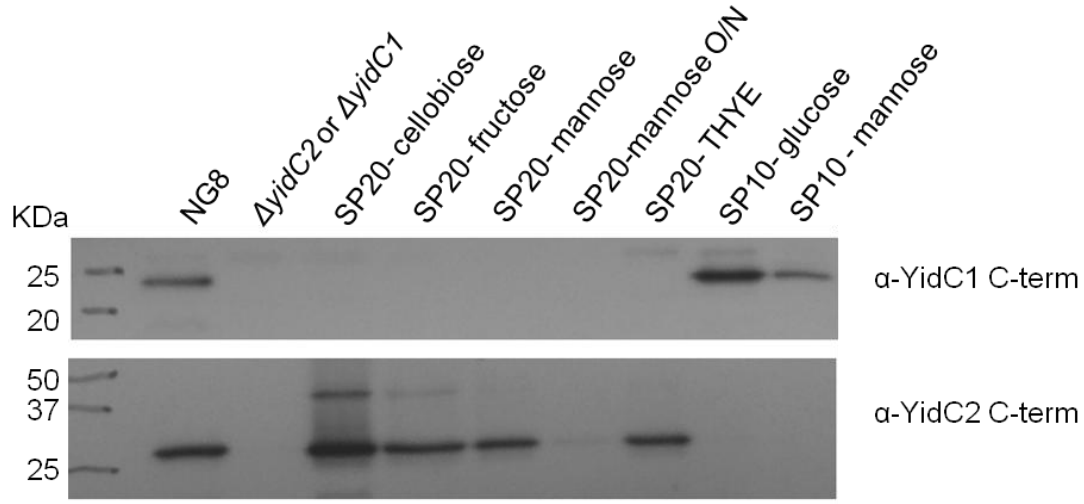

Figure 2-8. Western blots of whole cell lysates from YidC2 depletion strains SP20 and SP10 grown in TDM 0.5% sugar or in THYE. SP10 and SP20 contain promoter fusions of *yidC2* to PcelB. SP20 was made from SP10 by replacing *yidC1* with a spectinomycin marker. NG8, *ΔyidC1* (α-YidC1 C-term control) and *ΔyidC2* (α-YidC2 C-term control) were used as negative controls for antibody reactivity. Western blots were reacted with the indicated antibody and developed by ECL. O/N is an abbreviation for overnight culture.

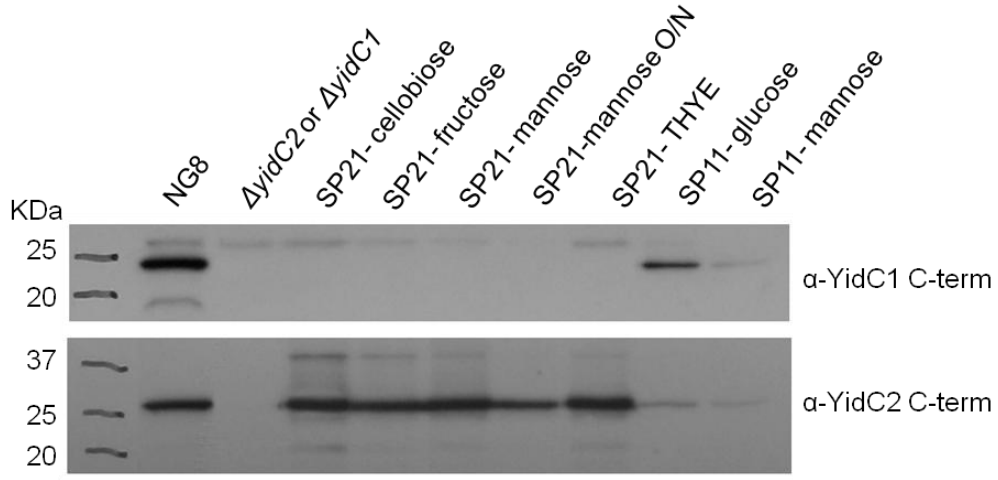

Figure 2-9. Western blots of while cell lysates from YidC2 depletion strains SP21 and SP11 grown in TDM 0.5% sugar or THYE. SP11 and SP21 contain promoter fusions of *yidC2* to P*celA.* SP21 was made from SP11 by replacing *yidC1* with a spectinomycin marker. NG8, Δ*yidC1* (α-YidC1 C-term control) and Δ*yidC2* (α-YidC2 C-term control) were used as negative controls for antibody reactivity. Western blots were reacted with the indicated antibody and developed by ECL.

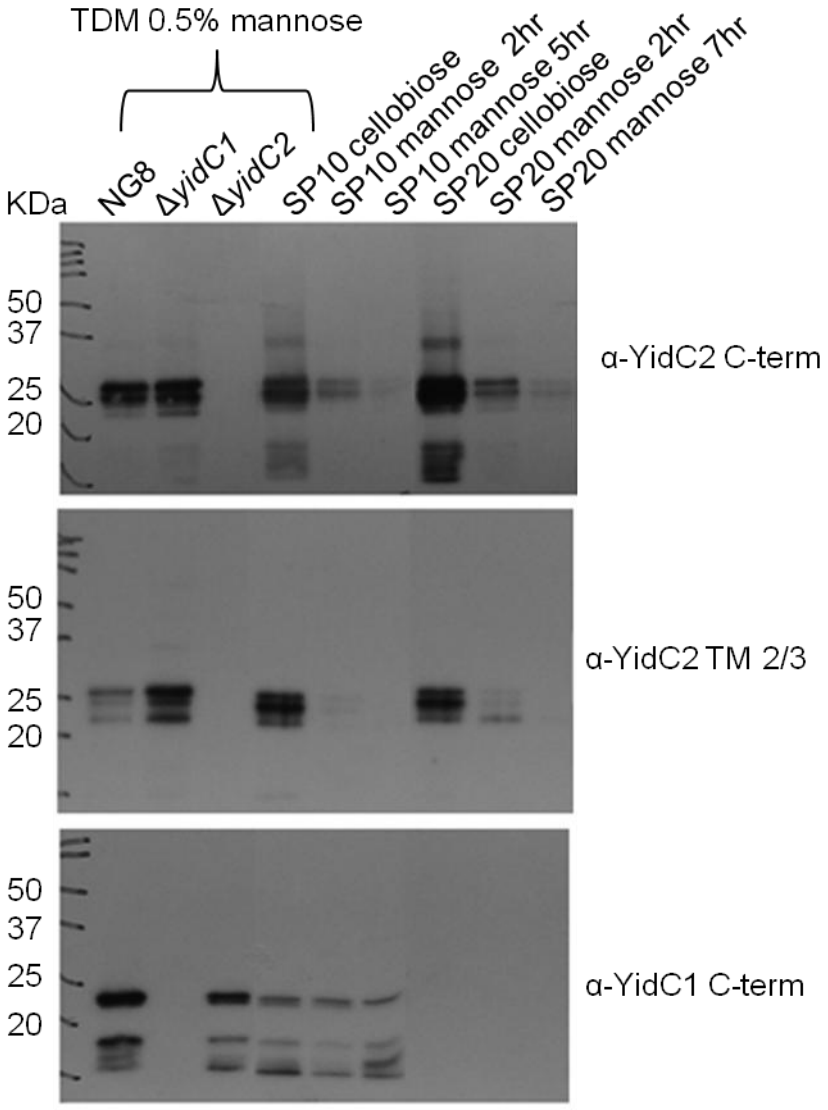

Figure 2-10. Western blots of membrane fractions from YidC2 depletion strains SP10 and SP20 grown in TDM 0.5% sugar. Cells were grown to mid-log phase in the indicated sugar, or in the case of SP10 and SP20 grown in mannose for the indicated times. Proteins were separated on 12% SDS-PAGE gels and reacted with the indicated antisera. When YidC2 expression was high (0.5% cellobiose), an unprocessed 34 kDa band was seen as well as a number of lower molecular weight breakdown products.

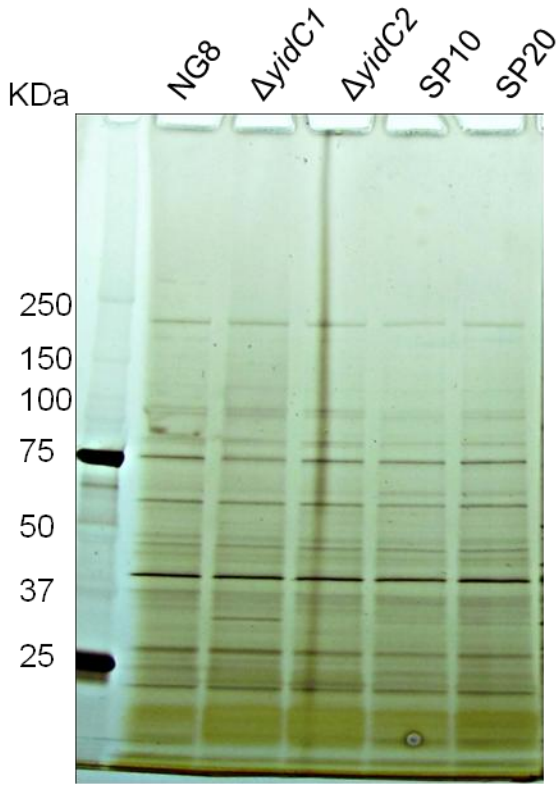

Figure 2-11. Cell wall extracts of *S. mutans* wildtype, *yidC* mutant strains, or YidC2 depletion strains SP10 and SP20. Cells were grown in TDM 0.5% mannose. Extracts were prepared by digestion of the cell wall with mutanolysin and lysozyme. Proteins were precipitated with TCA and separated on a 4-15% gradient Criterion gel and stained using the Silver Stains Plus Kit (BioRad).

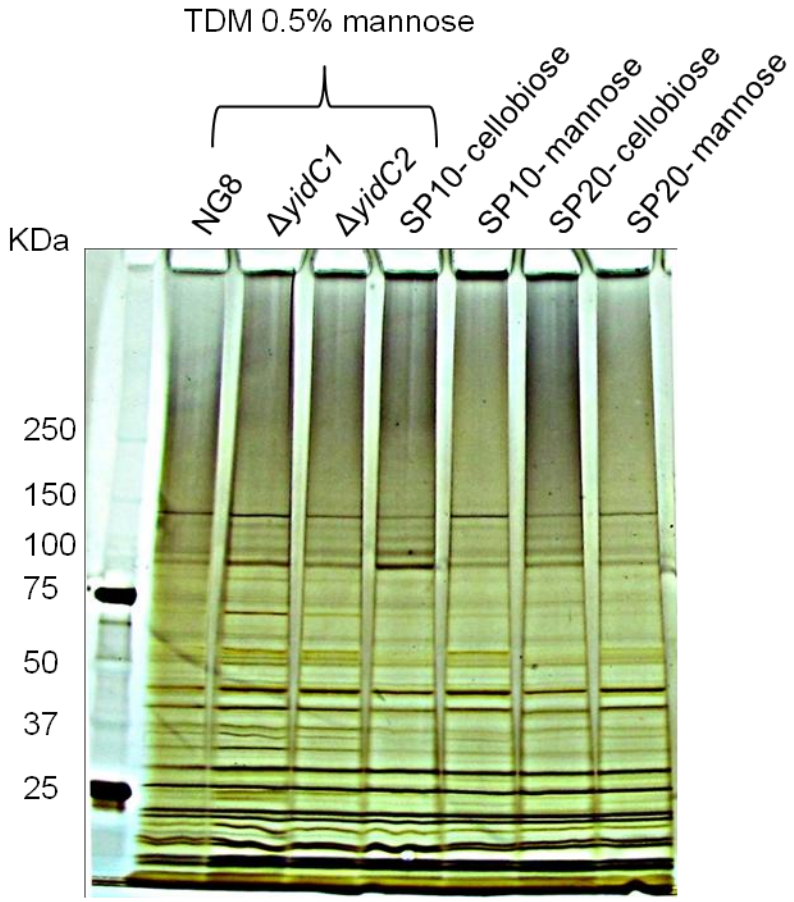

Figure 2-12. Cytoplasmic fractions of *S. mutans* wildtype, *yidC* mutant strains or YidC2 depletion strains SP10 and SP20, grown in TDM 0.5% of the indicated sugar. Proteins were precipitated with TCA and separated on a 4-15% gradient Criterion gel and stained using the Silver Stain Plus kit from BioRad.

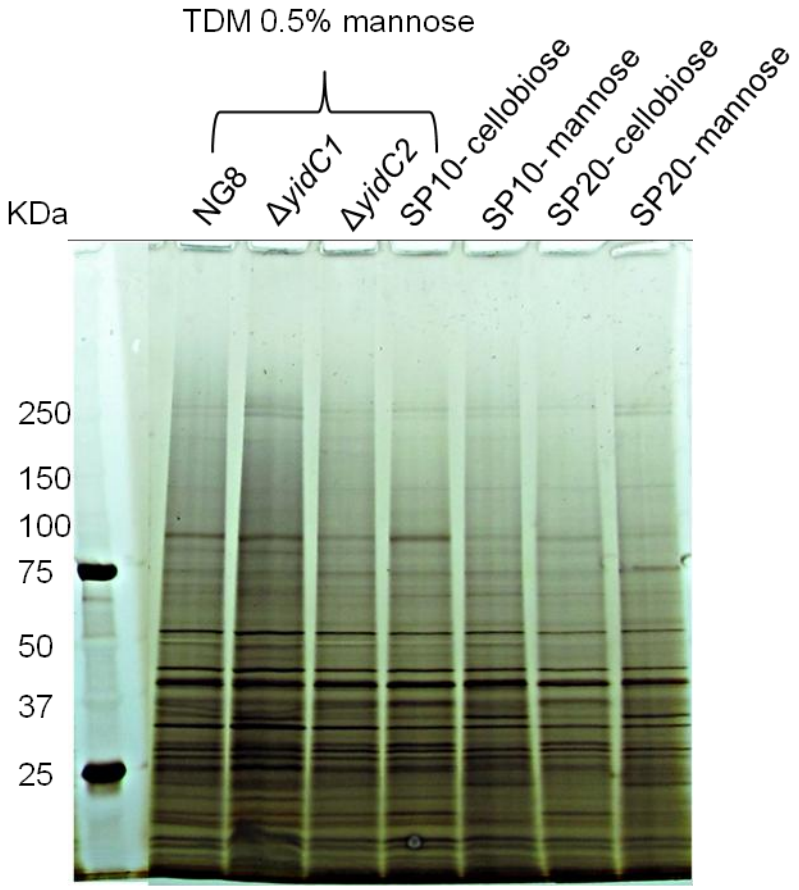

Figure 2-13. Membrane fractions of *S. mutans* wildtype, *yidC* mutants, or YidC2 depletion strains SP10 and SP20. Cells were grown in TDM with 0.5% of the indicated sugar. Proteins were separated on a 4-15% gradient Criterion gel and stained using the Silver Stains Plus kit from BioRad.

CHAPTER 3
EVALUATION OF YIDC1 AND YIDC2'S INVOLVEMENT IN THE ASSEMBLY OF THE F_1F_O ATP SYNTHASE

Rationale for Study

In *S. mutans* the F_1F_o ATPase plays a large role in acid tolerance, by pumping protons out of the cytoplasm. This contributes to maintenance of a hospitable pH for glycolytic enzymes during acid stress conditions created by metabolic end products. The F_1F_o ATPase is also important for maintenance of the proton motive force (PMF). Assembly of the F_1F_o ATP synthase has been studied in *E. coli*, and insertion of the integral membrane components were shown to involve the SecYEG-YidC, SRP, and YidC only pathways (29-30, 144-145). The mechanisms of insertion of the F_1F_o ATPase in *S. mutans* are not known; however mutations of *ffh* or *yidC2* decrease membrane-associated ATPase activity and acid tolerance (31, 74). In previous work a deletion of *yidC1* had no apparent effect on membrane-associated ATPase activity or acid tolerance (31), leading to the hypothesis that in *S. mutans* YidC2 and the SRP pathway are involved in the assembly of the F-ATPase, while YidC1 is not.

In this study, the ability of YidC1 and YidC2 to insert components of the F_1F_o ATPase was evaluated in the *E. coli* YidC depletion strain JS7131 in collaboration with Ross Dalbey at Ohio State University (142). A sequence alignment of the YidC proteins of *S. mutans* and *E. coli* using Clustal W shows that the 5 C-terminal transmembrane domains are conserved (Figure 3-1). Genes were engineered for expression of chimeric proteins of *E. coli* YidC, and YidC1 and YidC2 from *S. mutans*. The membrane topologies of the YidC proteins are shown in Figure 3-2 A. *E. coli* YidC demonstrates six transmembrane (TM) domains and a large periplasmic loop between TM 1 and 2. This architecture is conserved in gram-negative bacteria. YidC1 and YidC2 from *S.*

mutans are predicted to be lipoproteins that are processed by SPaseII, resulting in mature proteins with five transmembrane domains (Figure 3-2 A). To ensure proper membrane targeting in heterologous hosts, chimeric proteins between the *E. coli* YidC, and YidC1 and YidC2 from *S. mutans* were constructed as indicated in Figure 3-2 B. The chimeric *S. mutans* YidC1 and YidC2 proteins were then evaluated for their ability to complement growth in the *E. coli* YidC-depletion strain JS7131 and for their ability to function in the insertion and assembly of F_1F_o ATP synthase subunits in *E. coli.* This was measured by ATP hydrolysis and proton motive force assays at the University of Florida and by protease accessibility assays with model YidC substrates at Ohio State University. Additionally, a chimeric *E. coli* YidC protein was evaluated for its ability to restore stress tolerance to a *yidC2* mutant in *S. mutans.*

The contribution of YidC1 and YidC2 to ATPase activity in membranes and whole cells from *S. mutans* was also evaluated using inverted membrane vesicles and permeablized whole cells. The membranes and permeablized cells were prepared from the strains described in Chapter 2. These produced chimeric proteins YidC1C2 (SP13) and YidC2C1 (SP14), as well as YidC2 lacking the C-terminus (AH412).

Materials and Methods

Chimeric *S. mutans yidC2-yidC E. coli* Construction

All plasmid preps and gel extractions were completed using QIAGEN QIAquick kits. Standard molecular cloning was performed using enzymes and buffers from New England Biolabs. DNA corresponding to amino acids 60-548 of *E. coli* YidC was amplified by PCR using plasmid DNA from pACYC184-YidC (provided by Ross Dalbey, Ohio State University) with vent DNA polymerase and the forward primer SP1F 5' AAACTGCCTAGGGGTTAAGACCGACGTG 3' with an engineered *Avr*II site indicated,

and the reverse primer AH41R 5' TTTCCCGGGTTATTTCTTCTCGCGGCTATG 3' with an engineered *Sma*I site indicated. The resultant 1.4 Kb product was cloned into the Zero Blunt® TOPO® PCR cloning vector from Invitrogen and transformed into Invitrogen chemically competent TOP10® *E. coli* cells. Transformants were screened for orientation by enzyme digestion. A clone with the correct insert orientation was subjected to enzyme digestion using the *Hind*III site in the vector and the engineered *Avr*II site in the PCR product, to release a 1.5-Kb fragment. Next, DNA corresponding to the promoter region and encoding the first 50 amino acids (a.a.) of YidC2 was amplified by PCR using Vent polymerase from *S. mutans* NG8 genomic DNA. The forward primer AH39F 5' CCCGGGAAATAAATGCCAACCTTCAATCA 3' was engineered with a *Sma*I site (underlined) and the reverse primer SP1R 5' AAAACCTAGGGATAACACTTCC-CATTGG 3' with an *Avr*II site. The resulting PCR product was ligated to pACYC184 that had been restricted with *Eco*RV, through a blunt ligation reaction. The ligation product was transformed into Invitrogen chemically competent TOP10® *E. coli* cells. Transformants were screened for insert orientation by enzyme digestion. A clone with the correct orientation was restricted with *Avr*II and *Hind*III followed by gel purification to remove the resulting 80-bp fragment. The 1.5-Kb *Hind*III-*Avr*II fragment, containing the DNA of *E. coli* YidC, was then ligated to the gel purified DNA containing pACYC184 and part of the *yidC2* gene. The chimeric $yidC2^{1\text{-}50}$ $yidC^{EC\ 59\text{-}548}$ (2.2-Kb) gene, encoding the protein 50YidC, was then excised from pACYC184 by *Sma*I digestion and cloned into *Sma*I digested pDL289 (*E. coli* to *Streptococcus* shuttle vector) resulting in plasmid pSP4. The construction was

confirmed by DNA sequencing and pSP4 was transformed into AH398 (*S. mutans* Δ*yidC2* mutant) by electroporation as in (146), to create strain SP01.

E. coli YidC-Depletion Strain JS7131 with pACYC184 *S. mutans yidC1* and *yidC2* Constructs.

Construction of pCR2.1-*yidC1* and pCR2.1-*yidC2*. These plasmids were made by Dr. Adnan Hasona in the Brady lab (University of Florida) for use by Ross Dalbey in the generation of *S. mutans- E. coli* chimeric proteins at Ohio State University. The TOPO TA Cloning® kit from Invitrogen was used to clone *S. mutans yidC1* and *yidC2* into pCR®2.1-TOPO®. *YidC1* and *yidC2* were amplified by PCR from UA159 genomic DNA using the following primers, for *yidC1* AH30F 5' GTGAAAAAGAAATATAGAATT-ATTGGATT 3' and AH30R 5' GAGCCTTCATACGAGAAATACCCA 3' and for *yidC2* AH31F 5' GTGAAAAAAATTTACAAGCGTCTT 3' and AH31R 5' AGCTTATTGCTTATG-GTGACGC 3'. The PCR products were cleaned using QIAGEN QIAquick kits and cloned into pCR®2.1-TOPO® following the manufacturer's directions.

Chimeric *E. coli-S. mutans yidC1* and *yidC2* constructions. Genes encoding chimeric proteins between *E. coli yidC* and *S. mutans yidC1* and *yidC2* were constructed at Ohio State University, in the Ross Dalbey lab. This information was adapted from (142). The pCR®2.1 vector has a *Not*I (compatible with *EagI*) restriction enzyme site shortly upstream of cloned *yidC1* or *yidC2* and an *Eag*I site shortly downstream of them. To construct pACYC184-247YidC1, the *Eag*I fragment from pCR2.1-*yidC1* was inserted into pACYC184-YidC downstream of the *yidC* stop codon, to yield plasmid pACYC184-YidC-YidC1. Additional DNA sequences encoding amino acids after the 247th of YidC and before the 26th of YidC1 were deleted by oligonucleotide-directed loop-out mutagenesis using the Quick Change® method. The

same strategy was used to create pACYC184-YidC1, eliminating the DNA sequences between the 1st amino acid of *E. coli* YidC and the 2nd amino acid of YidC1 in pACYC184-YidC-YidC1. A similar strategy was used to construct pACYC184-247YidC2 and pACYC184-YidC2. To construct pACYC184-YidC1-YidC2, an *Eag*I site was introduced into pACYC184-YidC2 upstream of its *yidC* promoter region (note that the previous *Eag*I site was removed during construction of pACYC184-YidC2). Then the *Eag*I fragment from pACYC184-YidC2 containing the *yidC2* gene was inserted into pACYC184-YidC1 downstream of *yidC1*. Therefore expression of 247YidC1, 247YidC2, YidC1 and YidC2 were all under control of the *E. coli yidC* promoter. Recombinant plasmids were transformed into the *E. coli* YidC depletion strain JS7131 (147).

Growth Curves

***S. mutans*.** Overnight cultures of *S. mutans* wild-type strain NG8, AH374 (Δ*yidC1*), AH398 (Δ*yidC2*), and SP01 (AH398 with pSP4 encoding 50YidC) were diluted 1:20 in THYE, pH 7.0, without antibiotics and grown to an OD_{600} of 0.4. A 100-well Bioscreen C plate (Labsystems, Helsinki, Finland) was filled with 300 µl of pre-warmed media (THYE pH 7.0, THYE pH 5.0 or THYE pH 7.0 with 4% NaCl). Wells were inoculated in triplicate with 30 µl of culture and grown for 16 hours at 37ºC with absorbance at 600 nm recorded every 15 minutes.

***E. coli* YidC Depletion Strain JS7131.** To determine whether *S. mutans* YidC1 or YidC2 could restore growth to the *E. coli* YidC depletion strain JS7131 in broth, cells were grown overnight at 37ºC in LB medium containing 0.2% arabinose. Overnight cultures were diluted 1:10 into fresh LB medium containing 0.2% arabinose and grown

to an OD_{600} of 0.7-0.8. Cultures were washed once with LB (no sugar) and suspended at a 1:20 dilution in LB containing 0.2% glucose. Cultures were grown at 37ºC for 2 hours in order to deplete YidC. After YidC depletion, cultures were diluted 1:25 into fresh LB with 0.2% glucose (repressing sugar), or LB with 0.2% arabinose (inducing sugar). Then 200 µl of each culture was applied in triplicate to a 100 well Bio-screen C plate, which was inserted into a Bioscreen C machine (Labsystems, Helsinki, Finland), set at 37ºC to read OD_{600} every 15 minutes for 5 hours with shaking for 10 minutes in between readings. Spectinomycin (25 µg/ml) and chloramphenicol (50 µg/ml) were used where appropriate.

Growth on LB Agar Plates of *E. coli* JS7131 Expressing *S. mutans* YidC Proteins.

Complementation of growth of JS7131 by *S. mutans* YidC1 and YidC2 and derivatives on LB agar plates was also tested. The YidC depletion strain JS7131 and derivatives were grown at 37ºC overnight in LB medium supplemented with 0.2% arabinose. After being washed twice with plain LB, the overnight cultures were streaked onto LB agar plates containing 0.2% arabinose, or 0.2% glucose, and incubated overnight at 37ºC.

Preparation of Inverted Membrane Vesicles

E. coli. Strain JS7131 harboring *S. mutans yidC1* or *yidC2* constructs was grown in LB medium containing 0.2% arabinose. *E. coli* strain 1100ΔBC was grown in LB medium containing 0.2% glucose. After overnight incubation at 37ºC, bacterial cells were pelleted by centrifugation at 2,500 x g and washed once in LB medium. Cells were re-suspended in plain LB medium and transferred to 1 liter of LB medium with 0.2% glucose supplemented with 50 µg/ml chloramphenicol, and 25 µg/ml

spectinomycin where appropriate. Cultures were grown at 37^{o}C until they reached an OD_{600} of 0.5-0.55 (2.5-5 hours) and then immediately chilled on ice. Bacterial cells were collected by centrifugation at 6,000 rpm at 4ºC for 10 minutes. The cell pellets were washed once in 20 ml TM Buffer (50 mM Tris-HCl [pH 7.5], 10 mM MgSO4) and stored overnight (9 hours) at 4ºC. Inner membrane vesicles were made by the French press method using the procedure from Bhatt et. al., 2005 (148), with a few changes. The cell pellets were suspended in 3 ml TM Buffer and 20 Units of Ambion DNaseI were added. Cells were passed through a Fresh press twice at 12-14,000 PSI. Lysates were then cleared of cell debris by centrifugation at 9,000 rpm (16,000 x g) in a JA-10 Beckman rotor for 10 minutes at 4ºC. Supernatants were then subjected to another round of centrifugation at 9,000 rpm for 10 minutes. The resulting supernatants were again centrifuged at 100,000 x g at 4ºC for 1.5 hours in an ultracentrifuge using a Beckman 70.1 Ti rotor. The membrane pellets were suspended in 1 ml cold TM Buffer using a tissue homogenizer and centrifuged again at 100,000 x g for 1.0 hour. After a final ultracentrifugation step membranes were suspended in 1 ml TM buffer using a tissue homogenizer. Membrane protein concentrations were determined using a standard bicinchoninic acid (BCA) assay with bovine serum albumin (BSA) as the standard. Membranes were stored at 4ºC for up to 36 hours until biochemical assays were performed.

S. mutans. The 10 ml cultures were started from freezer stocks and after 8 hours of growth were used to inoculate 100 ml cultures of BHI (Brain Heart Infusion) broth supplemented with 20 mM DL-threonine, and incubated overnight at 37ºC. The overnight cultures were used to inoculate 1 liter of BHI with 20 mM DL-threonine and

grown to early log phase (OD_{600} 0.45-0.55). Cells were pelleted by centrifugation at 9,000 rpm (16,000 x g) in a JA-10 Beckman rotor for 10 minutes at 4ºC. Cells were washed once in 10 ml Buffer A (10 mM Tris-HCl [pH 6.8], 10 mM Mg acetate, in 25% sucrose), and transferred to a 40 ml tube for a JA-20 Beckman rotor and centrifuged at 10,000 rpm (4,354 x g) for 10 minutes at 4ºC. The pellet was resuspend in 5 ml Buffer A and 200 µl of 10 mg/ml lysozyme (final concentration 0.3-0.4 mg/ml) and 200 µl mutanolysin (10,000 U/ml, 2,000 U or 0.5 mg total) were added. Cells were incubated at 37ºC with gentle agitation for 45 minutes to 1 hour to protoplast cells (protoplast formation was monitored by Gram staining). The protoplasts were pelleted by low speed centrifugation at 6,000 rpm (4,353 x g) in a JA-20 Beckman rotor for 10 minutes at 4ºC and washed twice with 10 ml Buffer A. The pellet was resuspended in 3 ml of Buffer B (50 mM Tris-HCl [pH7.5] and 10 mM $MgSO_4$) and 200 ul of EDTA free protease inhibitor cocktail (Complete - Roche Tablet 25X stock solution), 10 ug/ml of DNase (50ul of DNase1 1mg/ml stock) and 10 µg/ml RNase (50ul of RNase A 1mg/ml stock) were added. Cells were lysed by passage through a French press at 12-14,000 PSI 2–3 times until cells appeared watery. Unlysed protoplasts and cell debris were removed by centrifugation in JA-20 Beckman rotor at 10,000 rpm (12,096 x g) for 10 minutes at 4ºC. Supernatants were transferred to a fresh 40 ml tube and centrifuged again. The resulting supernatant was ultracentrifuged at 100,000 X g (45K rpm) in a SW50.1 rotor for 1.5 hours (or overnight) at 4ºC. The membrane pellet was suspended in 0.5 to 1.0 ml of ice cold Buffer B using a Teflon homogenizer. The protein concentrations were determined by BCA assay, with BSA used as a standard.

ATP Hydrolysis Assays

***E. coli* inverted membrane vesicles.** ATP hydrolysis was determined by measuring the production of inorganic phosphate using a modification of the method of Fiske and Subbarow (149). All reactions were kept at 37ºC, and performed in 3 ml of 9.1 Buffer (50 mM tris-HCl, 1mM $MgCl_2$, pH 9.1) with 120 µg of membrane vesicles. Each strain preparation was assayed in triplicate. Reactions were started with the addition of 80 µl 0.15 M ATP (0.1 M ATP, 25 mM Tris-HCl [pH 7.5]) with a final concentration of 4 mM. Reactions were stopped after 2 minutes, 5 minutes and 7 minutes by adding a 435 µl aliquot of the reaction mix to 2 ml iced Stop Buffer (1.3 parts H_2O, 0.6 parts HCl/molybdate [2.5% $NH_4Mo_4O_2 \cdot 4H_2O$, 4.0 N HCl], 0.4 parts 10% SDS) and vortexing. Inorganic phosphate was measured by adding 100 µl of a 1:10 dilution of Eikonogen solution (1 M $NaHSO_3$, 0.1 M Na_2SO_3, 0.01 M 4-amino-3-hydroxyl-1-napthalenesulfonic acid) followed by incubation at room temperature for 30 minutes. The optical density at 700 nm was read with a spectrophotometer. A standard curve was generated using the following concentrations of phosphate in 1 ml of reaction buffer (9.1 Buffer): 0.02, 0.1, 0.2, 0.4, and 0.6 µmole of Pi (made from dilutions of 2 mM and 20 mM KH_2PO_4 buffers). A 435 µl aliquot of each standard concentration was added to 2 ml of iced Stop Buffer and processed as with samples containing membrane proteins. ATP hydrolysis specific activity was calculated for each membrane sample based on the standard curve and expressed as nMole Pi/min/mg membrane protein. Data was statistically analyzed by One-way ANOVA with Tukey's Multiple Comparison Post-Test using the GraphPad Prism 4.0 program.

***S. mutans* inverted membrane vesicles.** ATP hydrolysis assays with *S. mutans* inverted membrane vesicles were performed essentially the same as with *E. coli*, except each reaction was performed in ATPase Buffer 6.0 (50 mM Bis-Tris-HCL [pH 6.0], 10 mM $MgCl_2$) with 115 µg of membrane proteins. For assays with 50 µM orthovanadate (P-type ATPase inhibitor) membranes were incubated for 5 minutes at 37ºC with the inhibitor before ATP was added to start the reaction. Statistical analysis was calculated using One-way ANOVA followed by Bonferroni's Multiple Comparison or withTukey's Multiple Comparison Post-Tests, performed using the GraphPad Prism 4.0 program.,

Proton Motive Force Assays

The proton motive force (PMF) of inner membrane vesicles of the *E. coli* YidC-depletion strain JS7131 expressing *S. mutans* YidC1 or YidC2 was determined by the fluorescence quenching of 9-amino-6-chloro-2-methoxyacridine (ACMA) as previously described (150). Positive controls included JS7131 rescued with *E. coli* YidC, and the MC1060 wild-type parent strain of JS7131. Negative controls included JS7131 harboring the pACYC184 vector only, and the F_1F_o ATP synthase negative mutant strain 1100ΔBC (151). The assay was performed by adding 500 µg of membrane proteins to 3 ml of MOPS Buffer (50 mM MOPS, 10 mM $MgCl_2$, pH 7.3) in a quartz cuvette with a flea to stir the reaction. The cuvette was placed in the fluorescence spectrometer (Photon Technologies International [PTI], QuantaMaster 4), set to an excitation of 410 nm and an emission at 490 nm, which was recorded by the Felix32 software (PTI) provided with the spectrometer. A zero baseline was recorded for 30 seconds before the addition of 15 µl of 0.2 mM ACMA (final concentration of 1 µM). The reaction was started 45 seconds after ACMA was added by the addition of ATP to a

final concentration of 0.75 mM (15 µl of 0.15 M ATP, 25 mM Tris-HCL, [pH 7.5]). The acidification of the membrane vesicles was determined by monitoring the fluorescence quenching of ACMA for 300 seconds, which was recorded by the Felix32 software. Each trace was then combined in Adobe Photoshop. As a control the integrity of membrane vesicles was determined by the addition of 5 µl 0.1 mM β-nicotinamide adenine dinucleotide (NADH) instead of ATP to each sample and monitoring the fluorescence of ACMA.

Western Blots

Western blots were performed using 40 µg of protein loaded on a 10% SDS-PAGE (Laemmli) gel. Proteins of interest were detected by immunoblotting using the ECL Western blot detection kit (Amersham Biosciences). YidC proteins were identified with antisera from rabbits immunized with C-terminal synthetic peptides from *E. coli* YidC, or *S. mutans* YidC1 or YidC2. Western blots were also reacted with polyclonal antisera against *E. coli* full-length YidC or polyclonal antiserum to Lep (leader peptidase). Antibodies used to recognize YidC1 and YidC2 were described in the Material and Methods of Chapter 2. The C-terminal peptide (CLEKRGLHSREKKK) antiserum against *E. coli* YidC was obtained from Rosemary Stuart at Marquette University. Polyclonal antiserum against Lep was provided by Ross Dalbey at Ohio State University.

ATP Hydrolysis Activity of *S. mutans* Permeablized Whole Cells.

A 25 ml culture of each strain (SP22, AH374, AH378, SP13, SP14, and SP17) was grown to mid-log phase (OD_{600}=~ 0.5) in THYE pH 7.0 at 37ºC. Cells were pelleted and re-suspended in 2.5 ml Buffer B (50mM Tris-HCL, 10 mM $MgSO_4$, pH 7.5) and 250 µl of toluene was added. Cells were vortexed for 20 seconds and incubated in a 37ºC water

bath for 5 minutes. They were then snap frozen in an ethanol dry-ice bath and thawed at 37ºC. This was repeated two times. Cells were then pelleted and suspended in 1 ml of Buffer B and immediately used for ATP hydrolysis assays. For assay, 100 µl of permeablized cells were added to 3.0 ml assay Buffer 6.0 (50 mM Bis-Tris-HCL [pH 6.0], 10 mM $MgCl_2$). After 5 minutes 60 µl of 0.15 M ATP was added (3 mM final concentration). Time point zero was taken approximately 15 seconds later when a 435 µl aliquot was added to 2 ml iced Stop Buffer (1.3 parts H_2O, 0.6 parts HCl/molybdate [2.5% $NH_4Mo_4O_2 \cdot 4H_2O$, 4.0 N HCl], 0.4 parts 10% SDS) and vortexed. Another aliquot was taken at 5 minutes and again at 10 minutes. After all time points were taken, tubes were removed from ice and warmed for 10 minutes at room temperature. Inorganic phosphate was measured by adding 100 µl of a 1:10 dilution of Eikonogen solution (1 M $NaHSO_3$, 0.1 M Na_2SO_3, 0.01 M 4-amino-3-hydroxyl-1-napthalenesulfonic acid) to each tube and incubated at room temperature for 30 minutes. The optical density at 700 nm was read with a spectrophotometer. A standard curve was created from dilutions of 2 mM and 20 mM KH_2PO_4 Buffer (0, 0.02, 0.1, 0.2, 0.4 and 0.6 µMole Pi). Whole cell protein concentration was measure by BCA assay using a 1/50 dilution of permeablized cells. BSA was used as a standard. Statistical differences were determined using Student's t-test.

Results and Discussion

Confirmation of Expression and Membrane Localization of YidC1 and YidC2 Constructs in JS7131

Western blot analysis was performed on 40 µg of membrane proteins from *E. coli* JS7131 grown in LB 0.2% glucose under YidC depletion conditions (Material and Methods), harboring pACYC184 alone or encoding YidC, 247YidC1, YidC1, 247YidC2,

YidC2, and control strains MC1060 (parent strain of JS7131) and 1100ΔBC (F_1F_o ATP synthase negative strain) (Figure 3-3). Western blots were reacted with antisera against C-terminal peptides from YidC, YidC1, and YidC2 and with a polyclonal antiserum against full length *E. coli* YidC that recognized the periplasmic loop included in 247YidC1 and 247YidC2. An antibody against Lep (leader peptidase) was used as a control. As can be seen in Figure 3-3 A, the wild-type copy of YidC was depleted under the assay conditions tested in strains that were producing *S. mutans* YidC1 and YidC2 constructs. Figure 3-3 also shows that 247YidC1 and YidC1 migrate at the predicted size of ~50 kDa and ~24 kDa respectively (Figure 3-3 B), and 247YidC2 and YidC2 at ~60 kDa and ~28 kDa respectively (Figure 3-3 C). Of note, both YidC1 and YidC2 appear to be processed in the *E. coli* background, as they are in *S. mutans*. In Figure 3-3 D, both 247YidC1 and 247YidC2 were recognized by the YidC polyclonal with the expected sized bands at ~50 kDa and ~60 kDa, respectively. Collectively these results indicate that *E. coli* chromosomal *yidC* was repressed under assay conditions and the *S. mutans* YidC1 and YidC2 protein constructs were produced appropriately.

Restoration of Growth of the *E. coli* YidC-Depletion Strain JS7131 by *S. mutans* YidC1 and YidC2 in Broth

Growth curves of strain JS7131 containing pACYC184 encoding either wild-type YidC from *E. coli*, or YidC1/YidC2, YidC1, YidC2, 247YidC1, or 247YidC2 are shown in Figure 3-4 and mean doubling times are shown in Table 3-1. As a negative control, the pACYC184 vector alone was also included. Cultures were grown in LB medium containing 0.2% glucose (YidC repressing conditions) or 0.2% arabinose (condition where *yidC* is expressed from the chromosome by way of the araBAD promoter). When strains were grown in the presence of 0.2% arabinose all strains grew similarly

regardless of which gene was expressed from pACYC184. However, when strains were grown in the presence of 0.2% glucose, in which expression of the chromosomal copy of *yidC* is repressed, a differential in growth was seen, with the vector only control displaying the slowest growth (doubling time, 175.1±1.83 minutes) and the strain producing wild-type YidC growing the best (doubling time, 89.7 ±0.4 minutes). Expression of *S. mutans yidC1* (128.3±1.0 minutes) and *yidC2* (116.9 ±4.4 minutes) improved growth of JS7131 above the vector only control, even in the absence of the 247 periplasmic loop from *E. coli* YidC. Growth of JS7131 was improved more by 247YidC1, than by YidC1 without the periplasmic loop (107.1±2.1 minutes compared to 128.3±1.0), while there was little difference between 247YidC2 and YidC2 without the periplasmic loop (112.0±1.4 minutes compared to 116.9±4.4). Co-expression of both *yidC1* and *yidC2* together did not show improvement over expression of *yidC2* alone (113.7±1.2 minutes compared to 116.7±4.4).

Complementation of JS7131 Growth by *S. mutans* YidC1 and YidC2 on Solid Media

Growth on solid media, which presents a different set of challenges from growth in broth culture, of JS7131 containing plasmids encoding the *S. mutans* YidC1 and YidC2 constructs was also evaluated. Strains were grown overnight in 10 ml LB medium with 0.2% arabinose. Cells were pelleted and washed twice with 10 ml LB without sugar, before being streaked on LB agar plates supplemented with 0.2% arabinose or 0.2% glucose. Figure 3-5 shows growth of JS7131 producing *S. mutans* YidC1, YidC2 or chimeric constructs on LB agar plates. Under these conditions only constructs producing 247YidC2 and 247YidC1, and to a lesser extent YidC1 and YidC2 together were, able to restore growth to JS7131 on LB 0.2% glucose agar plates. Given the

results in broth cultures, this was somewhat surprising, but suggests a functional requirement of the periplasmic loop of YidC that can be overcome by co-expression of YidC1 and YidC2.

Rescue of F_1F_o ATPase Activity and PMF in JS7131 by *S. mutans* YidC1 and YidC2

The membrane ATPase activity in *E. coli* is associated primarily with the F_1F_o ATP synthase. In the absence of the F_1F_o ATPase, background ATPase activity is quite low, with roughly 300 nMol Pi/min/mg compared to 2,440 nMol Pi/min/mg in its presence (152). ATP hydrolysis is mediated by the F_1 portion of the enzyme, and is greatest under conditions when the F_1 is not attached to the F_0 (personal communication, Dr. Brian Cain). Inverted membrane vesicles were prepared from the *E. coli* YidC-depletion strain JS7131 containing the various *S. mutans* YidC1 and YidC2 constructs expressed from a plasmid and grown under repressing conditions for *yidC* (LB 0.2% glucose). The ATP hydrolysis activity of the membrane vesicles was measured in pH 9.1 Buffer, so that disassociation of the F_1 would occur and higher ATPase activity could be measured. The results of the ATP hydrolysis activity assays are shown in Figure 3-6. The YidC-depletion strain JS7131 harboring the vector only had 772±84 nMol Pi/min/mg protein of ATP hydrolysis activity. When JS7131 was complemented with *E. coli* YidC, the specific activity was restored to 1,225± 91 nMol Pi/Min/Mg. Both YidC1 (964±64 nMol Pi/Min/Mg) and 247YidC1 (1,159±120 nMol Pi/min/mg) improved the ATP hydrolysis activity compared to the vector only. Similarly, expression of YidC2 also restored specific activity (1081±101 nMol Pi/Min/Mg), which was comparable to 247YidC2 (1060±68 nMol Pi/Min/Mg). Therefore, in the case of ATP hydrolysis, both YidC1 and YidC2 were able to complement the *E. coli* YidC-depletion strain JS7131.

The function of the F_1F_o ATPase is directly related to the generation of a PMF in *E. coli*, which is generated by the translocation of protons through the F_o channel coupled to ATP hydrolysis by the F_1. Therefore another way to evaluate the insertion and function of the F_1F_o ATP synthase is by measuring the PMF of inverted membrane vesicles. There is no PMF generated in an F_1F_o ATPase mutant. The same inverted membrane vesicles used for ATP hydrolysis assays were used for PMF assays. The results for the PMF assays are shown in Figure 3-7. Both YidC1 and YidC2 functioned to insert and assemble components of the F_1F_o ATP synthase in *E. coli* and similar to the *E. coli* YidC, were able to restore the PMF above the vector only control. The restoration of PMF was not improved by appending the first 247 amino acids of *E. coli* YidC onto either YidC1 or YidC2.

To look at insertion of the individual subunits of the F_o complex by the YidC proteins from *S. mutans*, protease accessibility assays were performed at Ohio State University, by Yuxia Dong in Ross Dalbey's lab. In these assay protoplasts from the various JS7131 strains overexpressing the protein subunit of interest in the presence of a radiolabel, were exposed to proteinase K (PK) digestion, followed by immunoprecipitation of the protein subunits. If the protein was properly inserted into the membrane it was processed by PK, producing a smaller fragment, which was then visualized by phosphorimaging. The results from these experiments, which can be viewed in Dong and Palmer, et. al. 2008, Figure 4 (142), show that 247YidC1, 247YidC2, or YidC1/YidC2 together can each function to insert the "a" and the "c" subunits of the F_1F_o ATP synthase. The ability of *S. mutans* 247YidC1 and 247YidC2 to insert substrates not found in *S. mutans*, such as CyoA of cytochrome *bo* oxidase (94,

153) and a derivative of phage coat protein M13 (PClep), was also observed using protease accessibility assays. In these experiments 247YidC1, 247YidC2, or YidC1/YidC2 together were able to insert CyoA-N-P2 and PClep into the membrane of *E. coli,* Figure 6 (142).

E. coli* YidC can Restore Acid and Salt Tolerance to a *yidC2* Mutant in S*. mutans

The *yidC2* mutant of *S. mutans* displays a stress-sensitive phenotype, which is manifested by impaired growth at pH 5.0 or with 4% NaCl (31). The ability of *E. coli* YidC to complement this phenotype was evaluated in broth culture. For this purpose a chimeric gene was engineered (see Figure 3-2 for diagram of construction) that encodes the first N-terminal 50 amino acids of YidC2, including the targeting domain and SPaseII cleavage site, was appended to amino acids 59 to 548 of *E. coli* YidC (referred to as 50YidC) was engineered and expressed from plasmid pDL289 (*E. coli* to Streptococcal shuttle vector) under the control of the *yidC2* promoter (plasmid pSP4, Table 2-1). The recombinant plasmid was then used to transform the *yidC2* mutant strain AH398, resulting in strain SP01. SP01 was evaluated by growth curve under non-stress (THYE pH 7.0), acid-stress (THYE pH 5.0) and osmotic-stress (THYE, 4% NaCl) conditions. As shown in Figure 3-8, 50YidC was able to restore acid- and salt-tolerance to a Δ*yidC2* mutant of *S. mutans.* Figure 3-9 shows Western blot results with α-YidC1, α-YidC2, and α-YidC C-terminal antibodies, indicating appropriate expression of YidC1, YidC2 and the 50YidC protein in the Δ*yidC2* mutant background. When *yidC1* was deleted from this strain to produce SP25, mutants were barely viable and took three days to grow (data not shown). This indicates that while introduction of *E.*

coli YidC into the *ΔyidC2* strain was able to complement the stress sensitivity of the *yidC2* mutant, it could not do so in the absence of *yidC1.*

Involvement of *S. mutans* YidC1 and YidC2 in Membrane ATPase Activity

In order to measure membrane-associated ATPase activity in *S. mutans*, inverted membrane vesicles were made by first removing the cell wall through enzyme digestion (see Materials and Methods for details). Cells were broken by passage through a French press resulting in inverted membrane vesicles, which were isolated by high speed ultracentrifugation. ATP hydrolysis activity was determined by measuring the production of inorganic phosphate in the presence of ATP, as described above for *E. coli* membranes. However, reactions were performed in pH 6.0 Buffer instead of 9.1, because *S. mutans* F-ATPase functions optimally at pH 6.0. Also, it is not known if S. mutans F_1F_o ATPase displays the same properties as the *E. coli* F_1F_o ATPase in the presence of basic buffer. ATP hydrolysis assays were performed with or without 50 μM orthovanadate (a P-type ATPase inhibitor) using membranes from wild-type NG8, and *ΔyidC1*, and *ΔyidC2* mutants (Figure 3-10). There was a significant decrease in membrane-associated ATPase activity in both *yidC* mutants ($P< 0.01$, by ANOVA with Bonferroni's Multiple Comparison Test), with specific activities of 100 nMol Pi/min/mg protein in Δ*yidC1* (37% decrese) and 90 nMol Pi/min/mg protein in Δ*yidC2* (44% decrease), compared to NG8 membranes (160 nMol Pi/min/mg protein). There was a slight but not significant decrease (13%) in NG8 specific activity in the presence of the P-type inhibitor orthovanadate with a specific activity of 140 nMol Pi/min/mg protein. However, there was no inhibition in either of the *yidC* mutants' specific activities in the presence of P-type inhibitor. This suggests that the decrease seen in membrane-

associated ATPase activity in the mutants may be due in part to improper insertion of P-type ATPases as well as the F-type ATPase.

Membrane-associated ATPase assays were also performed on a panel of strains that were designed to evaluate the function of the C-terminal tails of YidC1 and YidC2 and described in Chapter 2. These included SP17, a Δ*yidC2* mutant complemented with YidC2, SP13 (Δ*yidC2* containing YidC1C2), and SP14 (Δ*yidC2* containing YidC2C1). Strain AH412, which has a chromosomal deletion of the C-terminal tail of *yidC2*, and SP22, which has an Erm^R marker inserted into the *gtfA* gene and thus serves as a control (Table 2-1 for strain details), were also included. Results are shown in Figure 3-11. Strain SP22 had the greatest level of specific activity with167±12 nMol Pi/min/mg protein, while strain AH412 had the lowest level of ATPase activity with 87± 0.6 nMole Pi/min/mg protein. Strain AH378 showed a significant decrease ($P < 0.01$) in activity compared to SP22 with a specific activity of 123±5 nMol Pi/min/mg protein. This activity was significantly restored in the presence of YidC1C2 (SP13) with 155±6 nMol Pi/min/mg protein ($P < 0.05$). Strain SP14, which contains YidC2C1, had similar ATPase activity to the *ΔyidC2* strain AH378 with 128±14 nMol Pi/min/mg. The positive control strain SP17, which contained a full-length wild-type version of YidC2 in the *gtfA* locus of the *ΔyidC2* background, had a specific activity of 136±8 nMol Pi/min/mg, which was not significantly different from the AH378 strain's specific activity of 128±14 nMol Pi/min/mg protein, nor was it significantly different from the positive control strain SP22 (analyzed by One-way ANOVA with Turkey's Multiple Comparison Test). However, this was not the complete level of complementation that would be expected for the wild-type YidC2 protein. To rule out contamination of cultures and confirm the proper level of

expression of chimeric proteins, Western blots were performed on the membrane samples used in these experiments. For Western blots 5 µg of membranes from each sample were separated on a 12% SDS-polyacrylamide gel, transferred to PDVF membranes and reacted with α-YidC2 C-terminal, α-YidC2 TM 2/3 and α-YidC1 C-terminal antibodies (Figure 3-12). Results show the expected reactivity with the α-YidC2 C-terminal and α-YidC1 C-terminal antibodies as seen in Figure 2-6. However, reactivity was weak in strain SP17 with the α-YidC2 TM 2/3 antibody (middle panel Figure 3-12), which recognizes a cytoplasmic loop of the YidC2 protein (Figure 2-3). A problem with expression can be ruled out since reactivity of the SP17 strain with the α-yidC2 C-terminal antibody was similar to that of the SP13 strain. DNA sequencing revealed no mutation is the y*idC2* gene from freshly grown SP17 cells. The ATP hydrolysis assay was repeated using permeablized whole cells instead of inverted membrane vesicles, which are technically more difficult to prepare. Results of ATPase assays of permeablized whole cells are shown in Figure 3-13. This time strains SP22, AH374, AH398, SP17, SP13 and SP14 were compared. While the ATPase activities of permeablized cells were lower in all strains compared to the activities of inverted membrane vesicles (Figure 3-10 and 3-11), the expected differential in activity between the control strains was similar to previous experiments. Strain SP22 (wildtype) had a specific activity of 70±8 nMol Pi/min/mg, while both *yidC* mutants had significantly less activity, AH374 (*ΔyidC1*) with a specific activity of 51±10 nMol Pi/min/mg ($P < 0.05$, by Student's t-test), and AH378 (*ΔyidC2*) with 30±4 nMol Pi/min/mg ($P < 0.01$) of specific activity. Strain SP17 (Δ*yidC2*, gtfA::*yidC2*) had 49±7 nMol Pi/min/mg of specific activity, which was significantly higher ($P< 0.05$) than AH378. Strain SP13 (Δ*yidC2*,

gtfA::*yidC1C2*) also had a specific activity which was significantly higher than AH378 (42±5 nMol Pi/min/mg, $P < 0.05$), while SP14 (Δ*yidC2*, gtfA::*yidC2C1*) had a specific activity of 32±5 nMol Pi/min/mg, which was comparable to the *ΔyidC2* mutant, AH378.

In summary, YidC1 and YidC2 from *S. mutans* were expressed in the *E. coli yidC* depletion strain JS7131 and evaluated for their ability to complement for growth (in broth and on solid media), restore ATP hydrolysis activity and PMF associated with a functional F_1F_o ATPase enzyme, as well as to insert the "a" and "c" subunits of the F_o integral membrane component of the F_1F_o ATP synthase. Both YidC1 and YidC2 were able to restore growth to JS7131 under YidC depletion conditions in broth (Figure 3-4). However, only the construct that contained both YidC1 and YidC2 or the chimeric versions of YidC1 or YidC2 (247YidC1 and 247YidC) in which the first 247 amino acid of *E. coli* YidC were appended, were able to restore growth on LB 0.2% glucose agar plates (Figure 3-5). In addition, both YidC1 and YidC2 were able to restore ATP hydrolysis activity to the YidC-depletion strain JS7131 (Figure 3-6). PMF was restored by YidC1 and YidC2, as well as the chimeric versions (247YidC1 and 247YidC2), to the same extent as with wild-type *E. coli* YidC.

When a chimeric version of *E. coli yidC* encoding amino acids 59-548 of YidC, was appended to *S. mutans* DNA incorporating the *yidC2* promoter and encoding the N-terminal first 50 amino acids of YidC2, including the signal sequence and lipoprotein processing signal, and the chimeric gene was expressed from a plasmid in the *ΔyidC2* mutant, tolerance to acid and osmotic stress was restored (Figure 3-8). This complementation is probably the result of cooperation between YidC1 and the 50YidC chimeric protein, since 50YidC could not complement a double deletion of *ΔyidC1* and

ΔyidC2. Also of note, when surface adhesin P1 was evaluated in this strain, a dominant-negative effect was seen, with barely any P1 detected on the surface of cells as analyzed by whole cell dot blot with a battery of monoclonal antibodies and polyclonal antiserum that recognize P1 (unpublished data). This suggests that the translocation machinery involved with P1 secretion was impeded by the presence of 50YidC. As mentioned earlier, deletion of *yidC1* results in increased anti-P1 immunoreactivity and hyper-adherence of *S. mutans* to salivary agglutinin, while deletion of *yidC2* decreases adherence and affects only some of the monoclonal antibodies, including those that recognize epitopes associated function. This suggests that YidC2 directly or indirectly contributes to the translocation and maturation of P1, and that balanced expression of YidC1 and YidC2 participate in cell surface biogenesis in *S. mutans.* The pronounced inhibitory effect of 50YidC on P1 immunoreactivity and function suggests that it may act as a sink for critical components of the translocation machinery while not supporting transport of cell surface localized proteins in this organism.

The contribution of YidC1 and YidC2 to membrane-associated ATP hydrolysis activity was evaluated in *S. mutans*, using a panel of mutants and complemented strains (Table 2-1). Inverted membrane vesicles prepared from wild-type NG8, Δ*yidC1* and Δ*yidC2* were evaluated for ATP hydrolysis activity with or without the P-type inhibitor orthovanadate (Figure 3-10). Both *yidC* mutants displayed significantly less membrane-associated ATPase specific activity than wild-type NG8, with only 63% of wildtype activity in *ΔyidC1* and 56% in *ΔyidC2.* Pre-incubation with orthovanadate had a modest but effect on wildtype ATPase activity, with 13% reduction in activity. There

was no effect on ATP hydrolysis activity of either *yidC* mutant. This suggests that YidC1 and YidC2 may be involved with insertion of P-type ATPases as well as F-type ATPases.

The ability of chimeric YidC1 and YidC2 proteins in which the C-terminal domains were swapped to restore membrane-associated ATPase activity to the *ΔyidC2* mutant was evaluated. Placing the C-terminal tail of YidC2 onto YidC1 (SP13) conferred on YidC1 an ability to significantly increase ATPase activity in the Δ*yidC2* mutant. However, when the C-terminal tail of YidC1 was placed onto YidC2 (SP14), no complementation was observed for ATPase activity (Figure 3-11 and 3-13) and growth was negatively affected further (Table 2-3). ATPase activity was also measured in the mutant and in the Δ*yidC2* mutant complemented with wild-type YidC2 (Figure 3-11). In this experiment ATPase activity of *yidC2ΔC* (AH412) was less than Δ*yidC2* (AH378), again indicating that the C-terminal tail plays an important role in this particular function of YidC2. The complemented mutant strain SP17 was evaluated in two ways for ATP hydrolysis activity, once using inverted membranes and once using permeablized whole cells. The assay performed with inverted membranes did not demonstrate full restoration of membrane ATPase activity to the *yidC2* mutant, as would be expected. Upon further evaluation of the membranes used in this experiment, it was noted that the SP17 sample showed decreased reactivity with a non C-terminal antibody against YidC2 (Figure 3-12). This antibody recognizes an epitope within the cytoplasmic loop between transmembrane domains 2 and 3 (Figure 2-3). Reactivity with the YidC2 C-terminal antibody was as expected (Figure 3-12). DNA sequencing of the *yidC2* gene in SP17, prepared from the original freezer stock indicated no mutations. When ATPase

assays were repeated using freshly grown permeablized whole cells (Figure 3-13), SP17 displayed improved ATP hydrolysis activity, but again not to wildtype levels. This may be due to the use of the *gtfA* promoter instead of the *yidC2* promoter to express the *yidC2* gene. Possibly the level or temporal aspects of *yidC2* expression contribute to proper integration and function of YidC2 within the membrane. It was recently shown that *yidC2* expression is upregulated under conditions that cause an envelope-stress response through the LiaFSR two-component system (45). It is possible that *yidC2* expression is regulated in other situations and by other TCSs. Alternatively a specific level of YidC2 may be required to restore ATP hydrolysis activity to wildtype levels. In future work,the *yidC2* gene including its own promoter should be placed into the *gtfA* locus in the *ΔyidC2* strain, as was done for *PcelB-yidC2*, and evaluated for ATP hydrolysis activity to determine if the promoter makes a difference in complementation. It would also be informative to test the effect of expressing the *yidC1* gene from the *yidC2* promoter.

```
YidC        NENLNISSKGGWVAMLQQYFATAWIPHNDGTNNFYTANLGNGIAAIGYKSQPVLVQPGQT 300
YidC2       SMLFFLSGCV-------------------------------------------------QMKN 29
YidC1       AALLFLSACG-------------------------------------------------RSQV 26
               : :*.                                                     :

YidC        GAMNSTLWVGPEIQDKMAAVAPHLDLTVDYGWLWFISQPLFKLLKWIHSFVGNWGFSIII 360
YidC2       GKPTGEGWVYKFFAAPMGSVIQYLANNLGL----------------------GFGFAIII 67
YidC1       TSHSSDAWEK--FVYFFAETIRFLSING------------------------RIGIGIIL 60
               ..  *    :   :. .  .*  .                           *:.**:

YidC        ITFIVRGIMYPLTKAQYT----SMAKMRMLQPKIQAMRERLG-----DDKQRISQEMMAL 411
YidC2       VTVIVRLLILPLGLSQVRKMTYQSEKMAYLKPVFDPIQERMKNAKTQEEKMAAQTELMQA 127
YidC1       FTFLIRTILLPLFNLQLK----SGQKMQELQPELKALQTKYP-GKDRESRMRMAEESQEL 115
            .*.::* :: **   *      .  **  *:* :..:: :       :.:     *

YidC        YKAEKVNPLGGC--FPLLIQMPIFLALYYMLMGSVELRQAPFALWIHDLSAQDPYYILPI 469
YidC2       QRHYGMSMFGGLGCLPLLIQMPFFSALYISTRYTKGIASA--SFLGIKLGS--PNMIITV 183
YidC1       YKKYGVNPYASL--FPLLIQMPVLWALYQALTRVEFLKTG--SFLWMDIGNKDPYFILPV 171
             :   :.  ..   :*******.: ***        :  .  ::   .:.   *  *:.:

YidC        LMGVTMFFIQKMSPTTVTDPMQ---QKIMTFMPVIFTVFFLWFPSGLVLYYIVSNLVTII 526
YidC2       IIGILYLVQSWVSTLSVPEAQRQQTRNMMFMMPIMMVMISIGAPAGGALYWLVSGIFGLI 243
YidC1       LAAIFTFLSSWLTNKAAKERNG-MMITMNIILPIFILLIGFNLASGVALYWVVSNAYQVF 230
            : .:  :. . ::  :. :       .:  ::*::: :: :  .:* .**::**.   ::

YidC        QQQLIYR----------------------------------GLEKRGLHSREKKKS---- 548
YidC2       QQLITNHIIKPKLRKQIDEEFKKNPPKPFKSNARKDITPQANNDKKLITSKKQKSNRNAG 303
YidC1       QILLLN--------------------NPFKIIAER---QRLEDEARELEAKKRRAKKKAH 267
            *  :                                      : : : ::::: .

YidC        ------- 548
YidC2       KQRHHKQ 310
YidC1       KKRK--- 271
```

Figure 3-1. Clustal W alignment of the five C-terminal transmembrane domains from *E. coli* YidC and *S. mutans* YidC1 and YidC2. Predicted transmembrane domains are boxed. YidC1 and YidC2 are predicted to be lipoproteins and the SPaseII cleavage sites are underlined (113).

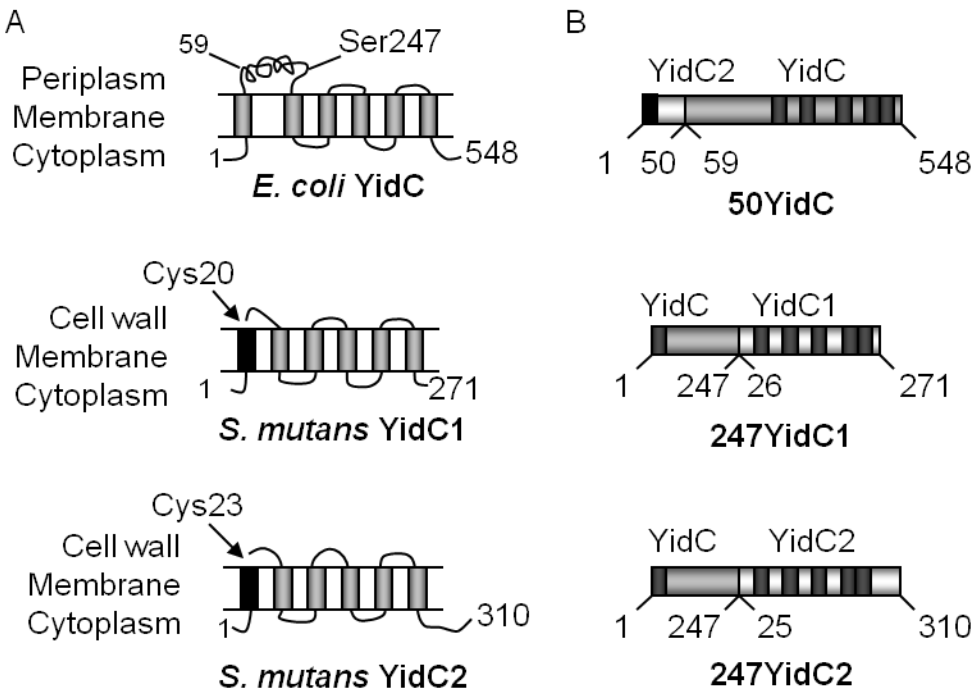

Figure 3-2. Predicted membrane topologies of *E. coli* YidC and *S. mutans* YidC1 and YidC2. Predictions are based on the TMPred prediction program. (A) YidC from *E. coli* spans the membrane six times, with the first transmembrane segment serving as an uncleavable signal sequence, followed by a large periplasmic loop. *S. mutans* YidC1 and YidC2 are each predicted to span the membrane five times, with an additional hydrophobic region functioning as a cleavable transmembrane targeting sequence. The predicted cleavage sites between amino acids 19 and 20 for YidC1 and amino acids 22 and 23 of YidC2 are indicated. (B) Schematic illustration of the chimeric proteins used in complementation studies. 50YidC is a fusion of amino acid residues 1 to 50 of YidC2 and 59 to 548 of *E. coli* YidC. The signal sequence and cleavage site of YidC2 is indicated by the black box. The transmembrane regions of *E. coli* YidC are indicated by dark grey boxes. 247YidC1 is a fusion of residues 1 to 247 of YidC and 26 to 271 of YidC1. 247YidC2 is a fusion of residues 1 to 247 YidC and 25 to 310 of YidC2. Each contains the uncleavable signal sequence and large periplasmic domain of *E. coli* YidC appended to the five transmembrane domains (grey boxes) of *S. mutans* YidC1 or YidC2.

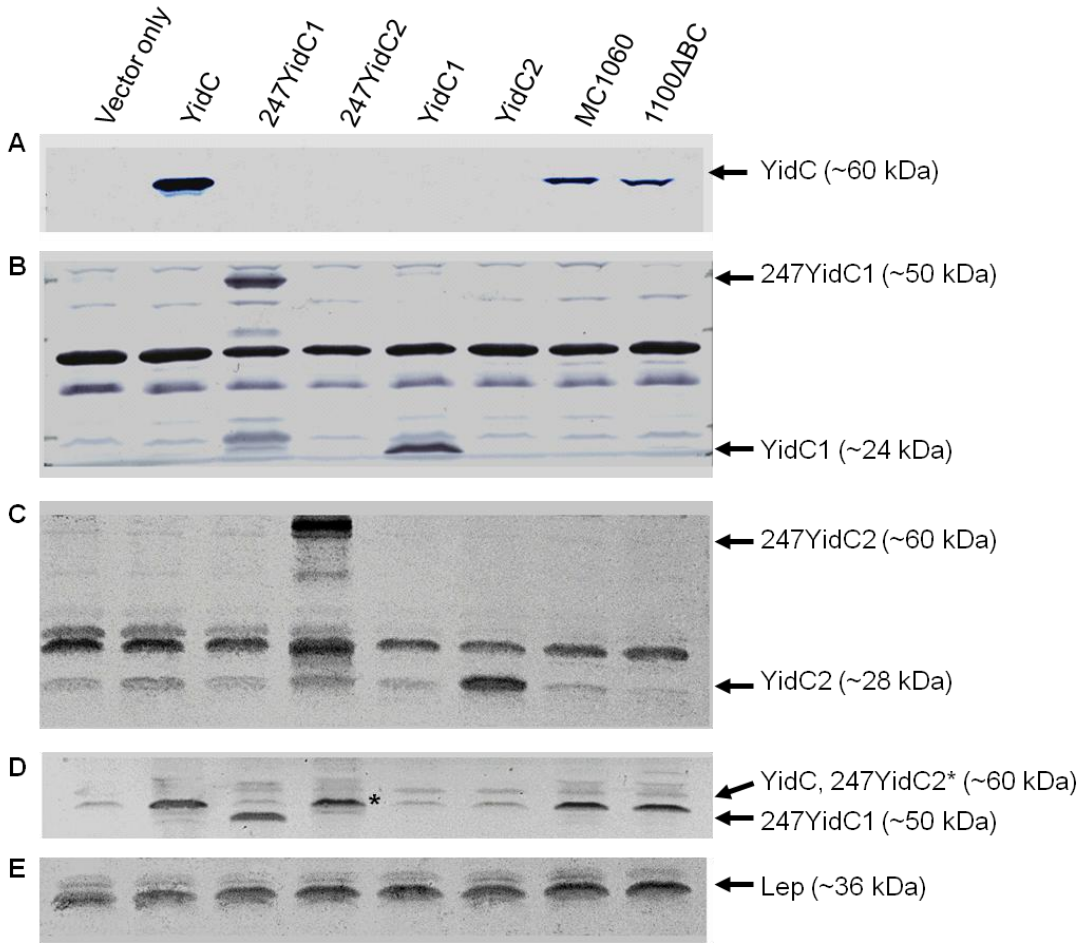

Figure 3-3. Confirmation of appropriate production of *E. coli* YidC and *S. mutans* YidC1 and YidC2 in the JS7131 YidC-depletion strain by Western blot analysis. Membranes were prepared from JS7131 harboring the pACYC184 vector only or the same vector containing genes encoding *E. coli* YidC, or *S. mutans* 247YidC1, 247YidC2, YidC1 or YidC2. The mutant and complemented strains were grown in 0.2% glucose to repress *E. coli* chromosomal *yidC* expression. The wild-type parental strain of JS7131, MC1060, and the *E. coli* mutant strain 1100ΔBC (34) that lacks a functional F_1F_0 ATPase but has not been manipulated with regard to *yidC*, were also evaluated. Proteins were resolved on a 10% SDS-PAGE gel and the YidC homologs were revealed by immunoblot analysis with rabbit antisera raised against C-terminal peptides of (A) *E. coli* YidC, (B*) S. mutans* YidC1 or (C) *S. mutans* YidC2, as well as with polyclonal antisera against (D) full-length *E. coli* YidC, or (E) leader peptidase (Lep), a YidC-independent membrane protein. The apparent molecular mass in kilodaltons of each protein of interest is indicated in parentheses. Asterisk indicates 247YidC2 is produced as a M_r ~60 kDa protein.

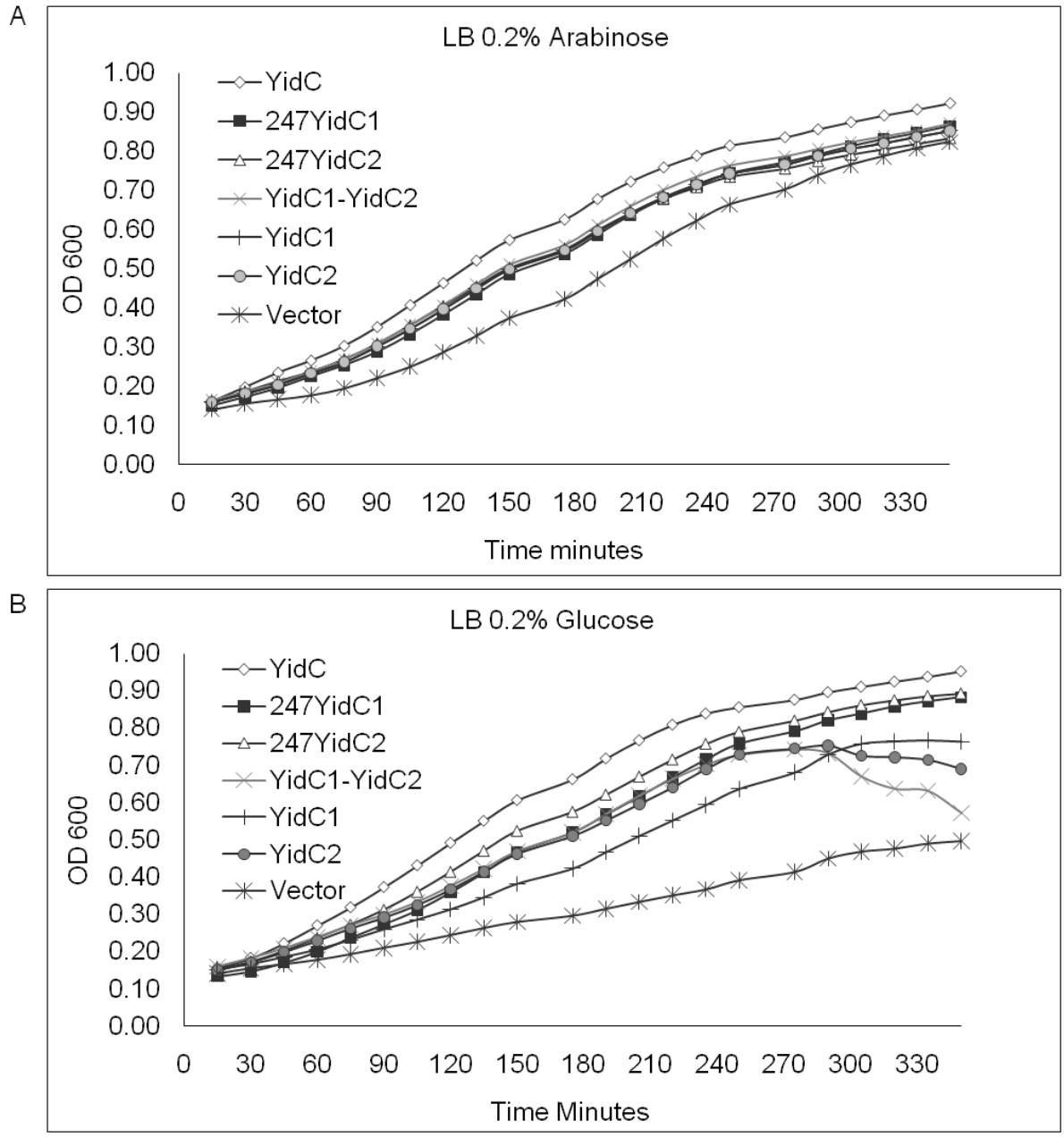

Figure 3-4. Growth curves of *E. coli* YidC-depletion strain JS7131 harbouring plasmid pACYC184 encoding various YidC constructs. Constructs contained within pACYC184 (vector) encoded YidC, 247YidC1, 247YidC2, YidC1-YidC2, YidC1 or YidC2. Growth curves were performed under yidC inducing (0.2% arabinose) and repressing conditions (0.2% glucose). Growth curves were completed in triplicate using a Bioscreen C machine in a 100 well Bioscreen C plate at 37oC. OD600 was recorded every 15 minutes with shaking for 10 minutes between readings.

Table 3-1. Complementation of growth of the *E. coli* YidC-depletion strain JS7131 with constructs encoding *S. mutans* YidC1 and YidC2

	Doubling time (min)[a]	
Protein produced from pACYC184	0.2% glucose	0.2% arabinose
None (vector only)	175.1 ± 1.8	106.7 ± 2.5
YidC	89.7 ± 0.4	97.8 ± 2.2
YidC1	128.3 ± 1.0	105.4 ± 2.9
YidC2	116.9 ± 4.4	107.3 ± 2.3
247YidC1	107.1 ± 2.1	104.3 ± 1.9
247YidC2	112.0 ± 1.4	101.5 ± 2.3
YidC1 and YidC2	113.7 ± 1.2	106.1 ± 5.8

[a] Mean of triplicate samples ±standard error. Growth in broth was determined in a 100-well plate by Bioscreen.C Machine (Labsystems, Helsinki, Finland).

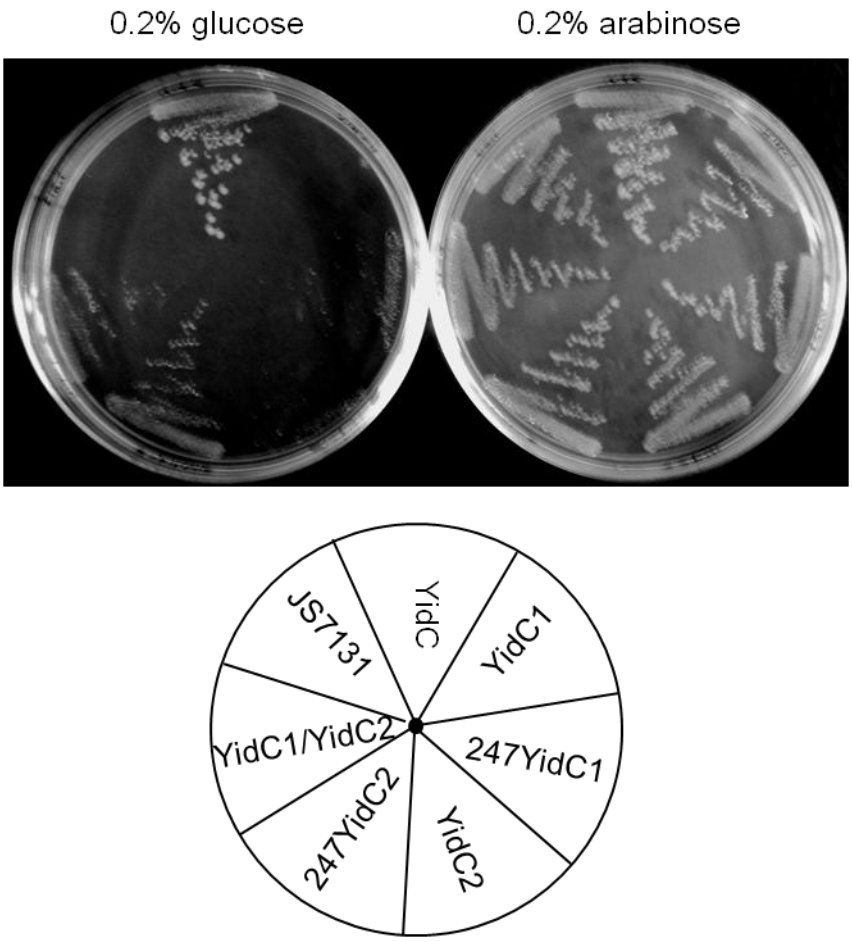

Figure 3-5. Growth on LB agar plates of the *E. coli* YidC-depletion strain JS7131 harboring pACYC184 encoding various YidC constructs. The top panel shows growth of JS7131 with pACYC184 encoding either YidC, YidC1, 247YidC1, YidC2, 247YidC2, YidC1/YidC2 or pACYC184 on 0.2% glucose (left) or 0.2% arabinose (right). The key is shown in bottom panel.

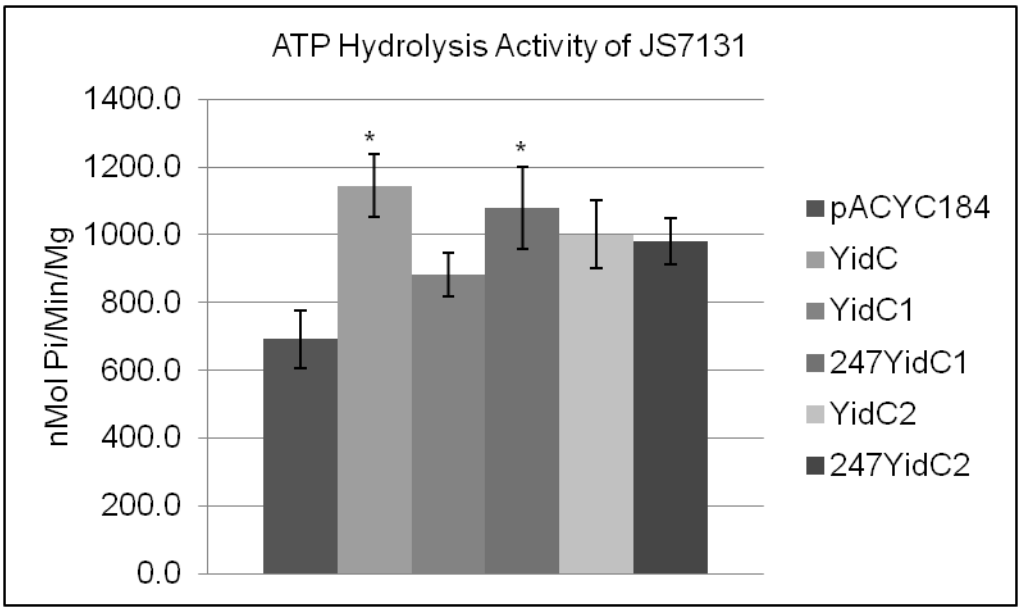

Figure 3-6. ATP hydrolysis activity of *E. coli* YidC-depletion strain JS7131 containing pACYC184 encoding the indicated YidC constructs. ATP hydrolysis activity was determined using inner membrane vesicles prepared as in Materials and Methods by measuring production of inorganic phosphate in the presence of 120 µg membrane proteins and 4 mM ATP using the acid molybdate method (154). Specific activity is expressed in nMol Pi/min/mg protein. Statistically significant differences are indicated, * = $P < 0.05$ compared to pACY184, analyzed by One-way ANOVA with Tukey's Multiple Comparison Post-Test.

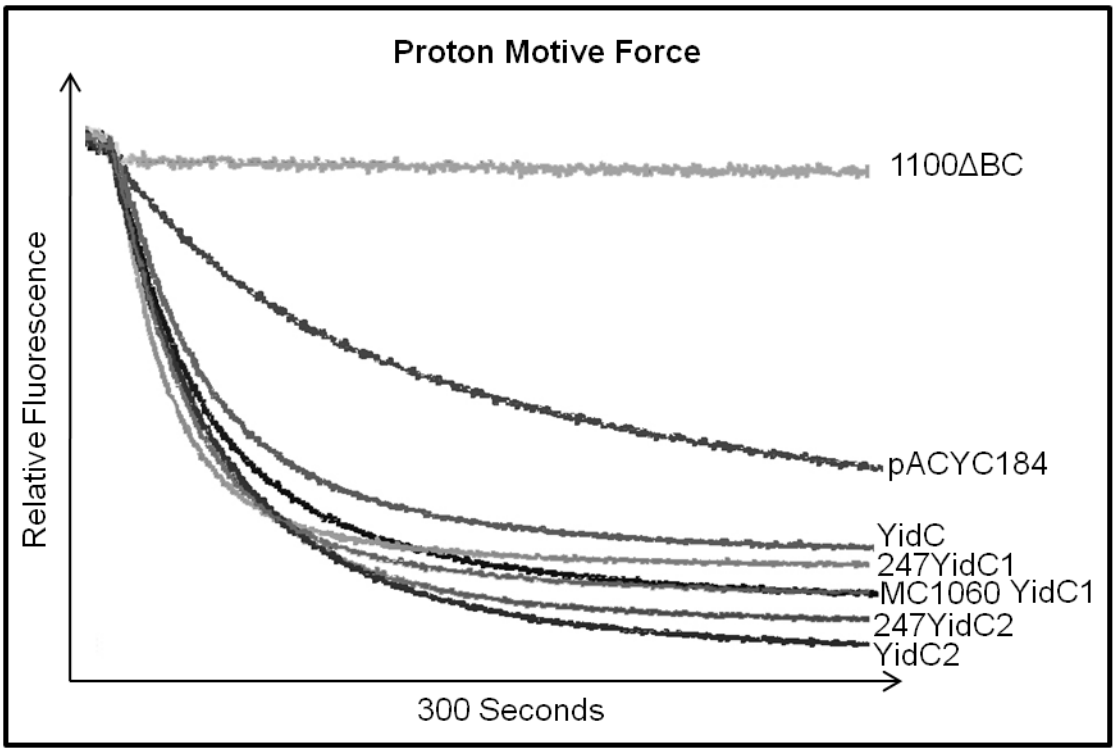

Figure 3-7. Proton motive force (PMF) of *E. coli* YidC-depletion strains JS7131 with pACYC184 encoding the YidC constructs, and the *E. coli* control strains indicated. Inner membrane vesicles were prepared as in Materials and Methods from *E. coli* 1100ΔBC (F_1F_o ATP mutant), MC1060 (parent stain of JS7131), JS7131 containing pACYC184 or complemented pACYC184 encoding *E. coli* YidC, *S. mutans* 247YidC1, YidC1, 247YidC2, and YidC2. Five hundred micrograms of membrane proteins were used to analyze PMF, through quenching of ACMA monitored with a fluorescence spectrometer. The integrity of membrane vesicles was confirmed by adding NADH to each sample and monitoring the fluorescence of ACMA (not shown).

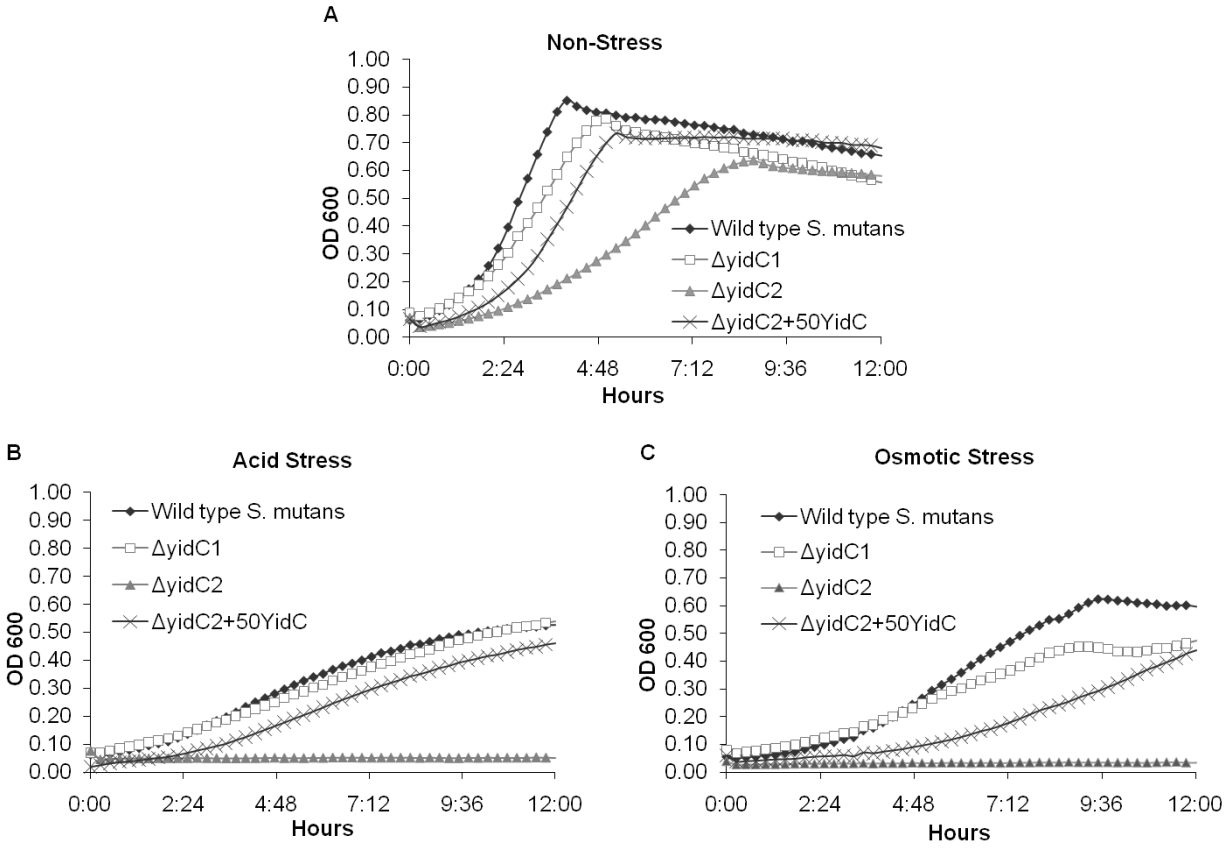

Figure 3-8. Growth curves of *S. mutans* wild-type NG8, *ΔyidC1*, *ΔyidC2* and *ΔyidC2* with chimeric *E. coli* 50YidC (YidC2 $^{1\text{-}50}$-YidC$^{59\text{-}548}$) under non-stress, acid- and osmotic-stress conditions. (A) Non-stress, THYE pH 7.0. (B) Acid stress, THYE pH 5.0. (C) Osmotic stress, THYE 4% NaCl. Growth curves were completed in triplicate using a Bioscreen C machine (Labsystems, Helsinki, Finland).

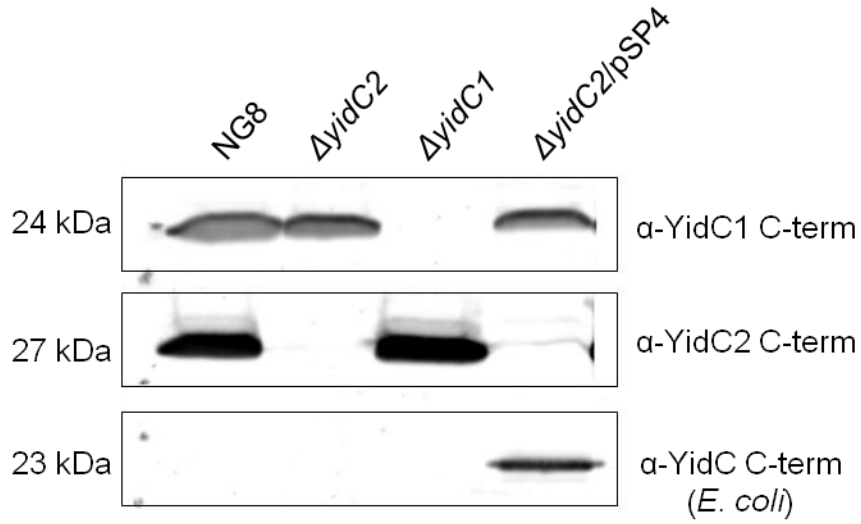

Figure 3-9. Western blot of whole cell lysates of *S. mutans* wildtype, Δ*yidC1*, Δ*yidC2* and *ΔyidC2* mutant with chimeric *E. coli* YidC (YidC2 $^{1-50}$-YidC$^{59-548}$). Proteins were resolved on 10% SDS-polyacrylamide gels and identified by reactivity with rabbit antisera raised against C-terminal peptides of *S. mutans* YidC1 or YidC2 and *E. coli* YidC.

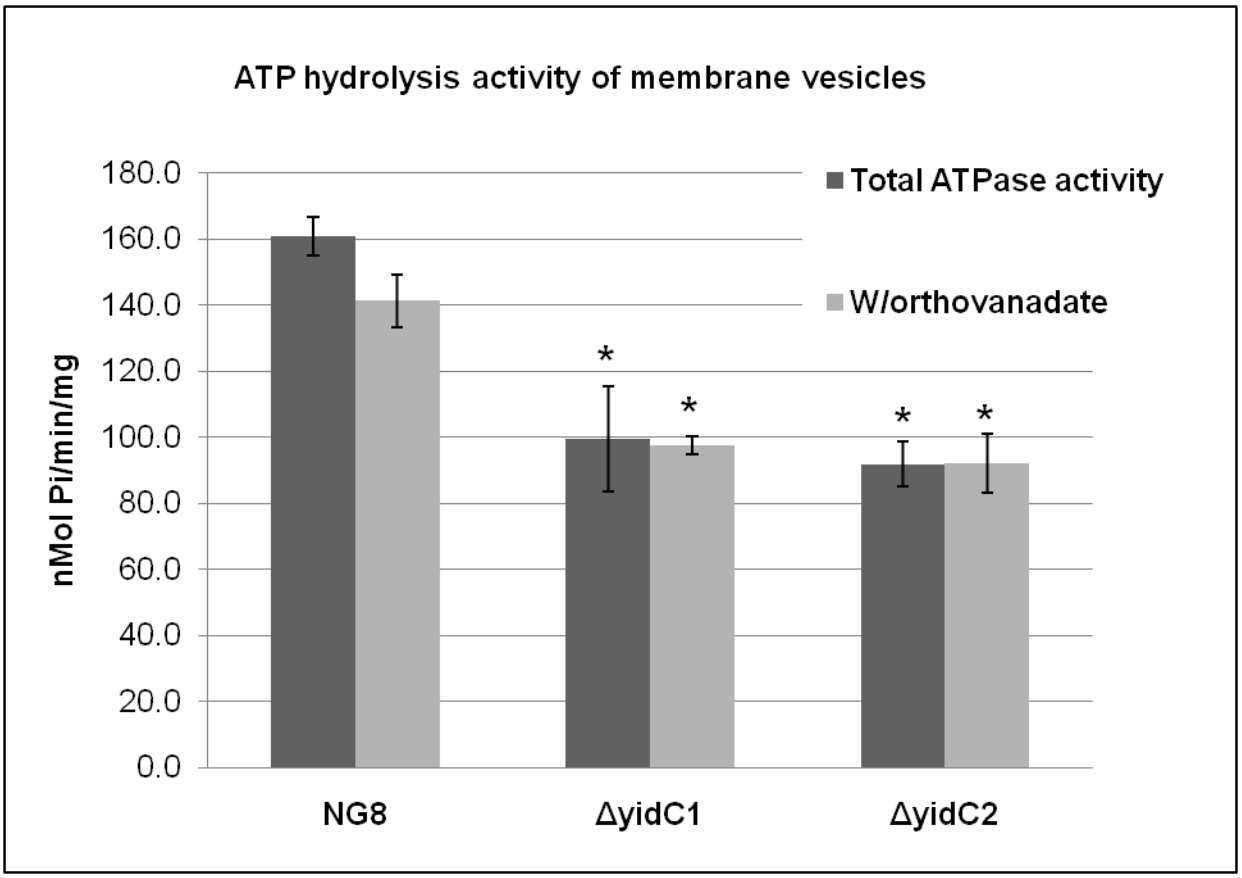

Figure 3-10. Membrane-associated ATPase activity in *S. mutans* NG8, Δ*yidC1* and Δ*yidC2* strains with or without the P-type ATPase inhibitor orthovanadate. Dark grey bars represent ATPase activity without orthovanadate. Light grey bars represent specific activity after membranes were incubated for 5 minutes with 50 μM orthovanadate. Specific activity is expressed as nMol Pi/min/mg of membrane proteins. Error bars represent standard deviation of the average specific activity resulting from duplicate assays. * indicates a significant difference compared to NG8 total ATPase activity, *P*-value < 0.01. Statistical analysis was performed using One-way ANOVA with Bonferroni's Multiple Comparison Post-Test.

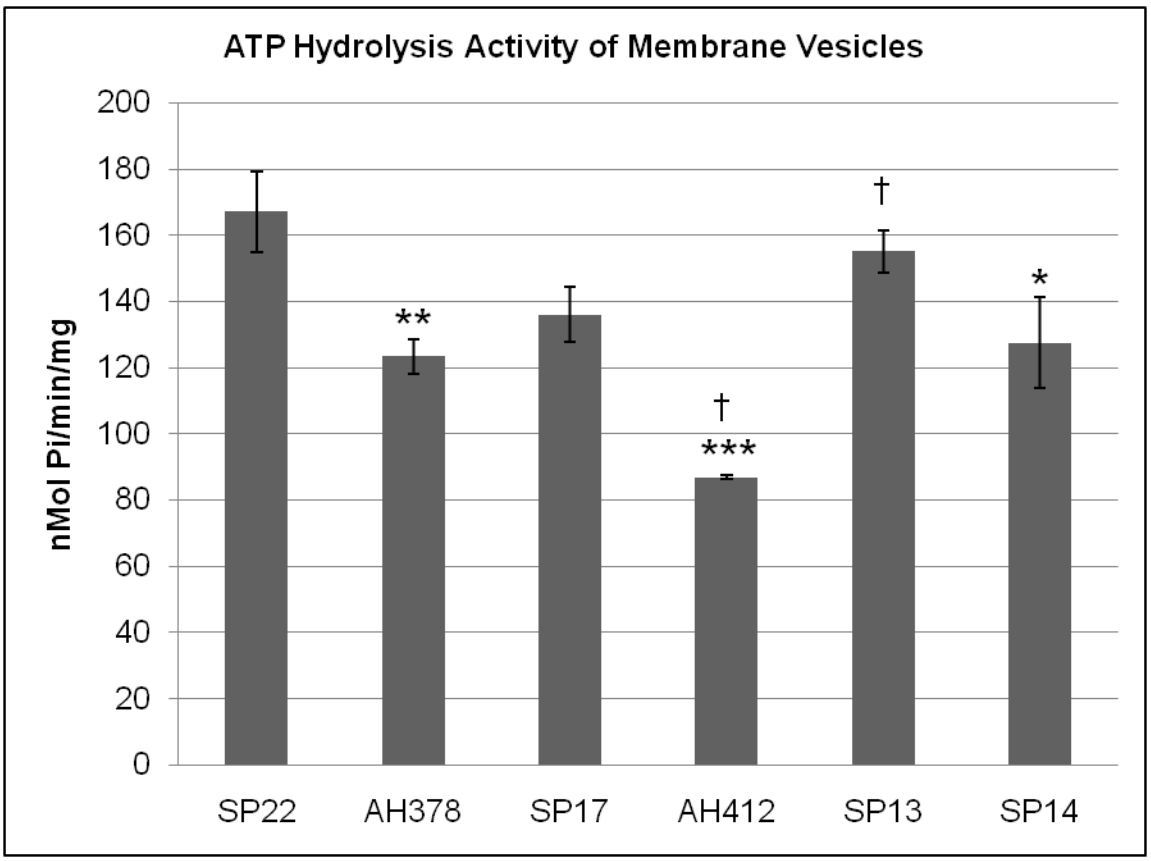

Figure 3-11. Membrane-associated ATP hydrolysis activity of *S. mutans* wildtype and Δ*yidC2* mutant strains expressing various YidC constructs. Mean specific activity is expressed as nMol Pi/min/mg membrane protein, calculated based on duplicate samples from three different time points. Standard deviation is indicated by error bars. Genotypes of strains are as follows: SP22-*gtfA::erm*, AH378-Δ*yidC2*, SP17-Δ*yidC2 gtfA::yidC2*, AH412-*yidC2*ΔC, SP13-Δ*yidC2 gtfA::yidC1C2*, and SP14-Δ*yidC2 gtfA::yidC2C1.* Statistically significant differences are based on One-way ANOVA followed by Tukey's Multiple Comparison Test, and are indicted; * = $P < 0.05$; ** = $P < 0.01$; *** = $P < 0.001$ compared to SP22, or † = $P < 0.05$ compared to AH378.

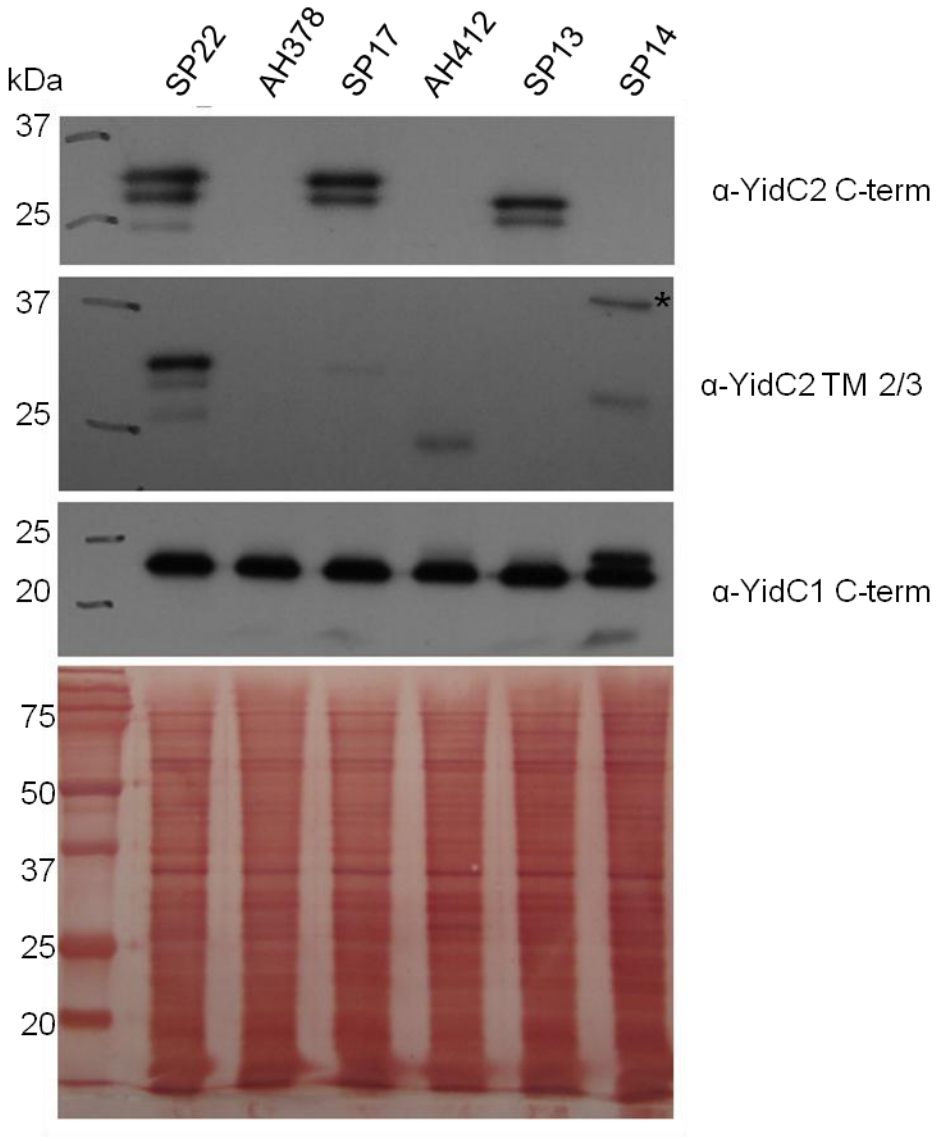

Figure 3-12. Western blots of membrane samples prepared from *S. mutans* strains used in ATP hydrolysis assays (Figure 3-11). For each indicated strain used in the ATPase assay (Figure 3-11), 5 µg of membrane proteins were loaded on a 12% SDS-PAGE gel. Proteins were transferred to PDVF membranes and reacted with the indicated affinity purified antibodies. Bottom panel shows colloidal gold protein stain. *, indicates a possible unprocessed version of the chimeric YidC2C1 protein. Genotypes of strains are as follows: SP22-*gtfA::erm*, AH378-Δ*yidC2*, SP17-Δ*yidC2 gtfA::yidC2*, AH412-*yidC2*ΔC, SP13-Δ*yidC2 gtfA::yidC1C2*, and SP14-Δ*yidC2 gtfA::yidC2C1.*

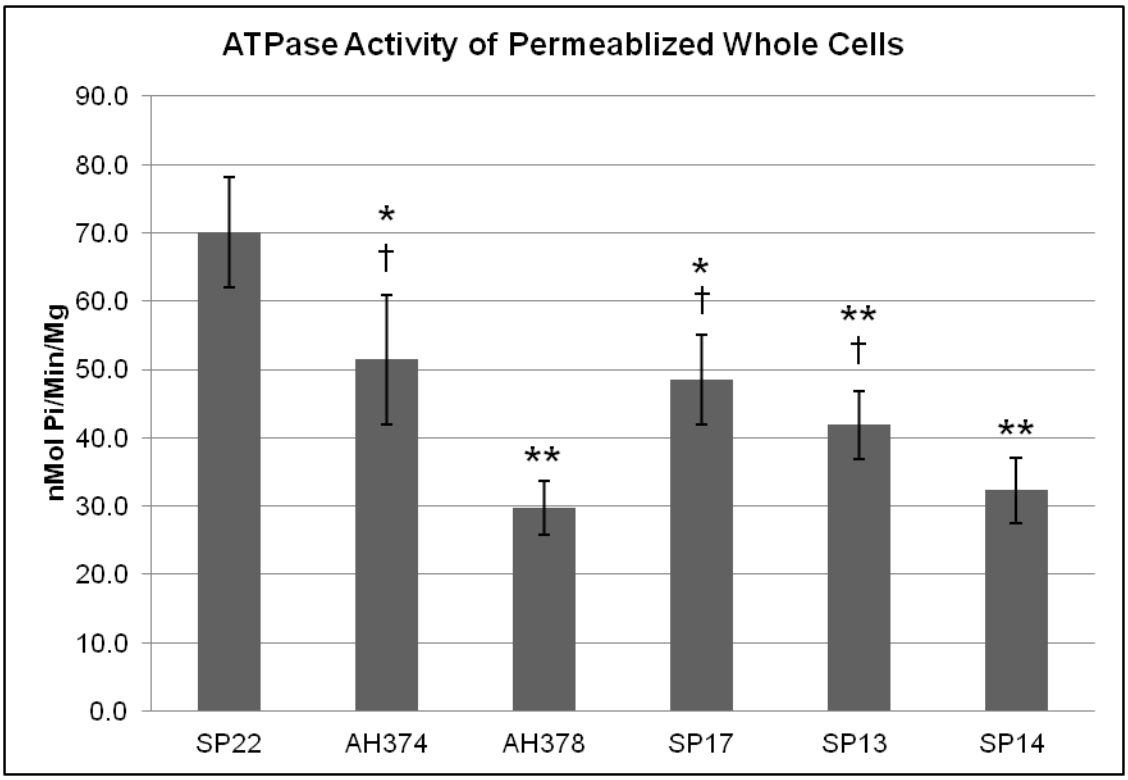

Figure 3-13. ATPase activity of *S. mutans* permeablized whole cells. Assay was performed in triplicate. Average specific activity is expressed in nMol Pi/min/mg whole cell protein, with error bars representing the standard deviation of the mean of triplicate assays. Genotypes of strains are as follows: SP22- *gtfA::erm*, AH378-Δ*yidC2*, SP17-Δ*yidC2 gtfA::yidC2*, AH412-*yidC2*ΔC, SP13-Δ*yidC2 gtfA::yidC1C2*, and SP14-Δ*yidC2 gtfA::yidC2C1.* Statistically significant differences are indicted, * = $P < 0.05$ and ** = $P < 0.01$ compared to SP22, or † = $P < 0.05$ compared to AH378. Significant differences were determined by Student's t-test.

CHAPTER 4
DIFFERENCES IN MEMBRANE PROTEIN COMPLEXES BETWEEN WILDTYPE AND YIDC1 AND YIDC2 MUTANTS USING BN-PAGE

Rationale for Study

Blue-Native polyacrylamide gel electrophoresis (BN-PAGE) was originally developed to separate enzymatically active membrane proteins, such as respiratory chain complexes located within the mitochondrial membrane (155). It has also been widely used to study chloroplast membrane protein complexes, such as the light harvesting chlorophyll binding proteins and twin arginine translocation pathway (156) (157). The BN-PAGE technique uses gentle non-ionic detergents to solublize proteins in their native conformations under non-denaturing conditions. Once membrane proteins are solublized in detergent micelles, the anionic dye Coomassie Brilliant Blue G-250 is added to the protein samples. The dye binds to the proteins causing a charge shift which allows for separation of protein complexes based on size in a gradient Blue-Native polyacrylamide gel. Protein complexes can be further analyzed by in gel enzyme assays, Western blot, mass-spectrometric analysis, or by second dimension PAGE, either 2D-BN/BN-PAGE or 2D-BN/SDS-PAGE.

BN-PAGE combined with second dimension SDS-PAGE is a powerful technique that allows protein subunits of complexes to be separated in a second dimension such that individual proteins can be isolated [reviewed in (158-159)]. This technique can also be combined with mass spectrometric analysis for applications in bacterial proteomics [reviewed in (160)]. This technique was successfully applied to inner membrane fractions from *E. coli*, identifying 43 distinct protein complexes of the inner membrane, including the F_1F_o ATP synthase subunits, as well as YidC, YajC, SecA, and a number

of transport complexes (161). Another study used 2D-BN/SDS-PAGE in conjunction with MALDI-TOF-MS (matrix-assisted laser desorption/ionization-time of flight-mass spectrometry) to analyze the membrane proteome of the green sulfur bacterium *Chlorobium tepidum* (162). This group was able to identify 63 membrane proteins out of 120 total proteins isolated, including membrane proteins containing up to 14 transmembrane domains. In a study by Tsirogianni, the composition of a phenol inducible multi-enzyme complex from a *Pseudomonas* species was identified, using BN-PAGE coupled with high-throughput mass spectrometry (163).

BN-PAGE can also be adapted to determine the molecular masses of membrane proteins as well as the oligomeric states of complexes, as was demonstrated for several well-characterized bacterial membrane transport proteins by Heuberger (164). Of note, this group found that membrane proteins migrate differently than the soluble proteins used as standards, and that by multiplying the predicted molecular mass based on amino acid sequence by a factor of 1.8 the apparent mass by BN-PAGE of membrane proteins can be estimated.

It is clear from the variety of studies using 2D-BN/SDS-PAGE, that this technique can be a useful proteomics tool. In addition it has applications in determining protein complex oligomeric states, as well as the potential to discover new protein-protein interactions within the membranes and the cytoplasms of cells. In the studies outlined in this Chapter, 2D-BN/SDS-PAGE followed by Western blot, was used to gain insight into potential protein-protein interactions between YidC1, YidC2 and SecY from *S. mutans*. Also, one dimensional BN-PAGE combined with LC-MS/MS (liquid chromatography-mass spectrometry/mass spectrometry) was used to begin to evaluate

differences in membrane protein complexes between wildtype and Δ*yidC1* and Δ*yidC2* mutants in *S. mutans*, in order to begin to understand the function of the YidC/Oxa1/Alb3 family of proteins in streptococci.

Materials and Methods

Membrane Fractions and DDM Solublization

Isolating cytoplasmic membranes from gram-positive bacteria can be complicated because the cell wall can make cell lysis difficult. For this reason cells have first been converted to protoplasts, by digesting the cell wall with lysozyme and mutanolysin. Chassy found that growth in 20 mM DL-threonine made cells more susceptible to lysozyme treatment by interfering with lysine incorporation into the cell wall and inhibiting cross-link formation (165). He also found that streptococci grown in Brain-Heart Infusion broth provided better lysis of proplasts than those grown in Todd Hewitt Broth. *S. mutans* cells in this study were grown in Brain-Heart Infusion broth (BHI, Difco) supplemented with 20 mM DL-threonine at 37ºC in a standard incubator without aeration.

Membranes from *S. mutans* wild-type strain NG8 were compared with those from AH374 (NG8, Δ*yidC1*::Erm) and AH398 (NG8, Δ*yidC2*::Erm). For each strain a 1 ml freezer vial (25% glycerol frozen back in mid-log) was used to inoculate 9 ml media in a 15 ml conical tube. After approximately 8 hours of growth, this culture was used to inoculate a 100 ml bottle of pre-warmed media and grown overnight. In the morning the 100 ml overnight culture was used to inoculate 900 ml of pre-warmed media in a 1 liter flask. The 1 liter culture was grown until it reached an OD_{600} of 0.5 to 0.6 (mid-log phase) and the flask was placed in an ice bath for at least 10 minutes to stop growth.

Each culture was then split into three 500 ml Beckman centrifuge tubes, and centrifuged at 9,000 rpm (16,000 x g) in a JA-10 Beckman rotor for 10 minutes at 4ºC to pellet the cells. Bacterial cells were resuspended in 10 ml Buffer A (10 mM Tris-HCl [pH 6.8], 10 mM Mg acetate, in 25% sucrose) and transferred to a 40 ml Beckman tube followed by centrifugation at 10,000 rpm (12,074 x g) in a JA-20 Beckman rotor for 10 minutes. The cell pellets were stored at -20ºC until needed. Freezing the cells before lysozyme and mutanolysin treatment resulted in more efficient protoplast formation.

To prepare protoplasts the cell pellets were thawed and suspended in 5 ml Buffer A , to which 200 µl lysozyme (10 mg/ml stock) and 2,000 U mutanolysin (200ul of a 10,000 U/ml stock, Sigma # M9901) were added. Cells were incubated at 37ºC with gentle agitation for approximately 1.5 hours and monitored by Gram stain until ~95% of cells were protoplasts (gram-negative). The protoplasts were pelleted by low speed centrifugation at 6,000 rpm (4,353 x g) in a JA-20 Beckman rotor for 10 minutes at 4ºC. They were then washed twice with 10 ml Buffer A. The protoplast pellets were suspended in 3 ml Membrane Buffer (50 mM Tris-HCL [pH7.5] and 10 mM $MgSO_4$) and 200 µl of EDTA free protease inhibitor cocktail (Complete® –Tablets, 25 x stock solution, Roche), and 10 µg/ml of both DNase1 (Sigma, D4527) and RNase A (Sigma, R5125) were added. Protoplasts were lysed by sonicating for 3 cycles, 15 seconds each (with cooling on ice between cycles) on setting 7 of a Fisher Scientific Sonic dismembrator 100. Cell lysis was confirmed by Gram stain. Unlysed protoplasts and cell debris was removed by centrifugation at 6,000 rpm (4,347 x g) in a JA-20 Beckman rotor for 10 minutes at 4ºC. The supernatants, containing membranes, were transferred to Beckman 5 ml (13 x 51 mm) tubes for a SW 50.1 Beckman rotor. The membranes were

pelleted by centrifugation at 100,000 X g (45,000 rpm) for 1.5 hours (or overnight) at 4ºC. The resulting membrane pellets were suspended in 500 µl of NativePAGE Sample Buffer (50 mM BisTris-HCL [7.2], 50 mM NaCl, 10% glycerol, 0.001% Ponceau S) using a teflon homogenizer. Protein concentrations were determined by BCA assay with a 1/500 dilution of membranes. A 1 mg/ml stock solution of bovine serum albumin (BSA) was used to make a standard curve. Each membrane preparation was adjusted to a protein concentration of 10 µg/µl.

For BN-PAGE, membrane proteins were solublized with the non-ionic detergent dodecylmaltoside (DDM). For the solublization step 800 µg of membrane proteins were combined with 4 µl of 20% DDM (1% of final volume). Samples were briefly vortexed and placed on ice for 15 minutes, with intermittent vortexing every 5 minutes. Samples were then ultracentrifuged at 100,000 x g (4ºC) for 15 minutes using a TLA-55 Beckman rotor in a Beckman Optima TLX tabletop ultracentrifuge. Supernatants were saved as the solublized fractions. Aliquots were frozen at -20ºC and used later in BN-PAGE experiments.

Blue-Native Polyacrylamide Gel Electrophoresis

The BN-PAGE protocol used in these experiments was adapted from the Invitrogen NativePAGE™ Novex® User Manual, which is based on the original protocol developed by Schägger and von Jagnow, (155, 166). Accordingly, solublized membrane proteins were combined with 5% Coomassie Blue G-250 solution (5% Coomassie Blue G-250 in 500 mM 6-aminohexanoic acid) at a detergent/dye ratio of 8 (gram/gram), which gives proteins a net negative charge, allowing for separation based on size in a polyacrylamide gel. BN-PAGE was performed using the Invitrogen XCell *SureLock* ™ Mini-Cell system. To prepare samples for electrophoresis, 80 µl of

solublized membrane proteins (1% DDM) were combined with 2 µl of 5% Coomassie Blue G-250 solution. Then 7.5 µl of each sample was loaded on a 10 well 3-12% Invitrogen NativePAGE™ Novex® Bis-Tris gel. The Invitrogen NativeMark™ Unstained Protein Marker (5 µl) was used as a standard. For electrophoresis, 600 ml of cold NativePAGE™ Anode Buffer (50 mM Bis Tris, 50 mM Tricine, pH 6.8) was poured into the lower chamber and 200 ml of cold NativePAGE Dark Cathode Buffer (50 mM Bis Tris, 50 mM Tricine, 0.02% Coomassie Blue G-250) was poured in the top chamber. Electrophoresis was performed in a cold room at 4ºC, with the XCell surelock cell connected to a PowerPac Basic Power Supply from BioRad set at 150 volts. Once the dye front had reached approximately 1/3 of the way to the bottom of the gel, after ~45 minutes, the dark blue cathode buffer was exchanged for NativePAGE Light Cathode Buffer (50 mM Bis Tris, 50 mM Tricine, 0.002% Coomassie Blue G-250) and continued to run at 250 volts until the dye front reached the bottom (~50 minutes). BN-PAGE gels were then further processed with one of the following protocols; Coomassie Blue R-250 stain, BioRad Silver Stain Plus Kit, BioRad Bio-Safe Coomassie Blue for Mass spectrometric analysis, transfer to PDVF membrane for Western blot analysis, or 2nd Dimension SDS-PAGE (protocols are described below).

Protein Staining of Blue-Native Polyacrylamide Gels

Coomassie Brilliant Blue R-250 stain. All membrane samples analyzed by BN-PAGE were stained with Coomassie Blue R-250 as a quality control step to ensure that the membrane protein banding patterns were consistent between each experiment. Coomassie Blue R-250 stain has a limit of detection between 50 to 100 ng of protein. When more sensitive staining was needed, gels were silver stained (BioRad Silver Stain Plus Kit, below). After the BN-PAGE run, gel were placed in approximately 100 ml

Fixative Solution (40% methanol, 10 % acetic acid) and microwaved on high for 45 seconds. The Gels were then placed on an orbital shaker for 15-30 minutes at room temperature. Next, Fixative Solution was decanted and 100 ml of Coomassie R-250 Stain (0.02% Coomassie R-250 in 30% methanol and 10% acetic acid) was added and microwaved on high for 45 seconds followed by incubation at room temperature on an orbital shaker for 15 to 30 minutes. Coomassie R-250 stain was removed and the gels were placed in 100 ml of Destain Solution (8% acetic acid solution) and microwaved again on high for 45 seconds. Gels were placed on an orbital shaker until the desired background was reached. Gels were stored in water until they were dried or photographed.

BioRad Silver Stain Plus. If a more sensitive protein stain was desired gels were silver stained. This method has a limit of detection of ~2 ng of protein per band. The BioRad Silver Stain Plus Kit was used following the manufacturer's directions with the following deviations. Immediately after BN-PAGE, gels were placed in a glass bowl (washed previously with 50% nitric acid) with 200 ml of Fixative Enhancer Solution (50% methanol, 10% acetic acid, 10% Fixative Enhancer, 30% distilled de-ionized water) and placed on an orbital shaker overnight at room temperature. In the morning Fixative Enhancer Solution was decanted, and gels were rinsed twice in 200 ml distilled de-ionized water for 10 minutes on an orbital shaker. During the last wash step the Silver Stain Plus solution was made according to product directions. A Teflon stir bar was added to a glass beaker (both cleaned with 50% nitric acid solution) on a stir plate and 35 ml of distilled de-ionized water was added and the stir plate turned on. To this, 5.0 ml of each of the following were added in this order; Silver Complex Solution, Reduction

Moderator Solution, and Image Development Reagent. The mixture was stirred for approximately 30 seconds more and then immediately added to the glass bowl with the gel to be stained and placed on an orbital shaker at room temperature to develop. Gels were constantly monitored for stain development and once desired staining was reached, the Silver Stain Plus solution was decanted and the gel was place in 5% acetic acid for 15 minutes to stop development. Gels were stored in water until photographed and dried.

BioRad Bio-Safe Coomassie Stain. Gels that were intended for Mass Spectrometry analysis were stained using Bio-Safe Coomassie from BioRad, according to the manufacturer's directions, with the following modifications. Immediately following electrophoresis, NativePAGE gels were washed a total of 3 times for 5 minutes each with 200 ml distilled de-ionized water. During the wash steps gels were placed on an orbital shaker at room temperature. After the water from the final wash step was decanted, enough Bio-Safe Coomassie was added to cover each gel. The gels were incubated for at least 1 hour in the stain on an orbital shaker. After staining, gels were de-stained in 200 ml of distilled de-ionized water for at least 30 minutes or until desired background was reached. Next, gels were placed on a glass plate on a light box and bands of interest were excised using a razor blade and placed in a 1.5 ml Eppendorf tube on ice. Samples were either immediately taken to the University of Florida ICBR Protein Core for LC-MS/MS analysis or frozen at -20ºC and taken to the ICBR Protein Core at a later time.

In-Gel Trypsin Digestion and LC-MS/MS (University of Florida, ICBR Core Facility Protocols)

Destain and SDS removal. The gel slice containing the band of interest was washed with 200 µl 50% acetonitrile solution while vortexing 2 times for 15 minutes. The wash solution was removed and the gel slice was dehydrated with acetonitrile (ACN). ACN was removed and the gel slice was rehydrated by incubation for 5 minutes in 50-100 µl 50 mM ammonium bicarbonate buffer (NH_4HCO_3). An equal amount of ACN was added (1:1 ratio of ammonium bicarbonate to ACN), and the sample was vortexed for 15 minutes. Then 200 µl of 50:50 ACN to 50 mM ammonium bicarbonate was added and the sample was vortexed for 15 minutes more to completely de-stain the gel slice.

Reduction, alkylation & trypsin digest. After the de-stain procedure, the wash was removed and the gel slice was dried in a Speedvac for 10-15 minutes (samples may have been stored at 4ºC at this point). The sample was rehydrated in 100 µl fresh 45 mM dithiothreitol (DTT), 50 mM ammonium bicarbonate at 55ºC for 45 minutes. Samples were allowed to come to room temperature and DTT solution was removed, then quickly replaced with 100 µl fresh 100 mM iodoactamide (IAA), then incubated in the dark at room temperature for 45 minutes. The IAA was removed and the gel slice was washed with 100 µl 50% ACN/50 mM ammonium bicarbonate by vortexing on low 3 times for 3 minutes each. The wash was removed and the gel piece was completely dried in a Speedvac (15 minutes). The sample may have been stored at 4ºC. If not, the sample was chilled in an ice bucket and enough Trypsin Solution (12.5 ng/ul trypsin in 50 mM ammonium bicarbonate) was added to cover the gel piece. The sample was incubated on ice for 10 minutes. Excess Trypsin Solution was removed and the gel was

overlaid with 30-50 µl of 50 mM ammonium bicarbonate. Trypsin digestion was performed at 37ºC for 12 to 16 hours.

Gel extraction. After trypsin digestion, the supernatant was removed and placed in a clean 1.5 ml tube. Then 200 µl 80:20 ACN:water containing 0.1% formic acid was added to the gel piece, and vortexed for 10-15 minutes. Buffer was removed and added to the previous supernatant. The gel piece was then dried in a Speedvac and resuspended in 15-20 µl Loading Buffer (3% ACN, 0.1% acetic acid, 0.01% TFA). The sample was sonicated in a water bath for 10 minutes, gently agitated on a vortex for 1 minute, then centrifuged at high speed for 15 minutes. The resulting supernatant was added to the other supernatant, and then analyzed by LC-MS/MS or stored at 4ºC.

LC- MS/MS. The enzymatically digested samples were injected onto a capillary trap (LC Packings PepMap) and desalted for 5 minutes with a flow rate 10 µl/min of 0.1% v/v acetic acid. The samples were loaded onto an LC Packing® C18 Pep Map HPLC column. The elution gradient of the HPLC column started at 3% Solvent A, 97% Solvent B and finished at 60% Solvent A, 40% Solvent B for 60 minutes for protein identification. Solvent A consisted of 0.1% v/v acetic acid, 3% v/v ACN, and 96.9% v/v H_2O. Solvent B consisted of 0.1% v/v acetic acid, 96.9% v/v ACN, and 3% v/v H_2O. LC-MS/MS analysis was carried out on a hybrid quadrupole-TOF mass spectrometer (QSTAR, Applied Biosystems, Framingham, MA). The focusing potential and ion spray voltage was set to 275 V and 2600 V, respectively. The information-dependent acquisition (IDA) mode of operation was employed in which a survey scan from *m/z* 400–1200 was acquired followed by collision induced dissociation of the three most

intense ions. Survey and MS/MS spectra for each IDA cycle were accumulated for 1 and 3 seconds, respectively.

Protein search algorithm. Tandem mass spectra were extracted by ABI Analyst version 1.1. All MS/MS samples were analyzed using Mascot (Matrix Science, London, UK; version 2.0.01). Mascot was set up to search the NCBInr database assuming the digestion enzyme was trypsin. Mascot was searched with a fragment ion mass tolerance of 0.30 Da and a parent ion tolerance of 0.30 Da. Iodoacetamide derivative of Cys, deamidation of Asn and Gln, oxidation of Met, are specified in Mascot as variable modifications. Scaffold (version Scaffold-01-06-03, Proteome Software Inc., Portland, OR) was used to validate MS/MS based peptide and protein identifications. Peptide identifications were accepted if they could be established at greater than 95.0% probability as specified by the Peptide Prophet algorithm (167). Protein identifications were accepted if they could be established at greater than 99.0% probability and contained at least two identified unique peptides. Protein probabilities were assigned by the Protein Prophet algorithm (168).

BN-PAGE with Western Blotting

In order to determine the locations of YidC1, YidC2 and SecY in membrane protein complexes separated by BN-PAGE, proteins were transferred to PDVF membranes and Western blots were performed with affinity purified antibodies (see Material and Methods, Chapter 2) against YidC1, YidC2, and SecY. The following protocol was used to transfer membrane protein complexes to PDVF membranes after the BN-PAGE run. Blue-Native gels were incubated in 0.1% SDS, 20 mM Tricine, 7.5 mM Imidazole (pH 7.0) for 10 minutes at room temperature on an orbital shaker. PDVF membranes were hydrated in 100% methanol for ~30 seconds and then rinsed in water

for 2 minutes on an orbital shaker. PDVF membranes were then equilibrated in Transfer Buffer (20 mM Tricine, 7.5 mM Imidazole [pH 7.0]) for 10 minutes. Proteins were blotted using the Hoefer Mighty Small TE 22 Mini Transfer Tank system. The Blue-Native gel was sandwiched between blotting sponges and blotting paper with the PDVF membrane placed on top of the gel. Once assembled, the cassette was placed in the transfer tank filled with Transfer Buffer, and electrophoresis took place at 50 volts for 45 minutes at room temperature. Once transfer was complete, proteins were fixed to the PDVF membrane in 20 ml 8% acetic acid solution for 15 minutes and rinsed in water to remove acid. The membrane was blocked in PBS, 0.3% Tween-20, 5% skim milk for at least 1 hour or overnight at 4ºC on an orbital shaker. Western blots were processed and developed following the Amersham (GE Healthcare) ECL protocol.

Two Dimensional BN/SDS-PAGE

Second dimension Tricine SDS/PAGE. Lanes cut from first dimension BN-PAGE gels were subjected to a reducing and alkylating step following the protocol from Invitrogen's NativePAGE™ Novex® Bis-Tris Gel System User Manual. Briefly, each excised lane was placed in a 15 ml conical tube with 5 ml Reducing Solution (1 x NuPAGE® LDS Sample Buffer with 50 mM DTT). The tube was placed on an orbital shaker at room temperature for 15 to 30 minutes. Reducing solution was decanted and replaced with 5 ml of Alkylating Solution (1 x NuPAGE® LDS Sample Buffer with 50 mM DMA (N,N-dimethylacrylamide) and incubated at room temperature on an orbital shaker for 15 to 30 minutes. Alkylating Solution was decanted and 5 ml of Quenching Solution (1 x NuPAGE® LDS Sample Buffer, 5 mM DTT, and 20% ethanol) was added and incubated at room temperature for 15 minutes. The gel strip was then placed on top of a 10% Tricine SDS-PAGE gel to run in the second dimension.

Tricine SDS-PAGE was performed essentially as described by Hermann Schägger's Nature Protocol from 2006 (169). Tricine gels were cast using the BioRad Mini-Protean II casting stands, with 12.5 cm x 6.5 cm x 1.5 mm glass plates with a prep well comb. Gels were made with a solution containing 1 M Tris-HCl (pH 8.45), 0.1% SDS (sodium dodecyl sulfate), 10% glycerol, 10% acrylamide (49.5% T, 3% C mixture), 0.05% ammonium per sulfate and 0.0005% TEMED. Gels were made the day before or the same day that 2D SDS-PAGE was performed. For the second dimension, a Tricine gel was placed in a BioRad Mini-Protean II Cell and Cathode Buffer (100 mM Tris, 100 mM Tricine, and 0.1% SDS [~pH 8.25]) was poured into the upper buffer chamber. Equilibrated gel strips (reduced, alkylated and quenched) were then placed in the prep well of the Tricine gel, and 200 µl of 1 x LDS (lithium dodecyl sulfate) sample buffer was applied around the gel strip. Next, Anode Buffer (100 mM Tris-HCl [pH 8.9]) was poured into the lower buffer chamber and the Mini-Protean II Cell was connected to a BioRad PowerPac Basic Power Supply set at 150 volts. The gel was run for ~1 hour or until the dye front had reached the bottom of the gel. After electrophoresis, gels were either transferred to PDVF membranes for Western blotting (see below) or stained using the BioRad Silver Stain Plus Kit, as with 1st dimension BN-PAGE gels (described above).

Western blots of second dimension Tricine SDS-PAGE. Second dimension gels were transferred to PDVF membranes and Western blots were performed as described in Chapter 2 under Material and Methods under Western blotting. For these experiments, membranes were probed with affinity purified α-YidC1 (1:2000), α-YidC2

C-terminal (1:6000), and α-SecY (1:500) antibodies. Antibodies are described in detail in Chapter 2 in Materials and Methods under Synthetic Peptide Antiserum.

GAPDH Assays with Whole Cells

GAPDH activity was determined using cells grown overnight in THYE. Cells were pelleted and resuspended to an OD_{600} of 1.0, in 25mM Tris-HCL [pH 7.5], 5mM EDTA. For assay, 1 ml of cell suspension was placed in an Eppendorf tube, spun down and resuspended in 900 µl of GAPDH Assay Buffer (40 mM Triethanolamine, 50mM Na_2HPO_4, 5mM EDTA, pH 8.6). The OD_{600} for each strain was read and recorded again before the assay was performed. For each assay, 7 µl of glyceraldyhyde-3-phosphate (50 mg/ml, Sigma) was added along with 100 µl of 10 mM NAD+, at which point a timer was started and reactions were placed in a 37ºC water bath for 30 minutes. After incubation, cells were spun at 4ºC for 2 minutes and OD_{340} was read. Assay was performed in triplicate for each strain. Results are expressed as OD_{340}/OD_{600}.

Results and Discussion

Changes in Protein Complexes in YidC Mutant Membranes were Visible by First Dimension BN-PAGE

Membrane proteins were isolated from wild-type NG8, *ΔyidC1* and *ΔyidC2* mutant strains of *S. mutans*. The membrane proteins were solublized using 1% DDM (dodecylmaltoside), a non-ionic detergent that preserves membrane protein complexes. Samples were compared using the BN-PAGE technique which separates native membrane protein complexes based on size in a polyacrylamide gel. Shown in Figure 4-1 is the resulting banding patterns from wild-type NG8, Δ*yidC1* and *ΔyidC2* solublized membrane protein complexes after staining with BioRad's Silver Stain Plus Kit or

Coomassie Blue G-250 stain. There were visible differences in banding patterns between the *yidC* mutants and NG8 (Figure 4-1 and 4-2), particularly in high molecular weight complexes of NG8 between 480 and 720 kDa, which were not visible in either Δ*yidC1* or *ΔyidC2* mutants. There was also an apparent lack of a band at approximately 300 kDa in both *yidC* mutants (Figure 4-1). Additionally, there were a number of bands present in the mutants in lower molecular weight complexes that were not present or were less pronounced in NG8. These migrated roughly between ~146 and ~60 kDa in Figure 4-1, 4-2, and 4-5. Shifts in the location of bands could indicate that in the mutant membranes some protein complexes were disrupted or perturbed, there could have been a change in expression of certain proteins, or there was a defect in the assembly of multimeric protein complexes.

YidC1, YidC2 and SecY Co-Migrate in High Molecular Weight Complexes

In an attempt to determine whether YidC1, YidC2 and SecY are present in a complex together in *S. mutans*, BN-PAGE was used in conjunction with Western blotting. Figure 4-3 shows a large streak of reactivity with the YidC1 and YidC2 antibodies suggesting that both YidC1 and YidC2 are located in a number of high molecular weight complexes. The patterns of reactivity are not identical, with YidC1 ranging from the top of the gel to approximately 300 kDa, and YidC2 from the top of the gel to approximately 500 kDa. There appears to be an extension in the location of YidC1 in the Δ*yidC2* mutant sample, with the reactivity extending down to approximately 200 kDa. The SecY antibody reactivity was weak; however, there was also a long streak of reactivity seen starting at the top of the gel and extending to approximately

300 kDa, with a pronounced band at ~146 kDa in the NG8 and Δ*yidC1* lanes, that was absent in the Δ*yidC2* mutant.

Epitopes may be masked in Western blots of first dimension Blue-Native polyacrylamide gels if the epitope is not exposed in the native protein, or by other proteins located in the same complex. Combining BN-PAGE with second dimension SDS-PAGE followed by Western blot can separate proteins from complexes in the second dimension and allow for better epitope recognition (160). Figure 4-4 shows the results of second dimension SDS-PAGE Western blots with YidC1, YidC2, and SecY antibodies. As in the 1D- BN-PAGE Western blots (Figure 4-3), YidC1, YidC2 and SecY are located in a streak of unresolved high molecular weight complexes. The streak observed with the α-YidC1 antibody migrated at ~24 kDa and was only seen in the NG8 and Δ*yidC2* samples. Likewise, the streak observed with the α-YidC2 antibody migrated at ~28 kDa and was only seen in NG8 and the Δ*yidC1* samples. Second dimension Western blots with the α-SecY antibody produced reactivity in three different locations, corresponding to three different sizes. For the NG8 sample there was a ~75 kDa spot corresponding to the ~146 kDa band in first dimension Blue-Native gel, a horizontal streak running at ~37 kDa, and a horizontal streak at ~20 kDa. In the Δ*yidC1* mutant sample there were two SecY species, a ~75 kDa spot and a 37 kDa horizontal streak, as in NG8. There was only faint reactivity in the Δ*yidC2* mutant sample with the SecY antibody, corresponding to the 37 kDa streak only. The ~20 kDa streak that was present in the NG8 sample was absent from the Δ*yidC1* and Δ*yidC2* mutant samples.

SecY has a predicted Molecular Weight of ~48 kDa in *S. mutans*, however runs at about ~37 kDa on SDS-PAGE gels. Others have found that SecY from *E. coli* runs

aberrantly on SDS-PAGE gels, migrating at about ~35 kDa with a predicted Molecular Mass of ~48 kDa (170-171). It is not uncommon for very hydrophobic proteins to run aberrantly on SDS-PAGE gels. They bind more SDS and therefore migrate faster (172). The ~75 kDa species in *S. mutans* could be a dimeric form or possibly an unresolved heterotrimeric SecYEG complex, which would run at about that size. The oligomeric state of SecY is somewhat of a controversy in the protein translocation field, [reviewed in (52)]. It can clearly function as a monomer; however, some have reported it as a dimer or in higher oligomeric states when it is overexpressed (171, 173). SecY was identified in a 400 kDa complex containing SecYEG and FtsY, in *E. coli* using BN-PAGE combined with Western blot with a SecY antibody (174). SecY was also found as a 230 kDa complex containing a SecYEG dimer, as well as 440 kDa and 880 kDa complexes in *E. coli* when SecY was crosslinked as a dimer and co-expressed with SecA dimers (175).

The ~20 kDa moiety in the NG8 Western in Figure 4-4 probably corresponds to a breakdown product of SecY, which is known for its susceptibility to the protease FtsH (176). In studies by van Bloois (177) and Price (139), YidC was able to be crosslinked to FtsH, HtlC and HtlK, suggesting that in *E. coli*, YidC plays a role in quality control and maturation of membrane proteins. The decrease of SecY observed in the Δ*yidC2* mutant may indicate that YidC2 plays a regulatory role in FtsH activity or in the activity of other cellular proteases. A study in *E. coli* that investigated the FtsY protein's involvement in membrane protein biogenesis found that the amount of SecY was reduced in the membrane when FtsY was depleted (178). It is possible that FtsY could also be affected by deletion of *yidC2* in *S. mutans*. Additionally, SecE is also known to

require YidC for insertion in *E. coli* (179). Several studies have found that decreasing the level of SecE results in reduced SecY in the membrane (127, 180). Therefore, YidC2 could play a direct role in the insertion of SecY, or in the insertion or regulation of other proteins that effect SecY stability. Furthermore, SecY is located in an operon with ribosomal proteins, which could be down-regulated in the absence of YidC2 due to a cellular stress response. In microarray studies of an Δ*ffh* mutant in *S. mutans* (which has a similar growth and stress-sensitive phenotype to the Δ*yidC2* mutant), a number of proteases were up-regulated including; HtrA, putative ATP-dependent Clp protease (SMU.1672), a Zn-dependent protease (SMU.1438c), and class III stress-response related ATP-dependent Clp protease (SMU.2029) (75). In this same study there were also a number of down-regulated proteins involved in translation including several ribosomal proteins, putative translation initiation factor IF-1 (SMU.2004), 50S ribosomal proteins L7/L12, and L33. In *S. mutans* the *secY* gene (SMU.2006) is located upstream of translation initiation factor IF-1 (SMU.2004), which was down-regulated in the Δ*ffh* mutant, and could possibly be coordinately regulated. There is no microarray data yet available for the Δ*yidC1* or Δ*yidC2* mutants in *S. mutans*. However, considering the similar phenotype of the Δ*ffh* and Δ*yidC2* mutants, it is likely that many of the same pathways involved in stress tolerance would be affected.

Interestingly, the smear recognized by α-YidC1 was longer in the Δ*yidC2* mutant for both Westerns of first dimension and second dimension gels, indicating that YidC1 may be located in different complexes in the absence of YidC2 than in the wildtype. In a study in *B. subtilis* using BN-PAGE and C-terminally His-tagged and over-expressed YidC homologs (SpoIIIj and YqjG), researchers found that both co-purify with a ~600

kDa complex (the F_1F_o ATP synthase) (116). In a study of human Oxa1L to evaluate its involvement in the biogenesis of the F_1F_o ATP synthase using BN-PAGE combined with Western blot, researchers found that Oxa1L was part of a 600-700 kDa complex containing the F_1F_o ATP synthase (181). In addition they noted that Oxa1L was also part of several lower molecular weight complexes, evidenced by a streak in the second dimension BN/SDS-PAGE Western.

Differences in Membrane Protein Complexes Between Wild-Type NG8 and *yidC* Mutants in *S. mutans* Determined by BN-PAGE/LC-MS/MS

Differences in first dimension Blue-Native polyacrylamide gels between wild-type NG8 and the *yidC* mutants were further analyzed by excision of bands followed by protein identification using LC-MS/MS. The locations of the bands that were excised from the Blue-Native gels are shown in Figure 4-5. There were four gel slices analyzed for each strain. Proteins that were identified by LC-MS/MS are summarized in Tables 4-1 through 4-3. In each summary table the number of peptides recognized by mass spectrometry and used to identify the indicated proteins from two separate BN-polyacrylamide gels, are shown. Summary Table 4-1 shows the results for proteins indentified in high molecular weight complexes from Bands 1 and 2 and are referred to as the ~700 kDa and ~400 kDa complexes, respectively. Shown in Table 4-2 are the proteins identified in the lower molecular weight complexes that were located in Bands 3 and 4, referred to as the ~70 kDa and ~64 kDa complexes. Table 4-3 shows a summary of the ribosomal proteins indentified for each strain in all four bands that were analyzed. Detailed descriptions of each protein indentified in Tables 4-1 and 4-2 (including accession number, predicted molecular weight, biochemical pathway, and gene) are included in Table 4-4. Information about the ribosomal proteins is detailed

(accession number, predicted molecular weight, gene, and additional information) in Tables 4-5 and 4-6.

Tables 4-7 through 4-25, are organized according to the band that was excised and protein categories. They indicate the number of peptides identified by mass spectrometry with the percentage of the identified protein covered by the peptides, for both Trial 1 and Trial 2. Tables 4-26 through 4-29 show the ribosomal proteins indentified, organized by band location. Trial 1 and Trial 2 indicate two separate mass spectrometry analyses of two different BN-PAGE experiments using the same membrane samples. When samples were compared, a greater number of peptides corresponding to a given protein was interpreted to mean there was more of that protein in the sample resulting in a higher percentage of protein coverage.

Glycolytic enzymes

There were a number of glycolytic enzymes identified, with differences in their abundance and location between the wildtype and *yidC* mutants. Several glycolytic enzymes with a greater abundance in the wildtype membranes compared to either *yidC* mutant, were located in high molecular weight complexes (Tables 4-1, 4-2, 4-7 through 4-10). These included pyruvate formate lyase, bifunctional acetaldehyde CoA/alcohol dehygrogense, and enolase. Additionally, there was a large increase in the number and variety of glycolytic enzymes in lower molecular weight complexes in both mutants with a more pronounced effect in the Δ*yidC2* mutant (Tables 4-2, 4-9 and 4-10). These proteins included glucose kinase, glucose-6-phosphate insomerase, fructose-bisphosphate aldolase, transketolase, glyceraldehyde-3-phosphate dehydrogenase, enolase, pyruvate kinase, and lactate dehydrogenase.

Pyruvate formate lyase (PFL) was found in the ~700 kDa band from NG8 and was also found in the ~300 kDa band in all three strains, but with a larger number of peptides indentified in NG8 then either *yidC* mutant. Bifunctional acetaldehyde-CoA/alcohol dehydrogenase (AdhE) was also found in the ~700 kDa band of NG8, but was lacking or under-represented in the *yidC* mutants in this complex. AdhE is located downstream of pyruvate formate lyase leading to the production of ethanol from acetyl Co-A and acetaldehyde, with 2 NADH oxidized to 2 NAD+, thus maintaining redox balance in the cell. In addition to the ~700 kDa complex, AdhE was found in the ~70 and ~64 kDa bands in NG8 and Δ*yidC1* mutant, but not in the Δ*yidC2* mutant. In a transcriptome analysis that evaluated genes regulated by the acid tolerance response by Chen, et al 2010 (182), it was found that *adhE* was down-regulated in response to low pH. Thus it would be consistent for the *yidC2* mutant to have less AdhE because of an inability to regulate cytoplasmic pH. In a proteomics study of *Clostridium thermocellum* in which 2D-BN/SDS-PAGE (with 1% DDM) was used, AdhE was found in a high molecular weight complex of ~800 kDa associated with membranes (183).

Glucose kinase, which phosphorylates glucose transported by a glucose permease, was found in both mutants in the ~64 kDa band but was not found in NG8 in either experiment. Phosphoglyceromutase, enolase, and pyruvate kinase were better represented in the *yidC* mutant samples in lower molecular weight complexes compared to the wild-type NG8 samples, with a more pronounced effect in the Δ*yidC2* mutant strain. These enzymes are involved in the last three steps of glycolysis leading to the production of pyruvate. Pyruvate kinase, which functions as a homotetramer, is thought to be the rate limiting step in glycolysis in *S. mutans* because it is completely dependent

on glucose-6-phosphate for activity and is inhibited by inorganic phosphate (184). Since these enzymes are known to function as dimers or trimers, their presence of in the lower molecular weight complexes could represent a disruption of a high molecular weight functional multi-enzyme complex in the *yidC* mutants.

Glucose-6-phosphate isomerase, fructose-bisphosphate aldolase, and transketolase, enzymes of the Pentose Phosphate Pathway and nucleotide biogenesis were, in at least one instance, found to be more highly represented in the Δ*yidC2* mutant than the *ΔyidC1* mutant or wild-type NG8. This effect was seen primarily in the ~64 kDa complex (Tables 4-2 and 4-10). Moreover, transketolase was more highly represented in both *yidC* mutants in the ~64 kDa complex than in NG8 (Table 4-10). This combined with the increased level of GAPDH (glyceraldehydes-3 phosphate dehydrogenase) in the mutants, suggests that glycolytic metabolites might be diverted to the Pentose Phosphate Pathway in the absence of YidC1 or YidC2. This could reflect an increased need for nucleotides due to up-regulation of stress genes in the mutants. In a membrane proteomics study by Saller et al. 2010, transketolase and GAPDH of *B. subtilis* were found to be up-regulated two- and three-fold, respectively, when SpoIIIJ was depleted in a *ΔyqjG* strain (117).

Lactate dehydrogenase converts pyruvate to lactate at the expense of $NADH_2$, and is located at an important branch point in metabolism. This protein was identified in all three strains in the ~700 kDa band in Trial 1, and only in the *yidC* mutants in Trial 2, (Table 4-1). It was also found in equal amounts in all three strains in the ~300 kDa band (Table 4-2). Lactate dehydrogenase was not represented in the ~70 kDa, but was

found in ~64 kDa band in all three strains. In Trial 1 there was a greater representation of this protein in Δ*yidC2*, than in Δ*yidC1* or NG8 (Tables 4-2 and 4-10).

(NAD+) specific glyceraldehyde-3-phosphate dehydrogenase (GAPDH) was found to be highly represented in all samples submitted for LC-MS/MS, but was more prominent in *ΔyidC2* mutant membranes in the lower molecular weight complexes. GAPDH (*gapC*) is an important glycolytic enzyme as it produces NADH and 1, 3-bisphosphoglycerate, which is converted to 3-phosphoglycerate with the production of one ATP by phosphoglycerate kinase. It also works in reverse to produce glyceraldehyde-3-phosphate, which can be directed into the Pentose Phosphate Pathway for nucleotide synthesis (*S. mutans* does not contain the oxidative branch of the Pentose Phosphate Pathway). Other investigators have reported changes in GAPDH amount/localization under defined circumstances. A study by Baev (185) that investigated the membrane association of a GTP binding protein induced by stress (186), found that GAPDH demonstrated an increased association with the membrane fraction during stationary phase. SGP (*Streptococcus* GTP-binding protein) was found to associate with the membrane during acid-stress, temperature-stress and during stationary phase (185). A study by Biswas (187), that investigated the effects of a deletion of the HtrA extracellular protease/chaperone, found that the level of extracellular GAPDH in media increased when HtrA was absent. This study also found that extracellular enolase was increased in the HtrA mutant background.

Citrate metabolic enzymes.

Three enzymes of the Citrate Cycle were present in wild-type NG8 in the ~700 kDa band, but not indentified in either the Δ*yidC1* or Δ*yidC2* mutants (Tables 4-1 and 4-

11). The three enzymes identified were a putative citrate lyase beta subunit, citrate lyase alpha subunit and citrate synthase. *S. mutans* has an incomplete TCA cycle, and the enzymes that it does possess are probably involved in creating precursors for amino acid synthesis (10).

Cell wall-associated proteins

A number of cell wall-associated proteins were identified including; PrsA, penicillin binding protein 1a (Pbp1a), Pac/P1, and HtrA (serine protease) (Tables 4-12 to 4-14). PAc/P1 (170 kDa sortase substrate, surface adhesin) was only found in the *yidC* mutants in the ~700 kDa band. HtrA was found in the ~700 kDa band of the Δ*yidC2*, but also in the ~70 kDa band of NG8 and the Δ*yidC1* mutant, indicating there may be a difference in the localization of this serine protease in the absence of *yidC2*. PrsA (foldase protein with PPIase activity) was also found in the ~700 kDa band, but was present in all three strains. Additionally, PAc/P1 was also found in the ~300 kDa band of the Δ*yidC2* mutant only. Penicillin binding protein 1a was indentified in all three strains in the ~700 kDa band, but only in the *yidC* mutants in the ~300 kDa band. The presence of cell wall-associated proteins in a high molecular weight complex associated with membranes from *S. mutans* may stem from an inefficiency in their secretion and subsequent accumulation and association with the membrane. The secretion of surface localized proteins is not well understood in streptococci but presumed to occur post-translationally via the general secretion pathway (188). It has further been proposed that secretion occurs through a localized micro-domain known as the Exportal (68). The presence of cell wall-associated proteins in the *yidC* mutants may indicate a defect in the assembly and/or function of the secretion machinery and Exportal. *S. mutans* P1

has been reported to co-localize with an Exportal-like structure (189). P1 maturation is negatively affected by deletion of *yidC2*, as indicated by decreased immunoreactivity of certain anti-P1 monoclonal antibodies with the Δ*yidC2* strain, while elimination of *yidC1* results in increased detection of P1 on the cell surface. The association of P1 with the membranes of the *yidC* mutants and not in the wildtype is consistent with the YidC proteins' involvement in the secretion of surface localized proteins through the membrane in gram-positive bacteria. In addition, the changes in function and antigenicity of cell surface-localized P1 further suggests a role of *S. mutans* YidC proteins in surface protein maturation.

Transport proteins

There were several transporters identified in the ~700 and ~300 kDa bands of the *yidC* mutants that were not found in NG8 (Tables 4-1, 4-15 and 4-16). These included an oligopeptide ABC transporter (substrate binding protein), putative mechanosensitive channel of large conductance (MscL), a putative ABC transporter (lipoprotein) and the maltose/maltodextrin ABC transporter sugar binding protein (MalX). MscL is a known substrate of the YidC only (Sec-independent) pathway in *E. coli* (97, 190). MalX (known as MalE in *E. coli*) is the substrate binding protein of the $MalXFGK_2$ ABC transporter, and also requires YidC for proper assembly in *E. coli* (99).

Chaperones

Several chaperone proteins were identified, with an increased representation of GroEL in the Δ*yidC1* mutant compared to NG8 or *ΔyidC2*, in the higher molecular weight ~700 kDa and ~300 kDa bands (Tables 4-1, 4-17 to 4-18). In the lower molecular weight ~70 kDa and ~64 kDa bands (Tables 4-2, 4-19 and 4-20), GroEL was equally

represented in NG8 and *ΔyidC1*, but was poorly represented in *ΔyidC2*. DnaK and GroES were also identified, with GroES only represented in the *yidC* mutants, and DnaK only found in NG8 or Δ*yidC1*. Overall, there appeared to be less molecular chaperones associated with the *ΔyidC2* membranes than either NG8 or *ΔyidC1*. In the case of GroEL there was more of it associated with the *ΔyidC1* mutant in the higher molecular weight complexes. Proteomics data of the *yidC* depletion strain in *E. coli*, showed an increase in GroEL and DnaK in the cytoplasm and membrane under *yidC* depletion conditions (139). In contrast, the doubly depleted SpoIIIJ/*ΔyqjG* strain in *B. subtilis* did not affect the level of GroELS or DnaKJ (117).

Amino acid metabolism

Proteins that were identified that are involved amino acid metabolism are shown in Tables 4-21 to 4-23. Branched-chain amino acid aminotransferase and aspartate-semialdehyde dehydrogenase were found in the ~64 kDa band of the Δ*yidC2* mutant, but not found in NG8 or the Δ*yidC1* mutant (Table 4-23). These enzymes are involved in the catabolism and biosynthesis of branch-chained amino acids. Leucine, isoleucine, and valine are found in high concentrations in membrane proteins. If membrane proteins were degraded because of an insertion defect, this pathway could be up-regulated to compensate for the increased need for catabolism of branch-chained amino acids (due to proteolysis). In addition to these enzymes, a branched-chain amino acid ABC transporter was also identified in both *yidC* mutants in the ~700 kDa band, but was absent in NG8 (Table 4-15), providing further evidence that this pathway may be up-regulated or perturbed in the mutants. Furthermore, NAD+ specific glutamate dehydrogenase (GdhA) was under-represented in the Δ*yidC2* mutant compared to NG8

and the Δ*yidC1* mutant in the ~300 kDa band, (Table 4-9). In a recent study by Chen, et al. 2010 (182) using microarray to investigate the role of GlnR in acid-mediated repression of genes related to glutamine and glutamate metabolism, the authors mention that *gdhA* was downregulated by 0.58 to 0.75 fold during ATR (182). Therefore, a decrease of GdhA in the *yidC2* mutant could be indicative of an acid adapted response, due to a decreased ability to regulate the cytoplasmic pH.

Butanoate, glutathione, and starch metabolic enzymes

Two proteins involved in butanoate metabolism were identified with increased representation in the *yidC* mutants; acetoin reductase and putative succinate semialdehyde dehydrogenase (Tables 4-24 to 4-25). In a proteomics study of *Corynebacterium glutamicum* in response to pH changes, researchers found that acetoin reductase was present in the membrane fraction and up-regulated during low pH conditions (at pH 6.0). Acetoin reductase (*butA* or *budC* in *S. mutans*) results in the production of 2, 3-butanediol from pyruvate with intermediates of acetolactate and acetoin. Acetoin and 2, 3-butanediol are neutral molecules, providing the cell with a means to eliminate pyruvate without producing acid. A study by Johansen (191) found that this pathway was induced by acetate in *Enterobacter aerongens*, and that mutations in this pathway resulted in a lower terminal culture pH. Studies in *S. mutans* have also implicated acetoin reductase in acid tolerance. A 2D-SDS-PAGE proteomics study of soluble proteins from *S. mutans* grown at low pH found that acetoin reductase was significantly up-regulated (192). In addition, a recent study by Chen, et al. 2010, using microarray, found that acetoin reductase was up-regulated fourfold under ATR conditions (182).

Glutathione reductase is an enzyme involved in oxidative stress tolerance in *S. mutans*, with increased activity when cells are grown with aeration (193). This enzyme was present in the ~70 kDa band in all three strains (Table 4-24). However, there was a higher representation in the *ΔyidC2* mutant compared to NG8 or *ΔyidC1*. Glutathione reductase was also found in the ~64 kDa band in Trial 1 in both NG8 and Δ*yidC2* mutant, with a greater representation in the *ΔyidC2* mutant (Table 4-25).

There were a number of enzymes involved in starch metabolism found in the ~70 kDa and ~64 kDa bands that were represented to a greater extent in the *yidC* mutants than in NG8 (Tables 4-24 and 4-25), with a greater effect in the *yidC2* than the *yidC1* mutant. Glucose-1-phosphate adenyltransferase was identified in both *yidC* mutants but absent in NG8. Additionally, glycogen phosphorylase was present in all three strains in the ~70 kDa complex in both trials, with a greater representation in the *ΔyidC2* mutant in Trial 1. Glycogen biosynthesis protein was also seen in the ~70 kDa band in the Δ*yidC1* and Δ*yidC2* mutants, but was not identified in the NG8 sample.

Ribosomal proteins

There was a pronounced decrease or lack of ribosomal proteins indentified in gel slices from the Δ*yidC1* and Δ*yidC2* mutants (Tables 4-3, and 4-26 to 4-27). A number of ribosomal proteins were associated with the membranes of wild-type NG8 in all bands submitted for LC-MS/MS identification, with an increase in number and variety seen in the lower molecular weight complexes (Tables 4-21 through 4-24). Conversely, there was almost a complete lack of ribosomal proteins associated with the Δ*yidC2* mutant membranes. There was also a notable decrease seen in the Δ*yidC1* mutant, but the effect was less severe than in the Δ*yidC2* mutant. This effect was not observed in a Δ*ffh*

mutant (data not shown), as there were a similar number of ribosomal proteins associated with the membranes from this strain as in NG8. For a detailed description of the ribosomal proteins identified see Tables 4-5 and 4-6.

Ribosomal proteins are small, ranging from 30 kDa to 6 kDa in size. In 2D BN/SDS-PAGE analysis of these strains (Figure 4-2), there was a lack of proteins in the lower right corner of the Δ*yidC2* mutant, below 20 kDa and corresponding to the lower molecular weight complexes in the BN- polyacrylamide gel. In comparison, in the NG8 and the Δ*yidC1* 2D-gels, there were lots of proteins stained in the area where ribosomal proteins are expected to run. Ribosomes are known to co-purify with membranes, and in one study researchers found that FtsY is required for ribosomal association with the membrane in *E. coli* (194). However, since the FtsY protein is dispensable in *S. mutans* (as is the entire SRP pathway) YidC1 or YidC2 may play a role in ribosomal association with membranes. The mass spectrometry data are consistent with a ribosome binding function of YidC2 involved with co-translational translocation, allowing for elimination of the SRP pathway. Cross-complementation studies performed in Yeast indicate that this function is dependent on the C-terminal tail of YidC2 (123). The current data provides the first evidence of a ribosomal association of YidC in *S. mutans*.

Two ribosomal proteins that are not found in the UA159 genome sequence (10) were identified in NG8, L2 and L23. Using PCR, Dr. Nathan Lewis from the Brady lab has confirmed that L23 and L2 are present in NG8 and UA159 (personal communication with Nathan Lewis and L.J. Brady). This indicates there was a mistake made during the sequencing of the UA159 genome. L23 is the ribosomal protein shown to be important for Ffh and trigger factor ribosome interactions in *E. coli*. It is the L23 homolog Mrp20 in

yeast mitochondria, which binds to the C-terminal tail of Oxa1. These genes are also present in *S. mutans* strain NN2025, which was recently sequenced (195).

Extracellular GAPDH Activity is Increased in *yidC* Mutants

GAPDH has been found on the surface of *S. mutans* and other streptococci, as well as a number of other cytoplasmic proteins. It is not known why this occurs or how they are transported because they do not contain signal peptides. In one study of *S. pneumoniae*, mutanolysin digestions of cells walls were analyzed by 2D-SDS PAGE combined with mass spectrometry (196). In this study, GAPDH, NADP-glutamate dehydrogenase, enolase, lactate dehydrogenase, DnaK, and fructose bisphosphate aldolase, among other proteins, were identified as associated with the cell wall. Tryptic digestion of *S. pyogenes* cell wall proteins combined with HPLC (high-performance liquid chromatography) separation of peptides and LC-MS/MS analysis, indentified 21 cytoplasmic proteins including GAPDH, enolase, 50S ribosomal proteins L7/L12/L5/L11, 30S ribosomal protein S8, pyruvate kinase, NADP-dependent GAPDH, phospho-glycerate kinase, pyruvate formate-lyase, RopA (trigger factor), and Hsp60 and Hsp10 homologs (197). The Staphylococcal transferrin receptor (Tpn) was identified as extracellular GAPDH, a 42 kDa protein that also possesses GAPDH activity. The functional conformation is a 170 kDa tetramer, which is necessary for GAPDH activity, while the monomer is capable of binding transferrin [reviewed in (198)].

Since there was more GAPDH associated with the membranes in the *ΔyidC2* mutant than NG8 or *ΔyidC1* (Tables 4-1 and 4-2), it was logical to test whether there was a difference in extracellular GAPDH activity. The various strains were grown overnight in THYE, and GAPDH activity of whole cells was measured (Materials and

Methods). Consistent with the increased levels of GAPDH in the mutants seen by BN-PAGE/LC-MS/MS, there was a significant increase in extracellular GAPDH activity in the *ΔyidC2* mutant compared to the *ΔyidC1* mutant or wild-type NG8 (Figure 4-6). The *yidC2ΔC* (AH412) strain was also evaluated for extracellular GAPDH activity, and demonstrated significantly increased surface-localized GAPDH activity, at a level similar to a complete deletion of *yidC2*. YidC1C2 (SP13) was able to complement and restore GAPDH activity toward wildtype levels in the Δ*yidC2* mutant. YidC2C1 did not complement and displayed GAPDH activity similar to that of the Δ*yidC2* mutant. When *yidC1* was deleted in the *yidC2ΔC* background, there was a significant decrease in GAPDH activity compared to *yidC2ΔC* (AH412) alone, indicating that whatever the cause for increased GAPDH activity, it is alleviated somewhat by deletion of *yidC1* in this background. The purpose of extracellular GAPDH is unknown in *S. mutans* and will require further investigation. It is possible that GAPDH is transported to the cell surface as part of a stress response, with an as yet unknown function. The increased surface localized activity seen in the mutants could be the result of an alteration in the maturation of GAPDH promoting the formation of tetramers (the enzymatically active form). It is possible that the cell wall is different in the mutants resulting in more GAPDH associated with the cell surface, whereas in the wildtype it is released into the culture supernatant.

Discussion

Other proteomics approaches have been used to investigate the function of YidC homologs in their parent organism. A recent study by Price (139) used metabolic labeling with $^{15}N/^{14}N$ of membrane proteins, combined with protein identification with

LC-MS/MS, to compare the effects of YidC depletion under aerobic and anaerobic growth. This study reported an increase in the number of ribosomes associated with membranes under aerobic growth conditions, as well as increased chaperones and a decrease in a number of ABC transporters. There were also effects seen in secreted proteins under aerobic conditions, as there was a decrease in periplasmic proteins. The effects of YidC depletion under anaerobic conditions were less severe. Protein aggregates were also isolated from YidC depleted cells in this study and found to contain a number of outer membrane proteins (indicating a secretion defect), periplasmic proteins (including DegP/HtrA and SurA /chaperone), ribosomal proteins, and several cytoplasmic chaperones.

In a microarray study of the *E. coli* YidC depletion strain JS7131 (199), there was up-regulation of genes for HflC and HflK, proteins that negatively regulate the activity of HflB/FtsH. YidC has been shown by others to interact with HflC/K and HflB/ FtsH (139, 177). This microarray study also found YidC depletion resulted in up-regulation of ribosomal genes, as well as *secY* (authors noted that *secE* and *secG* were not affected). Two genes that were most significantly affected by YidC depletion were *cadA* and *cadB*, which were up-regulated 32.8 and 20.7 fold respectively. These genes are located in the Cad operon (CadA is a lysine decarboxylase, CadB transports cadeverine), which is turned on during external acid-stress or anoxic growth conditions (200-201). CadA decarboxylates lysine producing CO_2 and cadeverine, effectively removing protons from the cytoplasm, cadeverine is then exported by CadB. The authors postulate that YidC depletion results in decreased cytoplasmic pH, due to impairment of the electron transport chain in the absence of YidC, inducing an acid

stress response. *S. mutans* has a similar system to CadBA that is induced by low pH, known as the agmatine deiminase system (AgDS) (202). In this system agmatine enters the cell through the *aguD* transporter, is hydrolysed by agmatine deiminase (*aguA*) to *N*-carbamolyputrescine and ammonia. *N*-carbamolyputrescine is phosphorylated by putrescine carbamoyltransferase (*aguB*) to yield putrescine and carbamoylphosphate. Carbamoylphosphate is in turn de-phosphorylated by carbamate kinase (*aguC*) producing ATP, CO_2 and NH_3. The anti-porter (*aguD*) then exchanges putrescine for agmatine (203). The AgDS was also shown to be regulated by multiple two component systems induced by acid and temperature stress (204). It would be interesting to test if AgDS is up-regulated in either the *yidC1* or *yidC2* mutants in future studies.

The results from this BN-PAGE study demonstrated differences in several biochemical pathways between wild-type NG8 and the *yidC* mutants, that are consistent with findings by Len (14) of acid adapted cells, that suggest the *yidC* mutants may be responding to low internal pH that is the result of decreased proton F_1F_o ATPase activity. There was evidence in the *yidC* mutants that pyruvate may be diverted to alternative pathways by the increase in Pentose Phosphate Pathway enzymes, and those involved in butanoate metabolism, which results in the production of the neutral compound acetoin. There was also an increase in or difference in the location of branched-chain amino acid aminotransferase (ilvE) and aspartate-semialdehyde dehydrogenase in the Δ*yidC2* mutant. Both are involved in branched-chain amino acid synthesis or degradation. Since production of branched-chain amino acids leads to production of ammonia, this would offset the increased internal pH resulting from

decreased F_1F_o ATPase activity. A number of other pathways were also affected by elimination of *yidC1* and *yidC2* including enzymes of the Citrate Cycle, which were absent in high molecular weight complexes in the *yidC* mutants, additionally, a number of transporters and cell wall-associated proteins were found in high molecular weight complexes in the mutants, but were absent in the wildtype. There was also a decrease in the number of ribosomal proteins associated with the *yidC* mutant membranes in low molecular weight complexes. Overall these results suggest a role for YidC1 and YidC2 in several pathways possibly involving assembly of complexes containing glycolytic enzymes, Citrate metabolism, and tethering of ribosomes to the membrane. Furthermore, effects on ABC transporters and cell wall-associated proteins and their detection in high molecular weight complexes suggest there may be a defect in protein transport resulting in a build-up of these proteins in the membranes of the *yidC* mutants.

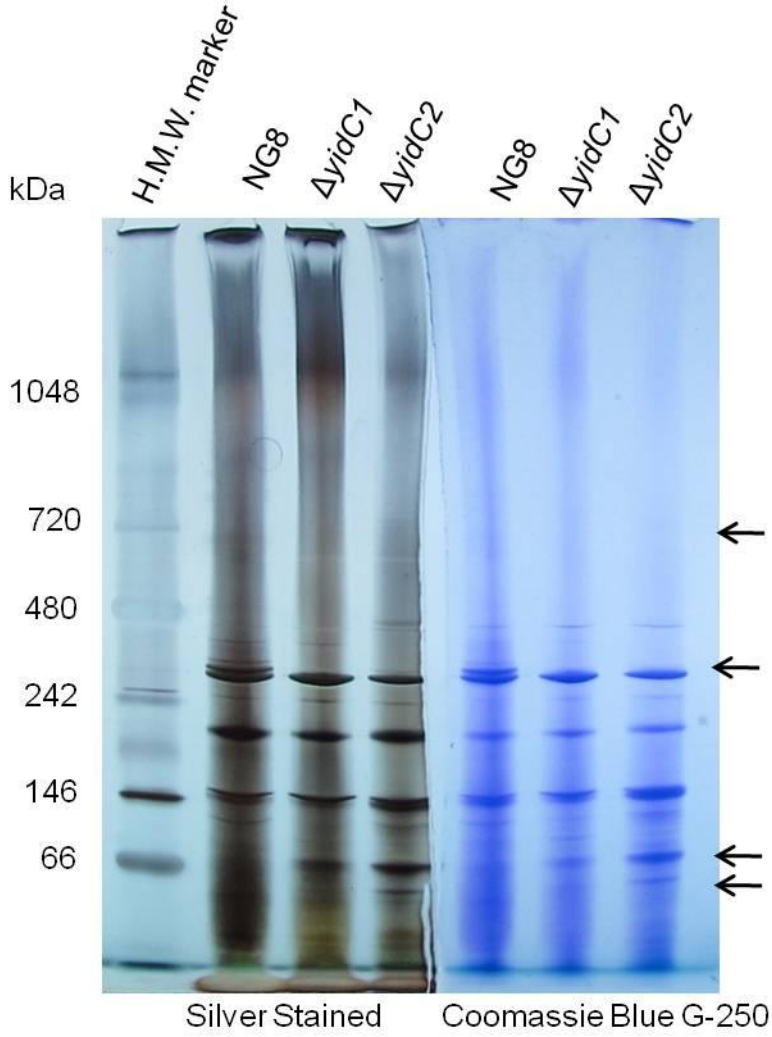

Figure 4-1. Silver stained versus Coomassie Blue G-250 stained first dimension Blue-Native polyacrylamide gels. Membranes were prepared from *S. mutans* wild-type NG8, Δ*yidC1* and Δ*yidC2* mutant strains. 50 µg of each sample was loaded per lane of an Invitrogen 3-12% NativePAGE™ Novex® Bis Tris Gel. Left panel shows results of gel stained with BioRad Silver Stain Plus Kit and right panel shows results with Coomassie Blue G-250 (see Materials and Methods for details). Arrows indicate bands of interest.

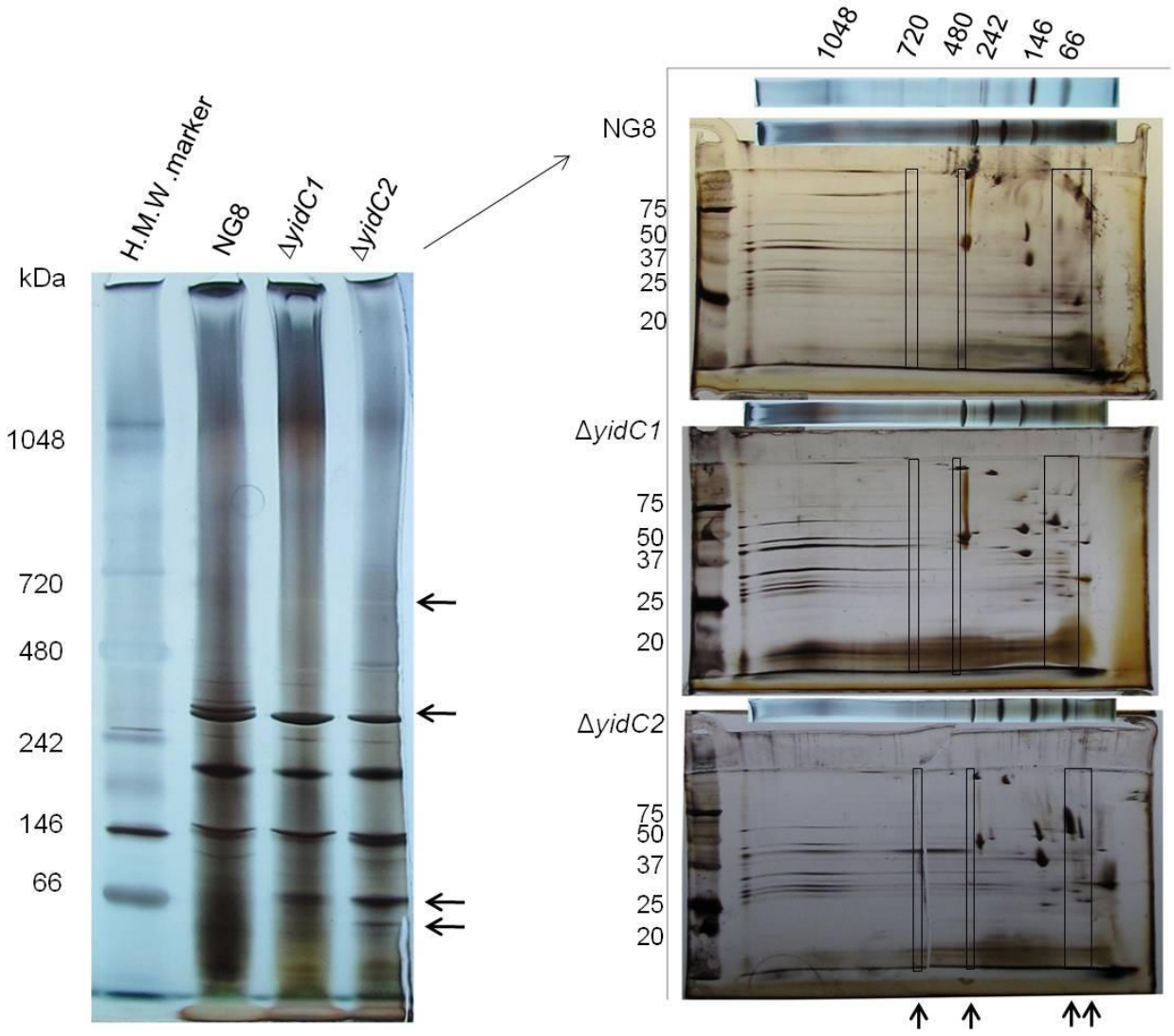

Figure 4-2. Silver stained first dimension Blue-Native polyacrylamide gel and second dimension Tricine-SDS polyacrylamide gels. Membranes were prepared from *S. mutans* wild-type NG8, Δ*yidC1* and Δ*yidC2* mutant strains. 75 µg of each sample was separated on an Invitrogen 3-12% NativePAGE™ Novex® Bis Tris Gel. Gel strips were cut out, reduced (50mM DTT), alkylated (50 mM DMA), and quenched (5 mM DTT, 20% ethanol) in LDS sample buffer. Gel strips were then applied to second dimension 10% Tricine-SDS polyacrylamide gels. Second dimension gels were silver stained using Silver Stain Plus kit from BioRad. Arrows indicate the bands of interest, and boxes indicate the respective areas of interest in the second dimension gels.

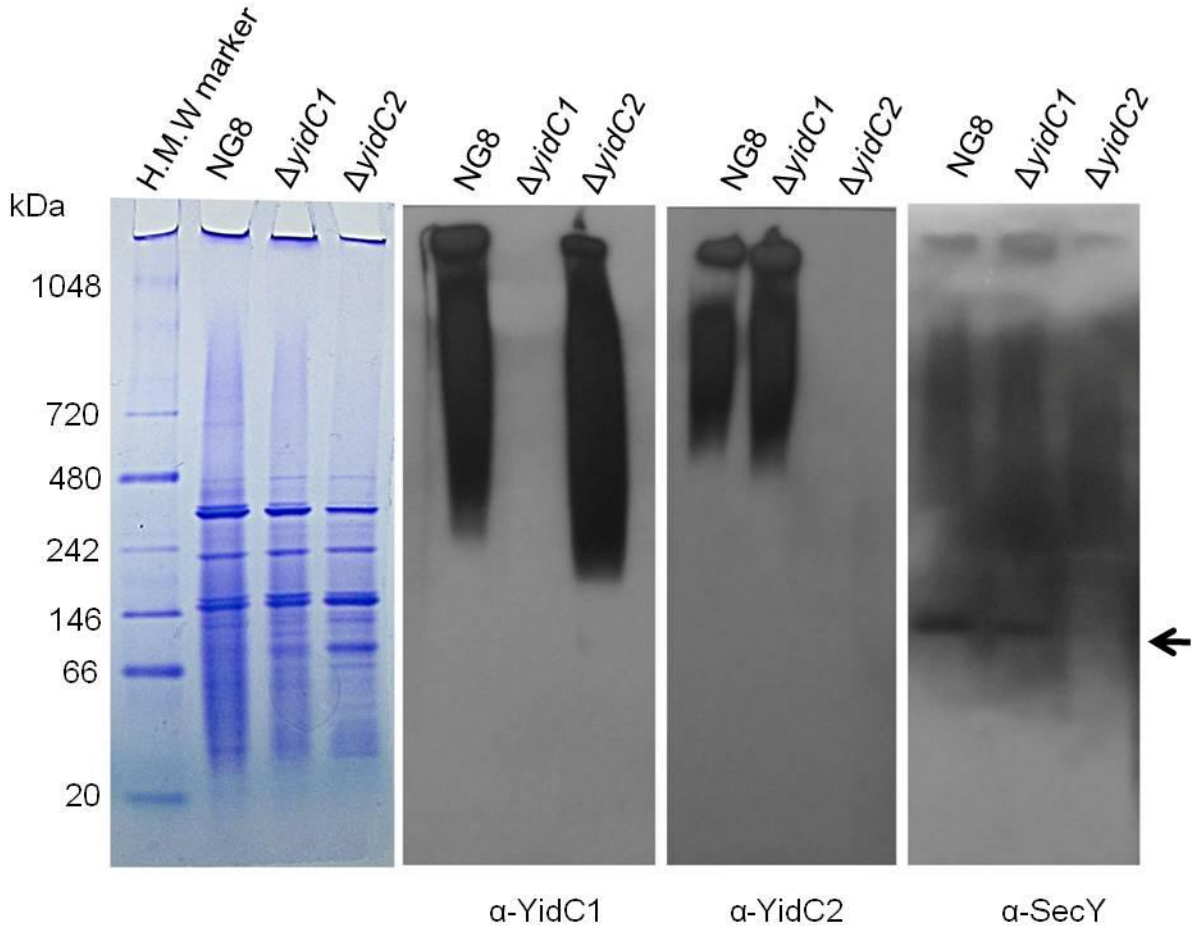

Figure 4-3. Western blots of Blue-Native polyacrylamide gels reacted with antibodies against YidC1, YidC2 and SecY. Membranes were prepared from *S. mutans* wild-type NG8, Δ*yidC1* and Δ*yidC2* mutant strains, and 50 µg of each sample was separated on an Invitrogen 4-16% NativePAGE™ Novex® Bis Tris Gel. Proteins were transferred to a PDVF membrane and reacted with affinity purified antibodies against C-terminal synthetic peptides (YidC1 or YidC2) or against 4 synthetic peptides of SecY (see Materials and Methods, Chapter 2 for description of antibodies). Arrow indicates a ~146 kDa band containing SecY.

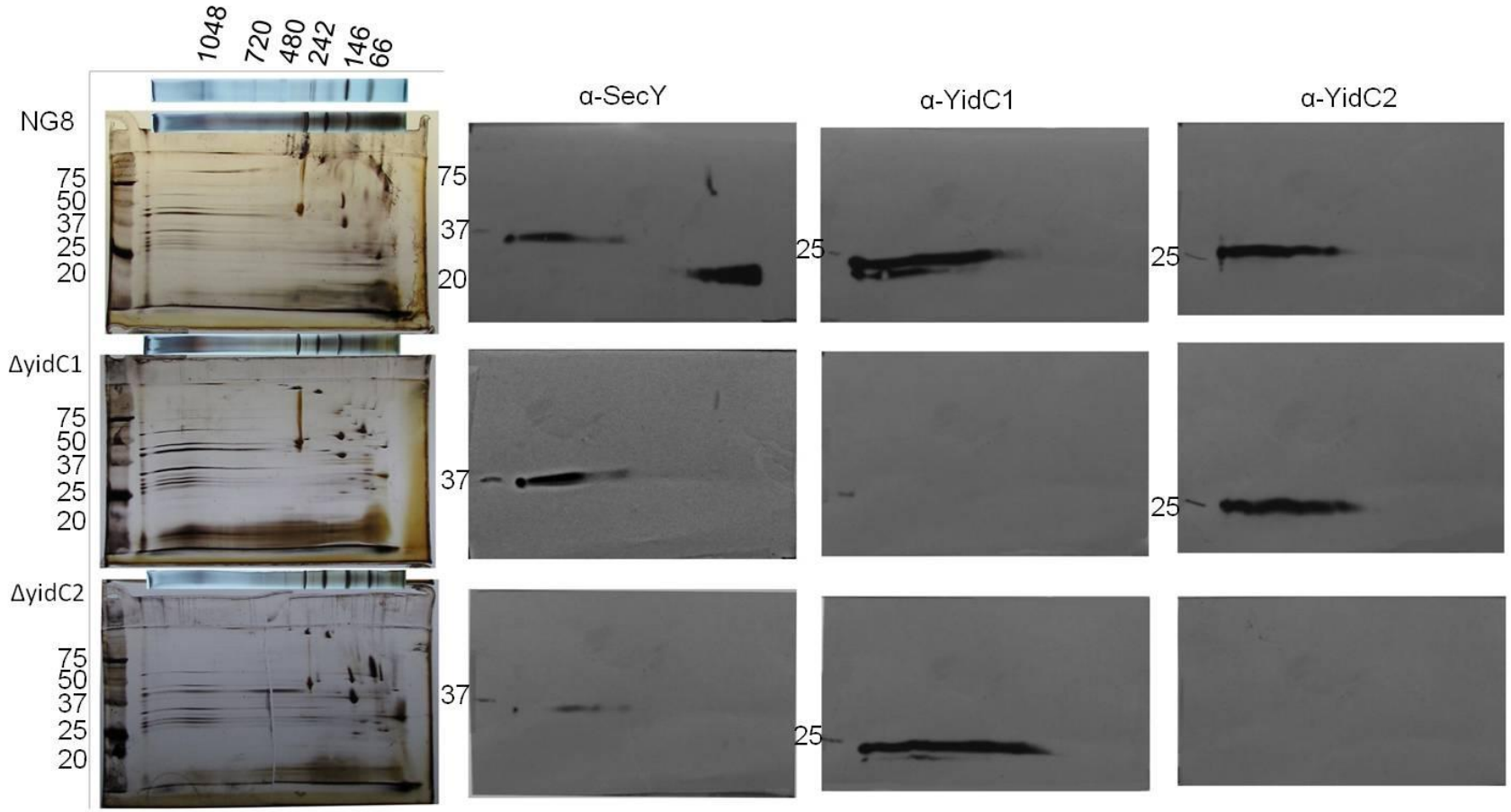

Figure 4-4. Western blot of second dimension BN/SDS-polyacrylamide gels reacted with affinity purified antibodies against SecY, YidC1, or YidC2. Left panel shows representative second dimension SDS-polyacrylamide silver stained gels for NG8, Δ*yidC1* and Δ*yidC2* strains. Right panels show Western blots for SecY (~75 kDa, ~37 kDa and ~20 kDa bands), YidC1 (expected ~24 kDa band) and YidC2 (expected ~28 kDa band).

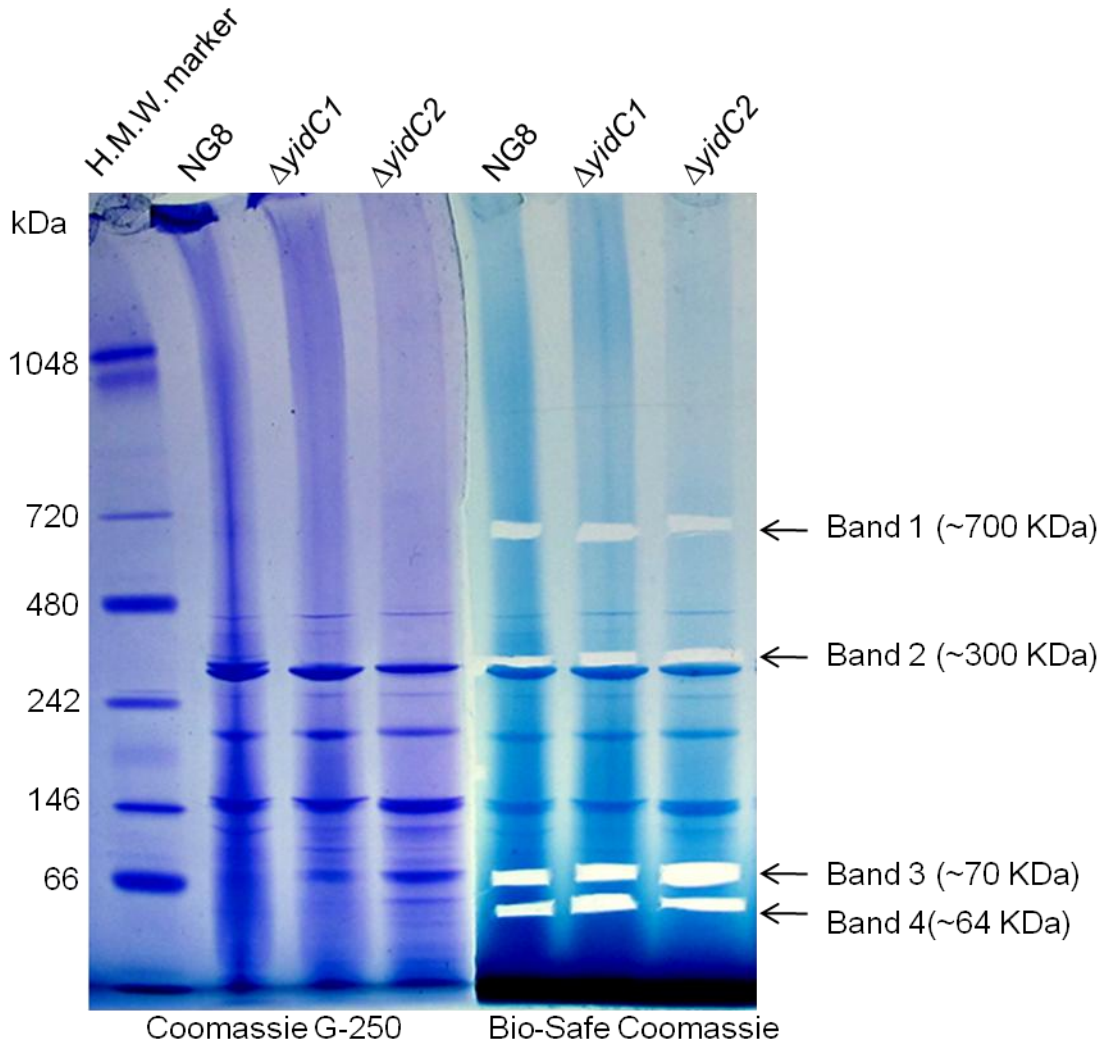

Figure 4-5. Blue-Native PAGE showing differences in membrane protein complex composition and indicating the gel slices analyzed by LC-MS/MS, for *S. mutans* wildtype NG8, *ΔyidC1* and *ΔyidC2* mutant strains. For each sample, 50 µg of DDM solublized membrane proteins were loaded per lane on a 3-12% Invitrogen Native PAGE™ Novex® Bis-Tris Gel (see Materials and Methods). Left panel shows a representative Blue Native gel stained with Coomassie Blue G-250. Right panel shows the other half of the same gel stained with Bio-Safe Coomassie (BioRad) with gel slices removed for LC-MS/MS analysis. Bands 1- 4 will be referred to in data Tables 4-1 through 4-29 summarizing proteins identified by LC-MS/MS.

Table 4-1 Summary of proteins identified by LC-MS/MS in BN-PAGE high molecular weight complexes from Bands 1 and 2

	Band 1 (~700 kDa)			Band 2 (~300 kDa)		
Identified Proteins	NG8	ΔyidC1	ΔyidC2	NG8	ΔyidC1	ΔyidC2
Glycolysis						
Glyceraldehyde-3-phosphate dehydrogenase	4[a] -0	0-7	2-7	2 -3	1-5	1-6
Phosphoglyceromutase	-	1-0	-	-	1-0	-
Enolase-phosphopyruvate hydratase	18-0	1-2	1-2	27-17	17-8	11-2
Pyruvate kinase	-	0-6	1-2	-	1-1	2-2
Pyruvate formate-lyase	1-0	-	-	9-1	2-2	1-0
Bifunctional acetaldehyde-CoA/alcohol dehydrogenase	12-0	-	-	-	-	-
L(+)-lactate dehydrogenase	3-0	2-3	3-1	1-1	3-1	2-1
Citrate cycle (TCA)						
Putative citrate lyase CilB, citryl-CoA lyase, beta subunit	4-0	-	-	-	-	-
Citrate lyase, alpha subunit	3-5	-	-	-	-	-
Citrate synthase	3-0	-	-	-	-	-
Cell wall biosynthetic proteins						
Foldase protein PrsA	3-0	1-3	2-1	-	-	0-1
Penicillin-binding protein 1a	1-0	5-3	3-0	-	1-0	1-0
PAc/P1 Major cell-surface adhesin	-	-	2-5	-	-	0-5
Serine protease HtrA	-	-	2-0	-	-	-
Transporters						
Branched-chain amino acid- ABC transporter (binding protein)	-	3-2	4-0	-	-	-
Oligopeptide ABC transporter, substrate-binding protein OppA	-	-	2-0	-	-	-
MscL–putative large conductance mechanosensitive channel	-	2-0	1-0	-	1-0	-
Putative ABC transporter (lipoprotein)	-	4-3	2-0	0-1	-	1-0
Maltose/maltodextrin ABC transporter, sugar-binding protein	-	1-0	1-0	-	-	-

Table 4-1. Continued

	Band 1 (~700 kDa)			Band 2 (~300 kDa)		
Indentified proteins	NG8	ΔyidC1	ΔyidC2	NG8	ΔyidC1	ΔyidC2
Charperones						
GroEL	-	5-0	-	2-0	8-0	1-0
DnaK	-	1-0	-	-	-	-
GroES	-	0-2	0-1	-	-	-
Amino Acid metabolism						
Aspartate-semialdehyde dehygrogenase	-	1-0	-	-	-	-
Glutamate dehydrogenase	-	-	-	17-11	7-15	3-0
Putative aminopeptidase P	-	-	-	1-0	1-0	4-0

[a] Number of unique peptides in the gel slice identified by LC-MS/MS that were used to identify the protein. Peptides indentified in Trials 1 and 2 are separated by dashes. – indicates no peptides were detected in either experiment.

Table 4-2. Summary of proteins identified by LC-MS/MS from BN-PAGE lower molecular weight complex from Bands 3 and 4.

	Band 3 (~70 kDa)			Band 4 (64 kDa)		
Identified Proteins	NG8	Δ*yidC1*	Δ*yidC2*	NG8	Δ*yidC1*	Δ*yidC2*
Glycolosis						
Phosphoenolpyruvate: sugar PTS enzyme 1	1-0[a]	2-0	3-0	-	-	-
Glucose kinase	-	-	3-0	-	4-7	16-7
Glucose-6-phosphate isomerase	-	-	2-1	-	1-0	15-4
Fructose-bisphosphate aldolase	-	-	1-0	1-0	2-0	7-0
Transketolase	4-0	5-2	5-1	6-1	5-8	17-6
Glyceraldehyde-3-phosphate dehydrogenase	1-0	4-0	11-0	4-3	0-5	13-7
Phosphoglycerate kinase (pgk)	-	1-0	1-0	1-1	0-4	5-2
Phosphoglyceromutase	-	1-0	-	1-0	3-1	4-2
Enolase	0-4	4-2	12-2	0-3	4-2	7-3
Pyruvate kinase	3-1	5-9	14-7	4-5	5-14	11-8
Bifunctional acetaldehyde-CoA/alcohol dehydrogenase	1-0	1-0	-	1-0	1-0	-
L(+)-Lactate dehydrogenase	2-2	2-1	4-0	2-2	2-2	7-1
Charperones						
GroEL	7-6	7-8	0-1	8-5	4-10	6-0
DnaK	2-0	2-0	-	-	-	-
GroES	-	0-2	0-1	-	-	-
Amino acid metabolism						
Branched chain amino acid aminotransferase	-	-	-	-	-	4-0
Aspartate-semialdehyde dehydrogenase	-	-	-	-	-	4-0
Butanoate metabolism						
Acetoin reductase	-	-	5-0	-	1-0	4-0
Putative succinate semialdehyde dehydrogenase	4-10	14-10	36-15	-	2-0	6-1

Table 4-2. Continued

Identified Proteins	Band 3 (~70 kDa) NG8	Δ*yidC1*	Δ*yidC2*	Band 4 (64 kDa) NG8	Δ*yidC1*	Δ*yidC2*
Glutathione metabolism						
Aminopeptidase N, PepN	1-0	-	5-0	-	-	-
Glutathione reductase	4-1	3-2	13-4	1-0	-	3-0
Starch and Sucrose metabolism						
Glucose-1-phosphate adenylyltransferase	-	-	4-1	-	1-0	9-4
Putative glycogen biosynthesis protein GlgD	-	1-0	5-0	-	-	-
Glycogen phosphorylase phsG	3-4	4-5	14-3	-	-	-

[a] Number of unique peptides in the gel slice identified by LC-MS/MS that were used to identify the protein. Peptides indentified in Trials 1 and 2 are separated by dashes. – Indicates no peptides were detected in either experiment.

Table 4-3. Summary of ribosomal proteins identified by LC-MS/MS from BN-PAGE experiments.

	Band 1 (~700 kDa)			Band 2 (~300 kDa)			Band 3 (~70 kDa)			Band 4 (64 kDa)		
Protein	NG8	ΔyidC1	ΔyidC2	NG8	ΔyidC1	ΔyidC2	NG8	ΔyidC1	ΔyidC2	NG8	ΔyidC1	ΔyidC2
50S-L1	-	-	-	-	-	-	-	1-0	-	2-0	-	3-0
50S-L2	-	2-0[a]	-	2-0	1-0	-	1-0	1-0	-	2-0	-	-
50S-L5	-	-	0-1	-	-	0-1	0-3	-	-	0-2	-	-
50S-L6	-	-	-	-	-	-	2-1	1-0	-	2-3	1-0	-
50S-L10	-	-	-	-	-	-	1-0	1-0	-	2-0	-	-
50S-L14	-	-	-	2-0	-	-	-	-	-	-	-	-
50S-L17	-	1-0	-	-	1-0	-	1-0	1-0	-	1-0	1-0	2-0
50S-L18	3-0	-	-	-	1-0	-	2-0	-	-	2-0	1-0	-
50S-L19	-	-	-	3	-	-	0-1	-	-	-	-	-
50S-L20	-	-	-	-	-	-	1-0	1-0	-	2-0	-	-
50S-L22	-	-	-	-	-	-	2-3	-	-	1-3	-	-
50S-L23	-	-	-	-	-	-	0-3	0-1	-	0-3	-	-
50S-L27	-	-	-	-	-	-	0-1	-	-	0-2	-	-
30S-S2	3-0	-	-	-	-	-	-	-	-	1-0	-	-
30S-S3	2-0	-	-	-	-	-	-	-	-	-	-	-
30S-S4	-	1-0	-	0-2	-	-	2-5	-	-	1-4	-	-
30S-S5	-	-	-	7-8	2-0	1-0	0-3	0-1	-	0-4	-	-
30S-S7	-	-	-	-	-	-	1-4	0-1	-	3-4	0-1	-
30S-S8	-	-	-	-	-	-	3-2	1-1	-	2-3	0-2	2-0
30S-S9	2-0	-	-	1-0	-	-	-	-	-	1-0	1-0	-
30S-S10	-	-	-	-	-	-	0-2	-	-	0-2	-	-
30S-S11	-	-	-	-	-	-	1-0	-	-	2-0	-	-
30S-S12	-	-	-	-	-	-	3-0	-	-	2-0	-	-

[a] Number of unique peptides in the gel slice identified by LC-MS/MS that were used to ID the protein. Number of peptides indentified in Trials 1 and 2 are separated by dashes. – Indicates no peptides were detected in either experiment.

Table 4-4. Information regarding proteins identified by LC-MS/MS listed in Tables 4-1 to 4-2 including predicted location, molecular weight, gene name, biochemical pathway and accession number.

Accession number	Protein ID	Biochemical Pathway	Gene	M.W. (Da)	PSORTb v. 3.0.2
	Glycolysis-Central Metabolism				
24370669	Enolase- phosopyruvate hydratase	E.C. 4.2.1.11	Smu.1247 *eno*	46,727	Cyto (10.0)[a]
24379618	Pyruvate kinase	E.C.2.7.1.40	Smu.1190 *pykF*	54,236	Cyto (7.50)
24378857	Glyceraldehyde-3-P dehydrogenase	E.C.1.2.1.12	Smu.360 *gapC*	35,937	Cyto (9.97)
24378663	Bifunctional acetaldehyde-CoA/alcohol DH	E.C.1.1.1.1	Smu.148 *adhE*	96,862	Cyto (9.97)
24379547	L(+)-lactate dehydrogenase	E.C.1.1.1.27	Smu.1115 *ldh*	35,114	Cyto (9.97)
24379148	Phosphoenolpyruvate sugar PTS enzyme I	PTS	Smu.675 *ptsA*	63,267	Cyto (10.0)
24378895	Pyruvate formate lyase	E.C.2.3.1.54	Smu.402 *pfl*	87,475	Cyto (9.97)
24379074	Phosphoglyceromutase	E.C.5.4.2.1	Smu.596 *gpmA*	25,919	Cyto (7.50)
24379024	Putative glucose kinase	E.C.2.7.1.2	Smu.542 *glk*	33,504	Cyto (9.97)
24378809	Glucose-6-phosphate isomerase	E.C.5.3.1.9	Smu.307 *pgi*	49,291	Cyto (9.67)
24378620	Fructose-bisphosphate aldolase	E.C.4.1.2.13	Smu.99 *fbaA*	31,295	Cyto (7.50)
24378858	Phosphoglycerate kinase	E.C.2.7.2.3	Smu.361 *pgk*	41,914	Cyto (9.97)
24378794	Transketolase	E.C.2.2.1.1	Smu.291 *tkt*	70,945	Cyto (7.50)
	Citrate Cycle (TCA)				
24379459	Putative citrate lyase, citryl-CoA lyase β-subunit	E.C.4.1.3.6.	Smu.1020 *cilB*	32,808	Cyto (9.97)
24379460	Citrate Lyase, α-subunit	E.C.4.1.3.6.	Smu.1021 *cilA*	55,324	Cyto (9.97)
24379144	Citrate synthase	E.C.2.3.3.1.	Smu.671 *citZ*	42,580	Cyto (9.97)
	Cell wall biosynthetic proteins				
24379121	PrsA- foldase protein (PPIase)	E.C.5.2.1.8	Smu.648 *prsA*	39,961	Memb (9.68)[+]
24378955	Penicilin binding protein 1a	NA	Smu.467 *pbp1A*	77,631	Memb (8.77)
24379087	PAc- surface adhesin P1	NA	Smu.610 *spaP*	169,841	C Wall (10.0)[+]
24380491	HtrA- serine protease (DegP)	NA	Smu.2164 *htrA*	42,941	Unknown
	Transport				
24378763	Oligopeptide ABC transporter subs binding protein	NA	Smu.255 *oppA*	60,100	C Wall (9.21)
24380047	Branched chain amino acid ABC transporter	NA	Smu.1669 *livK*	41,087	Non Cyto [c]
24379274	Putative MscL	NA	Smu.819 *mscL*	13,494	Memb (10.0)
24379952	Maltose/maltodextrin ABC transporter	NA	Smu.1568 *malX*	45,043	Unknown
24379553	Putative ABC transporter (Lipoprotein)	NA	Smu.1121c *yufN*	36,510	Non Cyto

Table 4-4. Continued

Accession Number	Protein ID	Biochemical Pathway	Gene	M.W. (Da)	PSORTb v. 3.0.2
	Chaperones				
24380300	GroEL- 60 kDa chaperonin	NA	Smu.1954 *groEL*	56,970	Cyto (9.97)
24380301	GroES- 10 kDa chaperonin	NA	Smu.1955 *groES*	9,907	Cyto (9.97)
24378606	DnaK- heat shock protein 70	NA	Smu.82 *dnaK*	65,155	Cyto (9.97)
	Amino Acid Metabolism				
24380211	Aminopeptidase P	E.C.3.4.11.9	Smu.1850 *pepP*	39,568	Cyto (9.97)
24379429	Aspartate-semialdehyce dehydrogenase	E.C.1.2.1.11	Smu.989 *asd*	38,772	Cyto (9.95)
24379360	Glutamate dehydrogenase, NAD+ specific	E.C.1.4.1.4	Smu.913 *gdhA*	48,102	Cyto (9.67)
	Butanoate Metabolism				
24379736	Acetoin reductase- putative acetoin dehydrogenase	E.C.1.1.1.5.	Smu.1322 *budC*	26,773	Cyto (9.67)
24380458	Putative succinate semialdehyde dehydrogenase	E.C.1.2.1.16	Smu.2127	50,328	Cyto (9.67)
	Glutathione Metabolism				
24379293	Glutathione reductase	E.C.1.8.1.7	Smu.838 *gshR*	48,847	Cyto (9.67)
24379563	Aminopeptidase N	E.C.3.4.11.15	Smu.1132 *pepN*	96,701	Cyto (9.97)
	Starch Metabolism				
24379927	Glucose-1- phosphate adenyltransferase	E.C.2.7.7.27	Smu.1538 *glgC*	42,069	Cyto (7.50)
24379924	Glycogen phosphorylase	E.C.2.4.1.1	Smu.1535 *phsG*	90,920	Cyto (7.50)
24379926	Glycogen biosynthesis protein	E.C.2.7.7.27	Smu.1537 *glg D*	42,204	Cyto (7.50)

[a] Location prediction is based on PSORTb v3.0.2 (http://www.psort.org/psortb/). Scores closer to 10 have a better chance of being located in the predicted location.[b] Unknown, protein had a 2.50 score for cytoplasm, cytoplasmic membrane, cell wall, and extracellular

[c] Protein had a signal peptide detected and a 3.33 score for extracellular, 3.33 cell wall, and 3.33 for cytoplasmic membrane so protein is not located in cytoplasm. [+] Protein contains a signal sequence

Table 4-5. Details of 50S ribosomal proteins indentified by LC-MS/MS including accession number, molecular weight, gene, and additional information.

Accession Number	Ribosomal Proteins	Gene	M.W. (Da)	Location PSORTb	Additional Information
24380006	50S-L1	Smu.1626 *rplA*	24,379	Cyto (9.97)	Forms part of the L1 stalk along with 23S rRNA. Also functions as a translation repressor that binds its own mRNA.
157150843	50S-L2	Sgo.1982[a] *rplB*	29,794	Cyto (7.50)	Not found in *S. mutans* UA159 sequence. Is required for association of the 30S and 50S subunits to form the 70S ribosome.
2438035	50S-L5	Smu.2015 *rplE*	19,680	Cyto (7.50)	Part of 50S and 5S/L5/L18/L25 subcomplex; contacts 5S rRNA and P site tRNA; forms a bridge to the 30S subunit in the ribosome by binding to S13.
24380354	50S-L6	Smu.2011 rplF	19,305	Cyto (7.50)	Mutations confer resistance to aminoglycoside antibiotics such as gentamicin, localized to C-terminal domain.
24379400	50S-L10	Smu.957 *rplJ*	17,536	Cyto (9.97)	Binds the two ribosomal protein L7/L12 dimers and anchors them to the large ribosomal subunit
24380359	50S-L14	SMU.2017 *rplN*	13 kDa	Cyto (9.67)	Binds to the 23S rRNA between the centers for peptidyl transferase and GTPase
24380342	50S-L17	Smu.2000 *rplQ*	14,409	Cyto (9.97)	A component of the macrolide binding site in the peptidyl transferase center.
24380353	50S-L18	Smu.2010 *rplR*	12,763	Cyto (9.67)	Binds 5S rRNA along with protein L5 and L25.
24379704	50S-L19	Smu.1288 *rplS*	13,021	Cyto (9.97)	Located at the 30S-50S ribosomal subunit interface
24379170	50S-L20	Smu.699 *rplT*	13,620	Cyto (9.67)	Binds directly to 23S ribosomal RNA prior to in vitro assembly of the 50S ribosomal subunit.
24380364	50S-L22	Smu.2022 *rplV*	12,313	Cyto (9.67)	Binds to 23S rRNA during 50S assembly; makes contact with all 6 domains of the 23S rRNA in the assembled ribosome. Mutations in this gene result in erythromycin resistance.
290581287	50S-L23	Smu2025.1761 *rplW*	10,855	Unknown	Not listed in *S. mutans* UA159 but is in *S. mutans* NN2025. Part of exit tunnel.
24379304	50S-L27	SMU.849 *rpmA*	10,290	Cyto (9.67)	Involved in the peptidyltransferase reaction during translation
24380351	50S-L30	SMU.2008 *rpmD*	6,250	Cyto (9.67)	L30 binds domain II of the 23S rRNA and the 5S rRNA; similar to eukaryotic protein L7

[a] Peptide matched to a protein from *S. mutans* NN2025, *Streptococcus mutans* UA159 sequence does not list this protein.

Table 4-6. Details of 30S ribosomal proteins identified by LC-MS/MS including accession number, molecular weight, gene, and additional information.

Accession Number	Ribosomal Proteins	Gene	M.W. (Da)	Location PSORTb	Additional Information
24380374	30S-S2	Smu.2032 *rpsB*	28,962	Cyto (9.97)	One of the last subunits in the assembly of the 30S subunit and is required for an active 30S subunit
161486819	30S-S3	Smu.2021 *rpsC*	23,991	Cyto (9.97)	Forms a complex with S10 and S14, binding to the lower part of the 30S subunit head and the mRNA in the complete ribosome.
24380465	30S-S4	Smu.2135c *rpsD*	22,903	Cyto (7.50)	Primary rRNA binding protein, nucleates 30S assembly and is involved in translational accuracy with proteins S5 and S12.
24380352	30S-S5	Smu.2009 *rpsE*	16,990	Cyto (9.97)	Located at back of 30S subunit, plays a role in translational accuracy. Mutations result in spectinomycin resistance.
24378855	30S-S7	SMU.358	17,674	Cyto (7.50)	Binds directly to 16S rRNA where it nucleates assembly of the head domain of the 30S subunit
24380355	30S-S8	Smu.2012 *rpsH*	14,562	Cyto (9.97)	Binds directly to 16S rRNA central domain where it helps coordinate assembly of the platform of the 30S subunit.
24378685	30S-S9	Smu.170 *rpsI*	14,089	Cyto (9.67)	Is in direct contact with the tRNA during translation.
24379400	30S-S10	Smu.957 *rpsJ*	17,536	Cyto (9.97)	Binds two ribosomal protein L7/L12 dimers and anchors them to the large ribosomal subunit.
24380344	30S-S11	Smu.2002 *rs11*	13,268	Cyto (9.67)	Located on the 30S subunit platform, bridges several RNA helices of the 16S rRNA; forms part of the Shine-Dalgarno cleft in the 70S ribosome; interacts with S7 and S18 and IF-3
24378854	30S-S12	Smu.357 *rps*L	14,978	Cyto (9.67)	Interacts with bases of 16S rRNA involved in tRNA selection in A site and with mRNA backbone. Located at interface of the 30S and 50S subunits. Mutations confer streptomycin resistance.

Table 4-7. Glycolytic enzymes identified by LC-MS/MS from BN-PAGE Band 1 (~700 kDa complex) including the number of peptides and percentage of protein represented for each Trial.

Indentified Proteins	NG8 Trial 1[C]	Δ*yidC1* Trial 1	Δ*yidC2* Trial 1	NG8 Trial 2	Δ*yidC1* Trial 2	Δ*yidC2* Trial 2
Glyceraldehyde-3-phosphate dehydrogenase	4[a], 12%[b]	-	2, 7%	-[d]	7, 24%	7, 22%
Phosphoglyceromutase	-	1, 11%	-	-	-	-
Enolase	18, 59%	1, 4%	1, 3%	-	2, 6%	2, 6%
Pyruvate kinase	-	-	1, 2%	-	6, 15%	2, 4%
Pyruvate formatelyase	1, 1%	-	-	-	-	-
L(+)-lactate dehydrogenase	3, 11%	2, 11%	3, 15%	-	3, 12%	1, 4%
Bifunctional acetaldehyde-CoA/alcohol dehydrogenase	12, 17%	-	-	-	-	-

[a] Number of unique peptides in the gel slice identified by LC-MS/MS that were used to ID the protein
[b] Percent of indentified protein covered by the peptides.
[c] Gel slices from two separate gels were submitted for LC-MS/MS analysis and are represented as Trial 1 and Trial 2.
[d] - indicates not detected.

Table 4-8. Glycolytic enzymes identified by LC-MS/MS from BN-PAGE Band 2 (~300 kDa complex) including the number of peptides and percentage of protein represented for each Trial.

Identified Proteins	NG8 Trial 1	Δ*yidC1* Trial 1	Δ*yidC2* Trial 1	NG8 Trial 2	Δ*yidC1* Trial 2	Δ*yidC2* Trial 2
Glyceraldehyde-3-phosphate dehydrogenase	2, 7%	1, 5%	1, 3%	3, 12%	5, 17%	6, 20%
Phosphoglyceromutase	-	1, 11%	-	-	-	-
Enolase	27, 65%	17, 63%	11, 43%	17, 42%	8, 23%	2, 6%
Pyruvate kinase	-	1, 5%	2, 7%	-	1, 2%	2, 4%
Pyruvate formate-lyase	9, 14%	2, 5%	1, 3%	1, 1%	2, 3%	-
L(+)-lactate dehydrogenase	1, 4%	3, 16%	2, 11%	1, 4%	1, 4%	1, 4%

As in Table 4-7, the number of unique peptides identified by LC-MS/MS is indicated, with the percent of the total protein represented next to it. - indicates not detected.

Table 4-9. Glycolytic enzymes identified by LC-MS/MS from BN-PAGE Band 3 (~70 kDa complex) including the number of peptides and percentage of protein represented for each Trial.

Identified Proteins	NG8 Trial 1	Δ*yidC1* Trial 1	Δ*yidC2* Trial 1	NG8 Trial 2	Δ*yidC1* Trial 2	Δ*yidC2* Trial 2
Phosphoenolpyruvate: sugar PTS enzyme I	1, 3%	2, 7%	3, 5%	-	-	-
Putative glucose kinase	-	-	3, 15%	-	-	-
Glucose-6-phosphate isomerase	-	-	2, 4%	-	-	1, 3%
Fructose-bisphosphate aldolase	-	-	1, 8%	-	-	-
Transketolase	4, 10%	5, 16%	5, 10%	-	2, 4%	1, 3%
Glyceraldehyde-3-phosphate dehydrogenase	1, 5%	4, 22%	11, 48%	-	-	-
Phosphoglycerate kinase	-	1, 5%	1, 4%	-	-	-
Phosphoglyceromutase	-	1, 11%	-	-	-	-
Enolase	-	4, 16%	12, 46%	4, 14%	2, 6%	2, 6%
Pyruvate kinase	3, 10%	5, 15%	14, 38%	1, 3%	9, 18%	7, 16%
Bifunctional acetaldehyde-CoA/alcohol dehydrogenase	1, 3%	1, 3%	-	-	-	-
L(+)-lactate dehydrogenase	2, 11%	2, 11%	4, 14%	2, 7%	1, 4%	-

As in Table 4-7, the number of unique peptides identified by LC-MS/MS is indicated, with the percent of the total protein represented next to it. – indicates not detected. PTS- phosphotransferase system.

Table 4-10. Glycolytic enzymes identified by LC-MS/MS from BN-PAGE Band 4 (~64 kDa complex) including the number of peptides and percentage of protein represented for each Trial.

Identified Proteins	NG8 Trial 1	Δ*yidC1* Trial 1	Δ*yidC2* Trial 1	NG8 Trial 2	Δ*yidC1* Trial2	Δ*yidC2* Trial 2
Putative glucose kinase	-	4, 15%	16, 53%	-	7, 25%	7, 20%
Glucose-6-phosphate isomerase	-	1, 6%	15, 46%	-	-	4, 17%
Fructose-bisphosphate aldolase	1, 5%	2, 13%	7, 35%	-	-	-
Transketolase	6, 20%	5, 17%	18, 40%	1, 2%	8, 14%	6, 11%
Phosphoglycerate kinase	1, 5%	-	5, 15%	1, 4%	4, 11%	2, 8%
Phosphoglyceromutase	1, 11%	3, 20%	4, 27%	-	1, 4%	2, 9%
Enolase	-	4, 16%	7, 26%	3, 11%	2, 6%	3, 9%
Pyruvate kinase	4, 12%	5, 14%	11, 29%	5, 14%	14, 31%	8, 20%
Glyceraldehyde-3-phosphate dehydrogenase	4, 17%	-	13, 60%	3, 13%	5, 22%	7, 26%
Bifunctional acetaldehyde-CoA/alcohol dehydrogenase	1, 2%	1, 3%	-	-	-	-
L(+)-lactate dehydrogenase	2, 11%	2, 11%	7, 28%	2, 7%	2, 7%	1, 4%

As in Table 4-7, the number of unique peptides identified by LC-MS/MS is indicated in parentheses, with the percent of the total protein represented next to it. - indicates not detected.

Table 4-11. Proteins identified by LC-MS/MS in BN-PAGE gel Band 1 (~700 kDa) involved in citrate metabolism including the number of peptides and percentage of protein represented for each Trial.

Identified Proteins	NG8 Trial 1	Δ*yidC1* Trial 1	Δ*yidC2* Trial 1	NG8 Trial 2	Δ*yidC1* Trial 2	Δ*yidC2* Trial 2
Putative citrate lyase CilB, citryl-CoA lyase, beta subunit	4, 20%	-	-	-	-	-
Citrate Lyase, alpha subunit	3, 7%	-	-	5, 10%	-	-
Citrate synthase	3, 8%	-	-	-	-	-

As in Table 4-7, the number of unique peptides identified by LC-MS/MS is indicated, with the percent of the total protein represented next to it. – indicates not detected.

Table 4-12. Cell wall-associated proteins identified by LC-MS/MS in BN-PAGE gel Band 1 (~700 kDa) including the number of peptides and percentage of protein represented for each Trial.

Identified Proteins	NG8 Trial 1	Δ*yidC1* Trial 1	Δ*yidC2* Trial 1	NG8 Trial 2	Δ*yidC1* Trial 2	Δ*yidC2* Trial 2
PrsA- foldase protein	3, 9%	1, 6%	2, 11%	-	3, 11%	1, 5%
Penicillin binding protein 1a	1, 2%	5, 12%	3, 6%	-	3, 7%	-
PAc/P1- surface adhesin	-	1, 1%	2, 2%	-	-	5, 4%
HtrA – serine protease	-	-	2, 6%	-	-	-

As in Table 4-7 the number of unique peptides identified by LC-MS/MS is indicated, with the percent of the total protein represented next to it. - indicates not detected

Table 4-13. Cell wall-associated proteins identified by LC-MS/MS in BN-PAGE gel Band 2 (~300 kDa) including the number of peptides and percentage of protein represented for each Trial.

Identified Proteins	NG8 Trial 1	Δ*yidC1* Trial 1	Δ*yidC2* Trial 1	NG8 Trial 2	Δ*yidC1* Trial 2	Δ*yidC2* Trial 2
PrsA- foldase protein	-	-	-	-	-	1, 5%
Penicillin binding protein 1a	-	1, 2%	1, 2%	-	-	-
PAc/P1- surface adhesin	-	-	-	-	-	5, 4%

Table 4-14. Cell wall-associated proteins identified by LC-MS/MS in BN-PAGE gel Band 3 (~70 kDa) including the number of peptides and percentage of protein represented for each Trial.

Identified Proteins	NG8 Trial 1	Δ*yidC1* Trial 1	Δ*yidC*2 Trial1	NG8 Trial 2	Δ*yidC1* Trial 2	Δ*yidC*2 Trial 2
HtrA	2, 10%	2, 11%	-	-	-	-

Table 4-15. Proteins identified by LC-MS/MS in BN-PAGE Band 1 (~700 kDa) involved with transport including the number of peptides and percentage of protein represented for each Trial.

Identified Proteins	NG8 Trial 1	Δ*yidC1* Trial 1	Δ*yidC2* Trial 1	NG8 Trial 2	Δ*yidC1* Trial 2	Δ*yidC2* Trial 2
Branched chain amino acid ABC transporter	-	3, 8%	4,12%	-	2, 6%	-
Oligopeptide ABC transporter, substrate-binding protein OppA	-	-	2, 5%	-	-	-
Putative large conductance mechanosensitive channel	-	2, 17%	1, 17%	-	-	-
Putative ABC transporter (lipoprotein)	-	4, 21%	2, 7%	-	3, 10%	-
Maltose/maltodextrin ABC transporter, sugar-binding protein	-	1, 4%	1, 4%	-	-	-

As in Table 4-7, the number of unique peptides identified by LC-MS/MS is indicated, with the percent of the total protein represented next to it. – indicates not detected

Table 4-16. Proteins identified by LC-MS/MS in BN-PAGE Band 2 (~300 kDa) involved with transport including the number of peptides and percentage of protein represented for each Trial.

Identified Proteins	NG8 Trial 1	Δ*yidC1* Trial 1	Δ*yidC2* Trial 1	NG8 Trial 2	Δ*yidC1* Trial 2	Δ*yidC2* Trial 2
Putative large conductance mechanosensitive channel	-	1, 17%	-	-	-	-
Putative ABC transporter (lipoprotein)	-	-	1, 9%	-	-	-

Table 4-17. Chaperone proteins identified by LC-MS/MS in BN-PAGE gel Band 1 (~700 kDa) including the number of peptides and percentage of protein represented for each Trial.

Identified Proteins	NG8 Trial 1	Δ*yidC1* Trial 1	Δ*yidC2* Trial 1	NG8 Trial 2	Δ*yidC1* Trial 2	Δ*yidC2* Trial 2
GroEL - 60 kDa chaperonin	-	5, 20%	-	-	-	-
DnaK - heat shock protein 70	-	1, 4%	-	-	-	-
GroES - 10 kDa chaperonin	-	-	-	-	2, 21%	1, 12%

As in Table 4-7, the number of unique peptides identified by LC-MS/MS is indicated, with the percent of the total protein represented next to it. - indicates not detected

Table 4-18. Chaperone proteins identified by LC-MS/MS in BN-PAGE gel Band 2 (~300 kDa) including the number of peptides and percentage of protein represented for each Trial.

Identified Proteins	NG8 Trial 1	Δ*yidC1* Trial 1	Δ*yidC2* Trial 1	NG8 Trial 2	Δ*yidC1* Trial 2	Δ*yidC2* Trial 2
GroEL – 60 kDa chaperonin	2, 4%	8, 24%	1, 2%	-	-	-

Table 4-19. Chaperone proteins identified by LC-MS/MS in BN-PAGE gel Band 3 (~70 kDa) including the number of peptides and percentage of protein represented for each Trial.

Identified Proteins	NG8 Trial 1	Δ*yidC1* Trial 1	Δ*yidC2* Trial 1	NG8 Trial 2	Δ*yidC1* Trial 2	Δ*yidC2* Trial 2
GroEL – 60 kDa chaperonin	7, 24%	7, 24%	-	6, 15%	8, 17%	1, 3%
DnaK - heat shock protein 70	2, 7%	2, 7%	-	-	-	-
GroES – 10 kDa chaperonin	-	-	-	-	2, 21%	1, 12%

Table 4-20. Chaperone proteins identified by LC-MS/MS in BN-PAGE gel Band 4 (~64 kDa) including the number of peptides and percentage of protein represented for each Trial.

Identified Proteins	NG8 Trial 1	Δ*yidC1* Trial 1	Δ*yidC2* Trial 1	NG8 Trial 2	Δ*yidC1* Trial 2	Δ*yidC2* Trial 2
GroEL – 60 kDa chaperonin	8, 25%	4, 14%	6, 16%	5, 11%	10, 22%	-

Table 4-21. Proteins identified by LC-MS/MS in BN-PAGE gel Band 1 (~700 kDa) involved in amino acid metabolism including the number of peptides and percentage of protein represented for each Trial.

Identified Proteins	NG8 Trial 1	Δ*yidC1* Trial 1	Δ*yidC2* Trial 1	NG8 Trial 2	Δ*yidC1* Trial 2	Δ*yidC2* Trial 2
Aspartate-semialdehyde dehydrogenase	-	1, 6%	-	-	-	-

As in Table 4-7, the number of unique peptides identified by LC-MS/MS is indicated, with the percent of the total protein represented next to it. - indicates not detected

Table 4-22. Proteins identified by LC-MS/MS in BN-PAGE gel Band 2 (~300 kDa) involved with amino acid metabolism including the number of peptides and percentage of protein represented for each Trial.

Identified Proteins	NG8 Trial 1	Δ*yidC1* Trial 1	Δ*yidC2* Trial 1	NG8 Trial 2	Δ*yidC1* Trial 2	Δ*yidC2* Trial 2
Aminopeptidase P	1, 3%	1, 3%	4, 16%	-	-	-
Glutamate dehydrogenase, NAD+ specific	17, 47%	7, 27%	3, 10%	11, 28%	15, 43%	-

Table 4-23. Proteins identified by LC-MS/MS in BN-PAGE gel Band 4 (~64 kDa) involved with amino acid metabolism including the number of peptides and percentage of protein represented for each Trial.

Identified Proteins	NG8 Trial 1	Δ*yidC1* Trial 1	Δ*yidC2* Trial 1	NG8 Trial 2	Δ*yidC1* Trial 2	Δ*yidC2* Trial 2
Branched-chain amino acid aminotransferase	-	-	4, 17%	-	-	-
Aspartate-semialdehye dehydrogenase	-	-	4, 17%	-	-	-

Table 4-24. Proteins identified by LC-MS/MS in BN-PAGE gel Band 3 (~70 kDa) involved in butanoate, glutathione and starch metabolism including the number of peptides and percentage of protein represented for each Trial.

Identified Proteins	NG8 Trial 1	Δ*yidC1* Trial 1	Δ*yidC2* Trial 1	NG8 Trial 2	Δ*yidC1* Trial 2	Δ*yidC2* Trial 2
Butanoate metabolism						
Acetoin reductase- putative acetoin dehydrogenase	-	-	5, 29%	-	-	-
Putative succinate semialdehyde dehydrogenase	4, 16%	14, 47%	36, 82%	10, 21%	10, 22%	15, 32%
Glutathione Metabolism						
Glutathione reductase	4, 20%	3, 12%	13, 49%	1, 2%	2, 5%	4, 14%
Amino peptidase N	1, 2%	-	5, 8%	-	-	-
Starch Metabolism						
Glucose-1- phosphate adenyltransferase	-	-	4, 14%	-	-	1, 3%
Glycogen phosphorylase	3, 7%	4, 10%	14, 22%	4, 5%	5, 12%	3, 7%
Glycogen biosynthesis protein	-	1, 6%	5, 16%	-	-	-

As in Table 4-7, the number of unique peptides identified by LC-MS/MS is indicated, with the percent of the total protein represented next to it. – indicates not detected.

Table 4-25. Proteins identified by LC-MS/MS in BN-PAGE gel Band 4 (~64 kDa) involved in butanoate, glutathione and starch metabolism including the number of peptides and percentage of protein represented for each Trial.

Identified Proteins	NG8 Trial 1	Δ*yidC1* Trial 1	Δ*yidC2* Trial 1	NG8 Trial 2	Δ*yidC1* Trial 2	Δ*yidC2* Trial 2
Butanoate metabolism						
Acetoin reductase- putative acetoin dehydrogenase	-	1, 11%	4, 30%	-	-	-
Putative succinate semialdehyde dehydrogenase	-	2, 9%	6, 25%	-	-	1, 3%
Glutathione Metabolism						
Glutathione reductase	1, 8%	-	3, 21%	-	-	-
Starch metabolism						
Glucose-1- phosphate adenyltransferase	-	1, 7%	9, 33%	-	-	4, 13%

Table 4-26. Ribosomal proteins identified by LC-MS/MS in BN-PAGE gel Band 1 (~700 kDa) including the number of peptides and percentage of protein represented for each Trial.

Indentified Proteins	NG8 Trial 1	Δ*yidC1* Trial 1	Δ*yidC2* Trial 1	NG8 Trial 2	Δ*yidC1* Trial 2	Δ*yidC2* Trial 2
50S-L2[a]	-	2, 11%	-	-	-	-
50S-L5	-	-	-	-	-	1, 10%
50S-L17	-	1, 14%	-	-	-	-
50S-L18	3, 43%	-	-	-	-	-
30S-S2	3, 13%	-	-	-	-	-
30S-S3	2, 13%	-	-	-	-	-
30S-S4	-	1, 11%	-	-	-	-
30S-S9	2, 15%	-	-	-	-	-

[a] Peptides matched to a protein from *S. mutans* NN2025 (*S. mutans* UA159 genomic sequence does not list 50S-L2). BN-PAGE experiments were performed on *S. mutans* strain NG8.

Table 4-27. Ribosomal proteins identified by LC-MS/MS in BN-PAGE gel Band 2 (~300 kDa) including the number of peptides and percentage of protein represented for each Trial.

Proteins Indentified	NG8 Trial 1	Δ*yidC1* Trial 1	Δ*yidC2* Trial 1	NG8 Trial 2	Δ*yidC1* Trial 2	Δ*yidC2* Trial 2
50S-L2[a]	2, 12%	1, 5%	-	-	-	-
50S-L5	-	-	-	-	-	1, 10%
50S-L14	2, 19%	-	-	-	-	-
50S-L17	-	1, 14%	-	-	-	-
50S-L18	-	2, 25%	-	-	-	-
50S-L19	3, 28%	-	-	2, 20%	-	-
30S-S4	-	-	-	2, 10%	-	-
30S-S5	7, 54%	2, 12%	1, 7%	8, 59%	-	-
30S-S9	1, 8%	-	-	-	-	-

[a] Peptides matched to a protein from *S. mutans* NN2025 (*S. mutans* UA159 genomic sequence does not list 50S-L2). BN-PAGE experiments were performed on *S. mutans* strain NG8.

Table 4-28. Ribosomal proteins identified by LC-MS/MS in BN-PAGE gel Band 3 (~70 kDa) including the number of peptides and percentage of protein represented for each Trial.

Identified Proteins	NG8 Trial 1	Δ*yidC1* Trial 1	Δ*yidC2* Trial 1	NG8 Trial 2	Δ*yidC1* Trial 2	Δ*yidC2* Trial 2
50S-L1	-	1, 7%	-	-	-	-
50S-L2[a]	1, 6%	1, 5%	-	-	-	-
50S-L5	-	-	-	3, 22%	-	-
50S-L6	2, 15%	1, 16%	-	1, 11%	-	-
50S-L10	1, 17%	1, 17%	-	-	-	-
50S-L17	1, 14%	1, 14%	-	-	-	-
50S-L18	2, 25%	-	-	-	-	-
50S-L19	-	-	-	1, 10%	-	-
50S-L20	1, 18%	1, 18%	-	-	-	-
50S-L22	2, 25%	-	-	3, 35%	-	-
50S-L23[b]	-	-	-	3, 22%	1, 10%	-
50S-L27	-	-	-	1, 15%	-	-
30S-S4	2, 10%	-	-	5, 19%	-	-
30S-S5	-	-	-	3, 25%	1, 7%	-
30S-S7	1, 9%	-	-	4, 28%	1, 9%	-
30S-S8	3, 39%	1, 14%	-	2, 14%	1, 14%	-
30S-S10	-	-	-	2, 25%	-	-
30S-S11	1, 11%	-	-	-	-	-
30S-S12	3, 24%	-	-	-	-	-

[a] Peptides matched to a protein from *S. mutans* NN2025 (*S. mutans* UA159 genomic sequence does not list 50S-L2). BN-PAGE experiments were performed on *S. mutans* strain NG8.

[b] Peptides matched to L23 from *S. mutans* NN2025, *S. mutans* UA159 genomic sequence does not list 50S-L23 and the genome sequence is not available for NG8, the strain used in these experiments.

Table 4-29. Ribosomal proteins identified by LC-MS/MS in BN-PAGE gel Band 4 (~64 kDa) including the number of peptides and percentage of protein represented for each Trial.

Identified Proteins	NG8 Trial 1	Δ*yidC1* Trial 1	Δ*yidC2* Trial 1	NG8 Trial 2	Δ*yidC1* Trial 2	Δ*yidC2* Trial 2
50S-L1	2, 11%	-	3, 20%	-	-	-
50S-L2 [a]	2, 11%	-		-	-	-
50S-L5	-	-	-	2, 16%	-	-
50S-L6	2, 15%	1, 16%	-	3, 26%	-	-
50S-L10	2, 13%	-	-	-	-	-
50S-L17	1, 14%	1, 14%	2, 20%	-	-	-
50S-L18	2, 25%	1, 25%	-	-	-	-
50S-L20	2, 28%	-	-	-	-	-
50S-L22	1, 10%	-	-	3, 26%	-	-
50S-L23[b]	-	-	-	3, 22%	-	-
50S-L27	-	-	-	2, 25%	-	-
50S-L30	-	-	-	2, 50%	1, 23%	-
30S-S2	1, 4%	-	-	-	-	-
30S-S4	1, 5%	-	-	4, 16%	-	-
30S-S5	-	-	-	4, 35%	-	-
30S-S7	3, 35%	-	-	4, 29%	1, 9%	-
30S-S8	2, 29%	-	2, 14%	3, 35%	2, 14%	-
30S-S9	1, 8%	1, 8%	-	-	-	-
30S-S10	-	-	-	2, 25%	-	-
30S-S11	2, 24%	-	-	-	-	-
30S-S12	2, 9%	-	-	-	-	-

[a] Peptides matched to a protein from *S. mutans* NN2025 (*S. mutans* UA159 does not have 50S-L2). BN-PAGE experiments were performed on *S. mutans* strain NG8.

[b] Peptides matched to L23 from *S. mutans* NN2025, *S. mutans* UA159 does not have 50S-L23 and the genome sequence is not available for NG8, the strain used in these experiments.

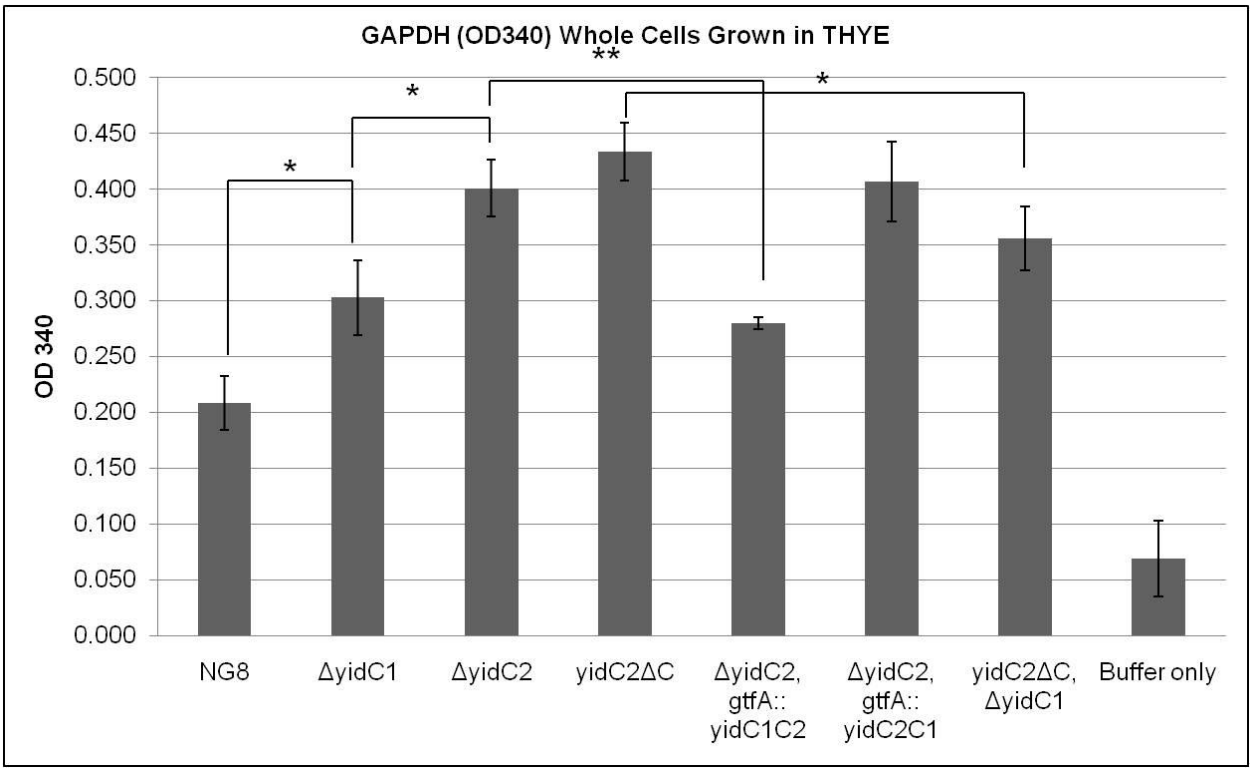

Figure 4-6. Extracellular GAPDH activity in *S. mutans* NG8 wild-type and various *yidC* mutants. Results are expressed as OD_{340}, standardized to the OD_{600} of the cells used for the assay. The assay was completed in triplicate with overnight cultures of each strain grown in THYE. The standard deviations of the average are indicated by error bars. Statistically significant differences are indicated (* indicates *P*-value ≤ 0.02, ** indicates *P*-value ≤ 0.001) and were determined by Student's t-test.

CHAPTER 5
CONCLUSIONS AND FUTURE DIRECTIONS

Development of Tools to Examine Compensatory or Redundant Functions in Membrane Biogenesis

Using *E. coli* as a model organism, techniques have been developed to purify membrane proteins and reconstitute them into proteoliposomes. This combined with *in vitro* transcription and translation, has allowed many advances to be made in the field of protein secretion and translocation thus facilitating dissection of the minimum requirements for this vital process. Additionally, the implementation of conditional expression systems to evaluate essential proteins in these pathways has furthered our knowledge of the *in vivo* requirements. Most of these studies have involved *E. coli,* with a few examples in *Bacillus subtilis*. Recent discoveries in gram-positive streptococcal species such as; the non-essentiality of the SRP pathway in *S. mutans* and *S. pyogenes*; the possibility of an Exportal micro-domain for secreted proteins; the existence of accessory SecA2/SecY2 in *S. gordonii, S. pneumoniae* and *S. parasanguinis;* and the presence of two YidC proteins with different functions in *S. mutans*, indicate there are likely other major differences between what is known in *E. coli* and what remains to be learned in the streptococci. There are still significant gaps in our knowledge of streptococcal protein translocation and membrane biogenesis that need to be filled before we can reach the same level of understanding available for *E. coli* and *B. subtilis.*

Streptococci have several redundant pathways for protein translocation and secretion, making it difficult to determine and/or evaluate essential functions of proteins in secretion. For example there are two YidC homologs, including one that may cooperate with the SRP to enable efficient co-translational translocation. Through work

conducted in this study, a number of tools have been developed, which can be used in future experiments to dissect the pathways involved in membrane biogenesis and secretion. A conditional expression system was developed using the *PcelB* promoter to allow controlled expression of *yidC2*, while eliminating *yidC1.* Depletion conditions were evaluated for this system and it was found that growth in TDM 0.5% mannose for 5 to 7 hours resulted in depletion of YidC2. Further optimization with different combinations of sugars may improve expression control, and improve the speed at which carbon catabolite repression occurs, resulting in more efficient repression. It should also be possible to use this system to conditionally express other essential genes, for example generation of strains that are depleted in YidC2 and the SRP pathway, and/or components of the SecYEG translocon.

The affinity purified antibodies described in Chapter 2 against C-terminal peptides of YidC1 and YidC2 and the cytoplasmic loop between TMD 2 and 3 of YidC2 will be useful reagents in future experiments. These antibodies can be covalently coupled to agarose beads and used in immunoprecipitation experiments to determine protein-protein interactions with the YidC proteins of *S. mutans*. Additionally a peptide antibody against SecY was also created and affinity purified to produce a mono-specific reagent that can be used to track SecY in *S. mutans.* This antibody may also be used in immunoprecipitation experiments to identify reacting partners of the uncharacterized SecY translocon of *S. mutans*. The development, purification, and characterization of these reagents against *S. mutans* membrane translocation components are necessary tools that can be used in combination with other previously made antibodies against *S.*

mutans' Ffh and FtsY to continue to decipher the proteins involved in targeting and insertion into *S. mutans* membranes.

A Function of the C-Terminal Tail of YidC2 in Stress Tolerance

A number of strains were constructed to investigate functional differences of the two YidC proteins in *S. mutans.* These strains were evaluated by growth curve under non-stress, acid-stress and osmotic-stress conditions. Results indicated a clear role of the C-terminal tail of YidC2 in stress tolerance. When the C-terminal tail was deleted, an intermediate growth phenotype was seen under non-stress conditions. However, when exposed to acid- or osmotic-stress, this partial mutant strain grew similarly to a complete deletion of *yidC2.* When *yidC1* was deleted in the *yidC2ΔC* background, a worse growth phenotype than complete elimination of *yidC2* resulted. Chimeric YidC1C2 (with the C-terminal tail of *yidC2*) restored stress tolerance to the Δ*yidC2* mutant, while YidC2C1, caused a dominant-negative effect, with slower growth than the un-complemented *yidC2* mutant, indicating that the C-terminal tails are important to each protein's function, perhaps in membrane protein complex assembly or protein-protein interactions within *S. mutans*.

Additional mutants need to be made to investigate further the functional domains of the YidC proteins of *S. mutans*. For example, a deletion of the C-terminal tail of the YidC1 protein needs to be evaluated to test whether this mutant behaves differently than a complete deletion of *yidC1*. Additionally, expression of *yidC1* from the *yidC2* promoter, and over-expression of *yidC1* in a *yidC2* negative background, should be evaluated for stress-tolerance.

YidC1 and YidC2 are Involved in ATPase Assembly

Experiments in Chapter 3 showed that YidC1 and YidC2 can both perform in *E. coli* to insert a functional F_1F_o ATPase, evaluated by ATP hydrolysis assays, PMF assays, and protease accessibility assays with the "a" and "c" subunits. Assays performed in *S. mutans* showed that elimination of either *yidC1* or *yidC2* resulted in decreased membrane-associated ATPase activity. In addition, the activity associated with the *S. mutans* Δ*yidC1* and Δ*yidC2* mutant membranes was not inhibited by the P-type inhibitor orthovanadate, while 13% of wildtype activity was, indicating that there is less P-type activity associated with *yidC* mutant membranes compared to wildtype. This could account for some of the decrease in overall ATPase activity seen in these mutants. The chimeric YidC1C2 protein was able to restore membrane associated activity to a Δ*yidC2* mutant. Additionally, AH412 (*yidC2ΔC*) showed a similar decrease in activity as AH378 (*ΔyidC2*), indicating the importance of the C-terminal tail of YidC2 to ATPase function. Future experiments need to be performed to evaluate membrane ATPase activity in the presence the F-type ATPase inhibitor N, N'-dicyclohexyl-carbodiimide (DCCD). By performing the ATPase assays with mutant membranes in the presence of DCCD, the true proportion of ATPase activity attributable to the F_1F_o ATPase can be determined.

YidC Mutants Showed Differences in Membrane Protein Complexes Compared to Wild-Type NG8 *S. mutans*

There were visible differences in membrane protein complexes between wildtype *S. mutans* and the *yidC* mutants (Figures 4-1and 4-5). There was an apparent shift in the location and intensity of bands from high molecular weight complexes present in wildtype but absent in both *yidC* mutants, to lower molecular weight complexes in both

yidC mutants that were absent in the wildtype. This effect was more pronounced in the Δ*yidC2* mutant. These differences could indicate a change in the protein expression profile in the *yidC* mutants and/or they could indicate a defect in the assembly process of multimeric protein complexes.

In the BN-PAGE experiments combined with LC-MS/MS analysis, differences seen in the Δ*yidC2* mutant were consistent with an acid tolerance response, perhaps stemming from an inability of the mutant to regulate cytoplasmic pH due to defects in the assembly of F_1F_o ATPase or other affected acid tolerance mechanisms related to the membrane. There was also a decrease in ribosomal proteins seen in membranes from both mutants but the effect was more pronounced in the Δ*yidC*2 mutant. This result is consistent with the C-terminal tail of YidC2 having a ribosome binding function that supports co-translational translocation. This has been hypothesized as the mechanism behind the dispensability of the SRP pathway in *S. mutans*. Additionally, GAPDH was more highly represented in the *ΔyidC2* mutant membranes than wild-type NG8. When extracellular GAPDH activity was measured in whole cells, the *ΔyidC2* mutant showed increased activity compared to wild-type NG8 (Figure 4-6). The Δ*yidC1* mutant also showed increased extracellular GAPDH activity compared to wildtype, but not to the same extent as the Δ*yidC2* mutant. The implications of increased extracellular GAPDH activity remain to be determined.

Given the apparent effect on membrane-associated protein complex localization of glycolytic enzymes, future experiments should be conducted to evaluate further the effects of *yidC2* mutation on glycolytic activity including measuring metabolic end products and by enzymatic assays. Also BN-PAGE could be applied to SP20, in which

yidC2 is depleted in a *yidC1* negative background, to analyze affects on membrane complexes in the absence of both YidC proteins.

The Functions of *S. mutans* YidC1 and YidC2

The purpose of this research was to determine the respective roles of YidC1 and YidC2 in membrane biogenesis in *S. mutans*. A working model is shown in Figure 5-1. Collectively, the knowledge gained from this work and the research of others from the Brady lab, indicate a pivotal role of YidC2 in membrane biogenesis and stress tolerance in *S. mutans* that depends on the presence of the C-terminal tail. Results are consistent with an ability of YidC2 to interact with ribosomes to mediate co-translational translocation in cooperation with the SRP pathway (Figure 5-1A), as evidenced by decreased ribosomes associated with membranes from the Δ*yidC2* mutants in BN-PAGE/LC-MS/MS studies, and the ability of YidC2 to complement an Oxa1 mutant in Yeast. Additionally, there is evidence that YidC2 is involved in several pathways that do not or only partially depend on the presence of its C-terminal tail, such as the effects seen in competence development, which is only partially affected in the *yidC2*ΔC strain (123), and on the surface adhesin P1 (a sortase substrate), which is not affected at all in the *yidC2*ΔC strain (represented by post-translational functions in Figure 5-1 B). There are also different effects seen between the Δ*yidC1* and Δ*yidC2* mutants on P1 function, with Δ*yidC1* mutant displaying a hyper-adherent phenotype, and the Δ*yidC2* mutant showing a marked decrease is adherence to salivary agglutinin. Additionally, both *yidC* mutants affect biofilm formation, but in different ways. The Δ*yidC1* mutant forms biofilms sooner, while the biofilms of the Δ*yidC2* mutant display a patchy architecture compared to wildtype (unpublished, personal communication with L. J. Brady). This

suggests a regulatory role for YidC1 in the secretion of proteins involved with biofilm formation and perhaps sortase substrates that are covalently linked to the cell wall. Furthermore, there is also evidence that both YidC1 and YidC2 are involved in the functional assembly of membrane proteins (Figure 5-1 C), revealed by functional assays with F_1F_o ATPase in *E. coli* and decreased membrane associated ATPase activity in both *yidC* mutants in *S. mutans*. Taken together, these results suggest that while YidC2 plays a larger role in the biology of *S. mutans*, at least in certain instances YidC1 and YidC2 cooperate in a balanced manner in protein assembly and secretion, thus partially explaining the inability to eliminate both paralogs simultaneously in this species.

There are still a number of questions that remain to be answered concerning protein translocation and secretion in *S. mutans.* There is not a SecB chaperone homolog for post-translational targeting in *S. mutans*. This raises the question, are proteins post-translationally targeted for secretion in *S. mutans*, and if so, are there other as yet undiscovered proteins involved? The Streptococci also lack a homolog for SecDF, which in *B. subtilis* is important for high levels of protein secretion, and in *E. coli* SecDF are known to associate with YajC. All gram-positive species encode a *yajC* gene; although YajC is not essential in *E. coli* and deletion has little effect. This raises the question of whether YajC has a more important function in *S. mutans* and in other gram-positive bacteria than in gram-negative species. Also, it is not known if YajC interacts with the SecY translocon in streptococcal species. Additionally, the SecYEG translocon has not been characterized in the streptococci, which makes one speculate that there could be other proteins associated with this complex in *S. mutans* that are not found in *E. coli*. Work is underway in the Brady lab to begin to answer some of these

questions. This work is vital to understanding the many differences in protein secretion between gram-negative bacteria and the medically relevant Streptococcal species.

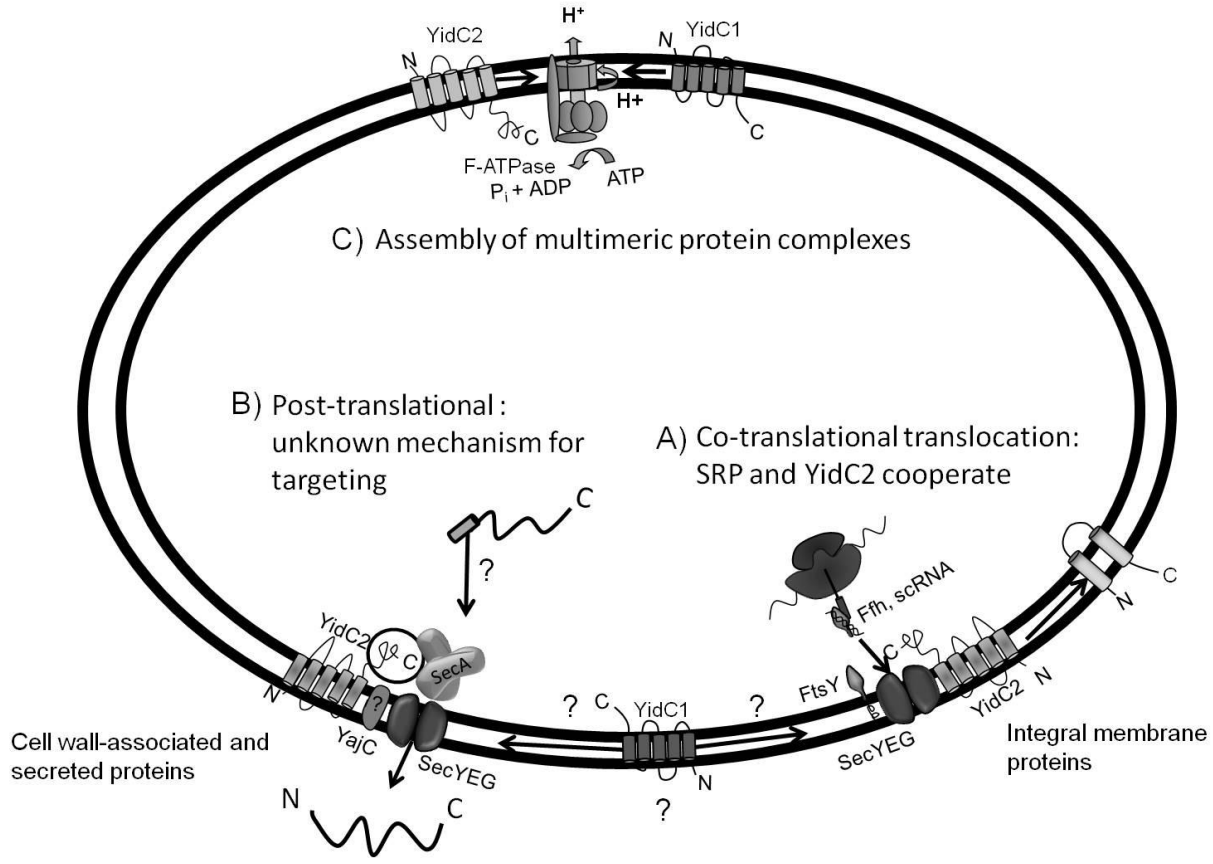

Figure 5-1. Current working model of YidC1 and YidC2's roles in protein translocation and membrane biogenesis in *S. mutans*. A) YidC2 and the SRP pathway may cooperate in co-translational translocation of integral membrane proteins. B) The mechanism of post-translational targeting in *S. mutans* is unknown. YidC1 and YidC2 may be involved in protein translocation, in either a regulatory role or to improve efficiency of secretion or maturation of certain proteins. C) YidC1 and YidC2 are likely involved in the insertion and assembly of multimeric protein complexes. The C-terminal tail of YidC2 is believed to be required in several of these pathways. A circle around the C-terminal tail indicates a variable requirement in the pathway depending on the substrate.

LIST OF REFERENCES

1. Facklam, R. (2002) What happened to the streptococci: overview of taxonomic and nomenclature changes. *Clin Microbiol Rev* 15**:**613-30.

2. Doern, C. D. & Burnham, C. A. (2010) It's not easy being green: the viridans group streptococci, with a focus on pediatric clinical manifestations. *J Clin Microbiol* 48**:**3829-35.

3. Nakano, K., Nomura, R., Nakagawa, I., Hamada, S. & Ooshima, T. (2004) Demonstration of *Streptococcus mutans* with a cell wall polysaccharide specific to a new serotype, k, in the human oral cavity. *J Clin Microbiol* 42**:**198-202.

4. Loesche, W. J. (1986) Role of *Streptococcus mutans* in human dental decay. *Microbiol Rev* 50**:**353-80.

5. Taubman, M. A. & Nash, D. A. (2006) The scientific and public-health imperative for a vaccine against dental caries. *Nat Rev Immunol* 6**:**555-63.

6. Abranches, J., Zeng, L., Belanger, M., Rodrigues, P. H., Simpson-Haidaris, P. J., Akin, D., Dunn, W. A., Jr., Progulske-Fox, A. & Burne, R. A. (2009) Invasion of human coronary artery endothelial cells by *Streptococcus mutans* OMZ175. *Oral Microbiol Immunol* 24**:**141-5.

7. Lemos, J. A. & Burne, R. A. (2008) A model of efficiency: stress tolerance by *Streptococcus mutans*. *Microbiology* 154**:**3247-55.

8. Banas, J. A. & Vickerman, M. M. (2003) Glucan-binding proteins of the oral streptococci. *Crit Rev Oral Biol Med* 14**:**89-99.

9. Jenkinson, H. F. & Demuth, D. R. (1997) Structure, function and immunogenicity of streptococcal antigen I/II polypeptides. *Mol Microbiol* 23**:**183-90.

10. Ajdic, D., McShan, W. M., McLaughlin, R. E., Savic, G., Chang, J., Carson, M. B., Primeaux, C., Tian, R., Kenton, S., Jia, H., Lin, S., Qian, Y., Li, S., Zhu, H., Najar, F., Lai, H., White, J., Roe, B. A. & Ferretti, J. J. (2002) Genome sequence of *Streptococcus mutans* UA159, a cariogenic dental pathogen. *Proc Natl Acad Sci U S A* 99**:**14434-9.

11. Margolis, H. C., Zhang, Y. P., Lee, C. Y., Kent, R. L., Jr. & Moreno, E. C. (1999) Kinetics of enamel demineralization in vitro. *J Dent Res* 78**:**1326-1335.

12. Dashper, S. G. & Reynolds, E. C. (1992) pH regulation by *Streptococcus mutans*. *J Dent Res* 71**:**1159-65.

13. Bender, G. R., Thibodeau, E. A. & Marquis, R. E. (1985) Reduction of acidurance of streptococcal growth and glycolysis by fluoride and gramicidin. *J Dent Res* 64**:**90-95.

14. Len, A. C., Harty, D. W. & Jacques, N. A. (2004) Proteome analysis of *Streptococcus mutans* metabolic phenotype during acid tolerance. *Microbiology* 150**:**1353-66.

15. Len, A. C., Harty, D. W. & Jacques, N. A. (2004) Stress-responsive proteins are upregulated in *Streptococcus mutans* during acid tolerance. *Microbiology* 150**:**1339-51.

16. Hamilton, I. R. & Buckley, N. D. (1991) Adaptation by *Streptococcus mutans* to acid tolerance. *Oral Microbiol Immunol* 6**:**65-71.

17. Fozo, E. M. & Quivey, R. G., Jr. (2004) The fabM gene product of *Streptococcus mutans* is responsible for the synthesis of monounsaturated fatty acids and is necessary for survival at low pH. *J Bacteriol* 186**:**4152-8.

18. Fozo, E. M. & Quivey, R. G., Jr. (2004) Shifts in the membrane fatty acid profile of *Streptococcus mutans* enhance survival in acidic environments. *Appl Environ Microbiol* 70**:**929-36.

19. Quivey, R. G., Kuhnert, W. L. & Hahn, K. (2001) Genetics of acid adaptation in oral streptococci. *Crit Rev Oral Biol Med* 12**:**301-14.

20. Carlsson , J. (1986) *Textbook of Cariology. Munksgaard, Copenhagen*.

21. Senior, A. E., Nadanaciva, S. & Weber, J. (2002) The molecular mechanism of ATP synthesis by F1F0-ATP synthase. *Biochim Biophys Acta* 1553**:**188-211.

22. Sheng, J. & Marquis, R. E. (2006) Enhanced acid resistance of oral streptococci at lethal pH values associated with acid-tolerant catabolism and with ATP synthase activity. *FEMS Microbiol Lett* 262**:**93-8.

23. Bender, G. R., Sutton, S. V. & Marquis, R. E. (1986) Acid tolerance, proton permeabilities, and membrane ATPases of oral streptococci. *Infect Immun* 53**:**331-8.

24. Sutton, S. V. & Marquis, R. E. (1987) Membrane-associated and solubilized ATPases of *Streptococcus mutans* and *Streptococcus sanguis*. *J Dent Res* 66**:**1095-8.

25. Kuhnert, W. L., Zheng, G., Faustoferri, R. C. & Quivey, R. G., Jr. (2004) The F-ATPase operon promoter of *Streptococcus mutans* is transcriptionally regulated in response to external pH. *J Bacteriol* 186**:**8524-8.

26. Magalhaes, P. P., Paulino, T. P., Thedei, G., Jr. & Ciancaglini, P. (2005) Kinetic characterization of P-type membrane ATPase from *Streptococcus mutans*. *Comp Biochem Physiol B Biochem Mol Biol* 140**:**589-97.

27. Gong, Y., Tian, X. L., Sutherland, T., Sisson, G., Mai, J., Ling, J. & Li, Y. H. (2009) Global transcriptional analysis of acid-inducible genes in *Streptococcus mutans*: multiple two-component systems involved in acid adaptation. *Microbiology* 155**:**3322-32.

28. Yi, L., Celebi, N., Chen, M. & Dalbey, R. E. (2004) Sec/SRP requirements and energetics of membrane insertion of subunits a, b, and c of the *Escherichia coli* F1F0 ATP synthase. *J Biol Chem* 279**:**39260-7.

29. Kol, S., Majczak, W., Heerlien, R., van der Berg, J. P., Nouwen, N. & Driessen, A. J. (2009) Subunit a of the F(1)F(0) ATP synthase requires YidC and SecYEG for membrane insertion. *J Mol Biol* 390**:**893-901.

30. van der Laan, M., Bechtluft, P., Kol, S., Nouwen, N. & Driessen, A. J. (2004) F1F0 ATP synthase subunit c is a substrate of the novel YidC pathway for membrane protein biogenesis. *J Cell Biol* 165**:**213-22.

31. Hasona, A., Crowley, P. J., Levesque, C. M., Mair, R. W., Cvitkovitch, D. G., Bleiweis, A. S. & Brady, L. J. (2005) Streptococcal viability and diminished stress tolerance in mutants lacking the signal recognition particle pathway or YidC2. *Proc Natl Acad Sci U S A* 102**:**17466-71.

32. Ajdic, D. & Pham, V. T. (2007) Global transcriptional analysis of *Streptococcus mutans* sugar transporters using microarrays. *J Bacteriol* 189**:**5049-59.

33. Postma, P. W., Lengeler, J. W. & Jacobson, G. R. (1993) Phosphoenolpyruvate:carbohydrate phosphotransferase systems of bacteria. *Microbiol Rev* 57**:**543-94.

34. Zeng, L. & Burne, R. A. (2010) Seryl-phosphorylated HPr Regulates CcpA-Independent Carbon Catabolite Repression in Conjunction with PTS Permeases in *Streptococcus mutans*. *Mol Microbiol*.

35. Titgemeyer, F. & Hillen, W. (2002) Global control of sugar metabolism: a gram-positive solution. *Antonie Van Leeuwenhoek* 82**:**59-71.

36. Korithoski, B., Levesque, C. M. & Cvitkovitch, D. G. (2008) The involvement of the pyruvate dehydrogenase E1alpha subunit, in *Streptococcus mutans* acid tolerance. *FEMS Microbiol Lett* 289**:**13-9.

37. Carlsson, J., Kujala, U. & Edlund, M. B. (1985) Pyruvate dehydrogenase activity in *Streptococcus mutans*. *Infect Immun* 49**:**674-8.

38. Mascher, T., Helmann, J. D. & Unden, G. (2006) Stimulus perception in bacterial signal-transducing histidine kinases. *Microbiol Mol Biol Rev* 70**:**910-38.

39. Biswas, I., Drake, L., Erkina, D. & Biswas, S. (2008) Involvement of sensor kinases in the stress tolerance response of *Streptococcus mutans*. *J Bacteriol* 190**:**68-77.

40. Senadheera, D., Krastel, K., Mair, R., Persadmehr, A., Abranches, J., Burne, R. A. & Cvitkovitch, D. G. (2009) Inactivation of VicK affects acid production and acid survival of *Streptococcus mutans*. *J Bacteriol* 191**:**6415-24.

41. bChong, P., Drake, L. & Biswas, I. (2008) LiaS regulates virulence factor expression in *Streptococcus mutans*. *Infect Immun* 76**:**3093-9.

42. aChong, P., Drake, L. & Biswas, I. (2008) Modulation of covR expression in *Streptococcus mutans* UA159. *J Bacteriol* 190**:**4478-88.

43. Banu, L. D., Conrads, G., Rehrauer, H., Hussain, H., Allan, E. & van der Ploeg, J. R. (2010) The *Streptococcus mutans* serine/threonine kinase, PknB, regulates competence development, bacteriocin production, and cell wall metabolism. *Infect Immun* 78**:**2209-20.

44. Mascher, T. (2006) Intramembrane-sensing histidine kinases: a new family of cell envelope stress sensors in Firmicutes bacteria. *FEMS Microbiol Lett* 264**:**133-44.

45. Suntharalingam, P., Senadheera, M. D., Mair, R. W., Levesque, C. M. & Cvitkovitch, D. G. (2009) The LiaFSR system regulates the cell envelope stress response in *Streptococcus mutans*. *J Bacteriol* 191**:**2973-84.

46. Yuan, J., Zweers, J. C., van Dijl, J. M. & Dalbey, R. E. (2010) Protein transport across and into cell membranes in bacteria and archaea. *Cell Mol Life Sci* 67**:**179-99.

47. Driessen, A. J. & Nouwen, N. (2008) Protein translocation across the bacterial cytoplasmic membrane. *Annu Rev Biochem* 77**:**643-67.

48. Papanikou, E., Karamanou, S. & Economou, A. (2007) Bacterial protein secretion through the translocase nanomachine. *Nat Rev Microbiol* 5**:**839-51.

49. Hoffmann, A., Bukau, B. & Kramer, G. (2010) Structure and function of the molecular chaperone Trigger Factor. *Biochim Biophys Acta* 1803**:**650-61.

50. Beck, K., Wu, L. F., Brunner, J. & Muller, M. (2000) Discrimination between SRP- and SecA/SecB-dependent substrates involves selective recognition of nascent chains by SRP and trigger factor. *EMBO J* 19**:**134-43.

51. Duong, F. & Wickner, W. (1997) Distinct catalytic roles of the SecYE, SecG and SecDFyajC subunits of preprotein translocase holoenzyme. *Embo J* 16**:**2756-68.

52. du Plessis, D. J., Nouwen, N. & Driessen, A. J. (2010) The Sec translocase. *Biochim Biophys Acta*.

53. Pogliano, J. A. & Beckwith, J. (1994) SecD and SecF facilitate protein export in *Escherichia coli*. *EMBO J* 13**:**554-61.

54. Bolhuis, A., Broekhuizen, C. P., Sorokin, A., van Roosmalen, M. L., Venema, G., Bron, S., Quax, W. J. & van Dijl, J. M. (1998) SecDF of *Bacillus subtilis*, a molecular Siamese twin required for the efficient secretion of proteins. *J Biol Chem* 273**:**21217-24.

55. Yamane, K., Bunai, K. & Kakeshita, H. (2004) Protein traffic for secretion and related machinery of *Bacillus subtilis*. *Biosci Biotechnol Biochem* 68**:**2007-23.

56. Murphy, C. K. & Beckwith, J. (1994) Residues essential for the function of SecE, a membrane component of the *Escherichia coli* secretion apparatus, are located in a conserved cytoplasmic region. *Proc Natl Acad Sci U S A* 91**:**2557-61.

57. Nakamura, K., Yahagi, S., Yamazaki, T. & Yamane, K. (1999) *Bacillus subtilis* histone-like protein, HBsu, is an integral component of a SRP-like particle that can bind the Alu domain of small cytoplasmic RNA. *J Biol Chem* 274**:**13569-76.

58. Honda, K., Nakamura, K., Nishiguchi, M. & Yamane, K. (1993) Cloning and characterization of a *Bacillus subtilis* gene encoding a homolog of the 54-kilodalton subunit of mammalian signal recognition particle and *Escherichia coli* Ffh. *J Bacteriol* 175**:**4885-94.

59. Swaving, J., van Wely, K. H. & Driessen, A. J. (1999) Preprotein translocation by a hybrid translocase composed of *Escherichia coli* and *Bacillus subtilis* subunits. *J Bacteriol* 181**:**7021-7.

60. Gutierrez, J. A., Crowley, P. J., Brown, D. P., Hillman, J. D., Youngman, P. & Bleiweis, A. S. (1996) Insertional mutagenesis and recovery of interrupted genes of *Streptococcus mutans* by using transposon Tn917: preliminary characterization of mutants displaying acid sensitivity and nutritional requirements. *J Bacteriol* 178**:**4166-75.

61. Gutierrez, J. A., Crowley, P. J., Cvitkovitch, D. G., Brady, L. J., Hamilton, I. R., Hillman, J. D. & Bleiweis, A. S. (1999) *Streptococcus mutans ffh*, a gene encoding a homologue of the 54 kDa subunit of the signal recognition particle, is involved in resistance to acid stress. *Microbiology* 145 (Pt 2)**:**357-66.

62. Rosch, J. W., Vega, L. A., Beyer, J. M., Lin, A. & Caparon, M. G. (2008) The signal recognition particle pathway is required for virulence in *Streptococcus pyogenes*. *Infect Immun* 76**:**2612-9.

63. Rigel, N. W. & Braunstein, M. (2008) A new twist on an old pathway--accessory Sec [corrected] systems. *Mol Microbiol* 69**:**291-302.

64. Bensing, B. A. & Sullam, P. M. (2002) An accessory sec locus of *Streptococcus gordonii* is required for export of the surface protein GspB and for normal levels of binding to human platelets. *Mol Microbiol* 44**:**1081-94.

65. Bensing, B. A., Siboo, I. R. & Sullam, P. M. (2007) Glycine residues in the hydrophobic core of the GspB signal sequence route export toward the accessory Sec pathway. *J Bacteriol* 189**:**3846-54.

66. Takamatsu, D., Bensing, B. A. & Sullam, P. M. (2004) Genes in the accessory sec locus of *Streptococcus gordonii* have three functionally distinct effects on the expression of the platelet-binding protein GspB. *Mol Microbiol* 52**:**189-203.

67. Rosch, J. W. & Caparon, M. G. (2005) The ExPortal: an organelle dedicated to the biogenesis of secreted proteins in *Streptococcus pyogenes*. *Mol Microbiol* 58**:**959-68.

68. Rosch, J. & Caparon, M. (2004) A microdomain for protein secretion in Gram-positive bacteria. *Science* 304**:**1513-5.

69. Hu, P., Bian, Z., Fan, M., Huang, M. & Zhang, P. (2008) Sec translocase and sortase A are colocalised in a locus in the cytoplasmic membrane of *Streptococcus mutans*. *Arch Oral Biol* 53**:**150-4.

70. Carlsson, F., Stalhammar-Carlemalm, M., Flardh, K., Sandin, C., Carlemalm, E. & Lindahl, G. (2006) Signal sequence directs localized secretion of bacterial surface proteins. *Nature* 442**:**943-6.

71. Campo, N., Tjalsma, H., Buist, G., Stepniak, D., Meijer, M., Veenhuis, M., Westermann, M., Muller, J. P., Bron, S., Kok, J., Kuipers, O. P. & Jongbloed, J. D. (2004) Subcellular sites for bacterial protein export. *Mol Microbiol* 53**:**1583-99.

72. Phillips, G. J. & Silhavy, T. J. (1992) The *E. coli ffh* gene is necessary for viability and efficient protein export. *Nature* 359**:**744-6.

73. Kremer, B. H., van der Kraan, M., Crowley, P. J., Hamilton, I. R., Brady, L. J. & Bleiweis, A. S. (2001) Characterization of the sat operon in *Streptococcus mutans*: evidence for a role of Ffh in acid tolerance. *J Bacteriol* 183**:**2543-52.

74. Crowley, P. J., Svensater, G., Snoep, J. L., Bleiweis, A. S. & Brady, L. J. (2004) An *ffh* mutant of *Streptococcus mutans* is viable and able to physiologically adapt to low pH in continuous culture. *FEMS Microbiol Lett* 234**:**315-24.

75. Hasona, A., Zuobi-Hasona, K., Crowley, P. J., Abranches, J., Ruelf, M. A., Bleiweis, A. S. & Brady, L. J. (2007) Membrane composition changes and physiological adaptation by *Streptococcus mutans* signal recognition particle pathway mutants. *J Bacteriol* 189**:**1219-30.

76. Li, Y. H., Tang, N., Aspiras, M. B., Lau, P. C., Lee, J. H., Ellen, R. P. & Cvitkovitch, D. G. (2002) A quorum-sensing signaling system essential for genetic competence in *Streptococcus mutans* is involved in biofilm formation. *J Bacteriol* 184**:**2699-708.

77. Zhang, Y. J., Tian, H. F. & Wen, J. F. (2009) The evolution of YidC/Oxa/Alb3 family in the three domains of life: a phylogenomic analysis. *BMC Evol Biol* 9**:**137.

78. Bonnefoy, N., Fiumera, H. L., Dujardin, G. & Fox, T. D. (2009) Roles of Oxa1-related inner-membrane translocases in assembly of respiratory chain complexes. *Biochim Biophys Acta* 1793**:**60-70.

79. van der Laan, M., Urbanus, M. L., Ten Hagen-Jongman, C. M., Nouwen, N., Oudega, B., Harms, N., Driessen, A. J. & Luirink, J. (2003) A conserved function of YidC in the biogenesis of respiratory chain complexes. *Proc Natl Acad Sci U S A* 100**:**5801-6.

80. Kiefer, D. & Kuhn, A. (2007) YidC as an essential and multifunctional component in membrane protein assembly. *Int Rev Cytol* 259**:**113-38.

81. Yen, M. R., Harley, K. T., Tseng, Y. H. & Saier, M. H., Jr. (2001) Phylogenetic and structural analyses of the oxa1 family of protein translocases. *FEMS Microbiol Lett* 204**:**223-31.

82. Bonnefoy, N., Chalvet, F., Hamel, P., Slonimski, P. P. & Dujardin, G. (1994) OXA1, a *Saccharomyces cerevisiae* nuclear gene whose sequence is conserved from prokaryotes to eukaryotes controls cytochrome oxidase biogenesis. *J Mol Biol* 239**:**201-12.

83. Yi, L. & Dalbey, R. E. (2005) Oxa1/Alb3/YidC system for insertion of membrane proteins in mitochondria, chloroplasts and bacteria (review). *Mol Membr Biol* 22**:**101-11.

84. Stuart, R. (2002) Insertion of proteins into the inner membrane of mitochondria: the role of the Oxa1 complex. *Biochim Biophys Acta* 1592**:**79-87.

85. Jia, L., Dienhart, M., Schramp, M., McCauley, M., Hell, K. & Stuart, R. A. (2003) Yeast Oxa1 interacts with mitochondrial ribosomes: the importance of the C-terminal region of Oxa1. *Embo J* 22**:**6438-47.

86. Saracco, S. A. & Fox, T. D. (2002) Cox18p is required for export of the mitochondrially encoded *Saccharomyces cerevisiae* Cox2p C-tail and interacts with Pnt1p and Mss2p in the inner membrane. *Mol Biol Cell* 13**:**1122-31.

87. Funes, S., Nargang, F. E., Neupert, W. & Herrmann, J. M. (2004) The Oxa2 Protein of *Neurospora crassa* Plays a Critical Role in the Biogenesis of Cytochrome Oxidase and Defines a Ubiquitous Subbranch of the Oxa1/YidC/Alb3 Protein Family. *Mol. Biol. Cell* 15**:**1853-1861.

88. Gaisne, M. & Bonnefoy, N. (2006) The COX18 gene, involved in mitochondrial biogenesis, is functionally conserved and tightly regulated in humans and fission yeast. *FEMS Yeast Res* 6**:**869-82.

89. Samuelson, J. C., Chen, M., Jiang, F., Moller, I., Wiedmann, M., Kuhn, A., Phillips, G. J. & Dalbey, R. E. (2000) YidC mediates membrane protein insertion in bacteria. *Nature* 406**:**637-41.

90. Saaf, A., Monne, M., de Gier, J. W. & von Heijne, G. (1998) Membrane topology of the 60-kDa Oxa1p homologue from *Escherichia coli*. *J Biol Chem* 273**:**30415-8.

91. Jiang, F., Chen, M., Yi, L., de Gier, J. W., Kuhn, A. & Dalbey, R. E. (2003) Defining the regions of *Escherichia coli* YidC that contribute to activity. *J Biol Chem* 278**:**48965-72.

92. van der Laan, M., Houben, E. N., Nouwen, N., Luirink, J. & Driessen, A. J. (2001) Reconstitution of Sec-dependent membrane protein insertion: nascent FtsQ interacts with YidC in a SecYEG-dependent manner. *EMBO Rep* 2**:**519-23.

93. Urbanus, M. L., Froderberg, L., Drew, D., Bjork, P., de Gier, J. W., Brunner, J., Oudega, B. & Luirink, J. (2002) Targeting, insertion, and localization of *Escherichia coli* YidC. *J Biol Chem* 277**:**12718-23.

94. Celebi, N., Yi, L., Facey, S. J., Kuhn, A. & Dalbey, R. E. (2006) Membrane biogenesis of subunit II of cytochrome bo oxidase: contrasting requirements for insertion of N-terminal and C-terminal domains. *J Mol Biol* 357**:**1428-36.

95. Chen, M., Xie, K., Nouwen, N., Driessen, A. J. & Dalbey, R. E. (2003) Conditional lethal mutations separate the M13 procoat and Pf3 coat functions of YidC: different YIDC structural requirements for membrane protein insertion. *J Biol Chem* 278**:**23295-300.

96. Kol, S., Nouwen, N. & Driessen, A. J. (2008) The charge distribution in the cytoplasmic loop of subunit C of the F1F0 ATPase is a determinant for YidC targeting. *J Biol Chem* 283**:**9871-7.

97. Facey, S. J., Neugebauer, S. A., Krauss, S. & Kuhn, A. (2007) The mechanosensitive channel protein MscL is targeted by the SRP to the novel YidC membrane insertion pathway of *Escherichia coli*. *J Mol Biol* 365**:**995-1004.

98. Price, C. E., Kocer, A., Kol, S., van der Berg, J. P. & Driessen, A. J. (2011) In vitro synthesis and oligomerization of the mechanosensitive channel of large conductance, MscL, into a functional ion channel. *FEBS Lett* 585**:**249-54.

99. Wagner, S., Pop, O. I., Haan, G. J., Baars, L., Koningstein, G., Klepsch, M. M., Genevaux, P., Luirink, J. & de Gier, J. W. (2008) Biogenesis of MalF and the MalFGK(2) maltose transport complex in *Escherichia coli* requires YidC. *J Biol Chem* 283**:**17881-90.

100. Nagamori, S., Smirnova, I. N. & Kaback, H. R. (2004) Role of YidC in folding of polytopic membrane proteins. *J Cell Biol* 165**:**53-62.

101. Beck, K., Eisner, G., Trescher, D., Dalbey, R. E., Brunner, J. & Muller, M. (2001) YidC, an assembly site for polytopic *Escherichia coli* membrane proteins located in immediate proximity to the SecYE translocon and lipids. *EMBO Rep* 2**:**709-14.

102. Sundberg, E., Slagter, J. G., Fridborg, I., Cleary, S. P., Robinson, C. & Coupland, G. (1997) ALBINO3, an Arabidopsis nuclear gene essential for chloroplast differentiation, encodes a chloroplast protein that shows homology to proteins present in bacterial membranes and yeast mitochondria. *Plant Cell* 9**:**717-30.

103. Moore, M., Harrison, M. S., Peterson, E. C. & Henry, R. (2000) Chloroplast Oxa1p homolog albino3 is required for post-translational integration of the light harvesting chlorophyll-binding protein into thylakoid membranes. *J Biol Chem* 275**:**1529-32.

104. Gerdes, L., Bals, T., Klostermann, E., Karl, M., Philippar, K., Hunken, M., Soll, J. & Schunemann, D. (2006) A second thylakoid membrane-localized Alb3/OxaI/YidC homologue is involved in proper chloroplast biogenesis in *Arabidopsis thaliana*. *J Biol Chem* 281**:**16632-42.

105. Gohre, V., Ossenbuhl, F., Crevecoeur, M., Eichacker, L. A. & Rochaix, J. D. (2006) One of two alb3 proteins is essential for the assembly of the photosystems and for cell survival in *Chlamydomonas*. *Plant Cell* 18**:**1454-66.

106. Aldridge, C., Cain, P. & Robinson, C. (2009) Protein transport in organelles: Protein transport into and across the thylakoid membrane. *FEBS J* 276**:**1177-86.

107. Schunemann, D. (2007) Mechanisms of protein import into thylakoids of chloroplasts. *Biol Chem* 388**:**907-15.

108. Pool, M. R. (2005) Signal recognition particles in chloroplasts, bacteria, yeast and mammals (review). *Mol Membr Biol* 22**:**3-15.

109. Lewis, N. E., Marty, N. J., Kathir, K. M., Rajalingam, D., Kight, A. D., Daily, A., Kumar, T. K., Henry, R. L. & Goforth, R. L. (2010) A dynamic cpSRP43-Albino3 interaction mediates translocase regulation of chloroplast signal recognition particle (cpSRP)-targeting components. *J Biol Chem* 285**:**34220-30.

110. Falk, S., Ravaud, S., Koch, J. & Sinning, I. (2010) The C terminus of the Alb3 membrane insertase recruits cpSRP43 to the thylakoid membrane. *J Biol Chem* 285**:**5954-62.

111. Klostermann, E., Droste Gen Helling, I., Carde, J. P. & Schunemann, D. (2002) The thylakoid membrane protein ALB3 associates with the cpSecY-translocase in *Arabidopsis thaliana*. *Biochem J* 368**:**777-81.

112. Benz, M., Bals, T., Gugel, I. L., Piotrowski, M., Kuhn, A., Schunemann, D., Soll, J. & Ankele, E. (2009) Alb4 of Arabidopsis Promotes Assembly and Stabilization of a Non Chlorophyll-Binding Photosynthetic Complex, the CF1CF0-ATP Synthase. *Mol Plant* 2**:**1410-24.

113. Sutcliffe, I. C. & Russell, R. R. (1995) Lipoproteins of gram-positive bacteria. *J Bacteriol* 177**:**1123-8.

114. Murakami, T., Haga, K., Takeuchi, M. & Sato, T. (2002) Analysis of the *Bacillus subtilis* spoIIIJ gene and its Paralogue gene, yqjG. *J Bacteriol* 184**:**1998-2004.

115. Tjalsma, H., Bron, S. & van Dijl, J. M. (2003) Complementary Impact of Paralogous Oxa1-like Proteins of *Bacillus subtilis* on Post-translocational Stages in Protein Secretion. *J. Biol. Chem.* 278**:**15622-15632.

116. Saller, M. J., Fusetti, F. & Driessen, A. J. (2009) *Bacillus subtilis* SpoIIIJ and YqjG function in membrane protein biogenesis. *J Bacteriol* 191**:**6749-57.

117. Saller, M. J., Otto, A., Berrelkamp-Lahpor, G. A., Becher, D., Hecker, M. & Driessen, A. J. (2011) *Bacillus subtilis* YqjG is required for genetic competence development. *Proteomics* 11**:**270-82.

118. Rubio, A., Jiang, X. & Pogliano, K. (2005) Localization of translocation complex components in *Bacillus subtilis*: enrichment of the signal recognition particle receptor at early sporulation septa. *J Bacteriol* 187**:**5000-2.

119. Chiba, S., Lamsa, A. & Pogliano, K. (2009) A ribosome-nascent chain sensor of membrane protein biogenesis in *Bacillus subtilis*. *EMBO J* 28**:**3461-75.

120. Sarker, S., Rudd, K. E. & Oliver, D. (2000) Revised translation start site for secM defines an atypical signal peptide that regulates *Escherichia coli* secA expression. *J Bacteriol* 182**:**5592-5.

121. Brady, L. J., Piacentini, D. A., Crowley, P. J. & Bleiweis, A. S. (1991) Identification of monoclonal antibody-binding domains within antigen P1 of *Streptococcus mutans* and cross-reactivity with related surface antigens of oral streptococci. *Infect Immun* 59**:**4425-35.

122. Oli, M. W., McArthur, W. P. & Brady, L. J. (2006) A whole cell BIAcore assay to evaluate P1-mediated adherence of *Streptococcus mutans* to human salivary agglutinin and inhibition by specific antibodies. *J Microbiol Methods* 65**:**503-11.

123. Funes, S., Hasona, A., Bauerschmitt, H., Grubbauer, C., Kauff, F., Collins, R., Crowley, P. J., Palmer, S. R., Brady, L. J. & Herrmann, J. M. (2009) Independent gene duplications of the YidC/Oxa/Alb3 family enabled a specialized cotranslational function. *Proc Natl Acad Sci U S A* 106**:**6656-61.

124. Jones, S. E., Lloyd, L. J., Tan, K. K. & Buck, M. (2003) Secretion defects that activate the phage shock response of *Escherichia coli*. *J Bacteriol* 185**:**6707-11.

125. Antiporta, M. H. & Dunny, G. M. (2002) ccfA, the genetic determinant for the cCF10 peptide pheromone in *Enterococcus faecalis* OG1RF. *J Bacteriol* 184**:**1155-62.

126. Terpe, K. (2006) Overview of bacterial expression systems for heterologous protein production: from molecular and biochemical fundamentals to commercial systems. *Appl Microbiol Biotechnol* 72**:**211-22.

127. Baars, L., Wagner, S., Wickstrom, D., Klepsch, M., Ytterberg, A. J., van Wijk, K. J. & de Gier, J. W. (2008) Effects of SecE depletion on the inner and outer membrane proteomes of *Escherichia coli*. *J Bacteriol* 190**:**3505-25.

128. de Gier, J. W., Mansournia, P., Valent, Q. A., Phillips, G. J., Luirink, J. & von Heijne, G. (1996) Assembly of a cytoplasmic membrane protein in *Escherichia coli* is dependent on the signal recognition particle. *FEBS Lett* 399**:**307-9.

129. Herskovits, A. A., Seluanov, A., Rajsbaum, R., ten Hagen-Jongman, C. M., Henrichs, T., Bochkareva, E. S., Phillips, G. J., Probst, F. J., Nakae, T., Ehrmann, M., Luirink, J. & Bibi, E. (2001) Evidence for coupling of membrane targeting and function of the signal recognition particle (SRP) receptor FtsY. *EMBO Rep* 2**:**1040-6.

130. Henner, D. J. (1990) Inducible expression of regulatory genes in *Bacillus subtilis*. *Methods Enzymol* 185**:**223-8.

131. Eichenbaum, Z., Federle, M. J., Marra, D., de Vos, W. M., Kuipers, O. P., Kleerebezem, M. & Scott, J. R. (1998) Use of the lactococcal nisA promoter to regulate gene expression in gram-positive bacteria: comparison of induction level and promoter strength. *Appl Environ Microbiol* 64**:**2763-9.

132. Bryan, E. M., Bae, T., Kleerebezem, M. & Dunny, G. M. (2000) Improved vectors for nisin-controlled expression in gram-positive bacteria. *Plasmid* 44**:**183-90.

133. Zeng, L. & Burne, R. A. (2009) Transcriptional regulation of the cellobiose operon of *Streptococcus mutans*. *J Bacteriol* 191**:**2153-62.

134. Van den Berg, B., Clemons, W. M., Jr., Collinson, I., Modis, Y., Hartmann, E., Harrison, S. C. & Rapoport, T. A. (2004) X-ray structure of a protein-conducting channel. *Nature* 427**:**36-44.

135. Heckman, K. L. & Pease, L. R. (2007) Gene splicing and mutagenesis by PCR-driven overlap extension. *Nat Protoc* 2**:**924-32.

136. Wen, Z. T. & Burne, R. A. (2001) Construction of a new integration vector for use in *Streptococcus mutans*. *Plasmid* 45**:**31-6.

137. LeBlanc, D. J., Lee, L. N. & Abu-Al-Jaibat, A. (1992) Molecular, genetic, and functional analysis of the basic replicon of pVA380-1, a plasmid of oral streptococcal origin. *Plasmid* 28**:**130-45.

138. Terleckyj, B., Willett, N. P. & Shockman, G. D. (1975) Growth of several cariogenic strains of oral streptococci in a chemically defined medium. *Infect Immun* 11**:**649-55.

139. Price, C. E., Otto, A., Fusetti, F., Becher, D., Hecker, M. & Driessen, A. J. (2010) Differential effect of YidC depletion on the membrane proteome of *Escherichia coli* under aerobic and anaerobic growth conditions. *Proteomics* 10**:**3235-47.

140. Abranches, J., Chen, Y. Y. & Burne, R. A. (2003) Characterization of *Streptococcus mutans* strains deficient in EIIAB Man of the sugar phosphotransferase system. *Appl Environ Microbiol* 69**:**4760-9.

141. Abranches, J., Candella, M. M., Wen, Z. T., Baker, H. V. & Burne, R. A. (2006) Different roles of EIIABMan and EIIGlc in regulation of energy metabolism, biofilm development, and competence in *Streptococcus mutans*. *J Bacteriol* 188**:**3748-56.

142. Dong, Y., Palmer, S. R., Hasona, A., Nagamori, S., Kaback, H. R., Dalbey, R. E. & Brady, L. J. (2008) Functional overlap but lack of complete cross-complementation of *Streptococcus mutans* and *Escherichia coli* YidC orthologs. *J Bacteriol* 190**:**2458-69.

143. Buckley, N. D., Lee, L. N. & LeBlanc, D. J. (1995) Use of a novel mobilizable vector to inactivate the scrA gene of *Streptococcus sobrinus* by allelic replacement. *J Bacteriol* 177**:**5028-34.

144. van Bloois, E., Jan Haan, G., de Gier, J. W., Oudega, B. & Luirink, J. (2004) F(1)F(0) ATP synthase subunit c is targeted by the SRP to YidC in the E. coli inner membrane. *FEBS Lett* 576**:**97-100.

145. Kol, S., Turrell, B. R., de Keyzer, J., van der Laan, M., Nouwen, N. & Driessen, A. J. (2006) YidC-mediated membrane insertion of assembly mutants of subunit c of the F1F0 ATPase. *J Biol Chem* 281**:**29762-8.

146. Ricci, M. L., Manganelli, R., Berneri, C., Orefici, G. & Pozzi, G. (1994) Electrotransformation of Streptococcus agalactiae with plasmid DNA. *FEMS Microbiol Lett* 119**:**47-52.

147. Samuelson, J. C., Jiang, F., Yi, L., Chen, M., de Gier, J. W., Kuhn, A. & Dalbey, R. E. (2001) Function of YidC for the insertion of M13 procoat protein in *Escherichia coli*: translocation of mutants that show differences in their membrane potential dependence and Sec requirement. *J Biol Chem* 276**:**34847-52.

148. Bhatt, D., Cole, S. P., Grabar, T. B., Claggett, S. B. & Cain, B. D. (2005) Manipulating the length of the b subunit F1 binding domain in F1F0 ATP synthase from *Escherichia coli*. *J Bioenerg Biomembr* 37**:**67-74.

149. Fiske, C. H. & Subbarow, Y. (1925) THE COLORIMETRIC DETERMINATION OF PHOSPHORUS. *Journal of Biological Chemistry* 66**:**375-400.

150. Sorgen, P. L., Bubb, M. R., McCormick, K. A., Edison, A. S. & Cain, B. D. (1998) Formation of the b subunit dimer is necessary for interaction with F1-ATPase. *Biochemistry* 37**:**923-32.

151. Stack, A. E. & Cain, B. D. (1994) Mutations in the delta subunit influence the assembly of F1F0 ATP synthase in *Escherichia coli*. *J Bacteriol* 176**:**540-2.

152. Welch, A. K., Claggett, S. B. & Cain, B. D. (2008) The b (arg36) contributes to efficient coupling in F(1)F (O) ATP synthase in *Escherichia coli*. *J Bioenerg Biomembr* 40**:**1-8.

153. du Plessis, D. J., Nouwen, N. & Driessen, A. J. (2006) Subunit a of cytochrome o oxidase requires both YidC and SecYEG for membrane insertion. *J Biol Chem* 281**:**12248-52.

154. Nieuwenhuis, F. J., Kanner, B. I., Gutnick, D. L., Postma, P. W. & van Dam, K. (1973) Energy conservation in membranes of mutants of *Escherichia coli* defective in oxidative phosphorylation. *Biochim Biophys Acta* 325**:**62-71.

155. Schagger, H. & von Jagow, G. (1991) Blue native electrophoresis for isolation of membrane protein complexes in enzymatically active form. *Anal Biochem* 199**:**223-31.

156. Neff, D. & Dencher, N. A. (1999) Purification of multisubunit membrane protein complexes: isolation of chloroplast FoF1-ATP synthase, CFo and CF1 by blue native electrophoresis. *Biochem Biophys Res Commun* 259**:**569-75.

157. Cline, K. & Mori, H. (2001) Thylakoid DeltapH-dependent precursor proteins bind to a cpTatC-Hcf106 complex before Tha4-dependent transport. *J Cell Biol* 154**:**719-29.

158. Krause, F. (2006) Detection and analysis of protein-protein interactions in organellar and prokaryotic proteomes by native gel electrophoresis: (Membrane) protein complexes and supercomplexes. *Electrophoresis* 27**:**2759-81.

159. Braun, R. J., Kinkl, N., Beer, M. & Ueffing, M. (2007) Two-dimensional electrophoresis of membrane proteins. *Anal Bioanal Chem* 389**:**1033-45.

160. Dresler, J., Klimentova, J. & Stulik, J. (2011) Bacterial protein complexes investigation using blue native PAGE. *Microbiol Res* 166**:**47-62.

161. Stenberg, F., Chovanec, P., Maslen, S. L., Robinson, C. V., Ilag, L. L., von Heijne, G. & Daley, D. O. (2005) Protein complexes of the *Escherichia coli* cell envelope. *J Biol Chem* 280**:**34409-19.

162. Aivaliotis, M., Karas, M. & Tsiotis, G. (2007) An alternative strategy for the membrane proteome analysis of the green sulfur bacterium Chlorobium tepidum using blue native PAGE and 2-D PAGE on purified membranes. *J Proteome Res* 6**:**1048-58.

163. Tsirogianni, E., Aivaliotis, M., Papasotiriou, D. G., Karas, M. & Tsiotis, G. (2006) Identification of inducible protein complexes in the phenol degrader Pseudomonas sp. strain phDV1 by blue native gel electrophoresis and mass spectrometry. *Amino Acids* 30**:**63-72.

164. Heuberger, E. H., Veenhoff, L. M., Duurkens, R. H., Friesen, R. H. & Poolman, B. (2002) Oligomeric state of membrane transport proteins analyzed with blue native electrophoresis and analytical ultracentrifugation. *J Mol Biol* 317**:**591-600.

165. Chassy, B. M. (1976) A gentle method for the lysis of oral streptococci. *Biochem Biophys Res Commun* 68**:**603-8.

166. Wittig, I., Braun, H. P. & Schagger, H. (2006) Blue native PAGE. *Nat Protoc* 1**:**418-28.

167. Keller, A., Nesvizhskii, A. I., Kolker, E. & Aebersold, R. (2002) Empirical statistical model to estimate the accuracy of peptide identifications made by MS/MS and database search. *Anal Chem* 74**:**5383-92.

168. Nesvizhskii, A. I., Keller, A., Kolker, E. & Aebersold, R. (2003) A statistical model for identifying proteins by tandem mass spectrometry. *Anal Chem* 75**:**4646-58.

169. Schagger, H. (2006) Tricine-SDS-PAGE. *Nat Protoc* 1**:**16-22.

170. Akiyama, Y. & Ito, K. (1985) The SecY membrane component of the bacterial protein export machinery: analysis by new electrophoretic methods for integral membrane proteins. *EMBO J* 4**:**3351-6.

171. Bessonneau, P., Besson, V., Collinson, I. & Duong, F. (2002) The SecYEG preprotein translocation channel is a conformationally dynamic and dimeric structure. *EMBO J* 21**:**995-1003.

172. Rath, A., Nadeau, V. G., Poulsen, B. E., Ng, D. P. & Deber, C. M. (2010) Novel hydrophobic standards for membrane protein molecular weight determinations via sodium dodecyl sulfate-polyacrylamide gel electrophoresis. *Biochemistry* 49**:**10589-91.

173. Tziatzios, C., Schubert, D., Lotz, M., Gundogan, D., Betz, H., Schagger, H., Haase, W., Duong, F. & Collinson, I. (2004) The bacterial protein-translocation complex: SecYEG dimers associate with one or two SecA molecules. *J Mol Biol* 340**:**513-24.

174. Angelini, S., Boy, D., Schiltz, E. & Koch, H. G. (2006) Membrane binding of the bacterial signal recognition particle receptor involves two distinct binding sites. *J Cell Biol* 174**:**715-24.

175. Duong, F. (2003) Binding, activation and dissociation of the dimeric SecA ATPase at the dimeric SecYEG translocase. *EMBO J* 22**:**4375-84.

176. Kihara, A., Akiyama, Y. & Ito, K. (1995) FtsH is required for proteolytic elimination of uncomplexed forms of SecY, an essential protein translocase subunit. *Proc Natl Acad Sci U S A* 92**:**4532-6.

177. van Bloois, E., Dekker, H. L., Froderberg, L., Houben, E. N., Urbanus, M. L., de Koster, C. G., de Gier, J. W. & Luirink, J. (2008) Detection of cross-links between FtsH, YidC, HflK/C suggests a linked role for these proteins in quality control upon insertion of bacterial inner membrane proteins. *FEBS Lett* 582**:**1419-24.

178. Seluanov, A. & Bibi, E. (1997) FtsY, the prokaryotic signal recognition particle receptor homologue, is essential for biogenesis of membrane proteins. *J Biol Chem* 272**:**2053-5.

179. Yi, L., Jiang, F., Chen, M., Cain, B., Bolhuis, A. & Dalbey, R. E. (2003) YidC is strictly required for membrane insertion of subunits a and c of the F(1)F(0)ATP synthase and SecE of the SecYEG translocase. *Biochemistry* 42**:**10537-44.

180. Akiyama, Y., Kihara, A., Tokuda, H. & Ito, K. (1996) FtsH (HflB) is an ATP-dependent protease selectively acting on SecY and some other membrane proteins. *J Biol Chem* 271**:**31196-201.

181. Stiburek, L., Fornuskova, D., Wenchich, L., Pejznochova, M., Hansikova, H. & Zeman, J. (2007) Knockdown of human Oxa1l impairs the biogenesis of F1Fo-ATP synthase and NADH:ubiquinone oxidoreductase. *J Mol Biol* 374**:**506-16.

182. Chen, P. M., Chen, Y. Y., Yu, S. L., Sher, S., Lai, C. H. & Chia, J. S. (2010) Role of GlnR in acid-mediated repression of genes encoding proteins involved in glutamine and glutamate metabolism in *Streptococcus mutans*. *Appl Environ Microbiol* 76**:**2478-86.

183. Peng, Y., Luo, Y., Yu, T., Xu, X., Fan, K., Zhao, Y. & Yang, K. (2011) A Blue Native-PAGE analysis of membrane protein complexes in Clostridium thermocellum. *BMC Microbiol* 11**:**22.

184. Abbe, K. & Yamada, T. (1982) Purification and properties of pyruvate kinase from *Streptococcus mutans*. *J Bacteriol* 149**:**299-305.

185. Baev, D., England, R. & Kuramitsu, H. K. (1999) Stress-induced membrane association of the *Streptococcus mutans* GTP-binding protein, an essential G protein, and investigation of its physiological role by utilizing an antisense RNA strategy. *Infect Immun* 67**:**4510-6.

186. Wu, J., Cho, M. I. & Kuramitsu, H. K. (1995) Expression, purification, and characterization of a novel G protein, SGP, from *Streptococcus mutans*. *Infect Immun* 63**:**2516-21.

187. Biswas, S. & Biswas, I. (2005) Role of HtrA in surface protein expression and biofilm formation by *Streptococcus mutans*. *Infect Immun* 73**:**6923-34.

188. Scott, J. R. & Zahner, D. (2006) Pili with strong attachments: Gram-positive bacteria do it differently. *Mol Microbiol* 62**:**320-30.

189. Huang, M., Meng, L., Fan, M., Hu, P. & Bian, Z. (2008) Effect of biofilm formation on virulence factor secretion via the general secretory pathway in *Streptococcus mutans*. *Arch Oral Biol* 53**:**1179-85.

190. Pop, O. I., Soprova, Z., Koningstein, G., Scheffers, D. J., van Ulsen, P., Wickstrom, D., de Gier, J. W. & Luirink, J. (2009) YidC is required for the assembly of the MscL homopentameric pore. *FEBS J* 276**:**4891-9.

191. Johansen, L., Bryn, K. & Stormer, F. C. (1975) Physiological and biochemical role of the butanediol pathway in Aerobacter (Enterobacter) aerogenes. *J Bacteriol* 123**:**1124-30.

192. Wilkins, J. C., Homer, K. A. & Beighton, D. (2002) Analysis of *Streptococcus mutans* proteins modulated by culture under acidic conditions. *Appl Environ Microbiol* 68**:**2382-90.

193. Yamamoto, Y., Kamio, Y. & Higuchi, M. (1999) Cloning, nucleotide sequence, and disruption of *Streptococcus mutans* glutathione reductase gene (gor). *Biosci Biotechnol Biochem* 63**:**1056-62.

194. Herskovits, A. A. & Bibi, E. (2000) Association of *Escherichia coli* ribosomes with the inner membrane requires the signal recognition particle receptor but is independent of the signal recognition particle. *Proc Natl Acad Sci U S A* 97**:**4621-6.

195. Maruyama, F., Kobata, M., Kurokawa, K., Nishida, K., Sakurai, A., Nakano, K., Nomura, R., Kawabata, S., Ooshima, T., Nakai, K., Hattori, M., Hamada, S. & Nakagawa, I. (2009) Comparative genomic analyses of *Streptococcus mutans* provide insights into chromosomal shuffling and species-specific content. *BMC Genomics* 10**:**358.

196. Ling, E., Feldman, G., Portnoi, M., Dagan, R., Overweg, K., Mulholland, F., Chalifa-Caspi, V., Wells, J. & Mizrachi-Nebenzahl, Y. (2004) Glycolytic enzymes associated with the cell surface of Streptococcus pneumoniae are antigenic in humans and elicit protective immune responses in the mouse. *Clin Exp Immunol* 138**:**290-8.

197. Severin, A., Nickbarg, E., Wooters, J., Quazi, S. A., Matsuka, Y. V., Murphy, E., Moutsatsos, I. K., Zagursky, R. J. & Olmsted, S. B. (2007) Proteomic analysis and identification of Streptococcus pyogenes surface-associated proteins. *J Bacteriol* 189**:**1514-22.

198. Modun, B., Morrissey, J. & Williams, P. (2000) The staphylococcal transferrin receptor: a glycolytic enzyme with novel functions. *Trends Microbiol* 8**:**231-7.

199. Wang, P., Kuhn, A. & Dalbey, R. E. (2010) Global change of gene expression and cell physiology in YidC-depleted E. coli. *J Bacteriol*.

200. Soksawatmaekhin, W., Kuraishi, A., Sakata, K., Kashiwagi, K. & Igarashi, K. (2004) Excretion and uptake of cadaverine by CadB and its physiological functions in *Escherichia coli*. *Mol Microbiol* 51**:**1401-12.

201. Haneburger, I., Eichinger, A., Skerra, A. & Jung, K. (2011) New Insights into the Signaling Mechanism of the Ph-Responsive, Membrane-Integrated Transcriptional Activator Cadc of *Escherichia coli*. *J Biol Chem*.

202. Griswold, A. R., Jameson-Lee, M. & Burne, R. A. (2006) Regulation and physiologic significance of the agmatine deiminase system of *Streptococcus mutans* UA159. *J Bacteriol* 188**:**834-41.

203. Liu, Y., Zeng, L. & Burne, R. A. (2009) AguR is required for induction of the *Streptococcus mutans* agmatine deiminase system by low pH and agmatine. *Appl Environ Microbiol* 75**:**2629-37.

204. Liu, Y. & Burne, R. A. (2009) Multiple two-component systems of *Streptococcus mutans* regulate agmatine deiminase gene expression and stress tolerance. *J Bacteriol* 191**:**7363-6.

BIOGRAPHICAL SKETCH

Sara Marie Raser Palmer was born in Jackson, Michigan, the birthplace of the Republican Party. When she was 11 years old she moved to Somerset Center, Michigan to live with her Aunt and Uncle Carolynn and Terry Palmer, who made their living as artists. She later attended Addison High School in Addison, Michigan. With encouragement from her high school biology teacher, Mr. Ellis, Sara was the first person from her high school to attend a science fair. During her senior year, she won first place in the Tri-County, Regional, and State Science Fairs and then went on to compete in the International Science and Technology Science Fair in 2000, in Detroit Michigan, where she placed 4th in her category. After high school, she attended Jackson Community College, where she received an Associate in Science degree. Sara went on to attend Michigan State University and received a Bachelor's Degree in Microbiology. She moved to Gainesville, Florida in 2005, to pursue a graduate degree in The Interdisciplinary Program in Biomedical Sciences at the University of Florida. In her free time she enjoys cooking, reading, traveling and spending time with her friends and dog Jacopo.